A novel dental stem cell-based *in vitro* model for X-linked adrenoleukodystrophy: From development to therapeutic strategies

Claudia Pérez García

Thesis Director: Dr. Salvador Martínez Pérez

PhD Program in Neuroscience

Neuroscience Institute (UMH-CSIC)

Universidad Miguel Hernández de Elche

– 2025 –

The present Doctoral Thesis, entitled “A novel dental stem cell-based in vitro model for X-linked adrenoleukodystrophy: From development to therapeutic strategies”, is submitted as a conventional thesis with the following quality indicator:

- Hernandez-Lopez, J. M., Hernandez-Medina, C., Medina-Corvalan, C., Rodenas, M., Francisca, A., Perez-Garcia, C., Echevarria, D., Carratala, F., Geijo-Barrientos, E., & Martinez, S. (2023). Neuronal progenitors of the dentate gyrus express the SARS-CoV-2 cell receptor during migration in the developing human hippocampus. *Cellular and molecular life sciences: CMLS, 80*(6), 140. https://doi.org/10.1007/s00018-023-04787-8

Dr. Salvador Martínez Pérez, director of the doctoral thesis entitled **"A novel dental stem cell-based *in vitro* model for X-linked adrenoleukodystrophy: From development to therapeutic strategies"**

CERTIFIES:

That Mrs. Claudia Pérez García has carried out under my supervision the work entitled "A novel dental stem cell-based *in vitro* model for X-linked adrenoleukodystrophy: From development to therapeutic strategies" in accordance with the terms and conditions defined in her Research Plan and in accordance with the Code of Good Practice of the University Miguel Hernández of Elche, satisfactorily fulfilling the objectives foreseen for its public defence as doctoral thesis.

I sign for appropiate purposes,

Thesis Director

Dr. Salvador Martínez Pérez

Ms. Maria Cruz Morenilla Palao, Coordinator of the Neuroscience PhD programme at the Institute of Neuroscience in Alicante, a joint centre of the Miguel Hernández University (UMH) and the Spanish National Research Council (CSIC),

INFORMS:

That Mrs. Claudia Pérez García has carried out under the supervision of our PhD Programme the work entitled "A novel dental stem cell-based *in vitro* model for X-linked adrenoleukodystrophy: From development to therapeutic strategies" in accordance with the terms and conditions defined in her Research Plan and in accordance with the Code of Good Practice of the University Miguel Hernández of Elche, satisfactorily fulfilling the objectives foreseen for its public defence as doctoral thesis.

Which I sign for the appropiate purposes,

Dr. Maria Cruz Morenilla Palao
Coordinator of the PhD Programme in Neurosciences

To whom it may concern:

The doctoral thesis entitled “A novel dental stem cell-based in vitro model for X-linked adrenoleukodystrophy: From development to therapeutic strategies” carried out by Claudia Pérez García (DNI 74379888G) at Instituto de Neurociencias de Alicante, a joint centre of the Miguel Hernández University (UMH) and the Spanish National Research Council (CSIC), has been supported by Research Grants from Universidad Católica de Murcia (UCAM) and Walk on Project (WOP) Foundation (2019/00366/001).

A mi familia

"The important thing is not to stop questioning.
Curiosity has its own reason for existing.
One cannot help but be in awe when he
contemplates the mysteries of eternity, of life,
of the marvellous structure of reality. It is
enough if one tries merely to comprehend a
little of this mystery each day."

— *Albert Einstein, Old Man's Advice to Youth.*

Index

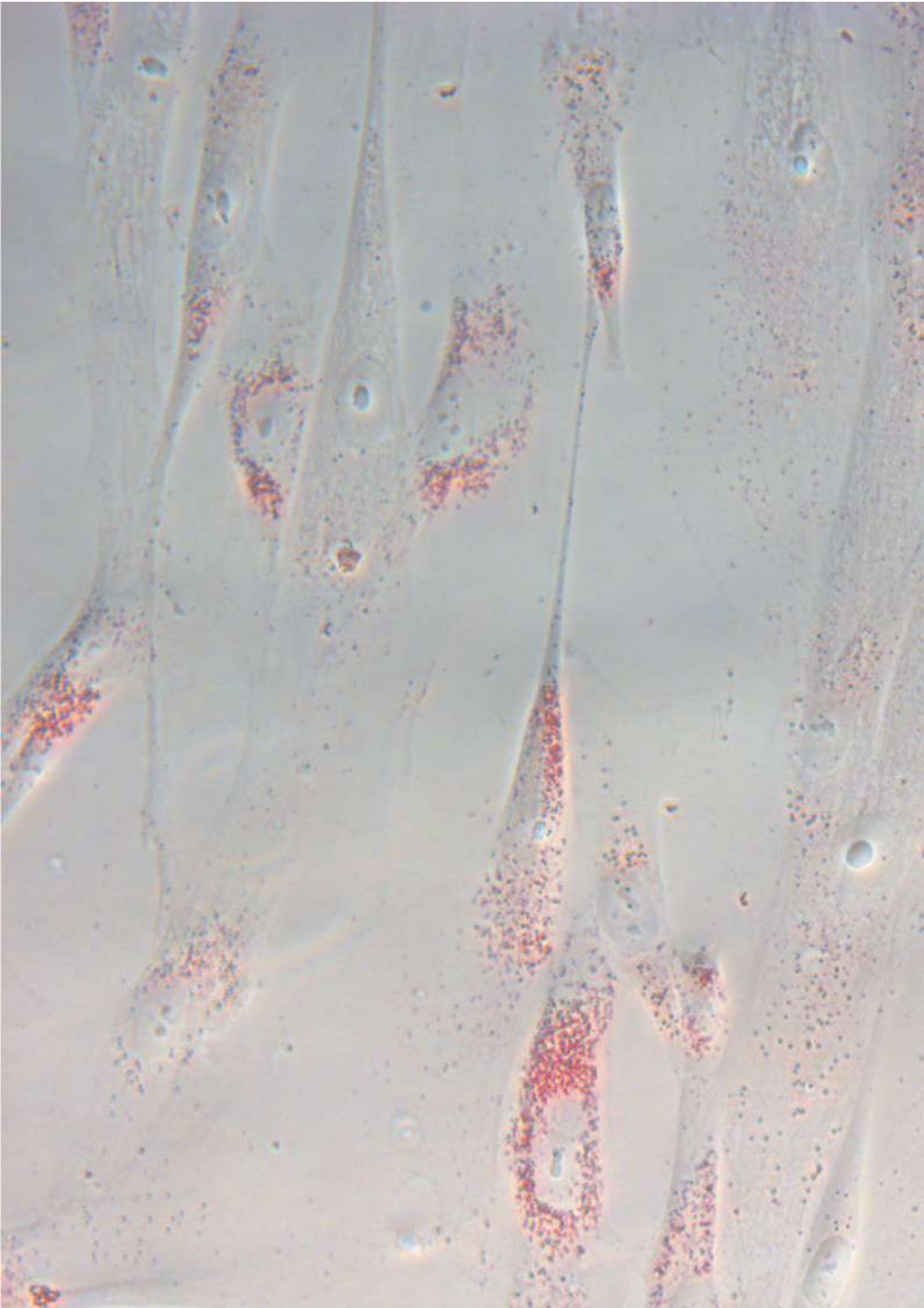

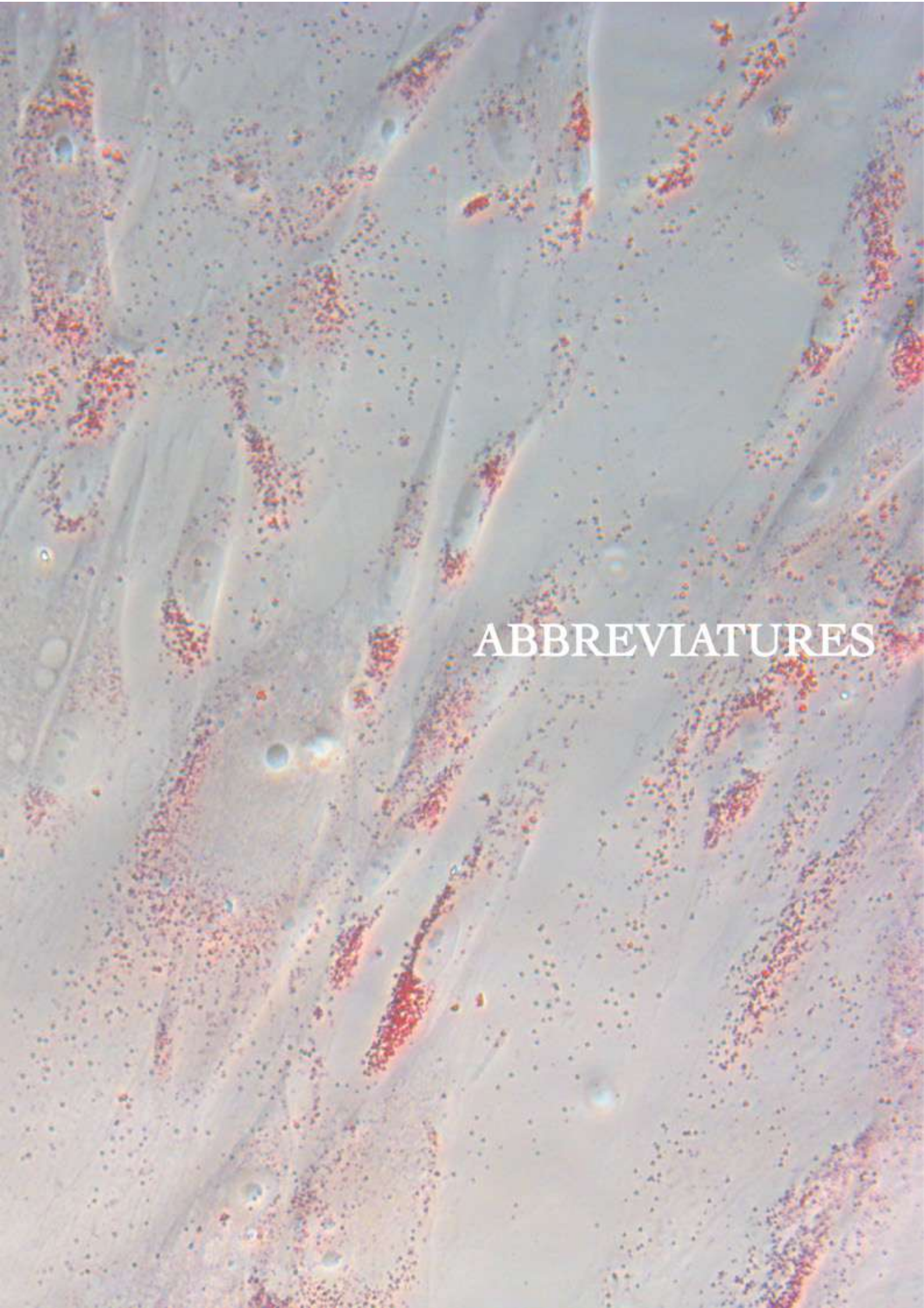

ABBREVIATURES

This image is property of Claudia Pérez García. Human dental pulp stem cells stained with Oil Red O evidencing neutral lipid accumulation. Image acquisition: Leica DMR fluorescence microscope.

Abbreviatures

AcALD	Adult cerebral adrenoleukodystrophy
Adol-cALD	Adolescent cerebral adrenoleukodystrophy
ADP	Adenosine diphosphate
ALDP	Adrenoleukodystrophy protein
AMN	Adrenomyeloneuropathy
APOs	Apoptotic bodies
ATP	Adenosine triphosphate
BBB	Blood-brain barrier
BCSFB/BBB	Blood-cerebrospinal fluid/blood-brain barrier
BDNF	Brain-derived neurotrophic factor
BMSCs	Bone marrow-derived mesenchymal stem cells
BSA	Bovine serum albumin
C18:0	Octadecanoic acid
C22:0	Docosanoic acid
C24:0	Tetracosanoic acid
C26:0	Hexacosanoic acid
CAM	Cell adhesion molecules
cALD, ccALD	Cerebral adrenoleukodystrophy, Childhood cerebral adrenoleukodystrophy
CM	Conditioned media
CNS	Central nervous system
CRISPR/Cas9	Clustered regularly interspaced short palindromic repeats

CTCF	Corrected Total Cell Fluorescence
Cx	Connexin
DAPI	4′,6-diamidino-2-phenylindole
dbcAMP	Dibutyryl cyclic adenosine monophospate
DMEM	Dulbecco's Minimal Essential Medium
DPSCs	Dental pulp stem cells
ELOVL	Elongation of very long-chain fatty acids
ENO-2	Enolase-2
ESCs	Embryonic stem cells
ETC	Electron transport chain
etOH	Ethanol
EVs	Extracellular vesicles
Exo	Exosomes
FBS	Fetal bovine serum
FGF	Fibroblast growth factor
FSC	Forward scatter
GBX	Gastrulation brain homeobox
gDNA	Genomic DNA
GDNF	Glial cell derived neurotrophic factor
GFAP	Glial fibrillary acidic protein
GJ	Gap junctions
Gpx	Glutathione peroxidase
GVHD	Graft-versus-host disease
H_2O_2	Hydrogen peroxide

hBMSCs	Human bone marrow-derived mesenchymal stem cells
hBMSCs-Exos	Human bone marrow stem cells-derived exosomes
hDPSCs	Human dental pulp stem cells
HEPES	4-(2-hydroxyethyl)-1-piperazineethanesulfonic acid
HGF	Hepatocyte growth factor
hMSCs	Human mesenchymal stem cells
HO·	Hydroxyl radical
$HO\cdot_2$	Hydroperoxyl radical
HOBr	Hypobromous acid
HOCl	Hypochlorous acid
HPCs	Hematopoietic progenitor cells
HRP	Horseadish peroxidase
HSCT	Hematopoietic stem cell transplantation
IDO	Indoleamine-pyrrole 2,3-dyoxygenase
IFN-γ	Interferon gamma
IGF-1	Insulin-like growth factor
IL	Interleukin
iNOS	Inducible-nitric oxide synthase
iPSCs	Induced-pluripotent stem cells
ISCT	International Society for Cell Therapy
ITG	Integrins
KLF4	Kruppel-like factor 4
LCFA	Long chain-fatty acids
LEVs	Large extracellular vesicles

LPC	Lysophosphatidyl choline
MAP2	Microtubule-associated protein 2
MAP2ab	Microtubule-associated protein 2ab
MIM	Mitochondrial inner membrane
miRNA	Micro-RNA
MISEV	Minimal Information for Studies of Extracellular Vesicles
MOM	Mitochondrial outer membrane
mPTP	Mitochondrial permeability transition pore
mRNA	Messenger RNA
MSC-Exos	Mesenchymal stem cell-derived exosomes
MSCs	Mesenchymal stem cells
mtDNA	Mitochondrial DNA
MVB	Multivesicular body
MVs	Microvesicles
NBD	Nucleotide-binding domain
NCP	Neural crest progenitors
NEAA	Non-essential aminoacids
NK	Natural killer
NP-1	Neuropilin-1
O^{-}_{2}	Superoxide anion
O2	Singlet oxygen
OCT3/4	Octamer-binding transcription factor 3/4
ORO	Oil Red O
OXPHOS	Oxidative phosphorylation system

PAX-6	Paired box-6
PBS	Phosphate buffered saline
PCR	Polymerase chain reaction
PDLSCs	Periodontal ligament stem cells
PFA	Paraformaldehyde
PGE2	Prostaglandin E
PMP70	70 kDa peroxisomal membrane protein
PPAR-γ	Peroxisome proliferator-activated receptor gamma
PUFA	Polyunsaturated fatty acids
RMI	Magnetic resonance imaging
RNS	Reactive nitrogen species
RO·	Alkosyl radical
RO·2	Peroxyl radical
ROS	Reactive oxygen species
RT	Room temperature
RT-qPCR	Real-time quantitative polymerase chain reaction
RUSP	Recommended Uniform Screening Panel
SCAP	Stem cells from apical papilla
SCDF	Stem cells from dental follicle
sEVs	Small extracellular vesicles
SD	Standard deviation
SHED	Stem cells from exfoliated deciduous teeth
Shh	Sonic hedgehog
SOD	Superoxide dismutase

SOX-2	Sex determining region Y-box 2
SSC	Side scatter
TEM	Transmission electronic microscopy
TGF-β	Tumor growth factor-beta
TGF-β1	Transforming growth factor- beta 1
Th17	T helper 17 cell
TLR	Toll-like cell receptor
TMD	Transmembrane domain
TNF-α	Tumor necrosis factor- alpha
TNTs	Tunneling nanotubes
TUJ-1	Tubulin-beta- III
VLCFAs	Very long-chain fatty acids
VMC	Vascular smooth muscle cells
X-ALD	X-linked adrenoleukodystrophy

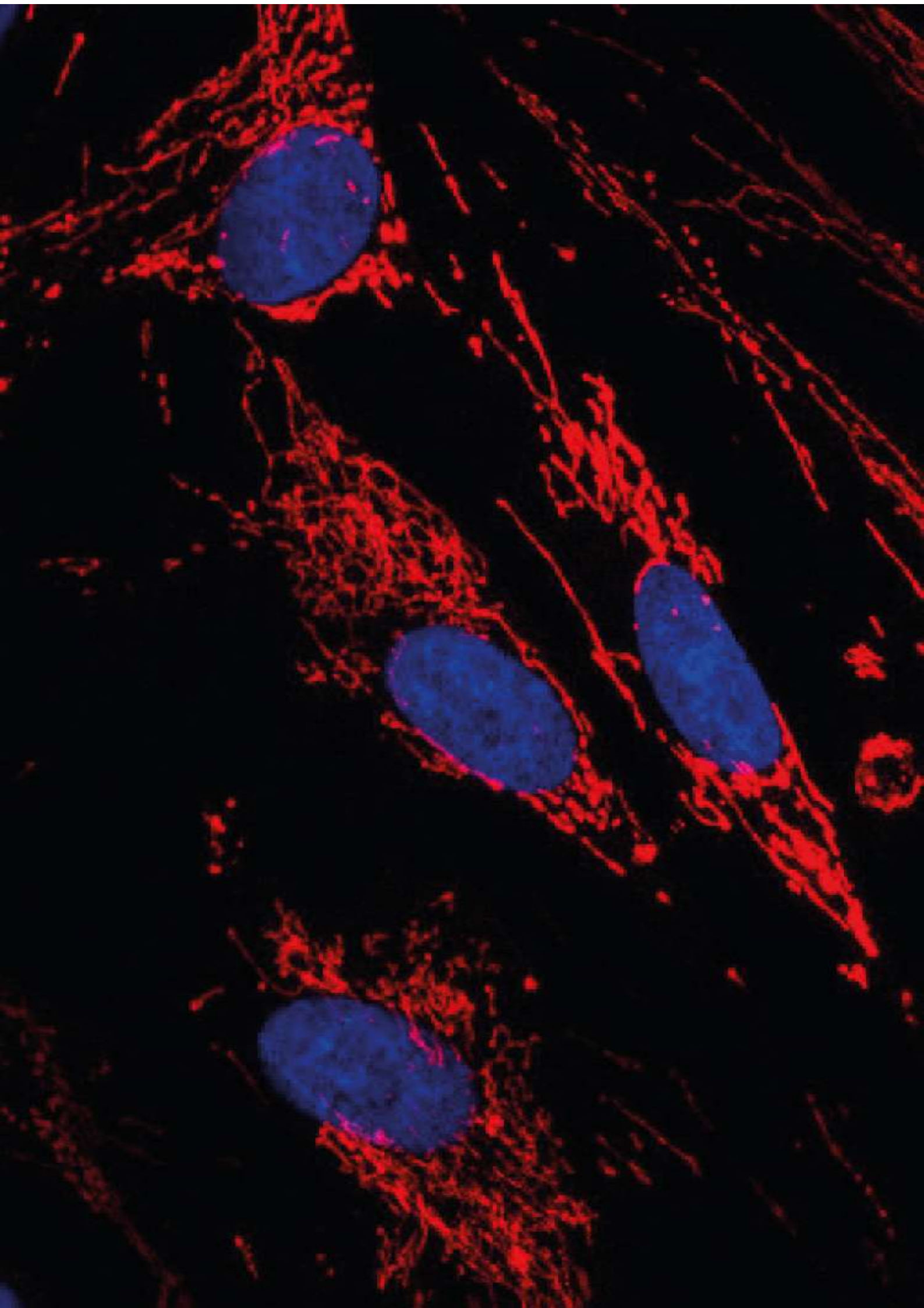

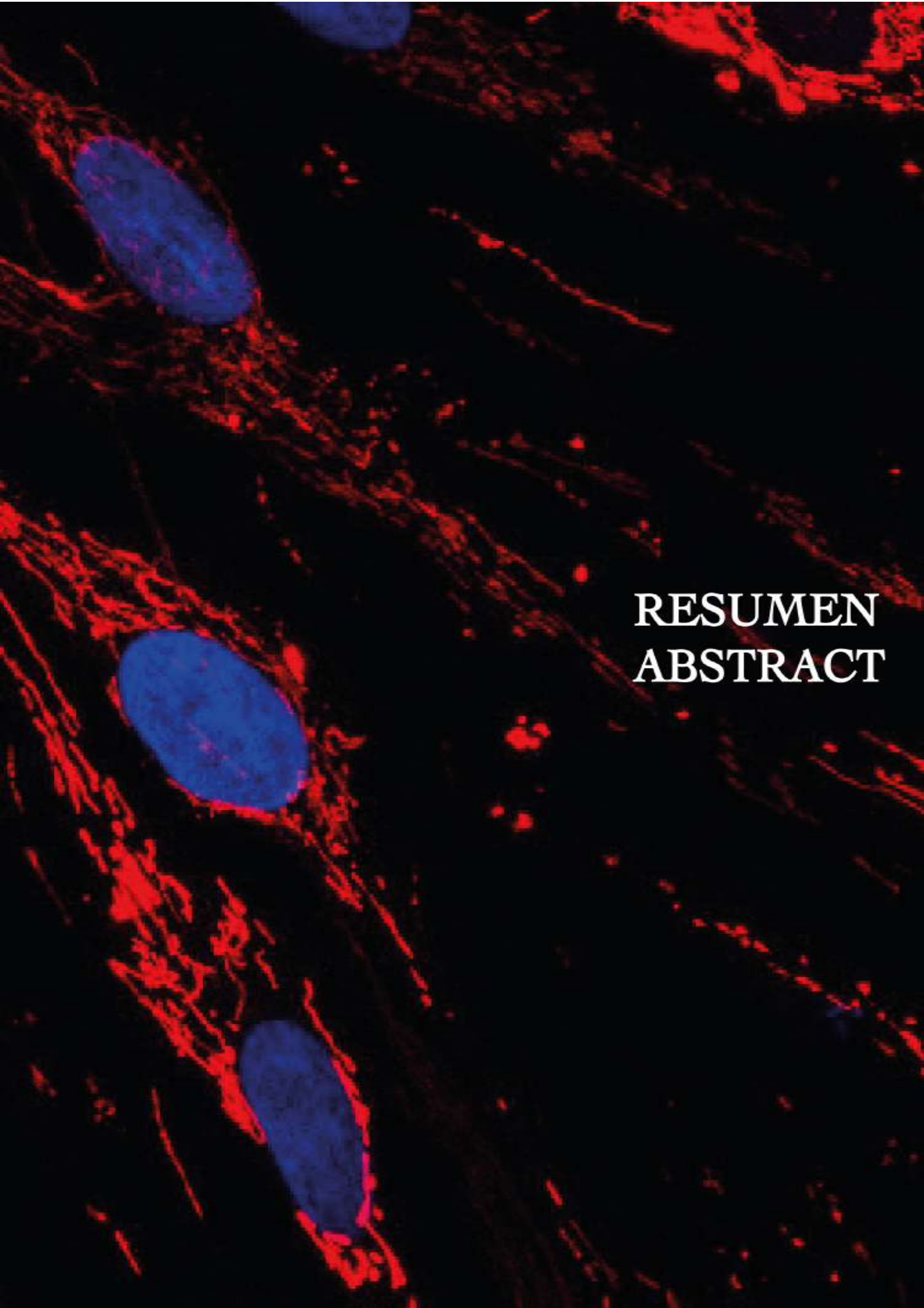

RESUMEN
ABSTRACT

This image is property of Claudia Pérez García. Immunofluorescence of transduced human bone marrow mesenchymal stem cells against RFP revealing mitochondria. Image acquisition: Leica SPEII confocal microscope.

Resumen

La adrenoleucodistrofia ligada al cromosoma X (X-ALD) es un trastorno genético raro causado por mutaciones en el gen ABCD1. Este gen codifica la proteína de la adrenoleucodistrofia (ALDP), una proteína de membrana peroxisomal crucial para el transporte de los ácidos grasos de cadena muy larga (VLCFA) hacia los peroxisomas, donde son degradados. En la X-ALD, las mutaciones en el gen ABCD1 provocan una disfunción de ALDP, lo que conduce a la acumulación de VLCFA en las células, afectando principalmente al sistema nervioso y glándulas suprarrenales. Esta acumulación produce una amplia gama de manifestaciones clínicas, que van desde insuficiencia suprarrenal hasta graves síntomas neurodegenerativos, incluyendo la desmielinización inflamatoria del sistema nervioso central, con consecuencias fatales. La complejidad y variabilidad en la progresión de la enfermedad, junto con las opciones terapéuticas limitadas, hacen que la X-ALD sea particularmente difícil de tratar, especialmente en los pacientes con las formas más graves de la enfermedad.

Uno de los principales obstáculos para comprender los mecanismos subyacentes de la X-ALD y desarrollar tratamientos específicos es la falta de modelos animales eficaces que reproduzcan el proceso de desmielinización observado en los seres humanos. Como resultado, numerosos autores han recurrido a modelos basados en células humanas para estudiar la enfermedad. Para avanzar en la comprensión de la X-ALD y explorar nuevas opciones de tratamiento, en esta Tesis Doctoral, se ha desarrollado un nuevo modelo celular de la enfermedad utilizando células madre de pulpa dental (hDPSCs) derivadas de un paciente con diagnóstico clínico de X-ALD. Estas células proporcionan un modelo único y clínicamente relevante, ya que expresan la proteína ALDP de manera similar a las células de individuos sanos, pero exhiben una acumulación anormal de lípidos neutros, lo que refleja la disfunción de ALDP observada en la X-ALD. Debido al natural potencial neurogénico característico de las hDPSCs, las células provinientes del paciente se pueden diferenciar en células neuronales, pudiendo estudiar el fenotipo patológico de forma más precisa. De este modo, se ha podido observar que las células diferenciadas procedentes del paciente de X-ALD, no sólo presentan una acumulación aberrante de lípidos neutros, sino que también muestran alteraciones en la cinética de las corrientes de sodio, sugeriendo una alteración en el proceso de diferenciación funcional en neuronas que no sucede en células derivadas de individuos sanos.

Además del desarrollo este modelo, se ha estudiado el potencial terapéutico de las células mesenquimales humanas derivadas de médula ósea (hBMSCs). Estas células son

conocidas por sus propiedades terapéuticas, tanto por el establecimiento de contactos directos entre células como por la secreción de moléculas solubles como las vesículas extracelulares (EVs).

En el contexto de la X-ALD, se ha investigado el efecto protector de la terapia celular con hBMSCs en el modelo celular de X-ALD desarollado en esta Tesis Doctoral. El medio condicionado (CM) derivado de las hBMSCs, rico en EVs, puede reducir la acumulación de lípidos neutros y proteger las células enfermas del estrés oxidativo y de los efectos citotóxicos derivados del exceso de VLCFAs, ambientes especialmente vulnerables en X-ALD. Además de los efectos paracrinos, las hBMSCs establecen una comunicación celular directa con las hDPSCs derivadas del paciente. Esta interacción permite la transferencia de mitocondrias y otros componentes citosólicos de las hBMSCs a las células afectadas, lo que podría ayudar a restaurar la función celular y, posiblemente, revertir el fenotipo de la enfermedad. Además, mediante el contacto directo célula-célula, las hBMSCs consiguen modificar el perfil de las corrientes de sodio de las células X-ALD diferenciadas, revertiendo el fenotipo electrofisiológico.

Las acciones combinadas de contacto célula a célula e indirectas (paracrinas) sugieren que las hBMSCs tienen un gran potencial terapéutico para el tratamiento de la X-ALD. A través del avance en los modelos celulares humanos y las estrategias terapéuticas, esta Tesis Doctoral tiene como objetivo mejorar la comprensión de la enfermedad y abrir nuevas vías para el desarrollo de terapias efectivas.

Abstract

X-linked adrenoleukodystrophy (X-ALD) is a rare genetic disorder caused by mutations in the ABCD1 gene. This gene encodes the adrenoleukodystrophy protein (ALDP), a crucial peroxisomal membrane protein responsible for transporting very long-chain fatty acids (VLCFAs) into peroxisomes, where these fatty acids are broken down. In X-ALD, mutations in ABCD1 lead to a malfunction in ALDP, resulting in the accumulation of VLCFAs in the body, particularly in the nervous system and adrenal tissues. This accumulation causes a spectrum of clinical manifestations that range from adrenal insufficiency to severe neurodegenerative symptoms, including inflammatory demyelination of the central nervous system, leading to debilitating and often fatal outcomes. The complexity and variability of symptoms, alongside limited therapeutic options, make X-ALD particularly challenging to treat, especially for patients with the most severe forms of the disease.

One of the primary obstacles in understanding X-ALD's underlying mechanisms and developing targeted treatments is the absence of effective animal models that accurately mimic the demyelination process observed in humans. As a result, researchers have turned to human cell-based models to study the disease. In this Doctoral Thesis, we sought to advance the understanding of X-ALD through the development of a novel *in vitro* model using human dental pulp stem cells (hDPSCs) derived from an affected patient. These cells provide a unique and clinically relevant model, as they express the ALDP protein similarly to cells from healthy individuals, but exhibit abnormal neutral lipid accumulation, reflecting the dysfunction of ALDP seen in X-ALD. This model is particularly promising because hDPSCs have natural neurogenic potential, meaning they can differentiate into neural-like cells that are capable of mimicking the pathological features of the disease, including increased neutral lipid accumulation, which is observed in the cellular bodies of differentiated neural lineage cells. In addition, impairments in sodium channel currents are also evidenced in X-ALD differentiated cells, suggesting an alteration in the process of functional neural differentiation. These characteristics make hDPSCs a valuable resource for studying X-ALD’s pathophysiology and testing potential therapeutic interventions.

In addition to this model, we also have highlighted the therapeutic potential of human bone marrow derived mesenchymal stem cells (hBMSCs). These cells are noted for their therapeutic properties, such as their ability to engage in direct cell-to-cell contact and secrete

several soluble molecules, including cytokines, growth factors, and extracellular vesicles (EVs). These molecules can act as paracrine signals to modulate the behaviour of target cells.

Based on their therapeutic potential, we have investigated the effects of hBMSCs on the *in vitro* X-ALD model developed from hDPSCs. The findings reveal that conditioned media (CM) from hBMSCs, containing EVs, can mitigate the abnormal lipid accumulation observed in X-ALD hDPSCs. Furthermore, hBMSCs protect these cells from oxidative stress and from cytotoxic effects derived from VLCFA, a condition that exacerbates cellular damage in many neurodegenerative diseases, including X-ALD. In addition to this paracrine signaling, hBMSCs also establish direct cellular communication with X-ALD hDPSCs. This direct interaction enables the transfer of healthy mitochondria and other cytosolic components from hBMSCs to the affected cells, which may help restore cellular function and potentially revert the diseased phenotype. Furthermore, through the establishment of cell-to-cell contacts, hBMSCs induce changes in sodium channel pattern of X-ALD differentiated cells, rescuing a healthy phenotype.

The combined actions of direct cell-to-cell contact and indirect (paracrine) signaling suggest that hBMSCs hold significant therapeutic promise for treating X-ALD. Their ability to not only protect but also potentially correct the pathological features of the disease at the cellular level represents a substantial advancement in X-ALD research. This doctoral thesis highlights the potential of hBMSCs and cell-derived products as a therapeutic tool for X-ALD. Through the advancement in human cell models and therapeutic strategies, this thesis aims to enhance the understanding of the disease and opens new avenues for developing effective therapies.

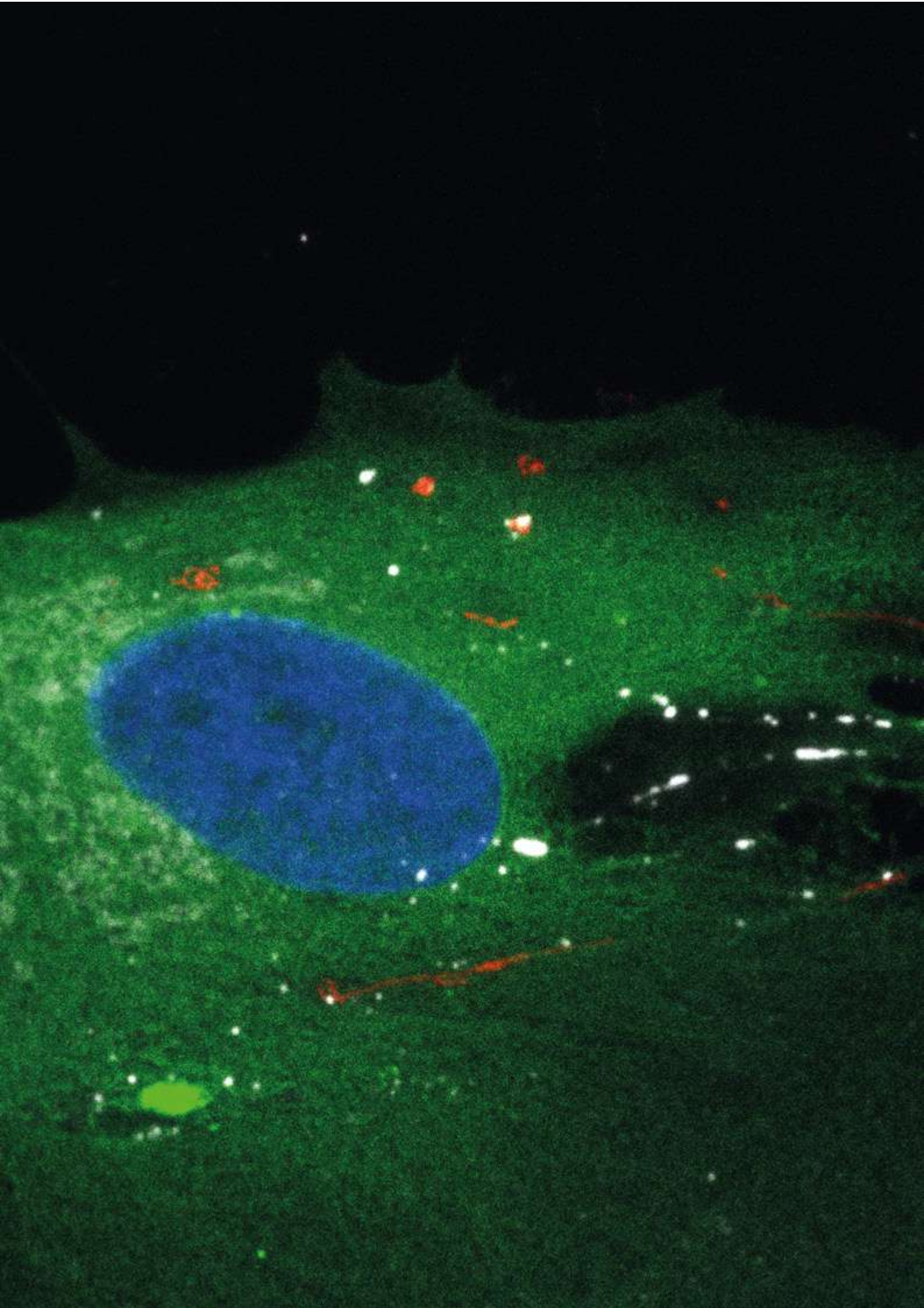

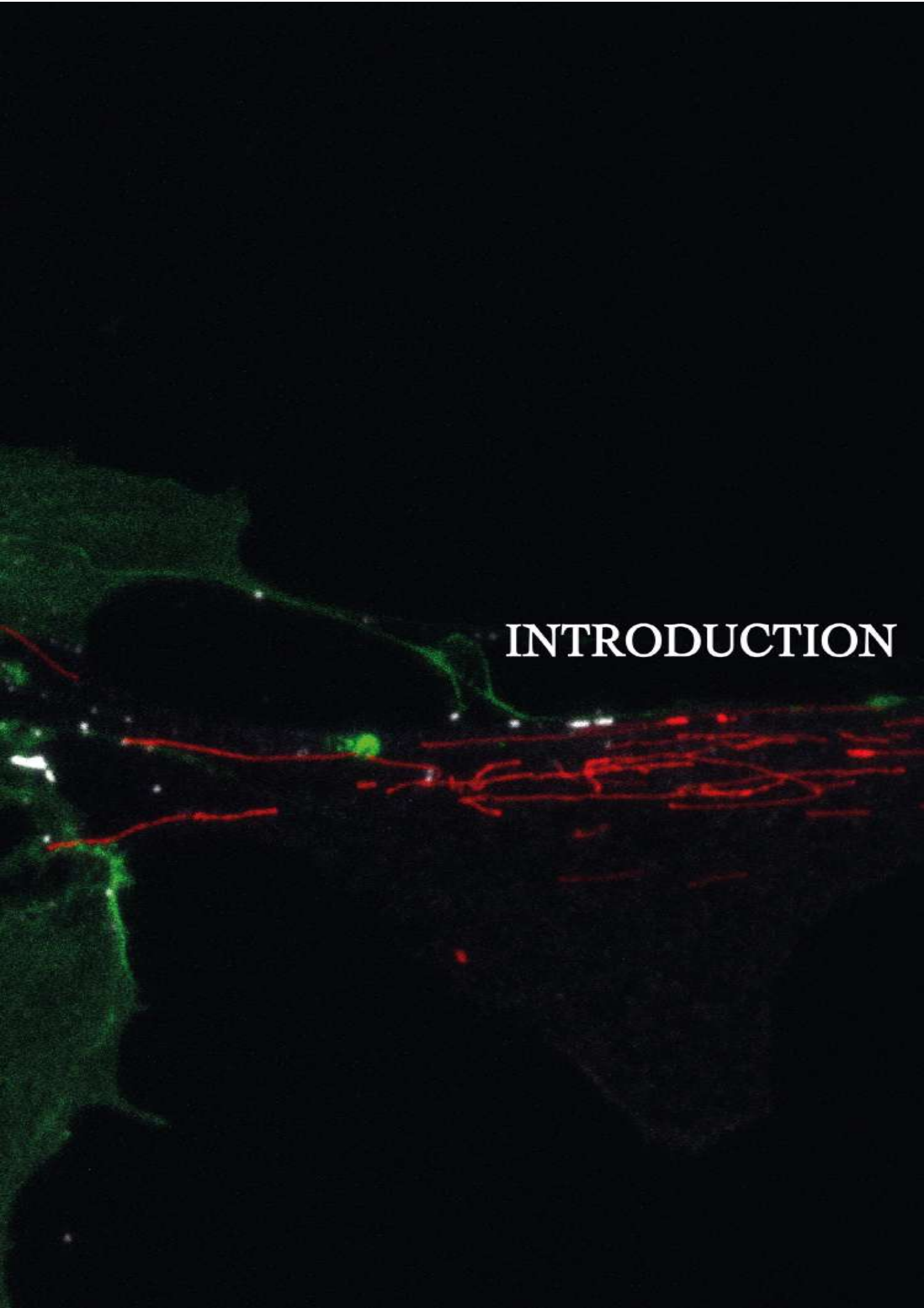

INTRODUCTION

This image is property of Claudia Pérez García. Immunofluorescence of direct co-cultures of human dental pulp and bone marrow stem cells against GFP, RFP and Connexin-43. Image acquisition: Leica SPEII confocal microscope.

Introduction

1. Human stem cells.

1.1 Definition and classifications.

Stem cells are unspecialized cells of the human body found both in embryo and adult stages. These cells are characterized not only by their ability to differentiate into any kind of cell of the organism but also by their capability of self-renewal. Based on their differentiation potential, these cell population can be classified in different groups: totipotent, pluripotent, multipotent, oligopotent and unipotent stem cell (Casado-Díaz, 2022; Zakrzewski et al., 2019) (Figure 1; subsequent figures as Fig.).

Totipotent stem cells are the most undifferentiated cells found in early stages of organism development. They are able to be differentiated into cells of the whole organism allowing cells to form both embryo and extra-embryonic structures (Rossant, 2001).

Pluripotent stem cells are cells that have the ability to form cells from any of the three-germ layer, but not extra-embryonic structures such as the placenta (De Miguel et al., 2010). Embryonic stem cells (ESCs), derived from the inner cell mass of the blastocyst (Evans & Kaufman, 1981) and induced-pluripotent stem cells (iPSCs), generated by reprogramming somatic cells (Takahashi & Yamanaka, 2006), are an example of these cell populations.

Multipotent stem cells are cell population that can be differentiated into discrete specific cells from the same blastodermic lineage (Ratajczak et al., 2012). An example of this type of stem cells are mesenchymal stem cells (MSCs), which their differentiation abilities are restricted to cell lineages derived from mesoderm. However, some multipotent stem cells can be differentiated into cells from other blastodermic lineages, in a process called trans-differentiation (Barzilay et al., 2009).

Oligopotent stem cells are characterised by their ability to differentiate into cells from two or more lineages within a specific tissue from a single blastodermic layer. A type of oligopotent stem cells are hematopoietic stem cells that are able to differentiated into cells of two lineages: myeloid and lymphoid (Marone et al., 2002).

Unipotent stem cells are those cells that have the narrowest spectrum of differentiation. They only can be differentiated into one specific cell type and form one single lineage (Dulak et al., 2015).

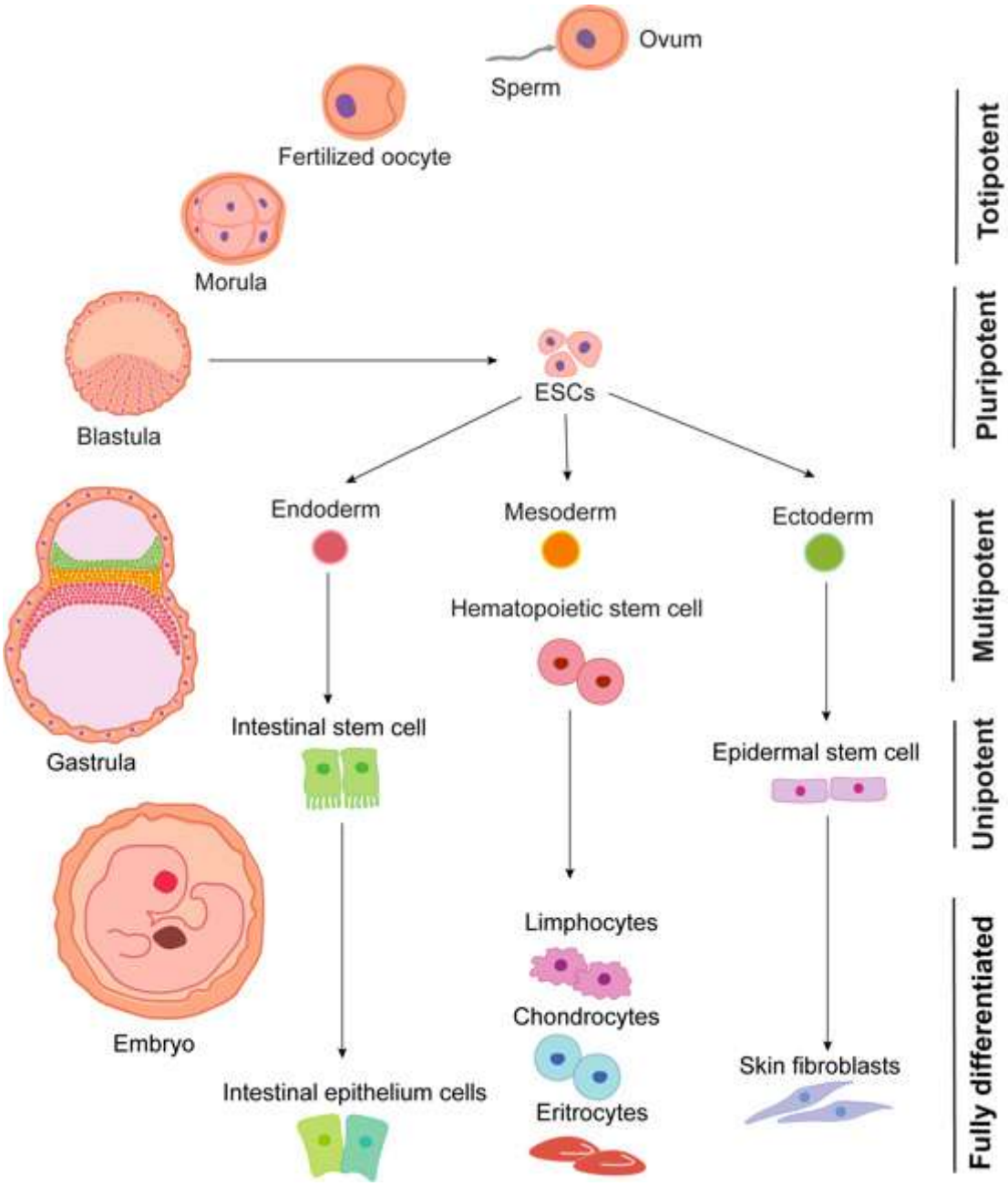

Figure 1. Types of human stem cells categorized by their potency.

As stem cells mature and become more specialized within their specific lineage, their capacity to differentiate into various cell types decreases. This figure illustrates a few stem cell lineages and examples of their resulting cell types. Illustration based on Balistreri et al (2020) (Balistreri et al., 2020).

Human stem cells can also be classified according to their origin in: ESCs, fetal and adult stem cells and iPSCs (Fig. 2).

ESCs are derived from the inner cell mass of the blastocyst (Evans & Kaufman, 1981). Due to their pluripotency, they can differentiate into cells from the three-germ layers, but also can be in an undifferentiated status for prolonged time (Yao et al., 2006).

Adult stem cells are found in adult tissue such as bone marrow, adipose tissue or teeth. Examples of adult stem cells are MSCs or stem cells found in placenta. These cells have ability of differentiation but they have limited capacity (Körbling & Estrov, 2003). They show beneficious advantages in the field of regenerative medicine and are proposed in transplants as therapeutic tool because of their lack of rejection or ethical controversies (McCormick & Huso, 2010).

As mentioned above, iPSCs are generated by genetically reprogramming of adult somatic cells to achieve an ESCs-like status (Rossant, 2008). They were first developed by Takahashi and Yamanaka (2006) by transducing mouse fibroblasts with 4 genes that encodes the following transcription factors: octamer-binding transcription factor 3/4 (OCT3/4), RY-related high-mobility group box protein-2 (SOX2), the oncoprotein c-MYC, and Kruppel-like factor 4 (KLF4) (Takahashi & Yamanaka, 2006). A year later, the same group (2007) developed iPSCs from human fibroblasts using the same 4 factors. These reprogrammed cell population displayed ESCs features in terms of morphology, proliferation, surface antigens, gene expression, epigenetic status of pluripotent cell specific-genes, telomerase activity and they were able to differentiate into cells from the three-germ layer *in vitro* (Takahashi et al., 2007).

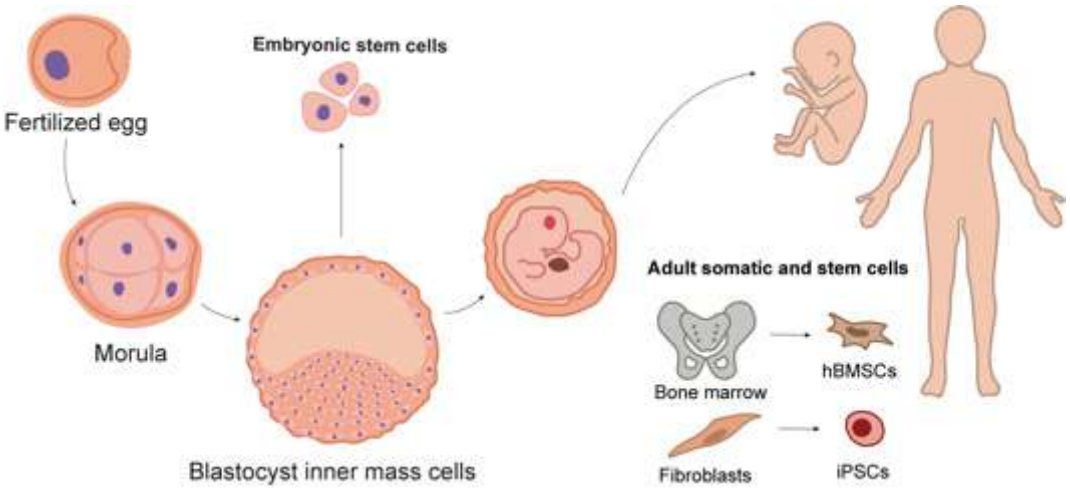

Figure 2. Types of human stem cells based on their origin.

Stem cells can be found in embryonic and adult sources. ESCs derive from the inner cell mass of blastocyst during embryo development. However, when human body is fully developed, adult stem cells can be observed at certain tissues such as bone marrow, where hBMSCs are located. In addition to natural sources of stem cells, fibroblasts are being used to obtain induced iPSCs through reprogramming methods. hBMSCs: human bone marrow derived mesenchymal stem cells; iPSCs: induced-pluripotent stem cells. Illustration based on Shevde (2012) (Shevde, 2012).

1.2 Mesenchymal stem cells.

1.2.1 Definition and historical context.

Human mesenchymal stem cells (hMSCs) are adult stem cells that can differentiate into variety of mesodermal mature cell types including adipocytes, chondrocytes, osteocytes and myocytes (Bartsch et al., 2005; Pittenger et al., 1999; Wagner et al., 2005). Apart from this, hMSCs can be trans-differentiated into a wide variety of cells of other lineages such as mature type II pneumocyte (Della Sala et al., 2021), hepatocytes, (Anzalone et al., 2010; Stock et al., 2014; Wang et al., 2014), neurons (Bueno et al., 2013; Karakaş et al., 2020; Lian et al., 2021) and insulin-producing cells (Oh et al., 2004; Tang et al., 2004), among others (Fig. 3). This cell type can be found in many adult tissues such as adipose tissue (Schneider et al., 2017), dental pulp (Gronthos et al., 2009.; Huang et al., 2000), umbilical cord blood (Majore et al., 2011), bone marrow (Baghaei et al., 2017; Friendenstein, 1970) and so forth.

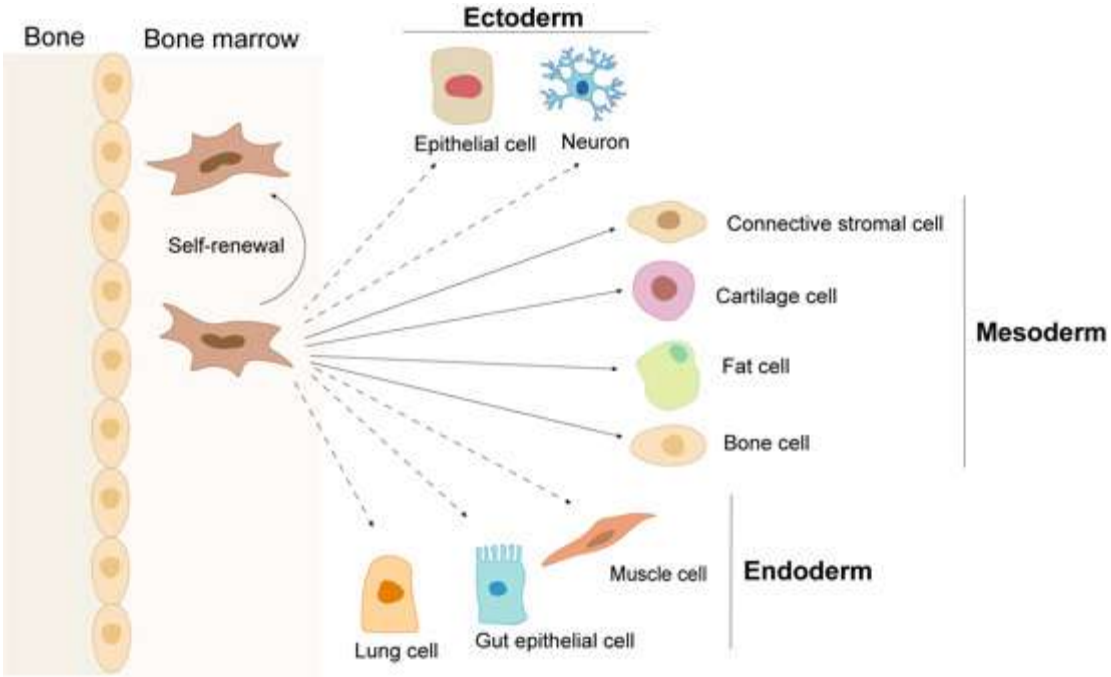

Figure 3. Multipotentiality of hMSCs.

hMSCs, located at bone cavity, are able to self-renew (curved arrow) and to differentiate into cells from mesodermal lineage under physiological conditions (solid arrows). Under *in vitro* and *in vivo* experiments, these cells are able to transdifferentiate into cells from ectoderm and endoderm lineages (dashed arrows). Illustration based on Uccelli et al (2008) (Uccelli et al., 2008).

MSCs derived from bone marrow (BMSCs) are the best-defined population of mesenchymal stem cells. They were the first MSCs population described by Friedenstein and colleagues (1970) in the 70's decade as "osteogenic stem cells" due to their ability to form ectopic bone (Friedenstein et al., 1970). However, it was not until 1991 when Caplan (1991) named these cell populations as "mesenchymal stem cells" remarking their natural capacity for multipotential differentiation into mesodermal lineage (Caplan, 1991) (Fig. 3). BMSCs can be easily isolated from bone marrow and exhibit advantages against other types of stem cells such as ESCs or iPSCs, since they present fewer ethical concerns when compared to ESCs and lower risk of teratoma formation than iPSCs (Steens & Klein, 2018).

In 2006, the International Society for Cell Therapy (ISCT) established standard criteria to define populations of MSCs. Ensuring compliance with minimal standards is essential to classify cells as MSCs. Firstly, they must exhibit plastic adherence and display a fibroblast-like morphology under standard culture conditions. Additionally, they should express specific markers including CD105, CD73 and CD90 while lacking expression of CD45, CD35, CD14 or CD11b, CD79-α or CD19 and HLA-DR surface molecules. Finally, these cells must demonstrate the ability to differentiate into osteoblasts, adipocytes and chondroblasts under *in vitro* conditions (Dominici et al., 2006). These criteria are important to define cell populations, but they are constrained by their lack of specific indicators for evaluating stemness. Nowadays, the terms of "mesenchymal stem cells" or "mesenchymal stromal cells" are widely used by scientific community but are still imprecise from their identity. Some authors propose the designation of "Medicinal Signalling Cells" according to their therapeutic functions (Caplan, 2017).

1.2.2 Therapeutic functions.

Over the last years, hMSCs are of special relevance for cell-based therapy in the treatment of several disorders such as cancer (Lan et al., 2021), inflammatory (Shi et al., 2018) or neurodegenerative (Issa et al., 2022) diseases. Their importance in therapeutics lies in their main biological functions: migration to target areas, the ability of immunomodulation and the secretion of paracrine factors that promote functional recovery.

- Cell-to-cell communication.

The crosstalk between hMSCs and other cell types may be mediated by cell fusion (Melzer et al., 2019; Shadrin et al., 2015), the establishment of gap junctions (GJ) (Gabashvili et al., 2015; Ogawa et al., 2022) and the formation of tunnelling nanotubes (TNTs). Consequences of these established contacts may vary according to the cell type and its status.

- Cell fusion.

Cell-cell fusion is a highly regulated biological event which plays an important role not only during embryonic development but also during different cellular processes throughout the whole life (Willkomm & Bloch, 2015). The cell fusion process can be generally categorized into three stages: initial contact between two distinct membrane compartments, hemifusion, and the subsequent formation of an enlarging fusion pore. This intricate process requires a substantial reorganization of the fusing cells. Although not entirely understood, this process is precisely regulated by proteins that convey the necessary information for membrane organization and regulation. Ultimately, fusion and fission act to merge and separate membrane lipids, respectively (Chernomordik et al., 2006). The regulation of this process involves various signals that facilitate communication between fusing cells and their local cellular and extracellular environments, triggering specific cell signalling pathways essential for the initiation of cell-cell fusion (Hindi et al., 2013; Larsson et al., 2008). Additionally, both genetic and epigenetic factors make a significant contribution to the regulation of these fusion processes (Aguilar et al., 2013).

The role of cell fusion in therapy and tissue regeneration attract interest in hMSCs research. In general, stem cells possess highly fusogenic potential with other stem cells or differentiated cells in order to maintain tissue homeostasis including the growth and regeneration of tissues (Dörnen & Dittmar, 2021). Several reports attribute the transdifferentiation capacity of administered MSCs to their ability to undergo cell fusion (Alvarez-Dolado et al., 2003; Vassilopoulos et al., 2003; Wang et al., 2003) and not only to secreted soluble factors. In the field of nervous system diseases, differentiation of administered MSCs through cell fusion appears as a spontaneous process and at extremely low frequencies, but promote neural recovery since they acquired phenotypic traits of cells with their fused allowing cell plasticity (Mezey et al., 2003; Terada et al., 2002; Ying et al., 2002).

- Establishment of cellular contacts.

In multicellular organisms, cell interactions and intercellular communication are fundamental to the survival of organism. These processes ensure the proper functioning of systems, maintenance of homeostasis and appropriate responses to environmental changes. Direct cell communication through the formation of intimal contacts is also a mechanism by which hMSCs exert their beneficial functions.

GJ are complexes of intercellular channels formed between the juxtaposed membranes of two adjacent cells which allow the intercellular transfer of ions, metabolites, soluble factors, and secondary messenger molecules smaller than 1200 Dalton (González-Nieto et al., 2015; Söhl & Willecke, 2004). These junctions are composed of oligomerized integral membrane proteins called connexins (Cx) (González-Nieto et al., 2015; Nielsen et al., 2012). GJ formation between hMSCs and other cell population is a common process and they mainly express Cx-43, Cx-40 and Cx-45 (Dorshkind et al., 1993; Valiunas et al., 2004). Through the establishment of Cx-mediated GJ, hMSCs transdifferentiate into neuron-like cells (Dilger et al., 2020), but also mediated cellular components exchange is reported in GJ-dependent manner. Among cellular material that can be transferred through GJ formation, mitochondria are of special interest (Golan et al., 2020; Islam et al., 2012; Yao et al., 2018). It is known that hMSCs can lead to neuronal survival due to GJ formation, among other cell-to-cell contacts, and exchange of cytoplasmatic material and mitochondria (Tarasiuk et al., 2022). This fact has gained special attention in recent years due to their promising potential in cell therapy, especially in those disorders with remarkable oxidative stress component and cell death (Liu et al., 2021).

- Tunneling nanotubes.

TNTs are long tubular structures rich in F-actin filaments that allow long-distance cell-to-cell contact and facilitate exchange of cytoplasmatic material (Rustom et al., 2004.). This structure is found in numerous cell types and in different biological conditions (Khattar et al., 2022).

Presence of TNTs in hMSCs population has also been reported. In pathological conditions, hMSCs can rescue damaged cells through TNTs suggesting that this particular structure acts as a mechanism of rescue and defence. Through the establishment of TNTs, different cargoes can be directly transferred between different cell populations, including mitochondria. hMSCs can transfer these organella to several different cell types, including epithelial cells, endothelial cells and cardiac myocytes, among others. These transfers are enhanced when the target cells

are under stress or damaged preventing their cell apoptosis (Liu et al., 2014). Special interest has been given to the process of intercellular proteostasis, which represents an intercellular mechanism that enhances protein management between damaged and normal cells (Kaushik & Cuervo, 2015). Intercellular proteostasis is defined by the exchange of exosomes and the establishment of TNTs that enable bidirectional transfer: the replenishment of proteostasis effectors from cells with more robust proteostasis to those with weaker proteostasis, and the transport of protein aggregates and damaged proteins in the reverse direction.

- Migration to target areas.

The homing effect of hMSCs is the *in vivo* capability of cell migration to damaged tissue. This migratory ability is regulated by a variety of signaling pathways and cellular processes, including interactions with extracellular matrix (ECM) components and the response to chemotactic signals. In systemic homing, hMSCs are administered or naturally recruited into the bloodstream. Subsequently, they undergo a multi-step process to exit circulation and migrate towards the injury site (Sackstein, 2005). By contrast, in non-systemic homing, hMSCs are introduced directly into the target tissue and then are guided to the injury area by chemokine gradient (Spaeth et al., 2008). Unfortunately, the homing efficiency of hMSCs is low because of physiological reasons (trapping) (Scarfe et al., 2018), lack of specific homing (low homing molecules) (Honczarenko et al., 2006; Rombouts & Ploemacher, 2003) and early death of administered cells (von Bahr et al., 2012). Strategies to increase homing efficiency using different procedures as magnetic guidance (Rombouts & Ploemacher, 2003), genetic modification (Cui et al., 2017; Shao et al., 2019) or priming (Ran et al., 2018; Zhang et al., 2012; Zhidkova et al., 2018) are being investigated.

Understanding hMSCs migration is essential not only for tissue engineering and regenerative medicine applications but also for developing *in vitro* specific models since migration dynamics can reveal important cellular behaviours in response to specific pathophysiological conditions. One key protein related to cell migration is angiotensin-converting enzyme 2 (ACE2), a membrane-bound protein that has recently gained attention as primary cellular receptor for SARS-CoV-2, the virus responsible for COVID-19 (Li et al., 2003). Nevertheless, beyond its role in viral entry, ACE2 is an important regulator within the renin-angiotensin system (RAS), which modulates blood pressure, inflammation and fibrosis (Tikellis & Thomas, 2012). The expression of this particular protein in hMSCs populations has been studied in recent years due to their potential therapeutic role in COVID-19 patients. Several authors reported little or no expression of this protein in various hMSCs cell populations isolated from different sources (Avanzini et al., 2021; Generali et al., 2022;

Hernandez-Lopez et al., 2023). However, studying ACE2 expression in hMSCs from other sources might elucidate questions about this topic.

- Direct immunomodulation.

hMSCs can modulate the immune response in diverse manners depending on physiological conditions, the microenvironment in which they are inserted, the levels of hypoxia and the stimulation of inflammatory factors (Weiss & Dahlke, 2019). After a tissue injury occurs, during the acute inflammatory phase, there is an increase of pro-inflammatory cytokines, which, consequently, activate hMSCs that may contribute to an immunosuppressive response (Planat-Benard et al., 2021). As the condition progresses to a chronic phase, there is shift with reduced production of pro-inflammatory cytokines and an increase of anti-inflammatory cytokines such as tumor growth factor-beta (TGF-β). Without the active stimuli of hMSCs, the reactivation of the immune response can be presented. Based on the inflammatory environment, hMSCs display functional adaptability exhibiting either immunotolerant or immunosuppressive activities (Renner et al., 2009).

Concretely, hMSCs have a direct effect on both adaptative and innate immune system cells with a result of maintenance of homeostatic immunity and inflammation regulation. The resulting immunomodulatory capacity of hMSCs is a consequence of their secreted released products which, in turn, depend on hMSCs phenotype at time. Phenotype of hMSCs is a result of the stimulation of specific cell surface receptor known as toll-like cell receptor (TLR) by paracrine factors placed at microenvironment. Thus, hMSCs can be classified by their immunomodulation capacity in pro-inflammatory phenotype (MSC-1), activated through TLR4 receptors or, on the other hand, an anti-inflammatory and immunosuppressive phenotype (MSC-2) activated by TLR3 (Waterman et al., 2010) (Fig. 5). Regarding adaptative immune system cells, hMSCs have a great influence on the action, survival and migration of T lymphocytes in presence of pro-inflammatory cytokines (Ren et al., 2008) as well as on proliferation, differentiation and expression of chemokine receptors of B cells (Corcione et al., 2006). hMSCs inhibit the expression and early activation markers during T cell activation (Ren et al., 2008). However, when the inflammatory process is not intense enough, hMSCs can adopt a pro-inflammatory phenotype and enhance the local immune response (Bernardo & Fibbe, 2013). In innate immune system, there is also evidence of direct effects of hMSCs modulating the expression, maturation and differentiation of natural killer (NK) cells (Moloudizargari et al., 2021; Spaggiari et al., 2006), dendritic cells (DCs) (Spaggiari et al., 2009), macrophages (Vasandan et al., 2016) and neutrophils (Raffaghello et al., 2008).

1.3 Extracellular vesicles.

The autocrine effect of hMSCs is mediated by secreted factors acting on stem cell itself. These secreted factors can influence on hMSCs differentiation capacity (Duque et al., 2009), maintenance of their stemness (Eom et al., 2014), regulation of immunomodulator factors release (Dumitru et al., 2014) and enhancement of their survival or proliferation (Lee et al., 2016).

Paracrine activity of hMSCs is driven by the release of a diverse range of bioactive molecules acting on neighbouring cells through a paracrine phenomenon. These secreted molecules and factors can be found in their free-form or bounded in extracellular vesicles (EVs). Among the different impact that might cause paracrine molecules from hMSCs, the main effects are: immunomodulation and promotion of cell survival.

EVs are nano to micro-sized membrane bounded vesicles that carry different cargoes (lipids, proteins, free acid nucleic, etc) into extracellular space as a form of intercellular communication. Depending on their biogenesis, release pathways, size, content and function, EVs can be classified into three main subtypes: microvesicles (MVs), apoptotic bodies (APOs) and exosomes (Exo). MV are larger vesicles (100-1000 nm) that bud directly from the plasma membrane. In contrast, APOs (500-2000 nm) are released during programmed cell death and contain cellular debris, including fragmented DNA, organelles and portions of the dying cell. Exos are much smaller (40-120 nm) and are derived from the endolysosomal pathway formed inside multivesicular bodies (MVB). They are secreted into the extracellular environment when MVBs fuse with the plasma membrane. In contrast to MVs, which bud from the plasma membrane, exosomes are derived from endolysosomal pathway (Vizoso et al., 2017; Zhou et al., 2023) (Fig. 4). While all three types of vesicles are involved in cellular communication, their origins and biological roles are distinct. Cargo content is heterogeneous in EVs depending on different factors not only restricted to their origin but also to cell status. However, they can be distinguished based on specific proteins that serve as markers for characterisation. Exos can be analysed by immunolabeling of exosomal surface proteins such as tetraspanins (CD9, CD63 and CD81), integrins (ITG) or cell adhesion molecules (CAM). Other critical markers for exosomes include ALIX, flotillin and TSG101, that play a key role in exosome biogenesis, and heat shock proteins (Hsp70 and Hsp90). These markers are being used for characterise and isolate exosomes from cell cultures. Criteria to standardize protocols for isolation, characterisation and purification of general and specific EVs are being in consideration through guidelines from Minimal Information for Studies of Extracellular Vesicles (MISEV) (Witwer et al., 2021).

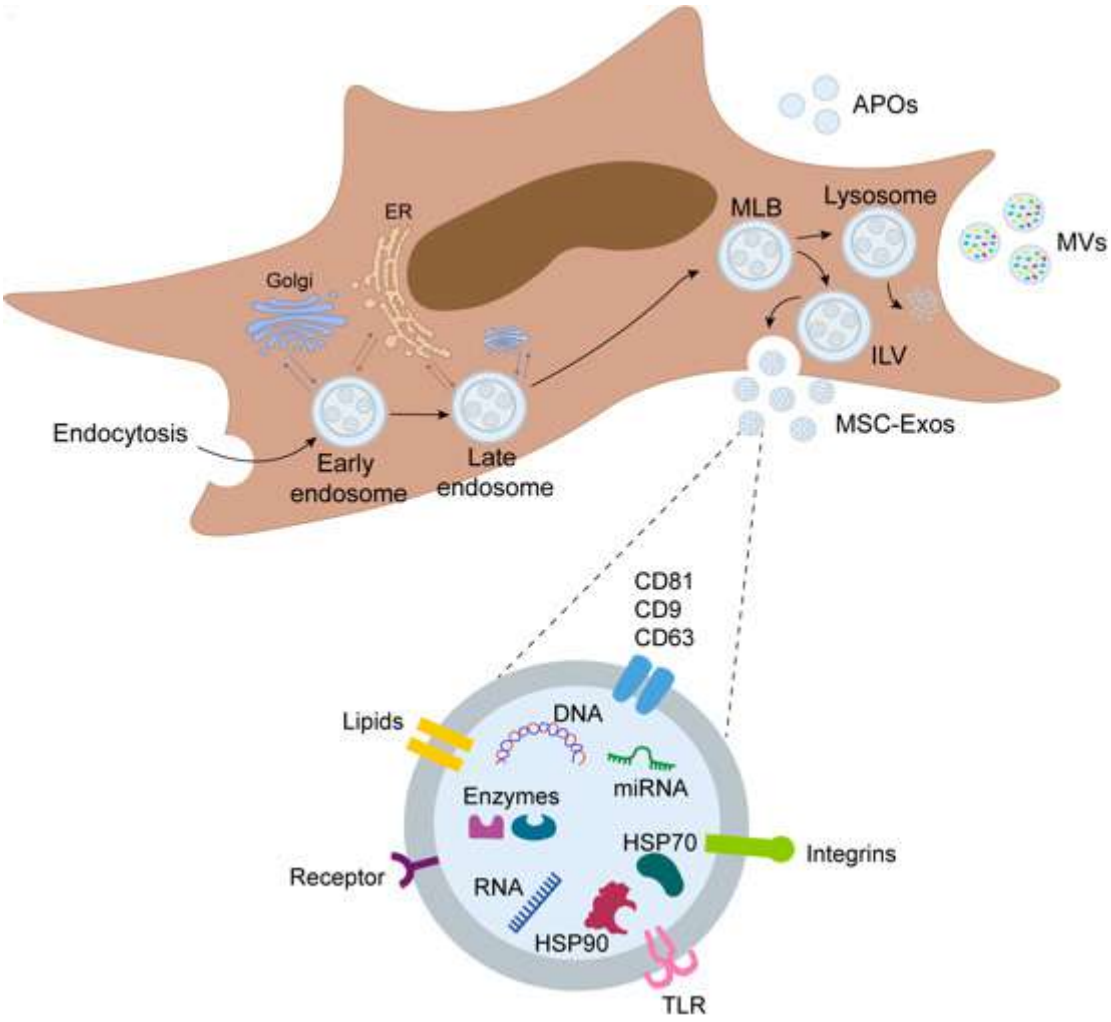

Figure 4. Development and composition of EVs derived MSCs.

Different types of EVs are depicted on the illustration: APOS, MVs and Exos. Exos are derived from endolysosomal pathway. The main components of Exos derived from MSCs are represented: several tetraspanins, lipids, DNA and heat shock proteins. ER: endoplasmic reticulum; MLB: multilamellar body; ILV: intraluminal vesicle; APOS: apoptotic bodies; MVs: microvesicles; MSC-Exos: exosomes derived from mesenchymal stem cells; TLR: toll-like receptor; HSP-; heat shock protein. Illustration based on Kou et al (2022) (Kou et al., 2022).

Mesenchymal stem cell-derived exosomes (MSC-Exos) have emerged as potent therapeutic agents due to their immunomodulatory and regenerative properties. These nanovesicles contain various bioactive molecules, including messenger RNAs (mRNAs), micro RNAs (miRNAs), cytokines and growth factors (Yu et al., 2014). MSC-Exos promote M2 macrophage polarization and induce regulatory T cells, contributing to their anti-inflammatory effects (Arabpour et al., 2021; Zhang et al., 2014). They stimulate the production of anti-inflammatory mediators like interleukin (IL) 10 (IL-10) and TGF-β while suppressing pro-inflammatory cytokines such as tumor necrosis factor-alpha (TNF-α), IL-1β and IL-6 (Zhang et al., 2014). MSC-Exos have shown therapeutic potential in various inflammatory and

autoimmune conditions, including central nervous system (CNS) diseases, inflammatory bowel disease, and graft-versus-host disease (GVHD) (Arabpour et al., 2021). Their mechanisms of action involve delivering immunoregulatory miRNAs and proteins to target cells, modulating immune responses, and promoting tissue repair by activating autophagy and inhibiting apoptosis in injured cells (Harrell et al., 2019). Human bone marrow-derived exosomes (hBMSCs-Exos) possess advantages compared to the administration of their cellular counterparts: determined dosage and potency, avoided invasive cell biopsy, higher chance of crossing the blood-brain barrier (BBB), lower or no risk of mutagenicity, oncogenicity and low immunogenicity. Also, they have more accessible transport with higher stability in storage conditions, which make them safer and more suitable than cellular therapy (Li et al., 2019; Yeo et al., 2013).

hMSCs also mediate immunomodulation via paracrine signalling secreting a variety of molecules known generally as the secretome. Among these secreted molecules, there are multifaceted cytokines, growth factors and chemokines that modulate the function of immune cells and include: transforming growth factor-beta 1 (TGF-β1), TNF-α, prostaglandin E2 (PGE2), interferon gamma (IFN-γ), hepatocyte growth factor (HGF), fibroblast growth factor (FGF), indoleamine-pyrrole 2,3-dyoxygenase (IDO) and nitric oxide, among many others (Salgado et al., 2010).

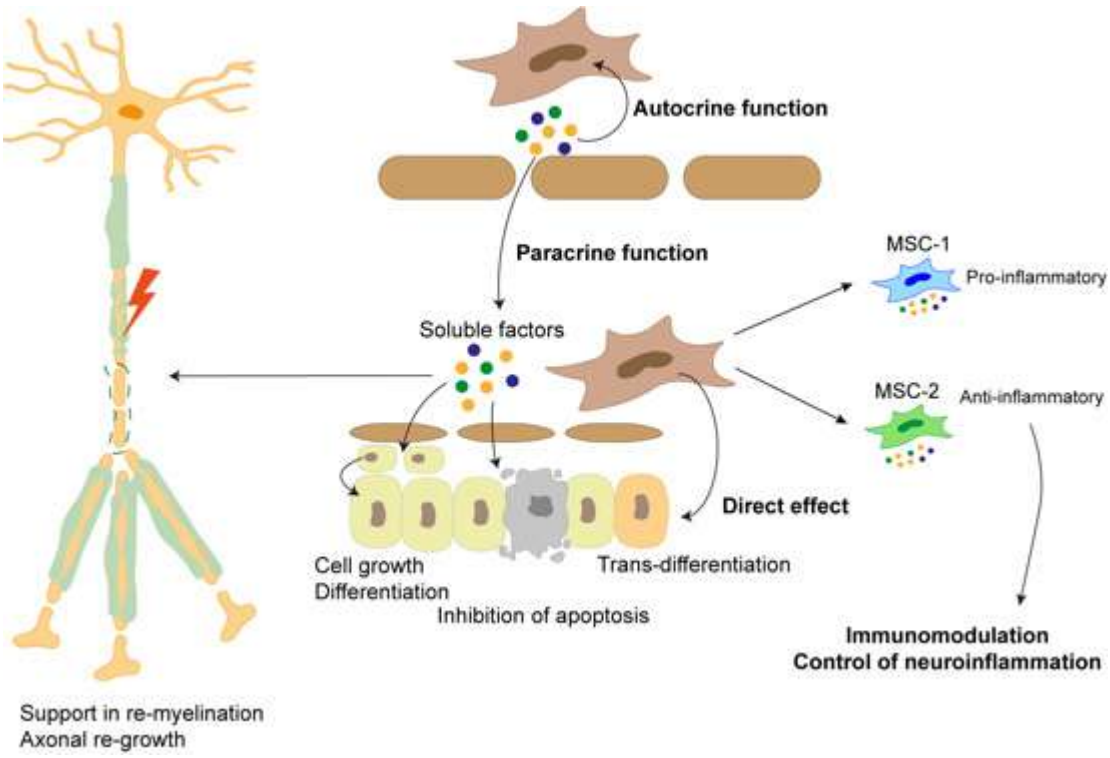

Figure 5. General therapeutic role of hMSCs.
The therapeutic function of hMSCs is exhibited due to their main functions. Through direct and indirect (paracrine) effect, hMSCs induce changes in host or co-cultured cells as inducing cell growth, differentiation and trans-differentiation, inhibiting cell apoptosis and modulating the expression of several immune cells in order to control neuroinflammation. Released soluble factors also show these beneficial effects with special attention to CNS diseases in which they support axonal re-growth and re-myelination.

On the adaptative immune system, hMSCs can act paracrinally especially with T cells. hMSCs inhibit T helper 17 cell (Th17) differentiation by inducing production of IL-2, PGE2 and inhibiting IL-17, IL-22 and IFN-γ (Ghannam et al., 2010). On the other hand, on the innate immune system, hMSCs interact with natural killers (NK) cells through secretion of cytokines that result in the improve of the defence against infections at the site of injury (Spaggiari et al., 2006). Also, hMSCs-derived IL-6 protect neutrophils from apoptosis (Raffaghello et al., 2008) as well as hMSCs derived-exosomes (Mahmoudi et al., 2019). Regarding its effect on monocytes, hMSCs-derived IL-6 prevent the differentiation of monocytes to an anti-inflammatory IL-10 producing phenotype (Melief et al., 2013) in contrast to hMSC-derived PGE-2 that induces the suppression of monocytes differentiation (Spaggiari et al., 2009). Derived EVs also have their impact on immune system since they play a critical role on macrophage polarization by promoting M2 macrophages downregulating IL-23 and IL-22 (Hyvärinen et al., 2018; Lo Sicco et al., 2017).

1.4 Dental stem cells.

1.4.1 Embryology and anatomy of teeth.

Teeth are calcified structures located in the oral cavity attached to upper and lower jaw. These structures are essential in basic human functions as eating, speech and are special important in proper facial aesthetics and interpersonal and psychosocial health and well-being (Zohrabian et al., 2015).

General anatomy of tooth divides this structure into two parts: the crown, the structure that is clearly visible in the oral cavity, and the root, part of tooth that is embedded into the bony ridge of the upper and lower jaw named as the alveolar process via attachment to the periodontal ligament (Zhang & Yelick, 2021; Zohrabian et al., 2015). Regarding different tissue found in teeth, these structures possess diverse hard and soft tissue types that are extremely organized. Among hard tissue, enamel is the hardest tissue in the body, embryological derived

from ectoderm cells, that protect the tooth crown. It is composed by a highly organized structure of carbonate-substituted hydroxyapatite mineral arranged in interlocking prisms. Dentin, in turn, is the most abundant tooth tissue and give shape and size to teeth. Its structure, characterised by minerals and organic components arranged in a complex organization of tubules filled with fluid, can flex and absorb force acting as a substructure to enamel. Cementum is located in the embedded part of the tooth and covers all surface of this root, placing the structure and attaching periodontal ligament to alveolar bone. Among soft tissue, dental pulp stands out for its neurosensory function and regenerative potential. Dental pulp is a highly vascularised and innervated tissue located at the core of the tooth. It is composed by an extracellular matrix enriched with blood vessels, nerves, odontoblasts and fibroblasts. Responding to external signals, providing nutrition and ameliorating neuronal sensitivity by repairing pulp through mineralisation are some of dental pulp's functions. Periodontal ligament is located between cementum and alveolar bone. It consists on a dense fibrous connective tissue that contains numerous cells, fibbers, rich vasculature and cellular components. This tissue participates in tooth anchorage, bone tissue development and homeostasis, nutrition-metabolic circulation and innervation (Abrahams et al., 1995; Zohrabian et al., 2015) (Fig. 6).

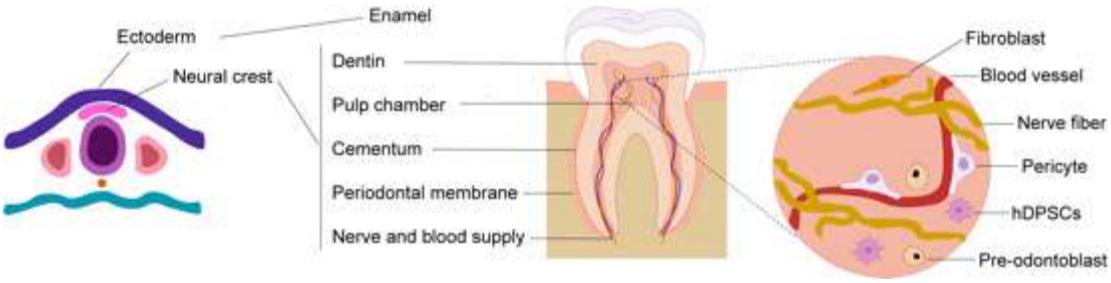

Figure 6. Human tooth development and anatomy.

Schematic outline for the tooth development: ectoderm cells contribute to the formation of tooth enamel, whereas, neural crest cells generate the rest of tooth tissues. The core of the tooth is composed of dental pulp, a highly vascularised tissue rich in different types of cells including dental pulp stem cells. hDPSCs: human dental pulp stem cells. Illustration based on Al Madhoun et al (2021) (Al Madhoun et al., 2021).

Odontogenesis, embryonic teeth development, is a complex interactive process involving cells of the first branchial arch (dental epithelium) and neural crest derived dental mesenchyme (Bilodeau & Hunter, 2021). This process begins at the sixth week of embryological development when the dental epithelium invaginates into the underlying mesenchyme to form the dental lamina. In the process, ten placodes (focal thickenings of oral epithelium) are formed both in mandibular and maxillary arches, the site of future teeth. As the dental epithelium develops, dental placodes are separated into the vestibule lamina (which gives rise to the

vestibular sulcus) and the dental lamina, whose development is associated to condensation in the associated mesenchyme. The proliferation within dental lamina continues giving rise to the formation of enamel organ which proceeds morphologically via the bud, cap and bell stages prior to initiation of dental hard tissue formation (Bilodeau & Hunter, 2021; Yu & Klein, 2020; Zohrabian et al., 2015). In parallel, the associated mesenchyme, originated from the neural crest, separates into two subsites: the dental papilla and the dental follicle. Dental papilla is enclosed by the developing cap/bell stage of enamel organ formation whereas dental follicle surrounds the entire enamel organ (Rothova et al., 2011). Dental hard tissue development is an inductive process that starts with the formation of the enamel knot in the inner enamel epithelium. This serves as a signalling centre in tooth development, leading to differentiation of dental papilla cells into odontoblasts adjacent to inner enamel epithelium. The resulted consequence of these differentiation processes is the final maturation of the inner enamel epithelium into secretory ameloblasts and the initiation of the enamel formation. The crown formation proceeds as the enamel organ's leading edge creates the cervical loop. This cervical loop will eventually progress into forming the tooth root, specifically as Hertwig's epithelial root sheath. This structure is essential for the development of root dentin, cementum, and the periodontal ligament (Guo et al., 2018; Wang & Feng, 2017). Odontogenesis, and more specifically the function of dental lamina and dental mesenchyme, is strictly regulated spatially and temporally by the activation of signalling pathways including Wnt, Shh (sonic hedgehog), and FGF, coordinated by a number of transcription factors (Thesleff, 1995; Yu & Klein, 2020). Moreover, a remarkable number of stem cells markers, such as Sex determining region Y-box 2 (SOX-2), are crucial in the function of dental lamina (Juuri et al., 2013). Due to the human dentition is heterodont, meaning that there are four different tooth types, different teeth erupt at different times, but they share the same pattern of odontogenesis (Zohrabian et al., 2015).

1.4.2 Dental ectomesenchymal stem cells.

The neural crest is a transient multipotent population of cells present during early stages of vertebrate embryogenesis. Neural crest originates at the lateral border of the neural plate and migrates throughout the embryo giving rise to a wide variety of differentiated cell types (Noden, 1983; Romer, 1972; Szabó & Mayor, 2018). After migration, differentiation of neural crest cells occurs in a region-specific manner. Cephalic neural crest cells give rise to specific components of the skull and facial structures, including sensorial and parasympathetic neurons of cranial nerve ganglia, vagal neural crest cells play a role in forming the aortic outflow track of the hearth and enteric nervous system and trunk neural crest cells contribute towards the most posterior region of enteric nervous system, dorsal root ganglia and the adrenal gland

(Szabó & Mayor, 2018). These migratory cells differentiate into multiple cells including MSCs, vascular smooth muscle cells (VMC), adipocytes, osteocytes, chondrocytes, melanocytes, neurons, glia and Schwann cells (Dupin & Sommer, 2012).

The ectomesenchyme is the specific tissue, derived from the neural crest, that contributes to the generation of craniofacial structures as oral muscles, bones tongue, craniofacial ganglia and nerves, teeth and dental ectomesenchymal stem cells or dental stem cells, which share a common origin with neural crest cells (Janebodin et al., 2011). Different types of dental stem cells are found in both adult and developing teeth (Fig. 7):

1.4.2.1 Dental stem cells from developing teeth.

- Stem cells from apical papilla (SCAP).

The apical papilla tissue is only present during tooth development before or during the tooth erupts into the oral cavity (Huang et al., 2008). Stem cells residing in this particular tissue have shown higher proliferative capacity and greater mineralisation potential *in vitro* compared to other adult dental stem cells (Bakopoulou et al., 2011; Sonoyama et al., 2006), which emphasises their therapeutic potential in bone and dental tissue regeneration.

- Stem cells from dental follicle (SCDF).

The dental follicle is an ectomesenchymal tissue that surrounds the developing tooth germ (Morsczeck et al., 2005). SCDF are direct precursors of periodontal tissues and can form periodontal ligament, cementum and alveolar bone. They are also characterised by their multidifferentiation capacity being able to differentiate into osteocytes, adipocytes, chondrocytes, neural cells and cardiomyocytes under proper induction environment (Yao et al., 2008).

1.4.2.2 Dental stem cells from adult teeth.

- Periodontal ligament stem cells (PDLSCs).

PDLSCs are specific dental stem cells population which were firstly discovered by Seo and colleagues (Seo et al., 2004). PDLSCs have shown expression of MSC markers (Lindroos et al., 2008) and neural crest progenitors (NCP) (Bueno et al., 2013) as well as multilineage

differentiation ability (Xu et al., 2009) and basal pluripotency markers (Trubiani et al., 2010), which makes them a suitable cell source in regenerative medicine.

- Stem cells from exfoliated deciduous teeth (SHED).

SHED are a population of dental stem cells are also found in dental pulp from primary exfoliated human teeth. These cells are notable for their greatly proliferation potential (Miura et al., 2003) and their basal expression of pluripotency markers (Kerkis et al., 2006). They have also been investigated because of their high neurogenic potential being able to differentiate into neuron-like cells and integrate in recipient brain tissues (Miura et al., 2003).

- Dental pulp stem cells (DPSCs).

In 2000, Gronthos et al (2000) first reported the existence of mesenchymal cell-like population within the pulp tissue of third molar impacted teeth (Gronthos et al., 2000). DPSCs are cell population that reside at the perivascular and periodontoblastic compartments within the adult tooth pulp (Shi & Gronthos, 2003). Biological function of this cells is to differentiate into odontoblast-forming dentin, playing a key role in dentinogenesis (Gronthos et al., 2000). DPSCs are the most widely used and understood type of dental stem cells (Campanella, 2018; Jain & Bansal, 2015; Mayo et al., 2014; Sharpe, 2016). As other dental stem cells, DPSCs are able to differentiate into multiples lineages including osteogenic (Liu et al., 2009; Rodriguez-Lozano et al., 2012), neurogenic (Arthur et al., 2008), adipogenic (Iohara et al., 2006) and chondrogenic (Iohara et al., 2006). In comparison to other populations of mesenchymal stem cells, such those derived from bone marrow, DPSCs show higher proliferation rates (Ponnaiyan & Jegadeesan, 2014) and a more potent immunomodulation effect suppressing T-cell reactivity (Özdemir et al., 2016; Pierdomenico et al., 2005).

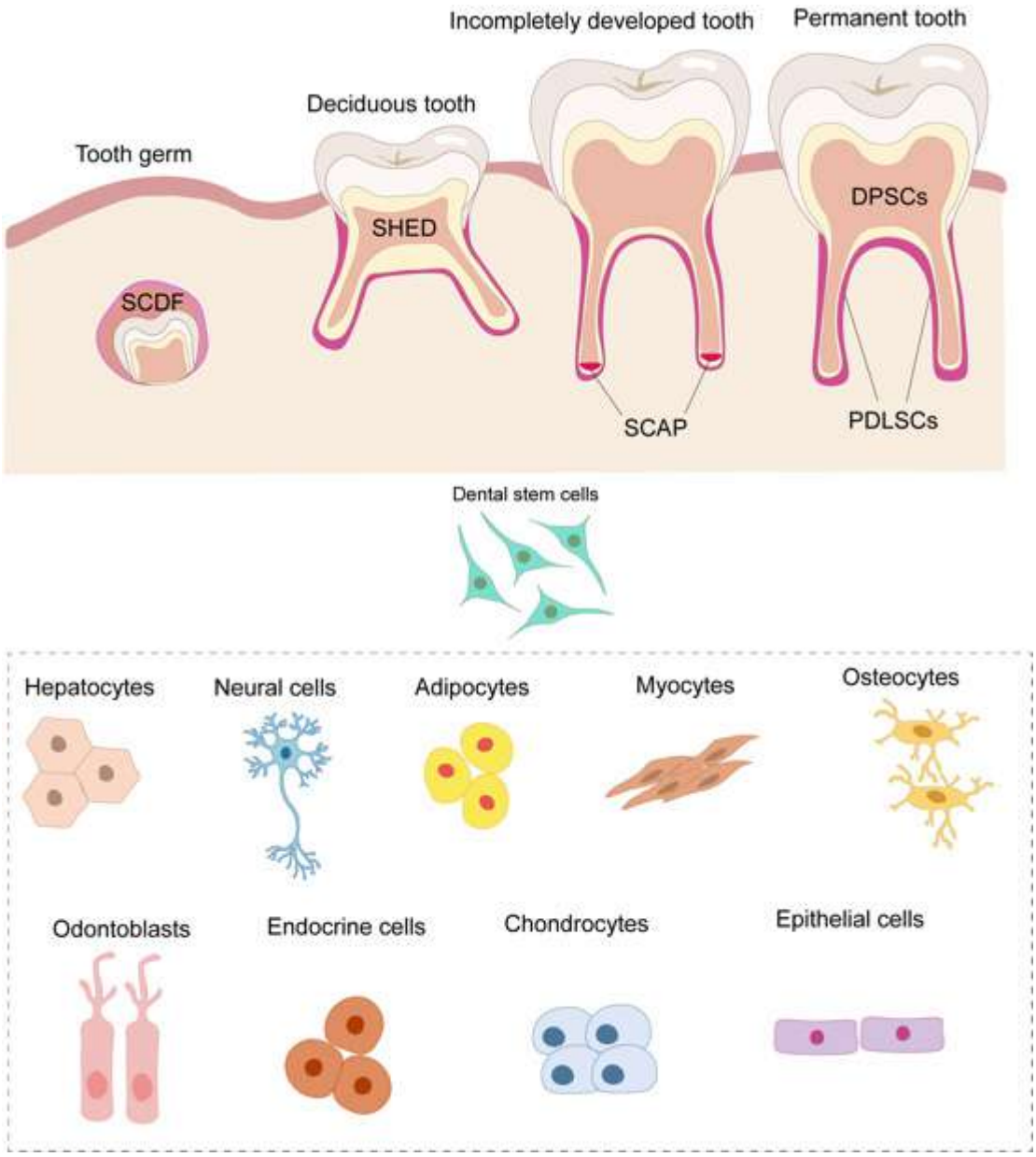

Figure 7. Sources of oral tissue and dental stem cells.

Different types of dental stem cells can be observed at different points of tooth development. Before tooth eruption, the developing tooth is surrounded by dental follicle, where SCDF can be found. In the deciduous tooth, SHED are located at the core of the tooth. Before or during tooth abruption, papilla tissue takes place with SCAP. Finally, the fully developed tooth is composed of two different types of dental stem cells: dental pulp and periodontal ligament stem cells. Dental stem cells, independently of their tissue source, have the ability of multi-differentiation into cells of different lineages. SCDF: stem cells from dental follicle; SHED: exfoliated deciduous stem cells; SCAP: stem cells from apical papilla; DPSCs: dental pulp stem cells; PDLSCs: periodontal ligament stem cells. Illustration based on Al Madhoun et al (2021) (Al Madhoun et al., 2021).

1.4.3 Neural differentiation of human dental stem cells.

Differentiation of adult stem cells into neurons or neural cell types allows a better knowledge about physiological and pathological processes in neurological environment. In order to both decipher mechanisms or to find therapeutic approaches to human neurodegenerative diseases, differentiation of adult stem cells into neurons might help since isolation of human neural cell types is strictly invasive.

In the case of human dental stem cells, they have shown a substantial capacity for neural differentiation. This important characteristic can be attributed to two main facts: their developmental origin from ectomesenchyme layer and their basal expression of pluripotency markers such octamer binding transcription factor 3/4 (OCT3/4), Nanog and TRA1-60, which enhance their neural differentiation natural ability (Kerkis et al., 2006; Takeyasu et al., 2006). All types of human dental stem cells are able to differentiate into neurons and neural cell types. Examples of this are studies that reported that human DPSCs (hDPSCs) have shown significant potential to generate dopaminergic and spinal motor neurons (Chang et al., 2014; Kanafi et al., 2014; Király et al., 2011; Osathanon et al., 2014; Urraca et al., 2015; Xiao & Tsutsui, 2013). Moreover, SHED have demonstrated similar differentiation capabilities into dopaminergic neuron-like cells (Nourbakhsh et al., 2011; Wang et al., 2010), Schwann cells (Yamamoto et al., 2016) and regenerate peripheral nerves (Sugimura-Wakayama et al., 2015). SCAP cells, in turn, also exhibit differentiation potential towards neuron-like cells (Bakopoulou et al., 2011). Interestingly, undifferentiated dental stem cells inherently express neural crest progenitor markers even without neural induction. This expression profile includes markers such as Nestin, SOX-2, tubulin-β III (TUJ-1), glial fibrillary acidic protein (GFAP), paired box 6 (PAX-6), gastrulation brain homeobox (GBX), microtubule-associated protein 2ab (MAP2ab), c-FOS, neurofilaments (NEF-H,NEF-L and NF-100), enolase-2 (ENO-2), Cx, microtubule-associated protein 2 (MAP2) and tenascin C, among others (Foudah et al., 2014; Martens et al., 2012, Bueno et al., 2013).

Despite their demonstrated neurogenic differentiation potential, there is not a standard neuronal differentiation protocol for human dental stem cells, which translates into high variability in endpoint differentiation results. Several factors such as the type of existing (or not) substrate, the induction media and the combination of various supplements including or not growth factors and small molecules, make it difficult to define the best and ideal protocol for neural induction in human dental stem cells.

2. Background of X-linked adrenoleukodystrophy.

2.1 Historical context of X-linked adrenoleukodystrophy.

The first clinical description of a patient with X-linked adrenoleukodystrophy (X-ALD) was reported by Haberfeld and Spieler in 1910. They described a 6-year-old boy with hyperpigmentation, impaired ocular acuity and academic failure. In the following months, the boy's condition worsened to become incapacitating and died at the age of 7. His older brother died at the age of 8.5 with a similar symptomatology. *Post-mortem* analysis revealed an inflammatory response with perivascular accumulation of lymphocytes and plasma cells in the nervous system and affected brain white matter (Haberfeld & Spieler, 1910). A few years later, in 1923, Siemerling and Creutzfeldt (1923) described a case with a similar disease progression but, also, with involvement of the adrenal cortex (Siemerling & Creutzfeldt, 1923). The disease, firstly called Schilder's disease, was renamed as "adrenoleukodystrophy" by Michael Blaw in 1970 (Blaw, 1970).

After decades since the first case reported, in 1976, X-ALD research completed a significant step forward when Igarashi et al (1976) found unusual high proportion of saturated very long chain-fatty acids (VLCFA, C22-C26:0) in cholesterol, phospholipids and gangliosides esters in brain and adrenal gland samples from X-ALD patients (Igarashi et al., 1976; Powers & Schaumburg, 1974). Subsequently, increased amounts of VLCFA were found in other complex lipids in all tissues from different X-ALD samples indicating that VLCFA, specially hexacosanoic acid (C26:0), could serve as a diagnostic marker (Moser et al., 1981). The initial association between the pathology and fatty acids classified X-ALD into the group of lipid storage disorders. However, it was accurately reclassified as a peroxisomal disorder when Singh et al (1981) discovered that VLCFA were not being degraded in X-ALD patients, a process that occurs within peroxisomes (Singh et al., 1981). In 1981, X-ALD gene was mapped to the terminal segment of the long arm of X-chromosome (Xq28), which confirmed X-linked inheritance (Fanconi et al., 1963). Several years later, in 1993, Moser et al. identified X-ALD gene through positional cloning (Mosser et al., 1993), which codes for a peroxisomal membrane ABC transporter called adrenoleukodystrophy protein (ALDP) (Mosser et al., 1994).

2.2 Gene, mutations and modifiers genes.

X-ALD patients possess a mutation in ABCD1 gene, located in X chromosome (Xq28) (Mosser et al., 1994). ABCD1 gene covers 19.9 kb and is composed of 10 exons that codes for

a 745 amino-acid protein (Sarde et al., 1994), an ATP-binding cassette transmembrane half transporter essential for the integration of VLCFA into peroxisomes for their subsequent degradation (Kemp et al., 2011; Mosser et al., 1994).

Since 1999, the ABCD1 variant database has catalogued the majority of (likely) pathogenic and (likely) benign variants in the ABCD1 gene (Kemp et al., 2001). Currently, more than 1220 unique variants in ABCD1 gene have been described in this database (see: x-ald.nl). The majority of reported ABCD1 variants (pathogenic, benign and unknown) arise from missense mutations (64.7%). Pathogenic variants are most frequently found in the transmembrane domain (exons 1 and 2, 40%) followed by the ATP-binding domain (exons 6-9, 30%) and exon 5 (14%) (Mallack et al., 2022). While most patients inherit the defective ABCD1 allele from one parent, between 4.1% and 19% of X-ALD cases have been reported to carry *de novo* mutations (Horn et al., 2013; Wang et al., 2011).

The phenotypic expression of the condition is unpredictable and all clinical manifestations can be presented in the same family (Berger et al., 1994; Gosalakkal & Balky, 2010). In 1996, a case-report described the existence of two monozygotic twins with the same genome and ABCD1 mutation, but different clinical manifestation. While one of them was asymptomatic with normal imaging resonance, the other showed evident brain demyelination that give rise to impairments in his gait and visual functions (Korenke et al., 1996). These evidences suggest that there is no correlation between genotype-phenotype and environment triggers and/or genetic factors may modulate the clinical outcome. One possible explanation to this fact is the “three-hit hypothesis” described by Singh and Pujol (2010). Based on this hypothesis, the metabolic derangements caused by excess of VLCFA, lower plasmalogens levels and induces oxidative stress (first hit) cause inflammatory disease with involvement of environmental, stochastic, genetic or epigenetic factors (second hit). Consequently, inflammatory response causes a generalized loss of peroxisome or peroxisome function (third hit), resulting in cell loss and progressive inflammatory demyelinating disease (Singh & Pujol, 2010) (Fig. 8).

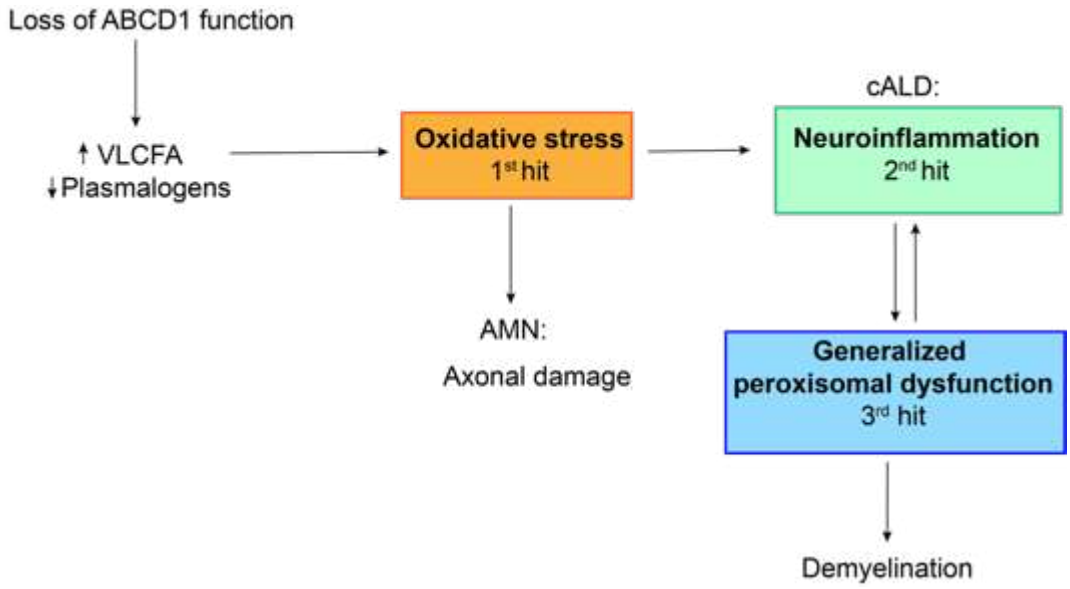

Figure 8. Representative scheme of the three-hit hypothesis.

Alterations in ABCD1 gene give rise to an altered ALDP protein with loss of function. This loss of function give rise to an increase of VLCFA levels and a decrease of plasmalogens levels that contribute to an oxidative stress status (first hit). Depending on X-ALD phenotype, this oxidative stress environment induces axonal damage (in adrenomyeloneuropathy patients) or neuroinflammation (in childhood cerebral X-ALD patients) by not fully understood mechanisms (second hit). The interplay between neuroinflammation and generalized peroxisomal disfunction (third hit) contribute to a final inflammatory demyelination, the main hallmark of childhood cerebral X-ALD patients. cALD: cerebral ALD. From (Singh & Pujol., 2010).

2.3 ABC transporters.

The protein responsible of X-ALD is belonged to ATP-binding cassette (ABC) transporters superfamily (Mosser et al., 1993). Structure of functional ABC transporters is composed of two analogous units, each with six transmembrane α-helices (TMD) and one hydrophilic nucleotide-binding domain (NBD) (Dean & Annilo, 2005) (Fig. 9). ABC transporters include membrane proteins responsible for transporting a wide range of substrates across cellular membranes, both intra- and extracellularly (Liu, 2019).

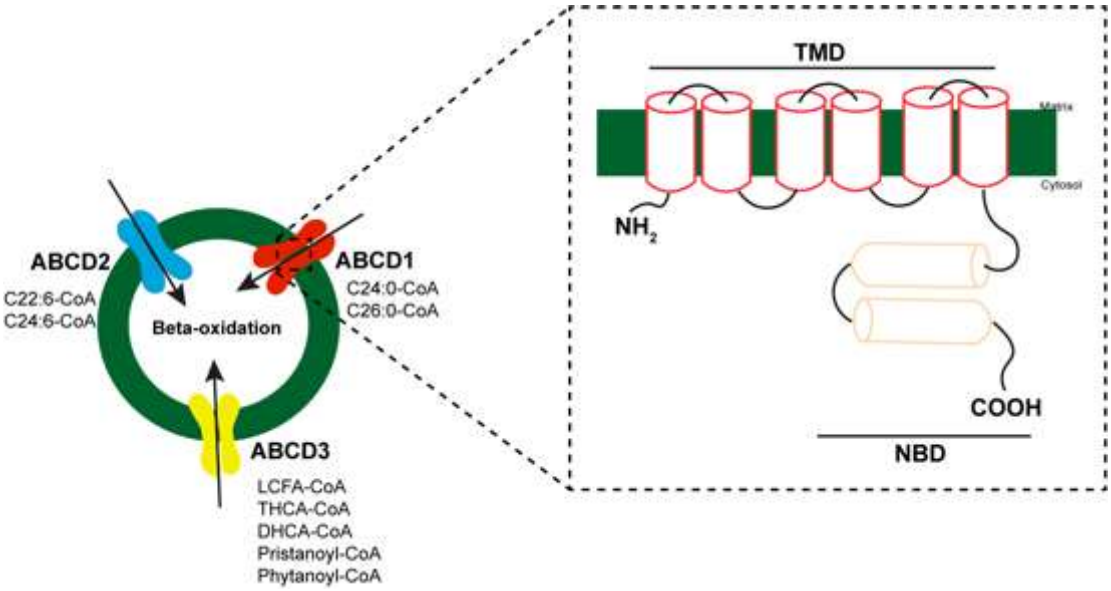

Figure 9. Human ABCD transporters in peroxisomes: substrates and molecular structure. Schematic representation of ABCD transporters found in human peroxisomes and their substrates. Molecular structure of ALDP protein containing a transmembrane domain (amino acids 75-352) and a nucleotide-binding domain, also named the ATP-binding region (amino acids 474-700). TMD: transmembrane domain; NBD: nucleotide-binding domain. Illustration based on Yan et al (2017) (Yan et al., 2017).

More specifically, protein related to X-ALD belongs to a specific subfamily called ABCD subfamily. ABCD transporters comprise four human genes: ABCD1, ABCD2, ABCD3 and ABCD4. Three of them encode proteins that are located in peroxisome (ABCD1, ABCD2 and ABCD3) whereas ABCD4 is found in lysosomes (Kashiwayama et al., 2009). Both ABCD1 and ABCD2 are involved in the transport of VLCFA and long-chain fatty acids (LCFA) (Van Roermund et al., 2008; Van Roermund et al., 2011) whereas ABCD3 transports branched-chain acyl-CoA into peroxisomes (Van Roermund et al., 2014) (Fig. 9). In contrast, ABCD4 is responsible of cobalamin transport (Coelho et al., 2012). These proteins are half-transporters as they function as homo- or hetero-dimers (Dean et al., 2022). There is evidence of both homodimerization and heterodimerization of ABCD1 with ABCD2 and ABCD3 *in vitro* (Geillon et al., 2014; Genin et al., 2011; Liu et al., 1999) although *in vivo* studies suggest that ABCD1 and ABCD3 act as homodimers (Guimarães et al., 2004). Larger structures such as tetramers formed by ABCD1 and ABCD2 have also been described (Geillon et al., 2017).

2.4 Biochemistry of X-ALD.

VLCFA levels analysis in plasma is the initial and main biomarker of X-ALD. As mentioned above, in X-ALD, VLCFA content is increased, principally, tetracosanoic acid (C24:0) and hexacosanoic acid (C26:0), in cholesterol esters and complex lipids such as gangliosides, phosphatidylcholine, sphingomyelin, cerebrosides and sulfatides (Igarashi et al., 1976; Moser et al., 1981).

VLCFA are partly absorbed by diet (Kishimoto et al., 1980), but majority of them are formed by elongation of long chain-fatty acids (LCFA) as Tsuji et al (1981) demonstrated using X-ALD fibroblasts and radiolabelling octadecanoic acid (C18:0) (Tsuji et al., 1981). Nowadays, it is known that restriction of VLCFA from diet do not reduce plasma levels of VLCFA in X-ALD patients (Brown et al., 1982) and, moreover, the elongation machinery of LCFA is elevated in these patients (Kemp et al., 2005). Endogenous synthesis of saturated VLCFA, monounsaturated VLCFA and polyunsaturated fatty acids (PUFA) occurs at the cytoplasmatic side of the endoplasmatic membrane. Four sequential reaction steps are involved in this elongation: condensation, reduction, dehydration and reduction (Kemp & Wanders, 2010). The enzyme that catalyses the first reaction is named as “elongation of very long-chain fatty acids” (ELOVLs) and plays an essential role in the rate of fatty acid elongation (Cook, 1996). There are seven human described ELOVLs (ELOVL 1-7) with characteristic substrate specificity (Jakobsson et al., 2006). Among all human ELOVLs, ELOVL-1 seems to be the main elongase that produce C26:0 in humans. Specifically, in X-ALD context, knocking down ELOVL-1 in X-ALD fibroblasts resulted in a decrease in C26:0 levels highlighting the importance of this enzyme in docosanoic acid (C22:0) to C26:0 elongation (Ofman et al., 2010). Moreover, two pharmacological compounds that inhibit ELOVL1 resulted in a decrease of C26:0 in X-ALD fibroblasts, lymphocytes and microglia. In animal models, inhibitors of ELOVL1 (compound 22 and 27), decreased C26:0 levels in blood and brain as well as C26:0 lysophosphatidyl choline (LPC), suggesting a promising therapeutic approach for X-ALD (Boyd et al., 2021; Come et al., 2021).

In X-ALD, peroxisomal β-oxidation is impaired due to mutations in ABCD1 gene. The fatty acid β-oxidation pathway is located in peroxisomes in all cell types and organisms ranging from yeast and plant cells to mammalian cells. In yeast and plants, this reaction occurs exclusively in peroxisome, whereas in eukaryotes, is found in both peroxisome and mitochondria. In mammals, peroxisomal β-oxidation is crucial for chain shortening of VLCFAs that cannot be degraded in mitochondria, main responsible of degradation of LCFA (Waterham

et al., 2016). β-oxidation in both organelles share catalytic mechanism of chain shortening fatty acids substrates by two carbons through a sequential reaction step: dehydrogenation, hydration, dehydrogenation and thiolytic cleavage. However, they differ in the way $FADH_2$ is reoxidized in the first step of dehydrogenation. While in peroxisomes, $FADH_2$ reacts with O_2 to generate H_2O_2 that is catalysed in H_2O and O_2 by peroxisomal catalase, in mitochondria, the reoxidation is coupled to the electron transport chain to produce adenosine triphosphate (ATP) (Van Veldhoven, 2010; Wanders & Brites, 2010) (Fig. 10).

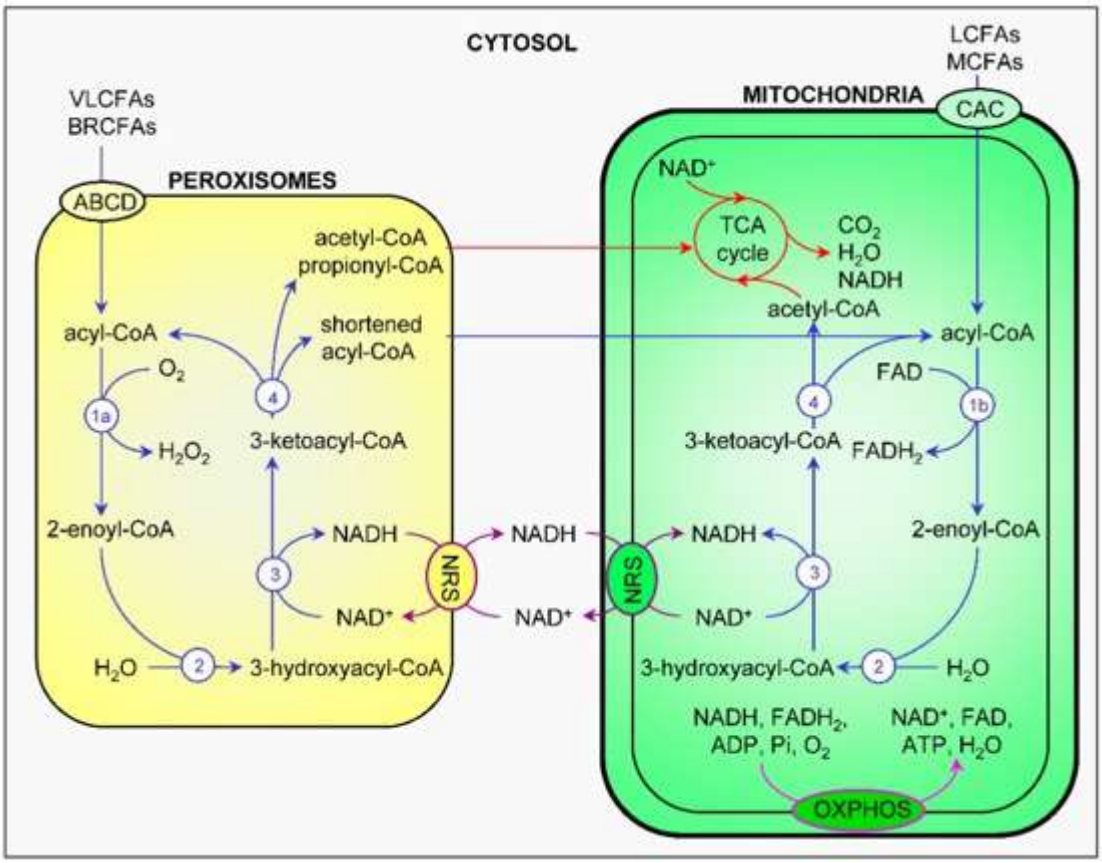

Figure 10. Human peroxisomal and mitochondrial fatty acid β-oxidation.

The process of fatty acid β-oxidation is the result of different reactions both in peroxisomes and mitochondria and their interplay. Fatty β-oxidation, NAD(H) redox shuttles, tricarboxylic acid cycle, and the electron transfer chain are represented in blue, purple, red and pink, respectively. The enzymes responsible of different depicted reactions are: 1a: acyl-CoA oxidase; 1b: acyl-CoA dehydrogenase; 2: enoyl-CoA hydratase; 3: 3-hydroxyacyl-CoA dehydrogenase; 4: 3-ketoacyl-CoA thiolase. ABCD: ATP-binding cassette transporters of subfamily D; ADP: adenine dinucleotide phosphate; BRCFA: branched-chain fatty acid; CAC: carnitineacylcarnitine carrier; FAD: flavin adenine dinucleotide; $FADH_2$: reduced FAD; LCFA: long-chain fatty acid; MCFA: medium-chain fatty acid; NAD: nicotinamide adenine dinucleotide; NADH; reduced NAD; NRS: NAD(H) redox shuttles; OXPHOS: oxidative

phosphorylation; TCA: tricarboxylic acid; VLCFA: very long-chain fatty acid. From Fransen et al (2017).

2.5 Clinical manifestations.

X-ALD is the most common peroxisomal and leukodystrophy disease with an estimate birth prevalence of 1 in 17000 subjects, including heterozygous women. Due to an aberrant accumulation of VLCFA, especially C24:0 and C26:0, X-ALD affects CNS white matter and the adrenal cortex (Moser et al., 2007; van der Knaap & Bugiani, 2018). X-ALD patients, although asymptomatic at birth, show a wide clinical spectrum ranging from adrenal insufficiency (Addison disease) to a progressive inflammatory demyelination (cerebral ALD, cALD). The two main phenotypes in male patients are:

- Adrenomyeloneuropathy.

Adrenomyeloneuropathy (AMN) is the most frequent phenotype and it is present in all affected patients that reach adulthood. It is characterised by peripheral neuropathy and distal axonopathy involving corticospinal tracts of the spinal cord without any involvement of neuroinflammation or brain demyelination (Powers et al., 2000). This phenotype is usually slowly progressive causing severe motor disability of the lower limbs over one or two decades while mild or none disturbances in upper body. Other disturbances are progressive spastic paraparesis, sensory ataxia with impaired vibration sense, sphincter dysfunction, impotence and scanty scalp hair at early ages (Harris-Jones & Nixon, 1955; Moser et al., 2007). Further, 70% of AMN patients present adrenocortical insufficiency (Moser et al., 1991). AMN may progress toward a cerebral phenotype with demyelination in different brain areas (De Beer et al., 2014). The exact prevalence of AMN patients developing demyelination remains unclear and depending on the study varies between of 20% to 63% of AMN patients (De Beer et al., 2014; Van Geel et al., 2001).

- Childhood cerebral ALD.

Childhood cerebral ALD (ccALD) is the most severe phenotype that appears during childhood between the ages of four and eight years with a peak at age of seven years. This phenotype is characterised by a rapid and severe progressive inflammatory demyelination. The first symptoms are related to cognitive dysfunction and behavioural problems often being misdiagnosed as attention deficit hyperactivity disorder (Kemp et al., 2016). Subsequently, specific neurologic alterations appear such as visual and auditory impairments, motor disability

and, occasionally, epileptic seizures. Symptoms progress rapidly and leads to total disability within six months to two years and death within five to ten years after diagnosis (Van Geel et al., 2001). White matter lesions on magnetic resonance images (RMI) precede clinical symptoms and, normally, are firstly originated in the splenium of corpus callosum and extend into the parietooccipital periventricular white matter (Melhem et al., 2000).

Other less frequent clinical manifestations of X-ALD have been reported:

- Asymptomatic or presymptomatic.

Asymptomatic X-ALD patients have been diagnosed after family screening. Those patients showed either genetic mutation or elevated VLCFA levels without any symptomatology, but they may develop cerebral demyelination or adrenocortical insufficiency (Kemp et al., 2001).

- Adolescent cerebral ALD.

Adolescent cerebral ALD (Adol-cALD) can be manifested between ages of ten to twenty-one. Adol-cALD patients show similar symptomatology as ccALD, but slower initial progression (Engelen et al., 2012c).

- Adult cerebral ALD (AcALD).

Inflammatory cerebral demyelination can be also be manifested at adulthood stages without any involvement of spinal cord. Diagnosis of these patients is normally delayed when no family X-ALD history is present and, as disease progresses, psychiatric symptoms can be manifested (Garside et al., 1999).

- X-ALD in women.

Despite its X-linked inheritance, several cases of X-ALD affected women have been reported suggesting that female are not just carriers of the disease. X-ALD women show an AMN-like phenotype, but with a delayed age of onset around the 4^{th} and 5^{th} decade (O'Neill et al., 1984). Cerebral involvement and adrenocortical insufficiency are clinical manifestations very rare in these patients (Engelen et al., 2012c).

- Addison-only.

Adrenal insufficiency is present in 80% of X-ALD patients and may be the initial symptom years before neurological involvement appears. However, there are reports of X-ALD patients with biochemical abnormalities related to adrenal insufficiency but any other clinical symptom (Dubey et al., 2005; Huffnagel et al., 2019).

2.6 Diagnosis.

Diagnosis of X-ALD is achieved by a combination of biochemical analysis and genetic tests. Detection of altered VLCFA levels in plasma is the main biochemical analysis to confirm X-ALD. Plasma VLCFA assay detects abnormal highly concentrations of C26:0-LPC and abnormal highly ratios C24:0/C22:0 and C26:0/C22:0. However, almost 15% of female carriers show normal levels of VLCFA (Moser et al., 1999; Valianpour et al., 2003) and cannot be diagnosed using this assay (Jaspers et al., 2020). Furthermore, genetic testing of ABCD1 gene is a more robust and specific assay for definitive X-ALD diagnosis (Wiesinger et al., 2015). Prenatal diagnosis of X-ALD can be conducted by VLCFA assay (A.Moser & H.Moser, 1999) or using polymerase chain reaction (PCR) sequencing via chorionic villous sampling and amniocentesis in subsequent pregnancies of women with affected children or family history of X-ALD. Preimplantation genetics have been used for both diagnose X-ALD and select healthy embryos (Lledó et al., 2007). In 2016, with the validation of a method for detecting C26:0-LPC in dried blood spots from new-born (Hubbard et al., 2009), X-ALD was included in the Recommended Uniform Screening Panel (RUSP) in the United States of America (USA) (Kemper et al., 2017). Nowadays, it is being applied in 43 states of the USA (See: "NewSTEPs Newborn screening status for all disorders" database). In Europe, Netherlands has recently approved the inclusion of X-ALD in the Dutch new-born screening program (Albersen et al., 2023) and it is expecting to be included in more countries in the upcoming years. New-born screening is essential to increase survivance of affected patients as it allows the identification of presymptomatically individuals.

Parieto-occipital white matter (maximum 4)	**Basal ganglia (maximum 1)**
Anterior temporal white matter (maximum 4)	
Frontal white matter (maximum 4) ▪ Periventricular ▪ Central ▪ Subcortical ▪ Local atrophy	**Visual pathway (maximum 4)** ▪ Optic radiation ▪ Meyer's loop ▪ Lateral geniculate body ▪ Optic tract
Corpus callosum (maximum 5) ▪ Splenium ▪ Genu ▪ Body ▪ Splenium atrophy ▪ Genu atrophy	**Auditory pathway (maximum 4)** ▪ Medial geniculate body ▪ Brachium of inferior colliculus ▪ Lateral lemniscus ▪ Pons
Global atrophy (maximum 4) ▪ Mild ▪ Moderate ▪ Severe ▪ Brainstem	**Cerebellum (maximum 2)** ▪ White matter ▪ Atrophy
	Projection fibbers (maximum 2) ▪ Internal capsule ▪ Brain stem

Table 1. MRI severity scale scoring.

Each region is given a score of 0 for normal, 0.5 for unilateral involvement and 1 for bilateral involvement or atrophy. The maximum score is 34. From Loes et al (1994) (Loes et al., 1994).

MRI is parallelly used along with genetic and biochemical assay to diagnose X-ALD cases. The X-ALD MRI Severity Scale is an imaging-based scoring system developed by Loes in 1994 that determines progression of cerebral disease based on the neuroanatomical involvement and the presence or absence of global atrophy. It is composed of 34 points and the resulting score helps in the prediction of disease course and in the selection of patients for several therapeutic approaches (Loes et al., 1994) (Table 1 and Fig. 11).

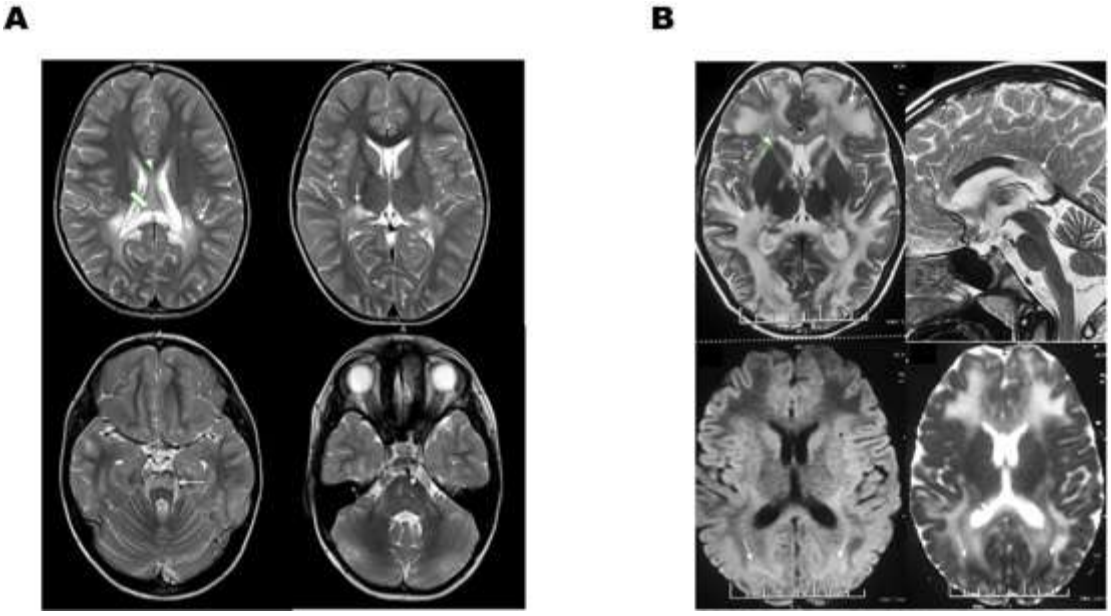

Figure 11. MRI of X-ALD cases.

MRI is used to decipher brain involvement in X-ALD patients even before clinical symptoms occur. A) Magnetic resonance images of a 9-year-old asymptomatic male with different areas with hyperintensity. Total Loes score: 9. B) Magnetic resonance images of symptomatic male with advanced disease. Total Loes score: 22. From Kumar et al (2021) (Kumar et al., 2021).

2.7 Therapeutic strategies.

Due to the wide spectrum of clinical manifestations of X-ALD, there is not an available therapy for all affected patients. Several therapeutic approaches have been addressed to reduce abnormal VLCFA levels and ameliorate neurological symptoms. Different therapeutic strategies are recapitulated in this chapter:

- Dietary's strategy: Lorenzo's oil.

Lorenzo's oil is a 4:1 mixture of oleic acid and erucic acid triglycerides that was designed to normalize the accumulation of VLCFA in brain. Mechanism of action of Lorenzo's oil was thought to be competitive inhibition preventing the synthesis of satured C26:0. Administration of this combined oil, along with dietary restriction of VLFCA, resulted in a reduction of VLCFA levels in the plasma of X-ALD patients suggesting a promising therapy (Moser et al., 1987). However, further studies with symptomatic and asymptomatic patients concluded that Lorenzo's oil does not reduce VLCFA levels in brain (Rasmussen et al., 1994). Moreover, it was demonstrated that this oil does not arrest disease progression neither in AMN nor in cALD (Aubourg et al., 1993; Rizzo, 1993; Van Geel et al., 1999).

- Metabolic modulators.

Modulation of crucial molecules or enzymes that are determinant in the synthesis of VLCFA or in the biochemical process of β-oxidation are other therapeutic approaches that have been studied.

Bezafibrate is an inhibitor of the enzyme ELOVL1, responsible of elongation of C24:0 to C26:0 as mentioned above (Ofman et al., 2010). Application of this inhibitor to X-ALD fibroblasts cultures resulted in a significant reduction of VLCFA levels (Engelen et al., 2012a), but it failed in clinical trials with AMN men and women (Engelen et al., 2012b).

The use of statins, such as lovastatin, was also studied in X-ALD context. Lovastatin reduces low-density lipoprotein (LDL) cholesterol and it was reported that normalized VLCFA levels in plasma of X-ALD patients (Singh et al., 1998). However, in subsequent studies, no normalization was reported (Engelen et al., 2010).

Upregulation of β-oxidation through the overexpression of determinant proteins such as ABCD2 or peroxisome proliferators is another strategy taken in account to reduce abnormal VLCFA in X-ALD. The use of histone deacetylase inhibitor (4-phenyl-butyrate, 4-PB), which promote the genetic transcription of ABCD2, brought promising results with a reduction of C24:0 levels in brain of Abcd1$^-$ knock-out mice (Kemp et al., 1998). However, there have not been any clinical trial of 4-PB. Other strategies are the use of thyroid hormone receptor agonist, which increase levels of ABCD2 mRNA (Hartley et al., 2017), or administration of pioglitazone, a peroxisome proliferator-activated receptor gamma (PPAR-γ) agonist, that restores mitochondria and halts axonal degeneration in Abcd1$^-$ mice (Morató et al., 2013).

- Anti-inflammatory strategies/immunomodulators.

The use of different anti-inflammatory molecules such as cyclophosphamide (Naidu et al., 1988; Stumpf et al., 1981), interferon-β (IFN-β) (Korenke et al., 1997), intravenous immunoglobulins (Miike et al., 1989), and monoclonal antibodies (NatalizumAb) (Berger et al., 2010) have been proven to halt neurological disease, but all of them failed.

- Antioxidant therapy.

Administration of antioxidants as a promising therapy for X-ALD is based on the importance of oxidative stress in the pathophysiology of the disease. Several groups proved antioxidant strategy and demonstrated that a combination of multiple high-dose antioxidants normalized halted axonal degeneration in Abcd1^{-} mice (López-Erauskin et al., 2011) and normalized inflammatory levels and oxidative stress markers (Casasnovas et al., 2019).

- Hematopoietic stem cell transplantation.

Allogeneic hematopoietic stem cell transplantation (HSCT) is the standard established therapy for the cerebral phenotype of X-ALD. Mechanism of action of this treatment is based on replacement of defective microglia by bone-marrow long-lived macrophages of allogeneic donor (Cartier et al., 2014; Moser & Mahmood, 2007; Schönberger et al., 2007). It is demonstrated that HSCT arrest neuroinflammation but, it is only effective when performed at early stages of the disease (Cartier & Aubourg, 2010). The X-ALD MRI Severity Scale developed by Loes in 1994 (Loes et al., 1994) determines progression of cerebral disease but, also, suitability to HSCT treatment. Only patients with a Loes score between 5 and 9 and without neurologic and neuropsychological deficits are adequate to this treatment with a presumable good prognostic (Loes et al., 2003). However, despite its successful therapeutic potential, risks and limitations associated to HSCT transplantation are reported. The main limitation of HSCT transplantation is the narrow therapeutic window which restricts treatment only to a few chosen patients. Moreover, severe GVHD along with immunodeficiency are risks associated to HSCT that must be taken in account when performed. Both monitoring X-ALD and diagnosis of early cases is essential to determine early onset of disease and treat appropriately to permanently arrest disease progression.

- Gene therapy.

Alternative to HSCT is gene therapy. Lentiviral gene therapy for X-ALD consists on administration of genetically modified positive CD34 cells (CD34^{+}) with the aim of introduce healthy ALDP to patient's cells. It was first administered to two 7-year-old boys that were candidates for HSCT, but no matched donors were available. Successful therapy was resulted with arrested progression of cerebral disease at 14 and 16 months (Cartier et al., 2009). Further studies including more patients showed similar results concluding that this type of therapy is, at least, as safe as allogeneic HSCT (Eichler et al., 2017). However, long-term studies might elucidate concerns about possible controversial adverse effects of this therapy.

2.8 Hallmarks of X-ALD.

- Oxidative stress.

Oxidative stress is a physiological condition characterised by an imbalance between the production of reactive oxygen/nitrogen species (ROS/RNS) and the ability of cells and tissues to detoxify or repair the resulting damage through antioxidants. Oxidative stress contributes to the development of various diseases such as cardiovascular diseases, neurodegenerative disorders and cancer.

ROS encompass a variety of molecules and free radicals (chemical species with one unpaired electron) that are physiologically generated from the metabolism of molecular oxygen (Halliwell, 2006). ROS include superoxide anion (O^{-}_{2}), hydrogen peroxide (H_2O_2), hydroxyl radical (HO·), peroxyl radical (RO·2), alkosyl radical (RO·), hydroperoxyl radical ($HO·_2$), hypochlorous acid (HOCl), hypobromous acid (HOBr) and singlet oxygen (O_2). They are highly reactive and can cause significant damage to cells and tissue (Halliwell, 2006). Therefore, animals have developed mechanisms to avoid or minimize the production of ROS from oxidative metabolism, as well as antioxidant defence systems to limit the pro-oxidant activity of these reactive species (Halliwell, 1999). In the antioxidant machinery, there are mainly three enzymes that are responsible of scavenging ROS: superoxide dismutase (SOD), glutathione peroxidase (Gpx) and catalase. SOD eliminates superoxide radical by converting it into oxygen and H_2O_2. Thus, Gpx and catalase eliminate H_2O_2 with differences in affinity and rates. Molecules such as vitamin C and E also take part of this complex antioxidant system. Concretely, vitamin C interacts with ROS to convert them in oxidized forms which can be reduced back again by NADPH-dependent (Rose & Bode, 1993) or GSH-dependent (Maellaro et al., 1994; Wells & Xu, 1994) dehydroascorbate reductases or by NADH-dependent plasma membrane ascorbate free radical reductase (Navas et al., 1994). In turn, antioxidant ability of vitamin E is due, in part, to their capability to inhibit propagation of lipid peroxidation in a chain reaction by reducing lipid peroxyl groups (Esterbauer et al., 1991).

In physiological conditions, components of antioxidant defence machinery counteract oxidative stress by neutralizing free radicals and repairing oxidative damage. However, when oxidative stress overwhelms these defence mechanisms, it can lead to chronic inflammation and tissue damage, highlighting the importance of maintaining a balance between oxidative stress and antioxidant defence for optimal health. Nevertheless, oxidative stress has been classically considered to be a common event in neurodegenerative diseases, characterised by apoptosis/necrosis and dysfunction of neuronal cells, leading to a notably damage. The brain

is more vulnerable to oxidative stress because of their high oxygen consumption rate, their enrichment in redox-active metals and their higher susceptibility to lipid peroxidation (McQuillen & Ferriero, 2004).

- Role of ROS and VLCFA in X-ALD.

In the case of X-ALD, oxidative stress is known to be a key feature in the pathogenesis of the disease (Singh & Pujol, 2010). First evidences of oxidative stress in X-ALD were given by studies that demonstrated higher oxidability of LDL in plasma of X-ALD patients (Di Biase et al., 2000) and the presence of inducible-nitric oxide synthase (iNOS) in X-ALD astrocytes and microglia from tissue (Gilg et al., 2000). Later studies confirmed evident oxidative stress in X-ALD, detecting it in plasma, erythrocytes and fibroblasts from X-ALD patients (Petrillo et al., 2013; Vargas et al., 2004), in adrenal cortex and brain tissue sections from ccALD phenotype (Powers et al., 2005) and in X-ALD derived lymphoblasts (Uto et al., 2008). Oxidative stress is notorious in X-ALD due to a decreased total antioxidant status, being evident in symptomatic but none in asymptomatic X-ALD cases (Deon et al., 2007). In the case of female carriers, oxidative stress is also present by an increase in lipid peroxidation and decreased antioxidant reactivity in plasma, whereas total antioxidant status is not altered (Deon et al., 2008).

Further, VLCFA accumulation is responsible of oxidative stress in X-ALD as several investigations demonstrated. The generation of ROS due to an excess of C26:0 is demonstrated in different cell types such as human X-ALD fibroblasts (Fourcade et al., 2008), immortalized neuronal and oligodendrocytes cells (Baarine et al., 2012; Zarrouk et al., 2012), and mitochondria and primary astrocytes from wild-type and Abcd1^{-} mice (Kruska et al., 2015). Concretely, in human X-ALD fibroblasts, the generation of ROS induced by C26:0 oxidized mitochondrial DNA (mtDNA) and impair the oxidative phosphorylation system (OXPHOS), triggering mitochondrial ROS production from electron transport chain complexes (López-Erauskin et al., 2013).

- Mitochondrial dysfunction.

Mitochondria are crucial regulators of energy metabolism and apoptotic pathways. Nowadays it is known that these essential organelles have been closely linked to the pathogenesis of several diseases including neurodegenerative disorders (Klemmensen et al., 2024).

- Mitochondria functions and components.

Mitochondria are intracellular organelles derived from α-proteobacterial endosymbionts (Gray, 2012). Their structure is characterised by a double membrane that separates mitochondrial matrix from cytoplasm. The external membrane, the mitochondrial outer membrane (MOM), is quite permeable whereas the internal, the mitochondrial inner membrane (MIM), is impermeable to most substances. Due to this particular structure, specific transport systems have been developed to allow movement of certain molecules in and out of the mitochondria. Mitochondria contain a genomic circular DNA, the mtDNA, that encodes 13 out of 1500 mitochondrial proteins, while others are encoded at nucleus. Thus, mitochondria form a dynamic network integrated with other cellular compartments.

The main function of mitochondria is the regulation of most of cell's function by the production of ATP through a process called OXPHOS. Given their essential role in energy metabolism, they are named as "the powerhouse of the cell" (Friedman & Nunnari, 2014). However, apart from their involvement in energy metabolism, they also participate in other important cellular functions such as the modulation of calcium signalling and homeostasis, the control levels of ROS and the stimulation of immune responses. Their highly dynamics and closely involvement in cell death pathways enable them an easily switch from the regulation of a normal cell status to the promotion of cellular stress.

The core of energy metabolism relies on mitochondrial respiratory chain, the basic structure for OXPHOS. During these processes, NAD^+ or FAD are reduced and form NADH and $FADH_2$. In the MIM, electrons are transferred from NADH/$FADH_2$ through the four complexes (complex I to IV) of the electron transport chain (ETC) and finally passed to O_2 to form H_2O. The oxidation of reducing agents (NADH/$FADH_2$) produces energy which allows the pump of protons from the matrix to the mitochondrial intermembrane space. Thus, an electrochemical gradient is generated across MIM and generated energy is used by ATP-synthase (or complex V) to generate ATP from adenosine diphosphate (ADP).

- Mitochondrial dysfunction in X-ALD.

Despite being originally classified as a peroxisomal disorder, there are evidences of mitochondrial dysfunction in X-ALD due to their oxidative stress status. Several investigations pointed out the cellular consequences of aberrant VLCFA accumulation at mitochondrial levels, suggesting that this organelle has an important role in the pathogenesis of the disease.

The precise mechanism by which VLCFA results in cell and tissue damage remains obscure, but there are several hypotheses about their relationship with alterations in mitochondria and/or mitochondrial processes. One of them is based on the disturbance of physiological membrane functions in mitochondria *in vitro* due to VLCFA storage in complex lipids such as LPC. This fact may lead to the formation of mitochondrial ROS and consequent tissue damage (Fourcade et al., 2008). There are other studies that reported that VLCFA decrease phospholipid bilayer stability in higher concentrations *in vitro* (Ho et al., 1995; Turk et al., 2020). In the case of myelin, dysfunction leads to a redistribution of Na^+/K^+ transporters along axons. This fact increases axonal ATP consumption, which also results in ROS formation due to a consequent hypoxia (Fourcade et al., 2008; Low & Ginhoux, 2018; Singh & Pujol, 2010; Turk et al., 2020). VLCFA-derived ROS are mainly originated in mitochondria and produce mitochondrial membrane depolarization along with the opening of mitochondrial permeability transition pore (mPTP) (Fourcade et al., 2008; López-Erauskin et al., 2013). Cytotoxicity of VLCFA was also studied in oligodendrocytes and astrocytes causing cell death within 24 hours (Hein et al., 2008). In addition to these hypotheses, transcriptomic functional analysis in X-ALD mice and human patients described a common abnormal metabolic pathway signature characterised by mitochondrial dysregulation, among others (Schlüter et al., 2012).

Overproduction of ROS is a common fact in neurodegenerative diseases (Kim et al., 2015) and it is not clear if it is a primary step in pathogenesis of X-ALD or if it is a consequence of another factors. Nevertheless, these studies demonstrated an interplay between oxidative stress and global mitochondrial dysfunction in the pathogenesis of X-ALD.

- Neuroinflammation.

The alteration of inflammatory response is one of the characteristics of neurodegenerative diseases. In a disease state, neuroinflammation and oxidative stress can stimulate one another since inflammatory cells can secrete reactive species that promote oxidative stress (Teleanu et al., 2022). These reactive species can further promote intracellular signalling cascades resulting in an increased expression of pro-inflammatory genes. In physiological conditions, inflammatory response is a mechanism of defence against diverse insults, but, when there is a redox imbalance, inflammatory response does not perform accordingly producing neuroinflammation in CNS. Thereby, neuroinflammation can be described as an inflammatory response in CNS to several factors that act against homeostasis (Ransohoff, 2016; Solleiro-Villavicencio & Rivas-Arancibia, 2018).

The main regulator of neuroinflammation is microglia. These cells are the resident macrophages in the brain that have numerous functions both in health and disease status (Cartier et al., 2014; Tremblay et al., 2011). Under physiological conditions, microglia exhibit a deactivated phenotype and exhibit beneficial roles in CNS homeostasis and in remodelling neuronal circuits. Nevertheless, imbalances in brain homeostasis due to stress, trauma, disease or pathology, induce changes in microglia phenotype converting them in activated microglia. This activation results in the promotion of several inflammatory and cytotoxic components to initiate the repair mechanism and, once the damage has been repaired, astrocytes turn to their deactivated form (Guo et al., 2022). However, if the damage persists, the amount of cytotoxic components leads to cell death (Wyss-Coray & Mucke, 2002).

- Role of VLCFA in neuroinflammation.

Inflammation in X-ALD is a critical factor as it is the main difference between cerebral phenotypes and AMN. The inflammatory brain lesion in cALD is characterised by impaired integrity of the blood-cerebrospinal fluid/blood-brain barrier (BCSFB/BBB) and recruitment of immune cells from the periphery (Powers et al., 1992). Increased levels of TNF-α and others pro-inflammatory mediators are found in demyelinating lesions of cALD (Gilg et al., 2000; Khan et al., 2010; Schlüter et al., 2012; Weinhofer et al., 2018). Alterations of VLCFA metabolism results in functional alteration of monocytes and macrophages (Weber et al., 2014). Moreover, there is a notable impairment of plasticity of X-ALD macrophages since they are less able to adopt an anti-inflammatory phenotype (Weber et al., 2014; Weinhofer et al., 2018).

Taking altogether, a possible explanation about inflammation in X-ALD could be an initial disruption of myelin sheets caused by VLCFA accumulation. This disruption causes myelin break down. Consequently, nearby astrocytes and macrophages are stimulated in response to the liberation of these myelin components and initiate TNF-cytokine cascade signalling resulting in demyelinating microenvironment. Several studies evaluated immune cells in X-ALD and demonstrated that monocytes, progenitors of macrophages, showed higher VLCFA accumulation suggesting more vulnerability to cALD (Weber et al., 2014). In addition to this fact, there is also evidence of alteration in oligodendrocyte maturation in the cerebral form of X-ALD (Schlüter et al., 2018) (Fig. 12).

Proteostasis impairment, endoplasmic reticulum stress or lipid imbalance are other hallmarks that have been analysed in the pathology of X-ALD. However, mechanisms involved in each specific factor are not fully covered and, consequently, there is a lack of knowledge of crucial aspects of pathogenesis of X-ALD and specifically of their different phenotypes.

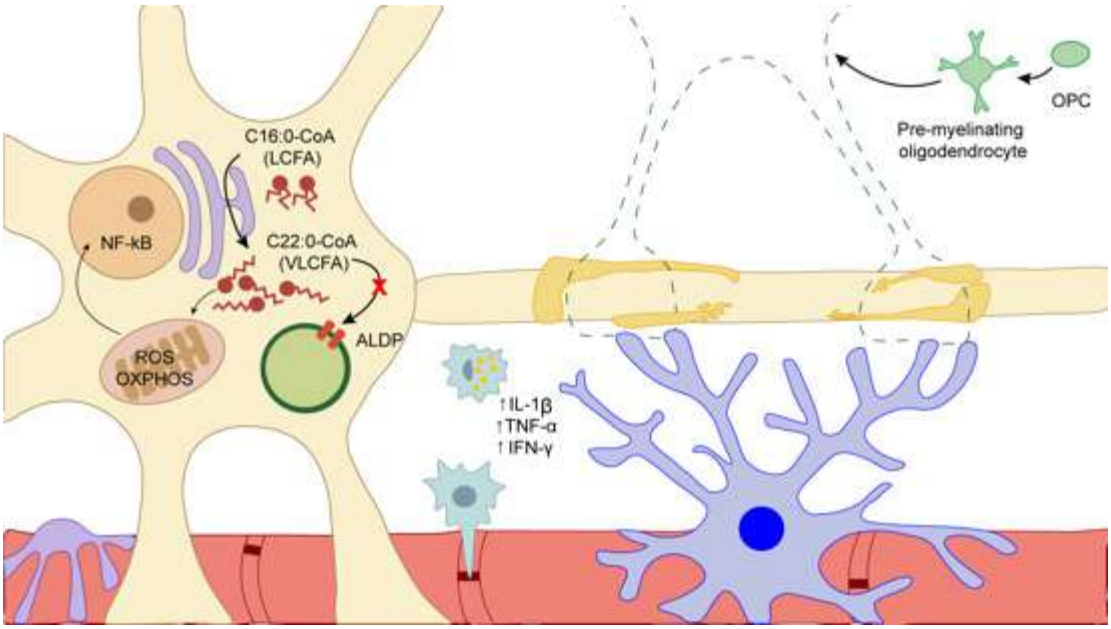

Figure 12. Mechanisms involved in inflammatory demyelination.

The absence or alteration of ALDP leads to an accumulation of VLCFA, originating from the elongation of LCFA through elongase enzymes (primarily ELOVL6 and ELOVL1). The increase in VLCFA levels causes severe damage to mitochondria, resulting in significant oxidative stress. Mitochondria exhibit alterations in OXPHOS, increased ROS and also promote the induction of the Nκ-B transcription factor. These events lead to an inflammatory state, which causes a recruitment of monocytes and other immune cells. Macrophages phagocytose parts of myelin, and together with astrocytes, release pro-inflammatory cytokines, further increasing the inflammatory state and leading to severe demyelination. In response to demyelination, the remyelination mechanism is activated by oligodendrocytes. OPCs migrate to the area and begin the differentiation process into mature oligodendrocytes capable of forming myelin. However, in ccALD, there is evidence of oligodendrocyte death and suppression of genes related to their maturation.

3. Modelling X-ALD

The development of animal models reproducing physiopathological processes of different diseases is crucial to understand mechanisms and find possible therapeutic options. In X-ALD context, animal models facilitate knowledge about unknown mechanisms of pathology. Nevertheless, there is still a lack of appropriate animal model to study cerebral involvement of the most devastating phenotype: ccALD. For this reason, the use of human cellular types isolated from specific X-ALD patients is an alternative in response to failed animal models. The specificity of *in vitro* strategies could shed light on X-ALD research.

3.1 Cellular models.

Due to the complexity of the disease and the resulting lack of an ideal and specific animal model, exploring the development of *in vitro* strategies, as a disease-specific cellular models, becomes a feasible option to study.

The first studies using human cell types in X-ALD context were focused on deciphering correlations between several basic characteristics of the disease, but any robust *in vitro* model was established. The use of human X-ALD fibroblasts to study the disease brought important findings: affected fibroblasts showed variable expression of ALDP (Kemp et al., 1996; Watkins et al., 1995), impaired VLCFA-CoA β-oxidation (Wiesinger et al., 2013) and reproduced an oxidative stress pattern due to VLCFA accumulation (Fourcade et al., 2008). Nevertheless, human *in vitro* strategies in X-ALD context were restricted to fibroblasts due to the inaccessibility to a more specific cell types related to the disease such as neural cell types.

The use of murine cell types allowed accessibility to specific cell types more appropriate to study CNS diseases. Several investigations were focused on silencing ABCD1 and ABCD2 of murine glial cells through RNA interference. These studies revealed a direct link between the build-up of VLCFA and oxidative stress by the presence of ROS levels and structural and functional changes in mitochondria (Baarine et al., 2012; Singh et al., 2013). Additionally, there was observed an association between induction of transcriptional factors involved in inflammation processes such as nuclear factor kappa light-chain enhancer of activated B cells (NF-κB) (Singh et al., 2009). In subsequent years, advancements in gene editing techniques led to the development of murine microglial models using clustered regularly interspaced short palindromic repeats (CRISPR/Cas9). These new models replicated key biochemical features of the pathology, including VLCFA accumulation and lipid inclusions

with similar profiles than observed in patients' macrophages (Raas et al., 2019). Once again, these findings highlight the connection between peroxisomal deficiencies and the onset of inflammation in ccALD. As mentioned, cellular models based on non-human cells replicate biochemical processes observed in the disease and have provided insights into mechanisms involved in the pathophysiology, complementing findings obtained from human patient fibroblasts. However, the introduction of advanced new technologies such as cellular reprogramming has been transformative in developing more suitable *in vitro* models. Since then, X-ALD derived fibroblasts have been successfully reprogrammed to iPSCs. These undifferentiated stem cells can be differentiated into cellular derivatives of any of the three-germ layers to obtain specific cell types with original mutations present in patients. Following this methodology, various researchers have developed cell models from fibroblasts. Jang et al (2011) differentiated AMN and ccALD fibroblasts into neurons and oligodendrocytes and found biochemical differences between phenotypes that had not been previously observed in fibroblasts (Boles et al., 1991; Moser et al., 1999). These studies indicated a higher VLCFA accumulation in oligodendrocytes derived from ccALD compared to those derived from AMN patients (Jang et al., 2011). Additionally, Baarine et al (2015) also obtained astrocytes and determined that those obtained from ccALD patients exhibited a higher expression of pro-inflammatory cytokines when cultured with a mixture of cytokines and/or lipopolysaccharide (Baarine et al., 2015). The results of both studies allowed, to some extent, the reproduction of biochemical aspects of both phenotypes and the study of epigenetic mechanisms involved in the synthesis of VLCFA in oligodendrocytes derived from ccALD and the pro-inflammatory response in ccALD astrocytes. An unresolved issue remains whether the epigenetic structure of cells derived from iPSCs is equivalent to non-reprogrammed cells in patients. Over the years more precise cellular models have been developed with the aim to understand specific pathophysiological aspects of different phenotypes of X-ALD. One example of this is the study of Lee et al (2018) that analysed the role of BBB in inflammatory demyelination of ccALD phenotype. They developed a robust BBB cell model from reprogrammed ccALD fibroblasts that were differentiated to specific BBB endothelial cells. Interestingly, these differentiated cells revealed differences in neutral lipid accumulation and also showed structural and functional impairments (Lee et al., 2018).

Most of the research on X-ALD using cells has been conducted either with reprogrammed human fibroblasts or with modified animal cells. While these studies have led to certain advancements, the mechanism by which the disease is triggered remains unknown. Therefore, developing cellular models that more closely reflect the pathogenic reality of patients is essential to study all the factors involved in the tissue context. This is also necessary to find an effective and definitive therapy to improve the prognosis of the disease.

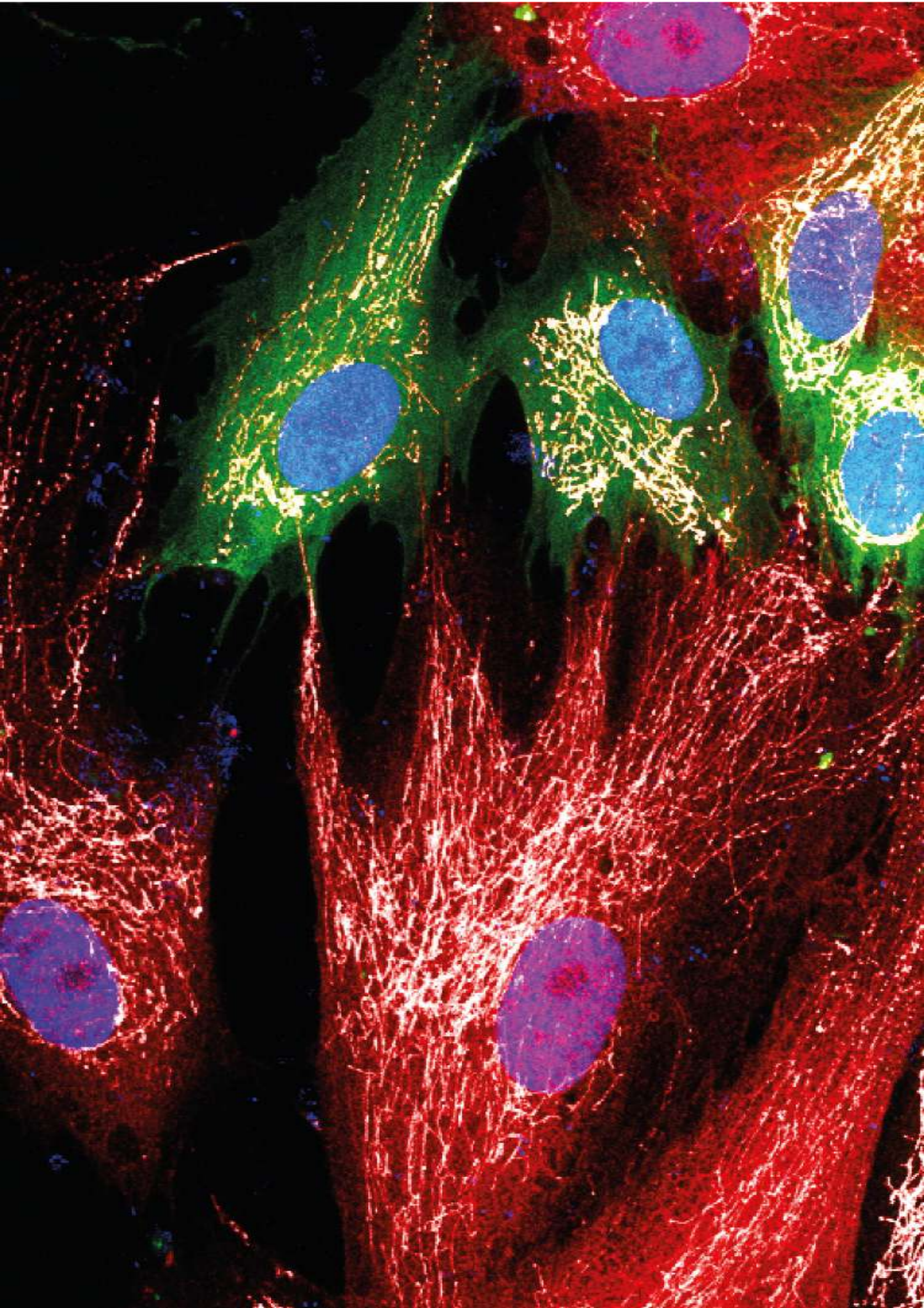

OBJECTIVES

This image is property of Claudia Pérez García. Immunofluorescence of direct co-cultures of human dental pulp and bone marrow stem cells against GFP, RFP and Human mitochondria. Image acquisition: Leica SPEII confocal microscope.

Objectives

The general objective of this Doctoral Thesis is to develop a novel *in vitro* model of X-linked adrenoleukodystrophy using dental pulp stem cells and to analyse the direct and indirect therapeutic effect of human bone marrow derived mesenchymal stem cell on this model.

These aims were accomplished by fulfilling the following objectives:

1) To analyse X-ALD hallmarks in human dental pulp stem cells derived from X-ALD patient. To accomplish this objective, we:

- Evaluated the genetical environment of X-ALD human dental pulp stem cells through sequencing.

- Analysed the expression of the protein responsible of the disease and its colocalization with peroxisomes.

- Studied the accumulation of neutral lipid through different neutral lipid staining and its comparison to healthy cells.

- Assessed cytotoxic effects related to X-ALD such as oxidative stress and higher concentrations of hexacosanoic acid.

- Investigated if differentiated neural cells maintain X-ALD phenotype through neutral lipid accumulation.

- Analysed functionality of X-ALD differentiated cells.

2) To evaluated the possible rescue of phenotype by the direct and indirect use of human bone marrow derived mesenchymal stem cells. To accomplish this objective, we:

- Established lentiviral transduction to clearly differentiate specific cell populations derived from human dental pulp and bone marrow.

- Performed direct co-cultures of these specifically labelled cells.
- Assessed exchange of cytoplasmatic and membrane material.

- Evaluated exchange of mitochondria derived from human bone marrow cell cultures and its inclusion in human dental pulp stem cell cytoplasm.

- Determined changes induced by direct effect of hBMSCs on X-ALD neural-like cells.

- Isolated microvesicles derived from CM of human bone marrow derived mesenchymal stem cells.

- Established indirect co-cultures through the addition of CM-containing EVs.

- Analysed the indirect effect of this conditioned media on neutral lipid accumulation of X-ALD dental cells.

- Evaluated the protective effect of this conditioned media in X-ALD cells exposed to oxidative stress and cytotoxic conditions.

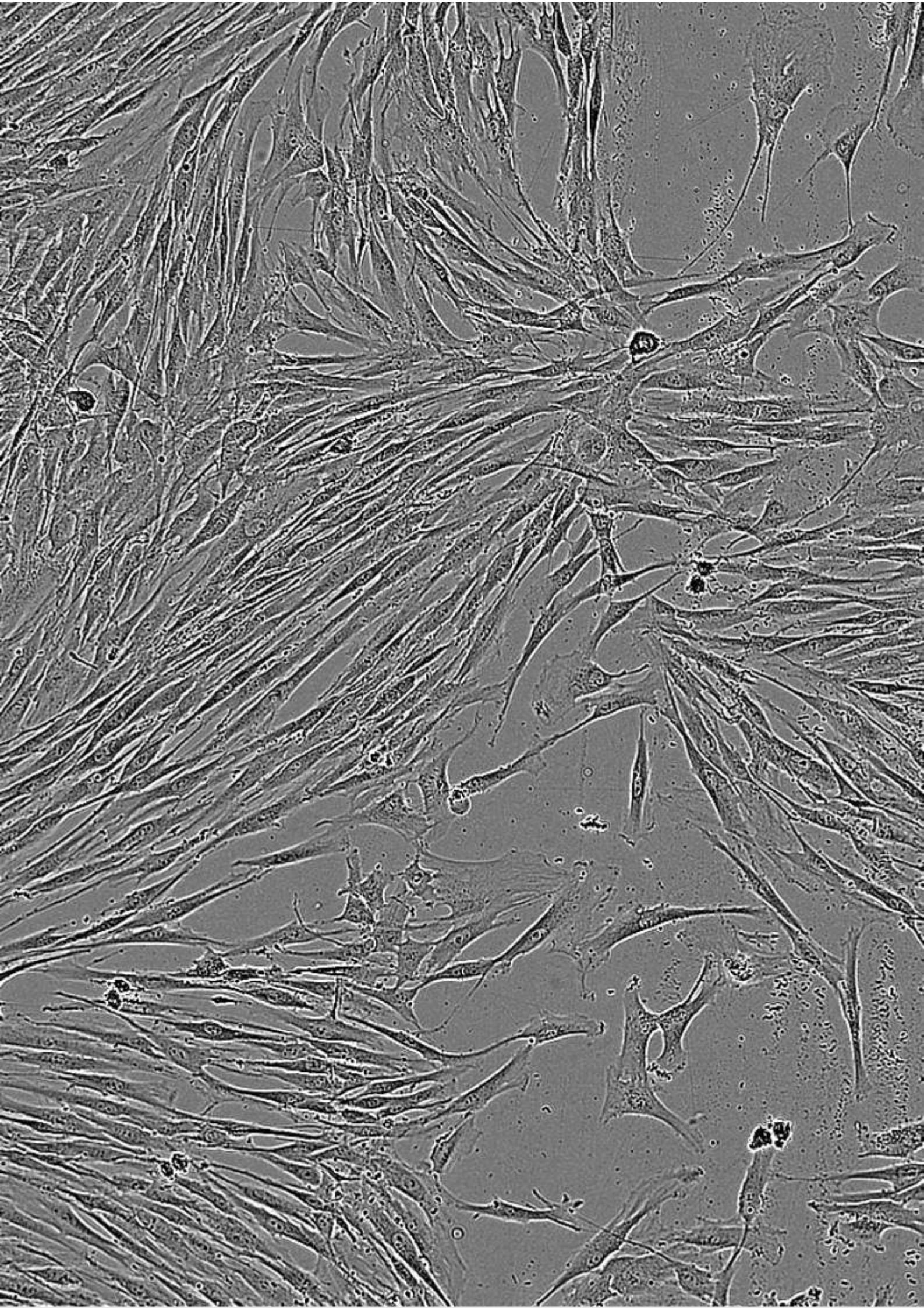

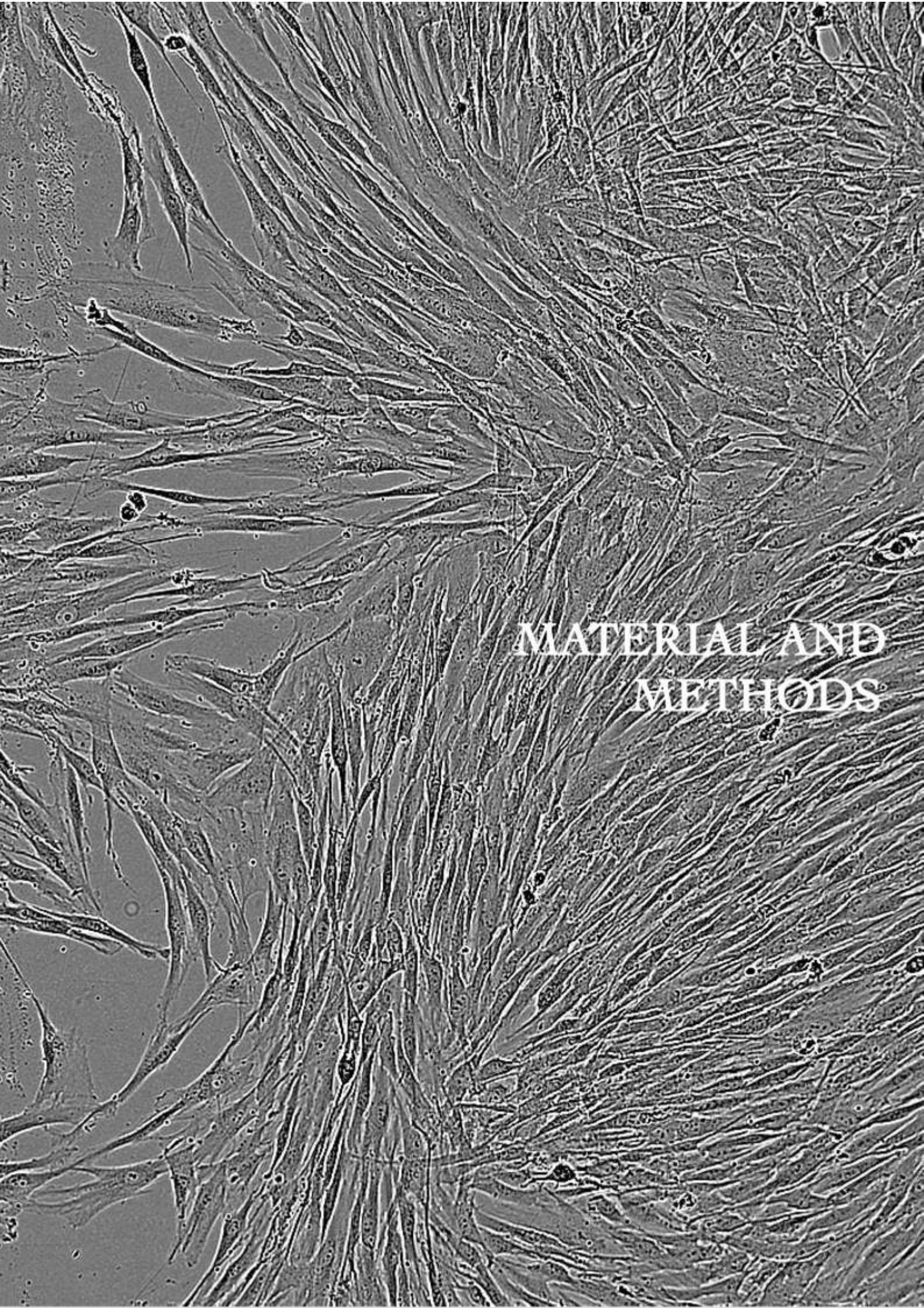

MATERIAL AND METHODS

This image is property of Claudia Pérez García. Phase contrast image of human dental pulp stem cells migrating in wound healing assay. Image acquisition: Sartorious InCuCyte s3.

Material and methods

1. Primary cultures.

All human-derived materials used in this study were obtained in strict adherence to ethical standards and regulations (ADH.NEU.SMP.CPG.23). Human teeth with X-ALD diagnostic were provided through donations facilitated by certified foundations (ELA Foundation, Spain) following approval by the corresponding ethics committee. Control teeth were obtained from donations to IMIB-Biobanc (National Biobanc Network, ISCIII) from children without known pathology story, following the same ethical committee approval. Informed consent was obtained from all authorized donors or their representatives, ensuring compliance with both institutional and international guidelines for research involving human subjects. Derived X-ALD hDPSCs were obtained from a 7-year-old male donor with clinical diagnostic but without genetic diagnostic of X-ALD.

1.1 hDPSCs isolation.

Human deciduous premolars were extracted and collected from three different healthy donors and one X-ALD patient. To obtain hDPSCs, dental pulp was harvested and, then, was digested with type I collagenase (3 mg/ml; Sigma-Aldrich; C7657) and dispase II (4 mg/ml; Sigma-Aldrich; D4693) in Dulbecco's Minimal Essential Medium (DMEM; Gibco; 11965092) 1X for 1 hour at 37ºC. The reaction was stopped by the addition of cold DMEM 1X. Dissociated dental pulp tissue was centrifuged at 1100 rpm for 5 minutes and the pellet, composed by hDPSCs, was resuspending in serum-containing media (designated as the basal media) composed of DMEM 1X supplemented with foetal bovine serum (15%; FBS; Fisher Scientific; 10309433), non-essential aminoacids (1%; NEAA; Gibco; 11140035), penicillin-streptomycin (100 units/ml; Gibco; 15140122) and L-glutamine (2mM; Gibco; 11500626). The cell suspension was plated into 6-well plates (Corning Falcon; CLS353934) and incubated at 37ºC and 5% CO_2.

1.2 hBMSCs isolation.

Bone marrow MSCs were obtained from Hemotology Service of Arrixaca Universitary Hospital and IMIB cell theraphy unit, from the analitical fraction of bome marrow donations, accomplishing the corresponding informed consent approval. Bone marrow was collected with

20 U/ml sodium heparin (Sigma-Aldrich; H3393), followed by a Ficoll density gradient-based separation by centrifugation at 540g for 20 minutes. After, mononuclear cell fraction was collected, washed twice with Ca^{2+}/Mg^{2+}-free phosphate buffered saline 1X (PBS 10X: 80 g NaCl, 2 g KCl, 14.4 g Na_2HPO_4, 2.4 g KH_2PO_4) and seeded into 175-cm^2 culture flasks (Nunc, Thermo Fisher Scientific) at a cell density of $1.5 \cdot 10^5$ cells/cm^2 in DMEM low glucose medium (Gibco; 11885084) supplemented with FBS (10%), GlutaMAX (1%; Gibco; 35050038) and penicillin-streptomycin (1%). After 3 days of culture, non-attached cells were removed and fresh complete medium was added.

2. Cell culture treatments.

2.1. Neural like differentiation of hDPSCs.

To induce neural differentiation, hDPSCs were allowed to adhere to plates or human collagen type IV (Sigma-Aldrich; C5533)-coated glass coverslip overnight. The following day, media was removed and hDPSCs were culture for 2 days in serum-free media (designated as the neural basal media) consisting in Dulbecco's modified Eagle's medium/F12 (DMEM/F12 Glutamax; Gibco; 11320033) supplemented with N2-supplement (1%; Gibco; 11520536), glucose (0.6%; Gibco; A2494001), 4-(2-hydroxyethyl)-1-piperazineethanesulfonic acid (5mM; HEPES; Gibco; 15630056), human serum albumin (0.5%; Sigma-Aldrich; A9080), heparin (0.0002%), non-essential aminoacids (1%) and penicillin-streptomycin (100 units/ml). On day 3, cells were cultured in neural induction media, consisting in the neural basal media supplemented with retinoic acid (500 nM; MedChemExpress; HY-14649), dibutyryl cyclic adenosine monophospate (1 mM; dbcAMP; Sigma-Aldrich; D0627) and a mix of growth factors: brain-derived neurotrophic factor (10 ng/ml; BDNF Gibco; 450-02), glial cell derived neurotrophic factor (10ng/ml; GDNF; Peprotech) and insulin-like growth factor (10 ng/ml; IGF-1; R&D systems).

2.2. Cell cultures with an excess of VLCFA.

Based on publication related to VLCFA topic (López-Erauskin et al., 2013), we choose 50 μM of C26:0 as a starting point of concentration to analyse the effect on hDPSCs. 5 mM of C26:0 (Sigma-Aldrich; 52200) stock solution was prepared combining heat and sonication in order to solubilize fatty acids in 100% ethanol (etOH; Montplet; #ALCH0321F5). Proper concentration of C26:0 was diluted in DMEM 1X and incubated with hDPSCs for 48 hours prior analysis.

2.3. Induction of oxidative stress.

Assessment of oxidative stress was studied by the addition of hydrogen peroxide (H_2O_2; Sigma-Aldrich; 95321) to cell cultures. Briefly, different concentrations of H_2O_2 (250, 500 and 1000 μM) were added to hDPSCs and incubated for 2 hours at 37ºC and 5% of CO_2. Then, changes in cell morphology and viability were evaluated. Based on previous report (Saleem et al., 2021) we chose 500 μM of H_2O_2 as standard concentration to induce oxidative stress on hDPSCs. hDPSCs grown on either bovine gellatin (0.4%; Sigma-Aldrich; G1890)-coated glass coverslips or in plastic surface of multi-well plates were previously washed with sterile PBS 1X and then incubated with 500 μM of H_2O_2 solution for 2 hours at 37ºC and 5% CO_2.

2.4. Indirect co-culture of hDPSCs and hBMSCs.

CM-containing EVs previously collected from hBMSCs flask cultures were added to hDPSCs cultures. Shortly, hDPSCs grown overnight were washed with sterile PBS 1X and, then, incubated with a dilution of CM-containing EVs with DMEM 1X in a ratio 1:1. Incubation of CM-containing EVs on hDPSCs were maintained for 72 hours before any type of analysis.

3. Preparation of CM from hBMSCs.

CM-containing EVs was obtained from 80-90% confluent hBMSCs. hBMSCs were previously washed with sterile PBS 1X and, then, incubated with DMEM 1X supplemented with penicillin-streptomycin (1%) for 48 hours. Supernatants, composed mainly of EVs, were then removed and stored at -80ºC prior to being used within culture experiments.

4. EVs isolation.

EVs were isolated from CM by ultracentrifugation. In brief, CM-containing EVs was removed from hBMSCs flask cultures and collected. Before EVs isolation, supernatants were centrifuged at 1100 rpm for 5 minutes at room temperature (RT) to eliminate cell debris. Then, supernatants were transferred to polycarbonate bottles with cap assembly (Beckman Coulter; 355618) and ultracentrifugated twice at 118000g for 1 hour at 4ºC (Beckman Coulter Optima XL-100K using Beckman type 70 Ti rotor with fixed angle). The resulting pellet was composed of a mixture of EVs of different their size: large EVs (LEVs) and small EVs (sEVs). EVs characterisation was performed by imaging flow cytometry and further confirmed by

transmission electronic microscopy (TEM), conducted exernally at Instituto de Investigación Sanitaria y Biomédica de Alicante (ISABIAL).

5. Wound healing assay.

In order to achieve a standardised and reproducible scratch assay, commercial two-well inserts were used (Ibidi; 80209). hDPSCs were seeded in wells in an appropriate cell density to achieve a cell monolayer within 24 hours (57.500 cells/well). The following day, insert was removed and a homogeneous wound area was clearly notable. Cell migration was then assessed by time-lapse imaging at different times using InCuCyte S3 incubator (Sartorious).

6. Immunoblotting.

hDPSCs cultured in T-25cm^2 flask cultures (Falcon; 353108) were washed with sterile PBS 1X and collected by trypsinization with trypsin/EDTA (0,25%; Gibco; 25200056). Cell pellets were lysed using RIPA lysis buffer (1%; Thermo Scientific; 89900) supplemented with a cocktail of protease inhibitors (Roche; 4693159001) and centrifuged at 12.000 rpm for 30 minutes. BCA assay (Thermo Scientific; 23227) was performed to quantify the concentration of total protein within each cell lysate sample according to manufacturer's instructions to ensure equal loading of cell lysates. BCA assay results were read on a plate reader (Infinite M nano; Tecan group) with proper settings for this assay. Lysates with equal amount of protein (10μg) were denatured by boiling in SDS-PAGE sample buffer (4X: 0.25M Tris-HCl pH:6.8; 8% sodium dodecyl sulfate (SDS), 40% glycerol, 0.02% bromophenol blue, 20% β-mercaptoethanol) at 95ºC for 5 minutes. Samples were then loaded into an SDS-polyacrylamide gel (Table 2) and separated by electrophoresis. Afterward, proteins were transferred into a nitrocellulose membrane (Amersham; GE10600007). blocked in bovine serum albumin (5%; BSA; Sigma-Aldrich; A7906), in TBS-T (20 mM Tris, 150 mM NaCl, 0.1% Tween-20, pH 7.6) and incubated overnight at 4ºC with gentle agitation in primary antibody (Table 3) diluted in blocking solution. The next day, membrane was incubated with appropriated secondary antibody horseradish peroxidase (HRP) conjugated antibody (Table 4), washed three times with TBS-T and visualized using an enhanced chemiluminescence (ECL) substrate (Immobilion Forte; Merck Millipore; WBLUF0100). Specific protein expression patterns were detected using an Amersham Imager 680 (GE Healthcare Life Sciences) western blot detection system.

Separating gel 7.5% of acrylamide/polyacrylamide	Stacking gel 4% of acrylamide/polyacrylamide	Source
H_2O	H_2O	-
Tris-HCl 1.5 M pH:8.8	Tris-HCl 0.5 M pH: 6.8	-
SDS	SDS	Sigma-Aldrich L4390
Acrylamide/Bis-acrylamide	Acrylamide/Bis-acrylamide	Sigma-Aldrich A3574
Tetramethylethylenediamine (TEMED)	TEMED	Sigma-Aldrich T9281
Ammonium persulfate (PSA)	PSA	Sigma-Aldrich A3678

Table 2. Composition of SDS-polyacrylamide gel of immunoblotting.

Antibody	Source	Reference	Dilution
α-ALDP (rabbit)	Abcam	AB197013	1:10000
α-β actin (mouse)	Sigma	A5441	1:7500

Table 3. Primary antibodies used for Western blot experiments.

Antibody	Source	Reference	Dilution
α-rabbit IgG (goat) HRP	Vector	PI-1000	1:4000
α-mouse IgG (goat) HRP	Dako	P0447	1:5000

Table 4. Secondary antibodies used for Western blot experiments.

7. Immunofluorescence.

A standard immunofluorescence protocol was used. First, hDPSCs cultured on coverslips were fixed in paraformaldehyde (4%; PFA; Merck-Sigma; #158127), washed, permeabilized with TritonX-100 (0.1%; Merck-Sigma; 9002-93-1) and blocked with goat serum (10%; Sigma-Aldrich; #S3772), BSA (5%) and PBS 1X. Afterward, they were incubated with primary antibody (Table 5) diluted with blocking solution overnight at 4ºC. The following day, hDPSCs were incubated during 1 hour with secondary antibodies, which were conjugated Alexa Fluor antibodies (Table 6). 4′,6-diamidino-2-phenylindole (1:10000; DAPI; Thermo Fisher Scientific; 11540206) was used to stain nuclei by incubating for 5 minutes at RT. The

coverslip was mounted onto Starfrost microscope slides (Knittel Glass) using Mowiol-NPG (Sigma-Aldrich; 475904) as antifaded mounting medium. Samples were observed and micrographs were taken under Leica SPEII confocal microscope (Leica Microsystems).

Antibody	Source	Reference	Dilution
α-ALDP (rabbit)	Abcam	AB197013	1:100
α-ACE2 (rabbit)	Abcam	AB15348	1:500
α-Connexin-43 (rabbit)	Cell Signalling	#3512	1:100
α-GFP (chicken)	Aves Labs	GFP-1010	1:500
α-MAP2 (chicken)	Invitrogen	PA1-10005	1:10000
α-Mitochondria (mouse)	Chemicon	MAB1273	1:300
α-Nestin (mouse)	Chemicon	MAB5326	1:200
α-Nav1.6 (rabbit)	Alomone Labs	ASC-009	1:200
α-PMP70 (mouse)	Merck	SAB4200181	1:100
α-RFP (rabbit)	Abcam	AB62341	1:500

Table 5. Primary antibodies used for immunofluorescence experiments.

Antibody	Source	Reference	Dilution
α-rabbit IgG (donkey) Alexa Fluor 488	Invitrogen	A 21206	1:500
α-rabbit IgG (donkey) Alexa Fluor 594	Molecular Probes	A21207	1:500
α-rabbit IgG (goat) Cy5	Molecular Probes	A10523	1:500
α-chicken IgY(IgG) (rabbit) FITC	Sigma	F8888	1:500
α-chicken IgG (goat)	Molecular Probes	A11042	1:500
α-mouse IgG (donkey) Cy5	Jackson Immuno Research	715-175-150	1:500
α-mouse IgG (goat) Alexa Fluor 594	Molecular Probes	A11032	1:500

Table 6. Secondary antibodies used for immunofluorescence experiments.

8. Neutral lipid staining.

For neutral lipid staining, hDPSCs cultured on glass coverslips were fixed with 4% PFA for 15 minutes at RT and subsequently washed with PBS 1X. Neutral lipids were stained using different stains: Oil Red O (ORO; Sigma-Aldrich; O1391), BODIPY 493/503 (Invitrogen; D3922) and LipidTOX Deep Red (Invitrogen; H34477).

For ORO staining, fixed cells were incubated with 0.3% of ORO staining solution in isopropanol at RT with agitation during 20 minutes. Excess of dye was removed washing with distilled water. After staining, coverslips were mounted on glass slides with mounting medium (Eukitt Classic Mounting Media; Aname; 15322-10) and sealed for imaging in Leica DMR fluorescence microscope.

BODIPY 493/503 staining was performed incubating fixed cells with 2μM of dye diluted in PBS 1X for 15 minutes at RT in the dark. Excess of dye was removed washing with PBS 1X. DAPI was used to stain nuclei. After staining, coverslips were mounted on glass slides with antifade mounting medium (Mowiol-NPG) and sealed for imaging in Leica SPEII confocal microscope.

LipidTOX Deep Red staining was performed incubating fixed cells with diluted dye (1:500 in PBS 1X) for 30 minutes at RT in the dark. Excess of dye was removed washing with PBS 1X. DAPI was used to stain nuclei. After staining, coverslips were mounted on glass slides with antifade mounting medium (Mowiol-NPG) and sealed for imaging in Leica SPEII confocal microscope.

9. Caspase 3/7 staining.

For analysing H_2O_2-induced stress on hDPSCs, we used Caspase 3/7 ready-reagent to evaluate cell apoptosis. In short, cells were washed twice with PBS and incubated for 30 minutes with CellEvent Caspase-3/7 Green Detection Reagent (ThermoFisher Scientific; C10423) in a dilution of 1:400 in DMEM1X. Then, cells were analysed using InCuCyte s3 incubator and processed by its software (Sartorious).

10. Flow cytometry experiments.

10.1 MSC characterisation.

Expression of MSC markers was analysed by flow cytometry. Briefly, hDPSCs and hBMSCs cultures were washed and harvested using trypsin digestion for 5 minutes at 37ºC, centrifuged for 5 min at 1100 rpm at RT and resuspended at a concentration of 10^6 cells/ml in DMEM 1X. Different concentrations of conjugated antibodies (Table 7) were added to 100 μl of cell resuspension tubes and incubated for 30 minutes at RT in the dark. Afterwards, cell resuspensions were washed by centrifugation and resuspended in staining buffer (3% BSA in PBS 1X) for further analysis in BD FACS Aria III cell sorter (BD Biosciences).

Antibody	Source	Reference	Dilution
α- CD105 (mouse) FITC	Biolegend	323203	1:20
α-CD34 (mouse) FITC	Biolegend	343603	1:20
α-CD44 (rat) APC	Biolegend	103011	1:100
α-CD45 (mouse) APC	Biolegend	368511	1:20
α-CD90 (mouse) FITC	Biolegend	328107	1:20

Table 7. Antibodies used for flow cytometry experiments for MSC characterisation.

10.2 EVs characterisation.

EVs characterisation was performed by imaging flow cytometry. For imaging flow cytometry, pellet was resuspended in PBS and incubated for 30 minutes at RT with appropriated primary antibodies (Table 8) for Exos characterisation based on MISEV recommendations (Witwer et al., 2021). Then, fluorophore-conjugated secondary antibodies (Table 9) were added and analysed using a cell sorter with cell imaging analysis (BD FACSDiscover S8 with BD CellView Image Technology and BD SpectralFX Technology, BD Biosciences).

Antibody	Source	Reference	Dilution
α- Calnexin (rabbit)	Cell Signalling	#2433	
α-CD63 (mouse)	Invitrogen	#10628D	1:100
α-Hsp70 (mouse)	Santa Cruz	SC-32239	

Table 8. Primary antibodies used for flow cytometry experiments for EVs characterisation.

Antibody	Source	Reference	Dilution
α-mouse IgG1 (goat) Alexa Fluor 488	Molecular Probes	A21121	1:1000
α-rabbit IgG (donkey) Alexa Fluor 594	Abcam	Ab10076	1:1000
α-mouse IgG (donkey) Cy5	Jackson ImmunoResearch	715-175-150	1:1000

Table 9. Secondary antibodies used for flow cytometry experiments for EVs characterisation.

10.3 Assessement of oxidative stress and CM-induced protection

The apoptotic effect of 500 μM H_2O_2 on hDPSCs for 2 hours and the protective outcome of CM-containing EVs on previously stressed hDPSCs after 72 hours was analysed using the PE-Annexin V Apoptosis Detection Kit (BD Biosciences; 559763) using flow cytometry according to the manufacturer's protocol. Briefly, cells were washed with PBS 1X, harvested by trypsinization and resuspended in binding buffer solution. Afterwards, they were incubated with PE-Annexin V and 7-AAD for 15 minutes at RT in the dark. Finally, cells were analysed using BD FACS Aria III cell sorter.

11. Lentiviral transduction.

Lentiviral particles were produced using three distinct constructs. Mitochondria were specifically labelled using a specific construct which target a mitochondrial specific sequence to direct the protein exclusively to the mitochondria (pLV-mitoDsRed; Addgene; #44386). hBMSCs and hDPSCs were transduced using two lentiviral constructs targeting the expression of GFP or RFP under the control of the ubiquitin promoter allowing fluorescent expression in cytoplasm. Lentivirus GFP and RFP were provided by Dra Guillermina Lopez-Bendito's laboratory). All constructs were packaged into lentiviral particles separately. For lentiviral production, HEK293T cells were transfected with each construct individually, along with packaging plasmids: RRE p312, RVE p313 and VSVG p314, following lipofectamine protocol as manufacturer's instructions indicate (LipoD93 In Vitro DNA Transfection Reagent; SignaGen Laboratories; #SL100668).

After 72 hours, supernatants containing lentiviral particles were collected, filtered and concentrated using Lenti-X Concentrator (ClonTech; 631231) for 72 hours. Then, lentiviral particles were centrifugated (1500g for 45 min at RT) and the resulting pellet was resuspended with PBS. Lentiviral particles were aliquoted and stored at -80ºC until use.

To perform transduction using lentiviral particles, hDPSCs and hBMSCs were seeded at an appropiate density and exposed to each lentiviral preparation separately depending on the aim of the experiment. Cells were incubated for 24-48 hours, followed by media replacement. Transduction efficiency was assessed after this time by visualization through InCucyte s3 incubator or by BD FACS Aria III cell sorter.

12. Whole-cell patch clamp.

Electrophysiological recordings of cell voltage and ionic membrane currents were performed under the whole cell configuration of the patch clamp technique (Hamill, Marty, Neher, Sakmann and Sigworth, 1981) using a MultiClamp 700B amplifier (Molecular Devices, USA). Cells were bathed in and extracellular solution at 32-33ºC; the composition of the extracellular solution was: 124 mM NaCl, 2.5 mM KCl, 1.25 mM $NaPO_4H_2$, 1 mM $MgCl_2$, 2 mM $CaCl_2$, 26 mM $NaCO_3H$, and 10 mM glucose; pH 7.4 when saturated with 95% O2 and 5% CO2. Borosilicate pipettes (1.5 mm outer diameter, 0,86 inner diameter, with inner glass filament) were used to pull patch electrodes with a vertical pipette puller (Narishige mod. P88, Narishige, Tokyo, Japan). The inner diameter of the tip pipette after pulling was approximately 0.5–1 μm. Filling of the pipette was carried out with an intracellular solution containing: NaCl (5 mM), KCl (5 mM), EGTA (5 mM), K-Gluconate (130 mM), HEPES (10 mM), Na-GTP (0.2 mM) and Mg-ATP (2 mM) at pH: 7.2. The electrical resistance of the pipettes was in the range of 4.8 MΩ, and the seal resistance was > 1 GΩ. Liquid junction potential was routinely corrected and a Ag-AgCl was used as reference. The cell voltage was maintained at −90 mV and depolarizing pulses of 750 ms duration were applied in steps of 5 mV. The recordings, the holding voltage and the pulses were digitalized and generated with a DigiData 1440A analog to digital converter and the pClamp 10.5 software (Molecular Devices, USA). Data were sampled at 20kHz kHz.

13. Direct co-cultures.

Once hDPSCs and hBMSCs populations were efficiently transduced with the indicated lentiviral constructs, different direct co-cultures were established. Direct co-cultures in a ratio 1:1 composed of hBMSCs-GFP and hDPSCs-RFP were cultured in order to analyse a possible exchange of cytoplasmatic and/or membrane components. Furthermore, following the same strategy, direct co-cultures composed by hBMSCs-mitoRED and hDPSCs-GFP were conducted with the aim of analyse a possible mitochondria trafficking. In brief, confluent transduced cells were washed and harvested by trypsinization. Once centrifuged at 1100 rpm for 5 minutes, cell pellets were resuspended with basal media and sorted through BD FACS Aria III cell sorter to assure pure cell cultures of transduced cells. Finally, cells were seeded on human collagen type IV-coated glass coverslips in a total cell density of 10000 cells/cm^2 for 72 hours prior to any analysis.

14. Conventional PCR.

Genomic DNA (gDNA) was isolated from confluent T25 cm^2 flasks of hDPSCs cultures. 100 µl of sodium hydroxide solution (50 mM; NaOH; Sigma-Aldrich; #72068) was added to cellular pellet and heated at 95ºC for 30 minutes. gDNA found in supernatant was then used for further studies.

Total gDNA extracted was used to study the ten-coding region the gene ABCD1. Thus, several PCR reaction tubes were prepared using different mix of primers corresponding to different fragments of ABCD1 exons (Table 8) and Kappa mix reactive (H_2O, polymerase, dNTPs and co-factors; Roche; KK5601). Amplification of PCR products was performed on a thermocycler (Biorad dual 48 well DNA engine thermal cycler; Bio-Rad laboratories) with the following thermal cycling conditions:

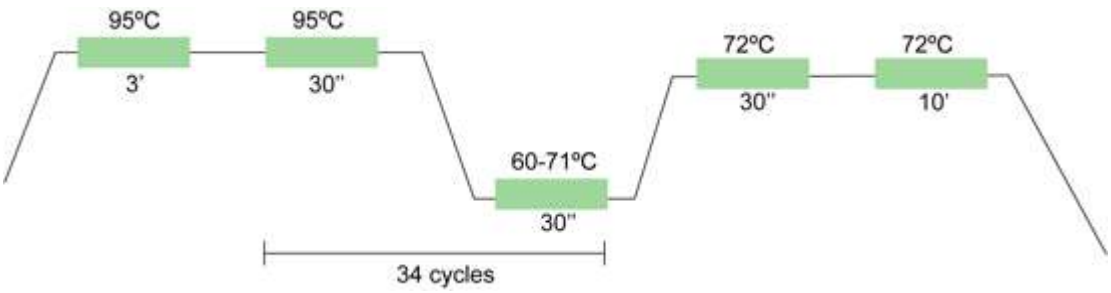

Exon	Primer sequence	Fragment length (bp)	Annealing temperature (ºC)
1a	F: ACAACAGGCCCAGGGTCAGA R: AGGAAGGTGCGGCTCACCA	422	62
1b	F: AACCGGGTATTCCTGCAGCG R: ACTGGTCAGGGTTGCGAAGC	385	60
1c	F: CCACGCCTACCGCCTCTACTT R: AGACTGTCCCCACCGCTC	484	60
2	F: GGCACTGGGAGACCCTG R: TCAGCACCCAGCGGTATGG	332	60
3,4	F: GCAGAAGAGCCTCGCCTTTC R: GCAGCAGGTCAGCACCTGCA	570	62
5	F: CTGCCAGGGATGGGAATGAG R: TCTCACCTTGACCTTGGCCC	337	60
6	F: GCCATAGGGTACGGGAAGGG R: GCCTCTGCAGGAAGCCATGT	276	60

7	F: CGATCCACTGCCCTGTTTTGG R: CTTCCCTAGAGCACCTGG	491	62
8,9	F: CTGAGCCAAGACCATTGCCCCCG R: TGCTGCTGCCGGGCCCGC	471	70
10	F: GAGGGGAGGAGGTGGCCTGGC R: GCGGGGTGCGTGCATGGGTGG	427	71

Table 8. Primer sequences used for ABCD1 gene PCR.

PCR amplificated products were visualized by electrophoresis. Samples were run in agarose gel (1%; Condalab; 8010.00) supplemented with GreenSafe Premium (2%; NYZTech; #MB13201) in TAE 1X (TAE 5X: 24.2g Tris base, 5.71 ml glacial acetic acid, 10 ml 0.5M EDTA). Fragments were visualised in an ultraviolet transilluminator (model TFX-20-M)

For Sanger Sequencing, corresponding PCR amplificated products from the ten coding regions of ABCD1 gene were pre-processed to clean-up primer sequences and nucleotides using ExoSAP-IT (Applied Biosystems; 78205). Afterward, samples were processed and sequences by Eurofins, an external facility (Eurofins company).

15. Cell imaging analysis.

15.1 ACE2 expression analysis

To quantify ACE2 expression in cultured cells of wound healing assay, three random images of the wound area were captured in each condition by Leica SPEII confocal microscope. Prior to quantification images were deconvoluted by Huygens professional software (Scientific Volume Imaging) to improve signal-to-noise ratio (SNR). Sum projections of deconvoluted images were analysed using Fiji software (Fiji is Just ImageJ) (Schindelin et al., 2012) (26 cells at t=0h and 22 cells at t=12h were quantified in terms of fluorescence intensity (Corrected Total Cell Fluorescence; CTCF; a.u: arbitrary units) with the following formula:

$$\text{CTCF (a.u): Integrated density} - \frac{\text{Area of selected cell}}{\text{Mean of background readings}}$$

15.2 Cell percentages of analysed cells

Depending on the aim of the experiment, different cell percentages were calculated from cell cultures images.

- Cell percentage of ORO^+ cells.

To analyse the percentage of cells with positive stain of ORO, five random images were selected. Using Fiji software, cells were counted using the multi-point tool. Cell percentage was calculated with the following formula:

$$ORO^+ \text{ cells } (\%): \frac{\text{Number of cells with ORO stain}}{\text{Total number of cells}} \text{ x } 100$$

- Cell confluence percentage determination.

To analyse in detail the effect of C26:0 and CM-containing EVs on cell growth, analysis of cell confluence, direct related to cell growth, was performed. Thus, time-lapse phase contrast images were obtained using InCuCyte incubator. We choose five random images of different times (0, 8, 16, 24, 32, 40 and 48h) and different conditions (healthy 50 μM vs X-ALD 50 μM or X-ALD 50 μM vs X-ALD 50 μM + CM) to analyse cell confluence. Numeric data of cell confluence was obtained using Fiji software. In brief, images were first transformed from RGB to 8-bit and adjusted to threshold. When adjusting to threshold, we assured total coverture of cells avoiding background. Data obtained from Fiji was %Area corresponding to the area of image full of cells.

- Cell viability percentage analysis.

To analyse the effect of C26:0 and CM-containing EVs in cell viability, we calculated the percentage of cell viability. Thus, five different images of time-lapse experiments at different times (0,8,16,24,32,40 and 48h) and conditions (Healthy 100 μM vs X-ALD 100 μM or X-ALD 100 μM vs X-ALD 100 μM +CM) were analyse using Fiji software. Thus, we used the multi-point tool to count total amount of cells and death cells. Then, we calculated the percentage of cell viability following the formula:

$$\text{Living cells } (\%): \frac{\text{Number of total cells} - \text{Number of dead cells}}{\text{Number of total cells}} \text{ x } 100$$

15.3 Fluorescence intensity of neutral lipids in hDPSCs cultures

To assess differences in neutral lipid accumulation in different hDPSCs cell populations, five randoms images of BODIPY and LipidTOX staining were captured by Leica

SPEII confocal microscope. Prior to quantification images were deconvoluted by Huygenes Professional software to improve SNR. Sum projections of deconvoluted images were analysed using Fiji software. Fluorescence intensity was calculated following the CTCF formula.

15.4 Number of peroxisomes analysis

To determine the number of peroxisomes of different cell populations of hDPSCs, immunofluorescence of the 70 kDa peroxisomal membrane protein (PMP70), a standard marker of peroxisomes, were conducted. Five random different images of each cell population were captured using Leica SPEII confocal microscope. The number of peroxisomes of each cell was obtained through a developed plugin called Squassh (Rizk et al., 2014).

15.5 Organelle inclusion

To confirm red mitochondria from hBMSCs included inside hDPSCS-GFP cell populations, different images of direct co-cultures were captured using Leica SPEII confocal microscope. Then, images were processed using both Imaris software (Bitplane) to perform tridimensional reconstruction of cells and orthogonal projections to confirm such inclusion. Fiji software was also used for orthogonal projection of images of hDPSCs-GFP and hDPSCs-RFP to confirm inclusion of $ALDP^+$ peroxisomes.

16. Statistical analysis.

All statistical analysis were performed using GraphPad Prism v8.0 (GraphPad software). Depending on the nature of variables, different statistical approaches were conducted. In brief, normality and lognormality tests were first proved in order to analyse if samples followed a normal distribution. If samples followed a normal distribution, then parametric tests were used to deciphering statistical differences between groups of samples (healthy and X-ALD hDPSCs). Non-parametric tests were applied when samples did not follow a normal distribution. Significance was represented attending APA normative as follows: *: $p<.05$; ** $p<.01$; *** $p<.001$.

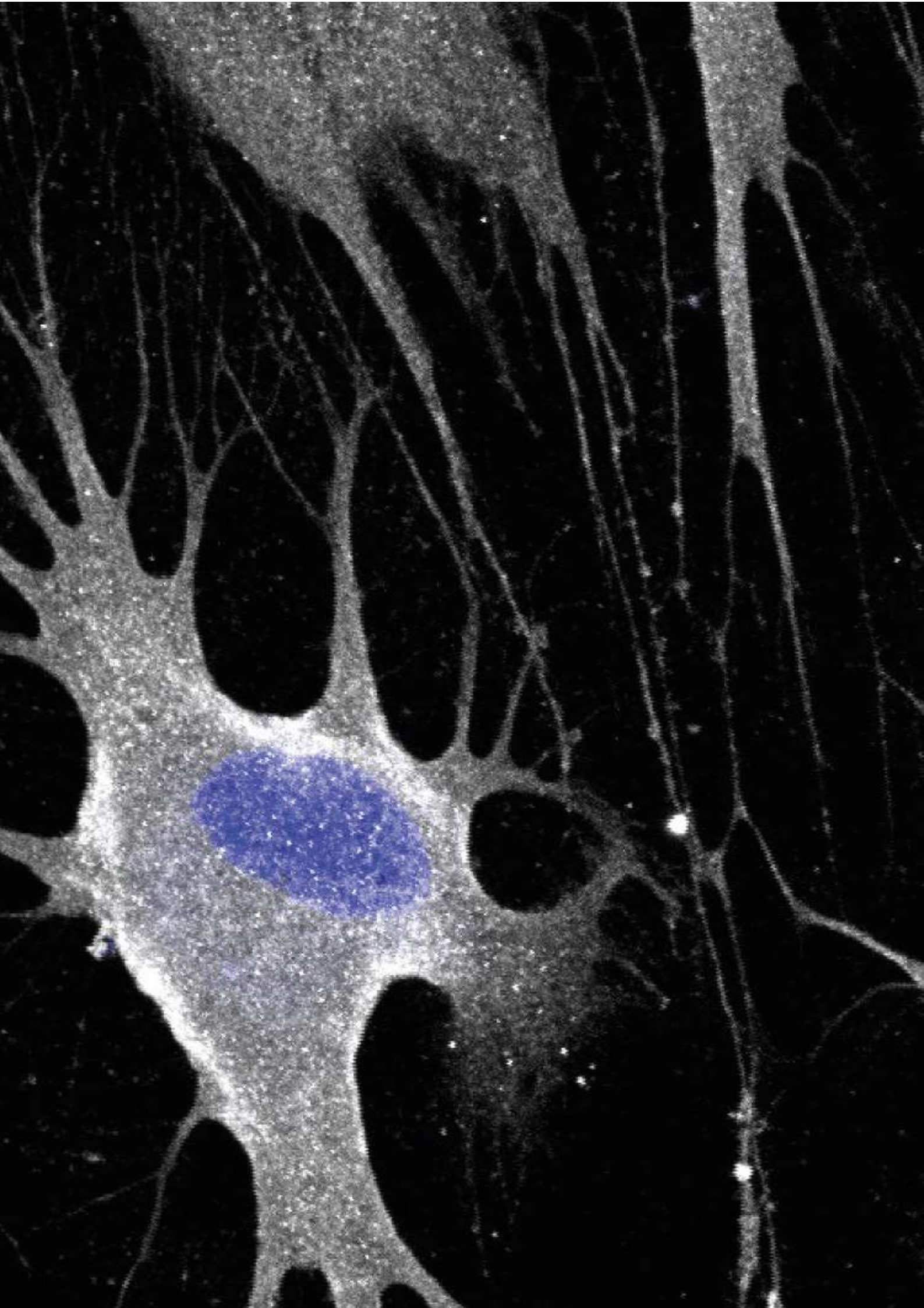

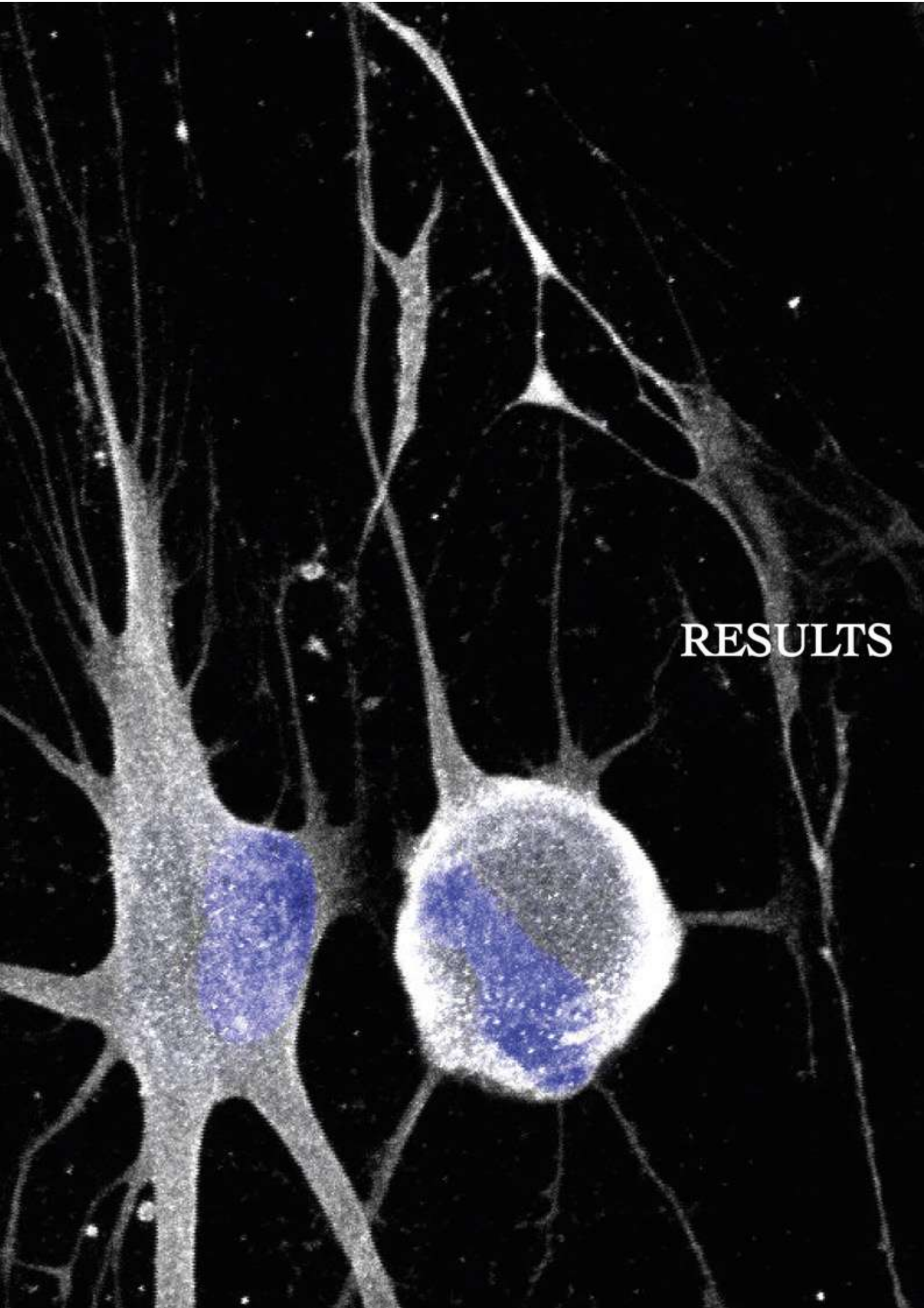

RESULTS

This image is property of Claudia Pérez García. Immunofluorescence of neural differentiated human dental pulp stem cells against Nav1.6. Image acquisition: Leica SPEII confocal microscope.

Results

1. Development of a novel *in vitro* model of X-ALD.

1.1 Analysis of cell migration of hDPSCs.

In the context of developing a cellular model for X-ALD using hDPSCs, understanding the migratory capacity and ACE2 expression profile of these cells becomes relevant. hDPSCs, derived from NCPs, possess inherent migratory abilities like those observed in neural crest cells, including polarization and directed movement. The expression of ACE2 in human cells has garnered significant interest, as it serves as the receptor for the SARS-CoV-2 coronavirus responsible for COVID-19. Notably, ACE2 is expressed in various human tissues, including the lungs, intestines, kidneys, brain and heart. Its expression in migrating cells suggests roles beyond viral receptor activity, potentially influencing cellular motility and intercellular communication.

To better characterise the developing *in vitro* model of X-ALD, we first explored the possible regulation of ACE2 expression in migrating healthy hDPSCs. One essential factor to study cell migration in hDPSCs is the fact that are a feasible source of NCPs *in vitro*. Neural crest cells are a transient cell population in the embryo that exhibits a variety of migratory mechanisms, including sheet and chain migration, in which neuropilin-1 (NP-1) expression is required (Szabó & Mayor, 2018). hDPSCs were cultured following the protocol described in material methods according to Bueno et al (2013) to derived mesenchymal stem cells that were molecular and functionally characterized as NCP (Bueno et al., 2013). The expression of Nestin has been used to confirm that our cultured cells are NCP (Fig. 13, A and A'). ACE2 immunofluorescence showed expression of ACE2 in the cytoplasm of cultured dental derived NCP, with perinuclear accumulation (Fig. 13, A and B). In cells with polarized morphology, which were suggestive of cell motility, ACE2 expression was stronger than in basal static fusiform or polygonal cells and also accumulated in the cellular membrane of the leading pole (Fig. 13, B'). To explore if ACE2 expression is modified by migratory activity, we used wound healing assay. Cells were grown to confluence and a thin "wound" was introduced by two-well inserts. Cells at the wound edge polarized and migrated into the wound space. Then minutes after the scratch (t0h), cells were fixed and processed by immunofluorescence to detect ACE2 expression. The cells at the wound edge strongly expressed ACE2 (Fig. 13, C and D). At 12–24 h (t12h, t24h) after the scratch, polarized elongated cells migrated into the wound with strong expression of ACE2 in the cellular membrane of leading processes and in intercellular

nanotubes (Fig. 13, E–I). At 48 h after the scratch, the wound was completely cellularized, with remnant expression of ACE2 in the cell membrane of some cells at the place where the wound was performed (Fig. 13, J). After quantification of ACE2 expression at 0 and 12 h after scratch, the increasing expression of ACE2 in migrating cells was significative in the cell membrane during a period of 12 h (the time with active cellular migration into the wound) without modification of ACE signal in the cytoplasm (Fig. 13, I).

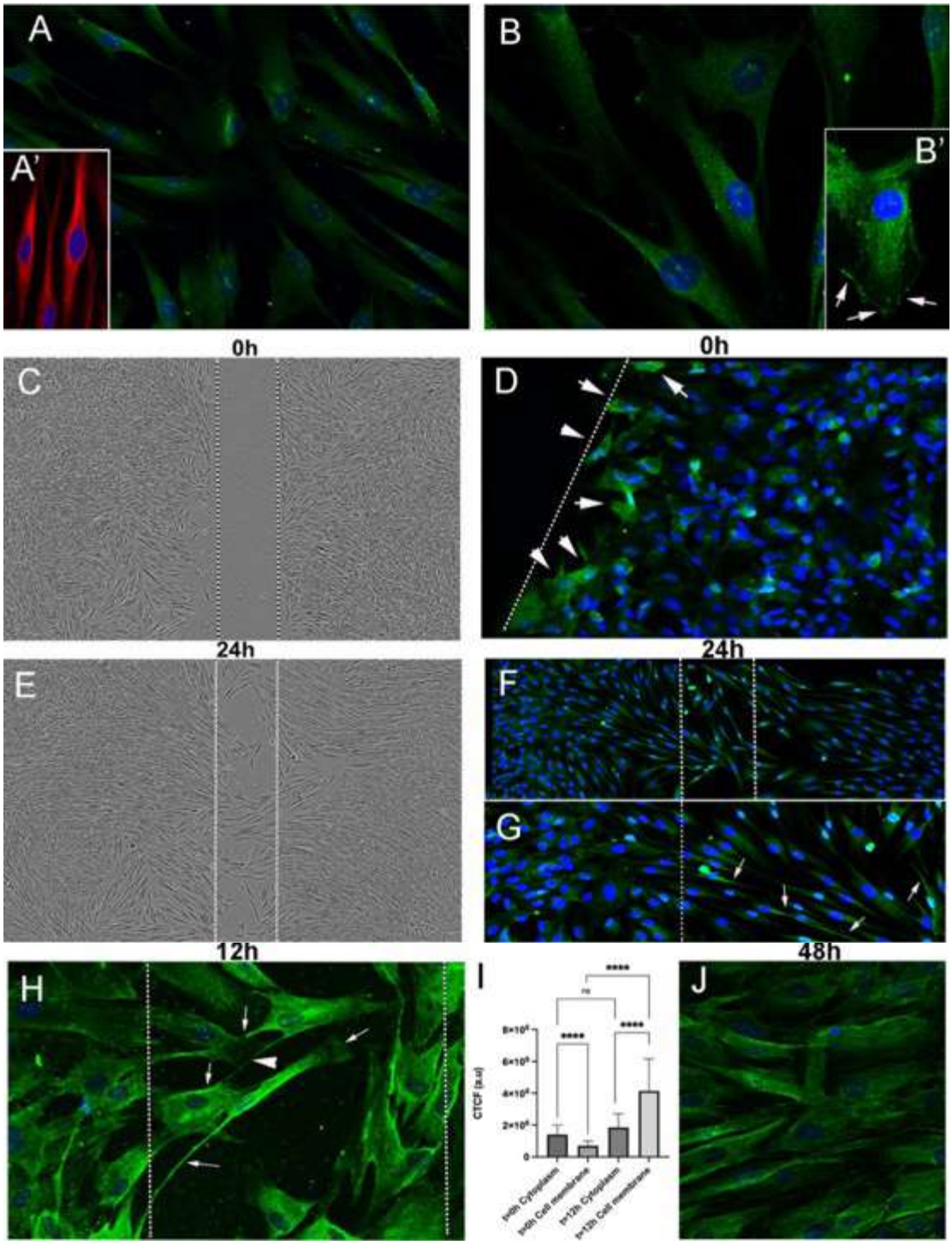

Figure 13. ACE2 expression in migrating hDPSCs.

Anti-ACE2 immunofluorescence showed expression of ACE2 in the cytoplasm of cultured hDPSCs, with perinuclear accumulation (A, B). hDPSCs express Nestin protein (red immunofluorescence) (A'). In cells with polarized morphology, ACE2 expression was stronger and accumulated in the cellular membrane of the progression pole (B', arrows). Scratch-wound assay in confluent cultures. D 10 min after the scratch (t0h) cells at the wound edge strongly expressed ACE2 (C-I, arrows). E–I At 12–24 h (t12h, t24h) after the scratch, polarized elongated cells migrated into the wound with strong expression of ACE2 in the cellular membrane of advance processes (arrows) including in intercellular nanotubes (arrows head in H). Quantification of ACE2 expression by immunofluorescence intensity and intracellular distribution with the ImageJ tool for measuring CTCF (I). Data shown as mean of CTCF and standard deviation (SD) bar errors. The number of cells analyzed were: T0h (cytoplasm or membrane) $n = 26$, T12h (cytosol or membrane) $n = 22$. Comparisons between cytoplasm and cell membrane at T0h and at T12h were made with tests for paired samples (Wilcoxon signed-rank test) and comparisons between cytoplasm at T0h and T12h or cell membrane at T0h and T12h were made with test for independent samples (Mann–Whitney test for T0h test), using the software GraphPad Prism. a.u: arbitrary units. Asterisks indicate p-value: **** $p < 0.0001$, ns not significant. At 48 h after the scratch the wound was completely cellularized with increased expression of ACE2 in some cell membranes of neighbouring cells at the place where the wound was performed (J, arrows). Images (20x and 40x) were taken using Leica SPEII confocal microscope.

1.2 Cell characterization of hDPSCs.

Based on ISCT criteria (Dominici et al., 2006), isolated cells from human dental pulp were characterized in terms of mesenchymal stemness. Cell population showed adherence to plastic surface and exhibited fibroblast-like morphology under *in vitro* standard conditions (Fig. 14, A). Furthermore, analysis of expression of different surface receptors aligned with established criteria as they expressed CD90 (99.4±0.2%), CD44 (96.9±2.5%) and CD105 (1.5±1.2%) while lacking expression of CD34 and CD45 (data not shown), more specific of hematopoietic progenitor cells (HPCs) (Fig. 14, B and C). CD105 is an included marker in ISCT criteria, but their expression has presented high variability among MSC populations (Izgi et al., 2017; Mark et al., 2013) and, in this case, healthy hDPSCs presented lower expression compared to CD90 and CD44.

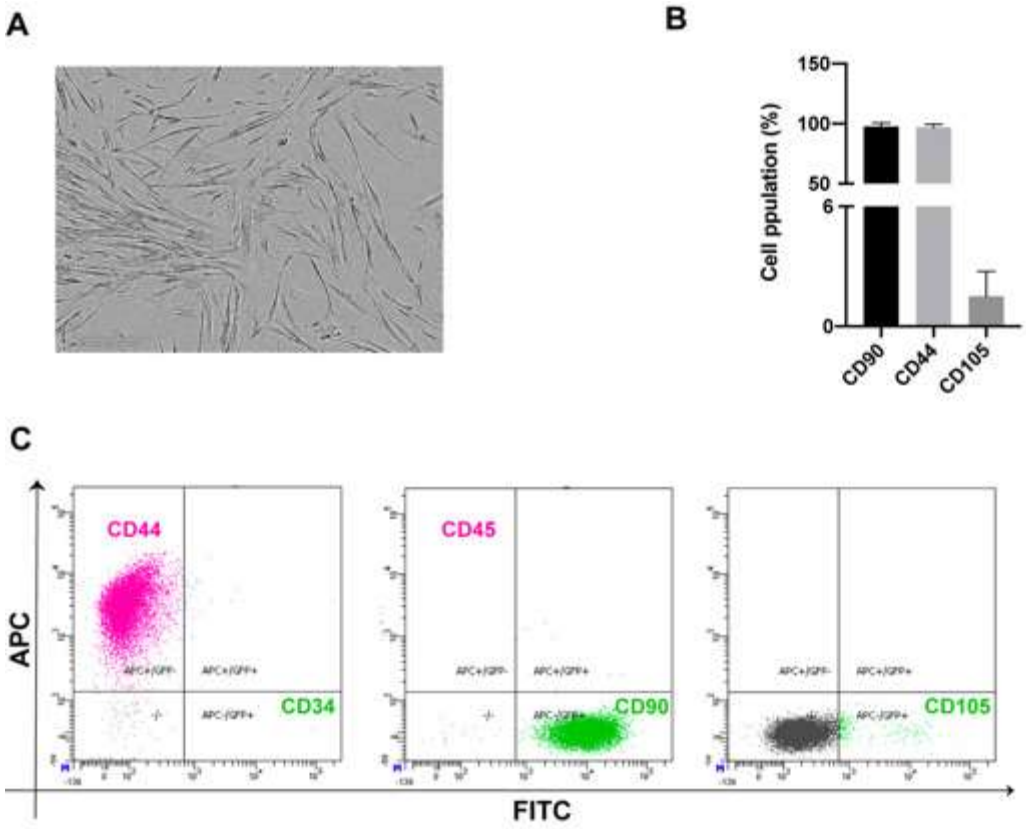

Figure 14. Cell characterisation of isolated hDPSCs.

Phase contrast image showing cell morphology and adherence in line with ISCT criteria (A). Graph exhibits the meaning of cell percentage (%) and SD bar errors of different stem cell markers such as CD90, CD44 and CD105 (B). Flow cytometry scatter plots of mentioned markers (C). Each dot represents an individual cell and the density of dots indicates the relative abundance of cells in each quadrant. The phase contrast image (10x) was taken by InCuCyte incubator and processed by InCuCyte software.

1.3 Analysis of healthy and X-ALD cell population by flow cytometry.

To assess differences in cell morphology and distribution between healthy and X-ALD cell population, a comparative analysis of cell cultures obtained from both groups was performed using flow cytometry strategies. Obtained forward (FSC) and side (SSC) scatter density plots from flow cytometry experiments allow the identification of cell population of interest and the exclusion of cell debris.

Under *in vitro* standard conditions, both healthy and X-ALD hDPSCs showed same morphology and adherence to plastic surface (Fig. 15, A and B). When analysed cell clusters in flow cytometry, we perceived differences between both populations. In the case of healthy hDPSCs, the cell cluster corresponding to the population is much more compact and denser

compared to X-ALD cell cultures (Fig. 15, C). In the X-ALD cell population, the cell cluster showed a slightly different distribution, being much more dispersed than healthy cell cluster (Fig. 15, D). This fact seems to indicate that X-ALD cell population exhibit differences in terms of complexity and size. Additionally, X-ALD cell cultures showed more cell debris than healthy hDPSCs even when analysed under the same conditions (Fig. 15, E). This could provide a basis for a more detailed analysis of distinct alterations observed in X-ALD hDPSCs, which could serve as a starting point to develop an *in vitro* model of the disease.

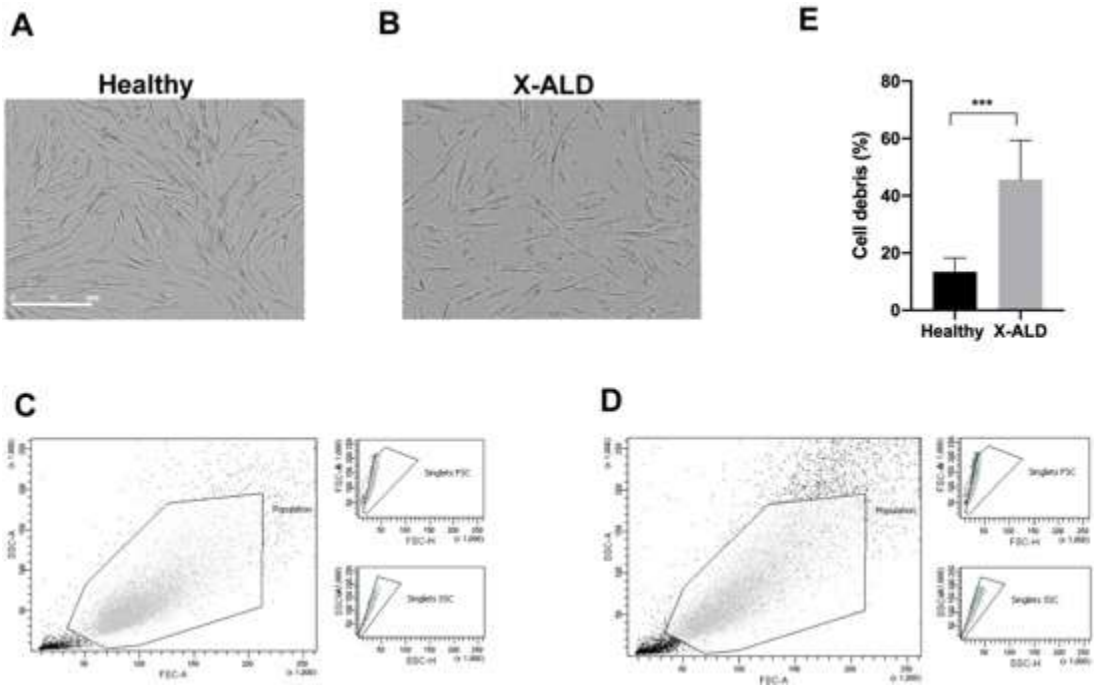

Figure 15. Flow cytometry cell clusters of healthy and X-ALD cell populations.
Phase contrast images of healthy (A) and X-ALD (B) hDPSCs under *in vitro* standard conditions. FSC vs SSC density plot from healthy (C) and X-ALD (D) cell populations. X-ALD cell population show higher density of cell debris and dispersion of cell cluster. Graph shows meaning of percentage of cell debris and SDs bar errors of healthy and X-ALD hDPSCs. Comparisons between healthy and X-ALD cell populations were made with tests for independent samples (Mann-Whitney test) (E). Images (10x) were acquired with InCuCyte incubator and processed by InCuCyte software. Asterisks indicate p value: p<.001 (***).

1.4 ABCD1 analysis.

As mentioned above, ABCD1 gene is composed of ten exons of different size that covers 19.9 kb (Fig. 16, A). In order to found any alteration in ABCD1 gene, we analysed this gene through conventional PCR and Sanger sequencing. We found that healthy and X-ALD hDPSCs expressed the ten coding regions that constitute human ABCD1 gene without differences

between cell populations (Fig. 16, B). Thus, gDNA from X-ALD hDPSCs was sequenced using Sanger sequencing method in order to find mutation across coding-regions. By Sanger sequencing we could not find any mutation in sequenced regions (Fig. 16, D). We could not confirm the existence of mutations in the untranslated regions of the gene (UTR sections). These results suggest that genetic alteration in X-ALD hDPSCs might be related to mutations that support translation of ABCD1 mRNA into a stable conformation of ALDP.

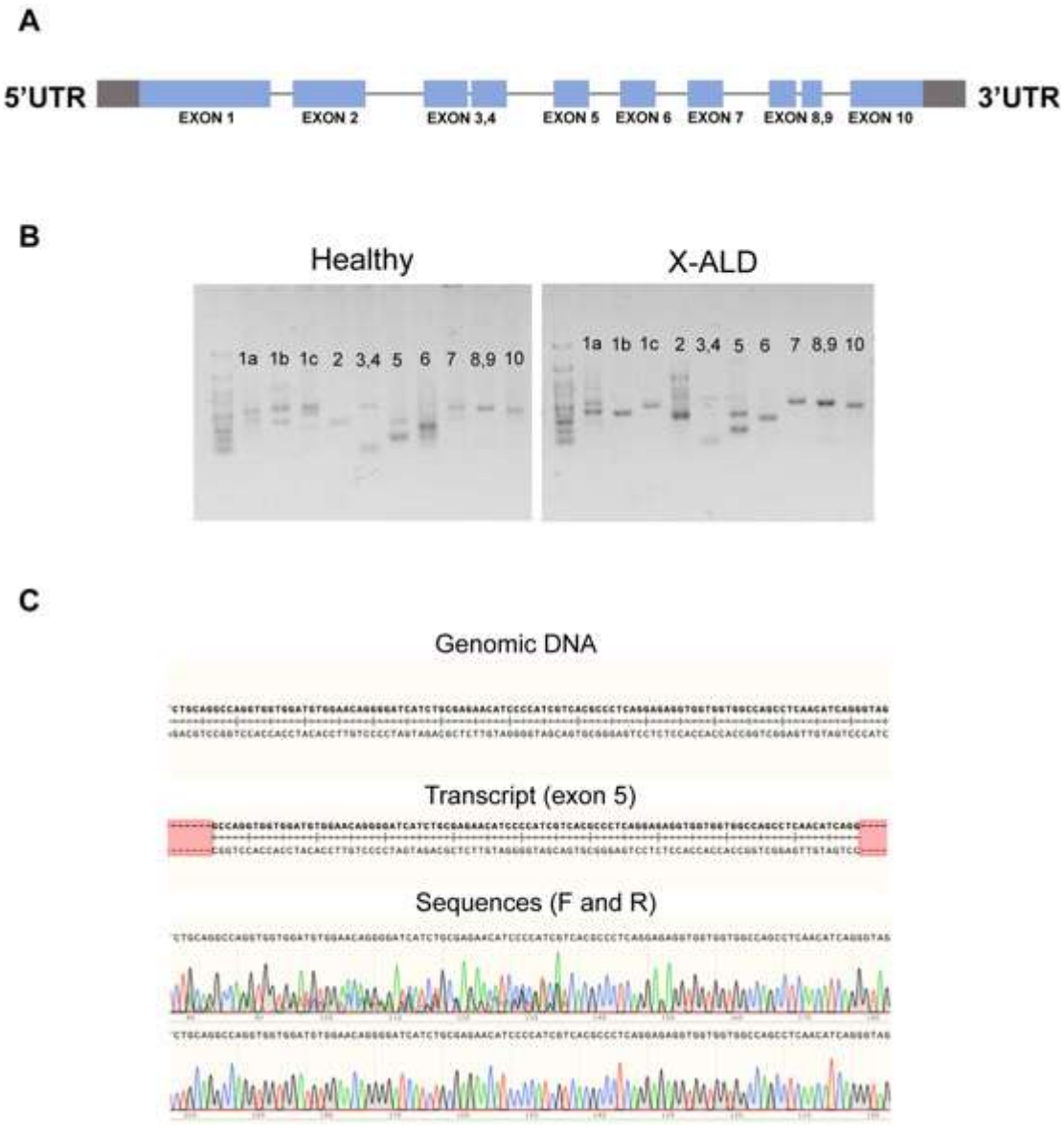

Figure 16. Genetic analysis of ABCD1 gene in X-ALD hDPSCs.

Representative structure of ABCD1 gene composed of ten coding regions or exons (A). Agarose gel electrophoresis results of conventional PCR for ABCD1 exons of healthy and X-ALD cells showing expression of coding regions in both cell populations (B). Illustrative results of Sanger sequencing of ABCD1 gene (exon 5) analysed by SnapGene software (version 6.0.2; GSL Biotech LLC) (D).

1.5 Analysis of ALDP expression in hDPSCs.

The expression pattern of ALDP in hDPSCs has not been studied before although the expression of several ABC transporters has been analysed in human stem cell populations (Erdei et al., 2014). In X-ALD context, ALDP expression was previously studied in cell cultures. Immunoreactivity to ALDP in fibroblasts derived from different X-ALD patients showed variability and three different case scenarios: absent, reduced and normal expression of this protein depending on genetic alterations of ABCD1 gene (Watkins et al., 1995). In our cells, immunofluorescence revealed that healthy and X-ALD hDPSCs showed positive immunoreactivity to human ALDP with similar expression pattern previously studied in human fibroblasts. ALDP was expressed in perinuclear zone and in cytoplasm, areas in which peroxisomes are located (Fig. 17, A-D). In addition to this, we analysed colocalization of stable ALDP with a standard peroxisomal marker such as PMP70 (Fig. 17, A'-D'). ALDP colocalized with PMP70 in all studied cases concluding that there was not any kind of disruption in peroxisome structure (Fig. 17, A"-D"). Healthy and X-ALD hDPSCs showed heterogeneity in peroxisome distribution and number per cell. We observed hDPSCs with a high number of peroxisomes across cytoplasm but, also, cells with a few peroxisomes were detected in both physiological and pathological conditions (data not shown). Overall, X-ALD hDPSCs showed significant higher number of peroxisomes compared to two healthy cell populations (Fig. 17, E). Despite this fact, normal ALDP expression in all hDPSCs populations was confirmed by further analysis by western blot (Fig. 17, F). Even when normal expression of ALDP was confirmed, we could not discard an impairment in protein function that give rise to pathophysiological hallmarks of X-ALD phenotype.

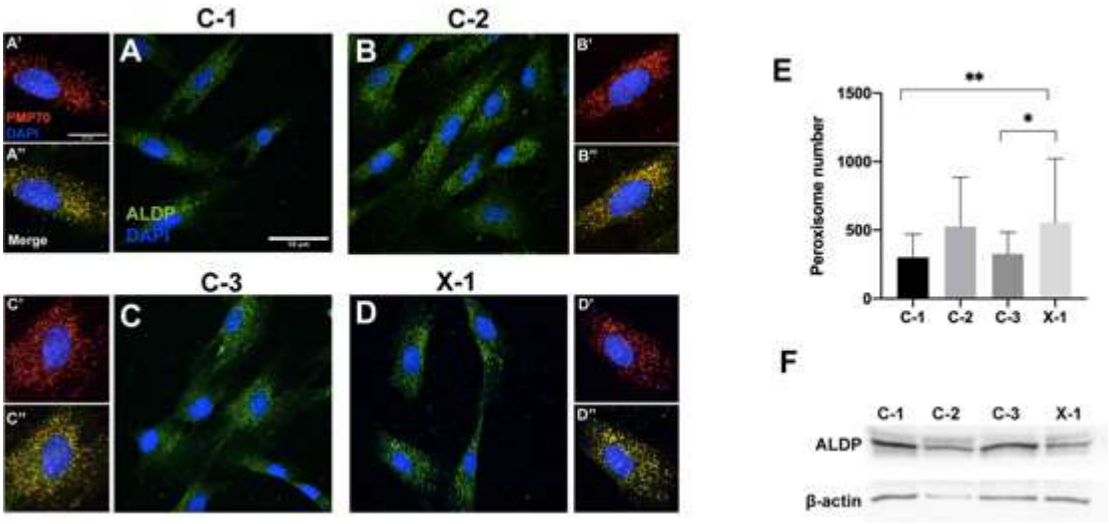

Figure 17. Peroxisomal analysis of X-ALD hDPSCs reveal normal expression pattern of ALDP. Deconvoluted confocal images of ALDP expression in healthy hDPSCs (A-C) and X-ALD hDPSCs (D) showing a punctuate expression pattern. ALDP colocalizes with PMP70 (A'-D'), a general marker of peroxisomes, in all studied cases (A"-D"). Significant differences were found in peroxisome number between X-ALD hDPSCs and two healthy cell population (E), but none in protein expression by western blot analysis (F). Images (40x) were acquired by Leica SPEII confocal microscope. Zoomed and cropped images were processed using Fiji software. Graph shows mean values of peroxisome number and SDs bar errors. Multiple comparisons between healthy and X-ALD cell populations were made with tests for independent samples (Kruskal-Wallis test). Asterisks indicate p value: p<.05 (*), p<.01 (**). C-1, C-2 and C-3: healthy hDPSCs; X-1: X-ALD hDPSCs.

1.6 Study of neutral lipid accumulation in hDPSCs.

Pathogenic accumulation of satured VLCFA, especially C26:0, is a critical hallmark of X-ALD (Engelen et al., 2012c; Turk et al., 2020). To demonstrate any alteration in ALDP function, we performed ORO staining experiments of healthy and X-ALD hDPSCs. ORO staining revealed higher accumulation of neutral lipid species in X-ALD hDPSCs in comparison to healthy hDPSCs (Fig. 18, A and B). Both cell populations showed positive staining of ORO, but X-ALD hDPSCs presented significant higher cell percentage population positive to this specific neutral lipid-staining (Fig. 18, C), suggesting an alteration in the removal of these lipid species.

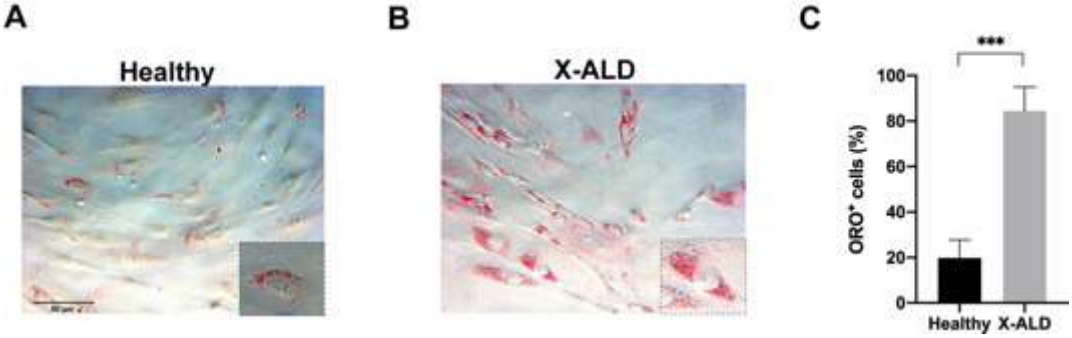

Figure 18. X-ALD hDPSCs showed aberrant neutral lipid accumulation by ORO staining. ORO staining revealed differences between healthy (A) and X-ALD cell population (B), with higher accumulation in X-ALD hDPSCs. Most of X-ALD hDPSCs were positive to ORO stain whereas healthy hDPSCs displayed less percentage of their population (B). Graph shows the meaning and SDs bar errors of the cell percentage presenting a positive stain of ORO. Comparison between healthy and X-ALD samples were made using independent tests (Mann-Whitney test) (C). Images (20x) were acquired using Leica DMR fluorescence microscope. Cropped sections were processed using Fiji software. Asterisks indicate p value: p<.001 (***).

Moreover, to analyse this fact in more detail, we choose different fluorophore dyes that bind to neutral lipids: BODIPY 493/503 and LipidTOX Deep Red. These types of stains showed similar results than ORO and confirmed our hypothesis. Both dyes showed similar specific neutral lipid stain with lipid-droplet pattern across cytoplasm. X-ALD hDPSCs revealed evident differences in neutral lipid accumulation in comparison to three different healthy hDPSCs (Fig. 19, A and B). Also, this fact could be studied by quantification of fluorescence intensity using values of CTCF. CTCF confirmed this alteration in neutral lipid accumulation (Fig. 19, C and D). These experiments concluded that X-ALD hDPSCs showed disease-specific characteristics making them suitable for further *in vitro* studies related to modelling X-ALD.

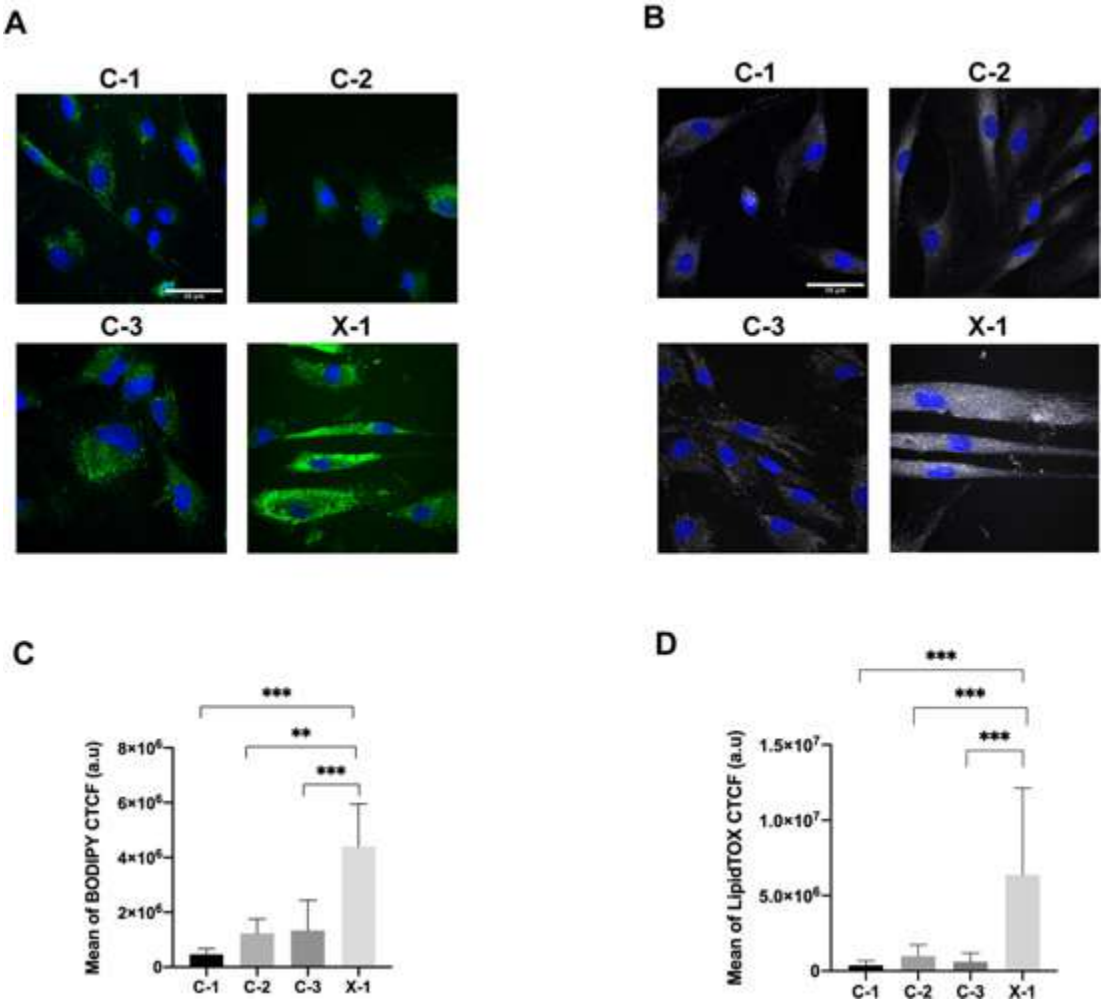

Figure 19. X-ALD hDPSCs showed aberrant neutral lipid accumulation by BODIPY 493/503 and LipidTOX Deep Red.

Fluorescent staining for neutral lipids, BODIPY 493/503 (A) and LipidTOX Deep Red (B) also demonstrated aberrant neutral lipid accumulation of X-ALD hDPSCs in comparison to three different hDPSCs. This finding was quantified in terms of CTCF both in BODIPY 493/503 (C) and LipidTOX

Deep Red (D) which revealed significant differences between X-ALD cell population and all healthy analysed cells. Graphs show the meaning and SDs bar errors of CTCF values of BODIPY 493/503 and LipidTOX Deep Red. Multiple comparisons were made with independent tests for multiple samples (Mann-Whitney tests; Dunn's multiple comparisons). Images (40x) were acquired using Leica SPEII confocal microscope and deconvoluted by Huygenes professional software prior to quantification. Asterisks indicate p value: p<.01 (**), p<.001 (***), a.u: arbitrary units. C-1, C-2 and C-3: healthy hDPSCs; X-1: X-ALD hDPSCs.

1.7 Effect of C26:0 on X-ALD cell cultures.

Cytotoxicity of C26:0 has been studied in different cell types remarking more vulnerability in X-ALD cell population and even resulting in cell death (Hein et al., 2008). In order to study the effect of C26:0 in our hDPSCs cell populations, we incubated cells with different concentrations of C26:0 for 24 hours. After this time, we studied changes in cell growth and viability. Both healthy and X-ALD cells survived to 50 μM of C26:0, but delayed cell growth was only apparent in X-ALD cell population suggesting an alteration in VLCFA metabolism (Fig. 20, A). Cell confluence of both cell populations was analysed and confirmed our hypothesis (Fig. 20, B). When concentrations of C26:0 increased to 100 μM, X-ALD hDPSCs did not survive and most of cells died at 24 hours (Fig. 20, C). Consequently, percentage of cell death was significantly increased in X-ALD hDPSCs (Fig. 20, D). This evident cell death was not present in healthy cell population, which apparently grown as basal condition. This fact suggests an evident alteration in VLCFA metabolism, more concretely in peroxisomal β-oxidation, one of disease-specific characteristics of X-ALD.

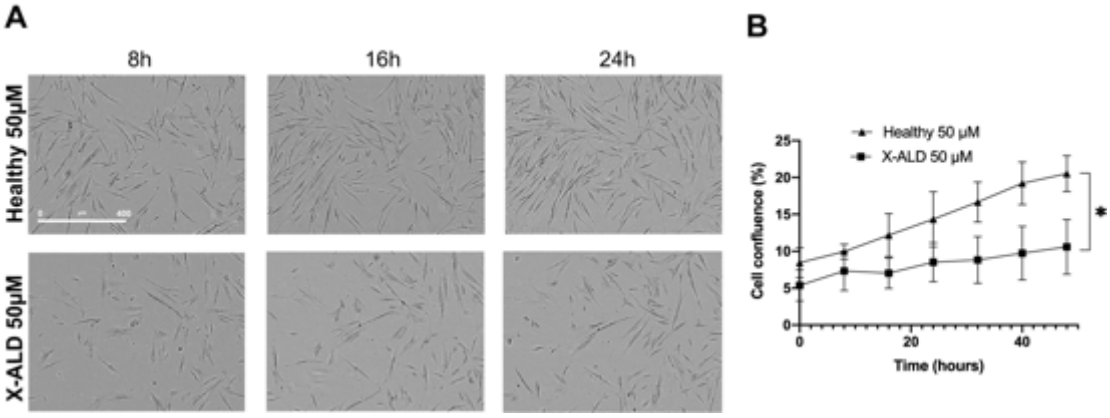

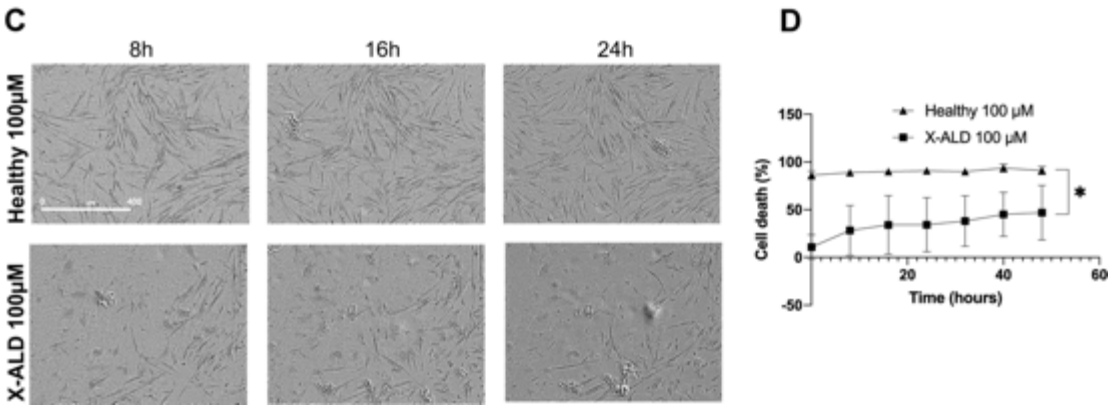

Figure 20. C26:0 induces changes in cell growth and viability in X-ALD hDPSCs.

The effect of 50 µM of C26:0 in both healthy and X-ALD hDPSCs was only evident in X-ALD population, delaying cell growth (A, B). Increased concentrations of C26:0 induced more notable changes present only in X-ALD hDPSCs, inducing evident cell death (C, D). Graphs show the meaning and SDs bar errors of cell confluence (B) and death (D). Comparison between samples were made through paired-samples tests (Willcoxon-signed rank test). Phase contrast images (10x) at different time points (8, 16 and 24h) were acquired and processed by InCuCyte incubator. Asterisks indicate p value: $p<.05$ (*).

1.8 Neural differentiation of hDPSCS.

hDPSCs are known by their ability to differentiate into the neural lineage (Nuti et al., 2016). We demonstrate that both healthy and X-ALD hDPSCs could differentiated into neural-like cells using a previous published protocol of our group (Bueno et al., 2021). We confirmed previous findings and analysed that healthy hDPSCs differentiated into neural lineage. After 48 hours of induction, differentiated cells showed rounded cell bodies and neurite extension (Fig. 21, A). In order to study presumable functionality of these differentiated cells, we performed whole-cell patch clamp experiments. Interestingly, neuron-like cells derived from healthy hDPSCs showed evident excitability when applied different voltages (from -90 mV to +95 mV) evidencing the activation and deactivation of currents (Fig. 21, B). In more detail, these cells exhibited sodium (Na^+) (Fig. 21, C) and potassium (K^+) (Fig. 21, D) typical currents.

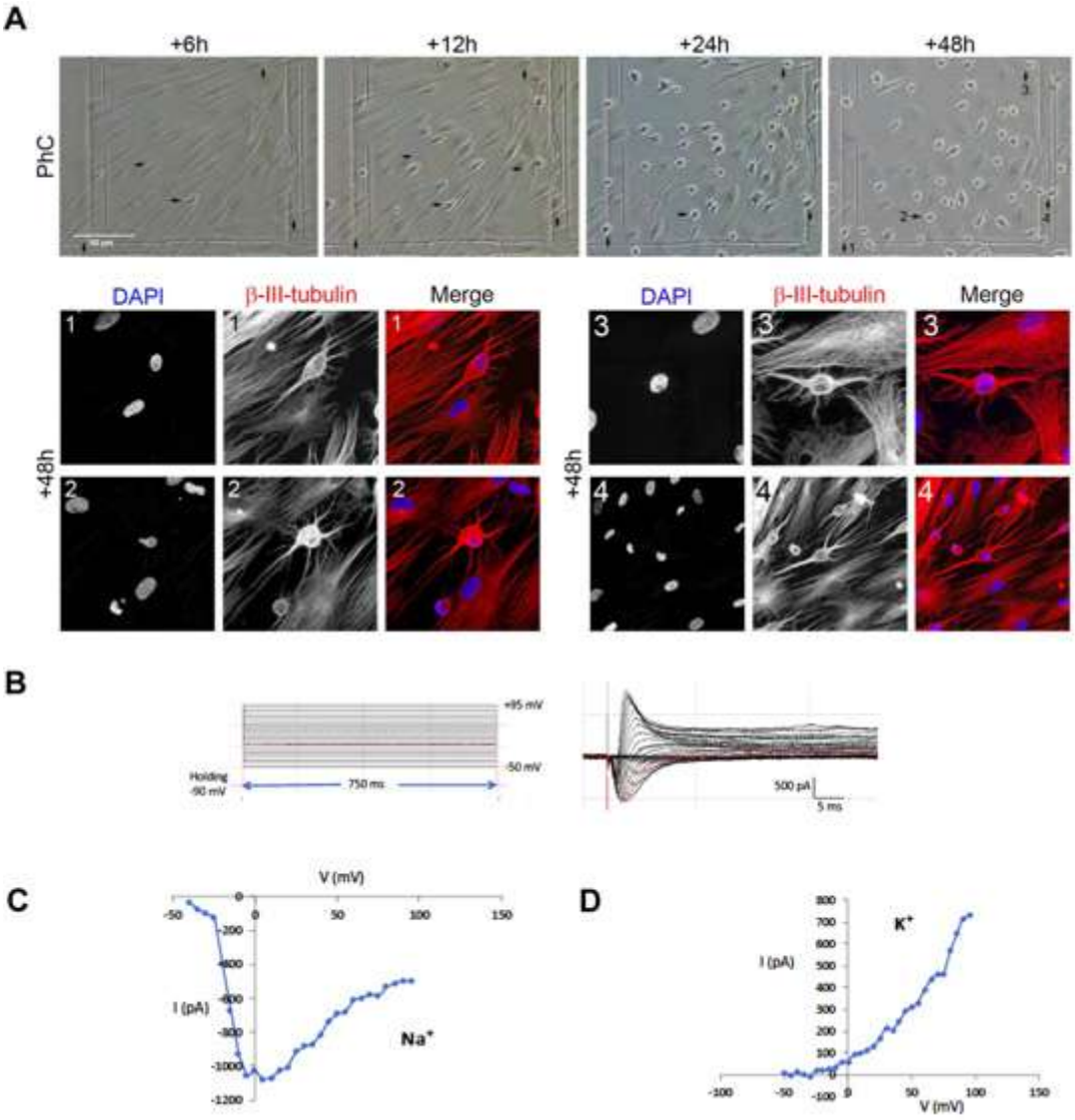

Figure 21. Neural differentiation of healthy dental pulp stem cells.

Time-lapse of healthy hDPSCs differentiating into neural-like cells. After 48 hours, cells became rounded and neurite extension appeared (A, upper). These neural-differentiated cells expressed β-III-tubulin (A, down). Representation of currents induced at different voltages (from -90 mV to +95 mV) in whole-cell patch clamp records of neuron-like cells from healthy hDPSCs, indicating neural activity (B). Na^+(C) and K^+ (D) currents of differentiated healthy cells evidencing inward and outward currents. Graphs show values of intensity (pico ampers, pA) vs voltage (milivoltages, mV) of both ions.

Regarding neural markers expression, we analysed several mature and immature neural markers. In their basal media, hDPSCs exhibited low expression of immature (Tuj-1) and mature neural markers (MAP2 and Nav1.6), whereas exhibited basal expression of NCP marker Nestin (Fig. 22, A). However, in differentiated cells, there was an increase of these markers (Fig. 22, B). This fact indicated that our protocol is suitable for studying mature specific neural cell types.

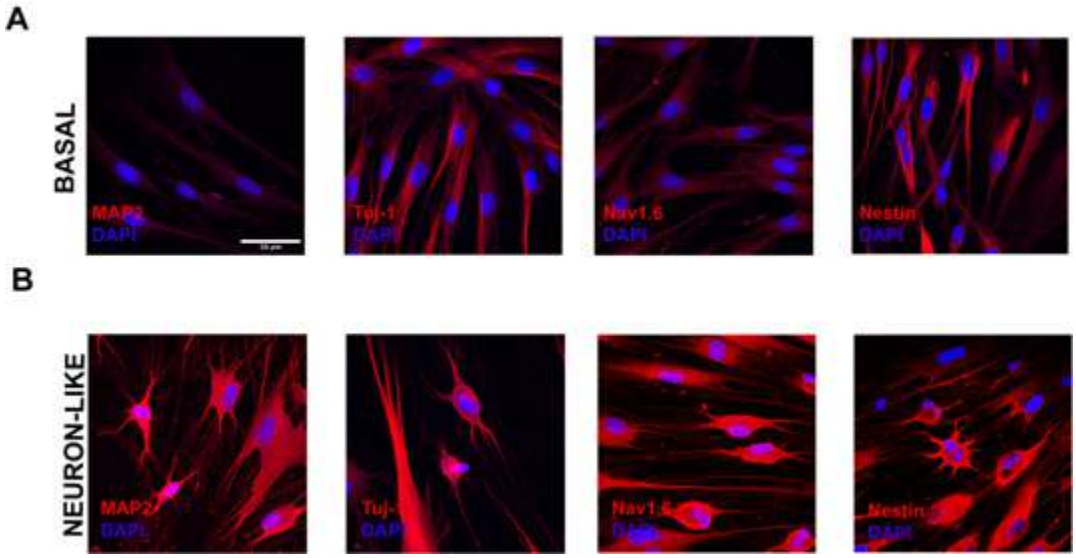

Figure 22. Neural markers expression in basal and differentiated hDPSCs.
In basal conditions, hDPSCs exhibited lower expression of different neural markers: MAP2, Tuj-1 and Nav1.6. Nestin expression was evaluated as NCP marker (A). By contrast, when they were differentiated into neural lineage, expression of these markers seemed to be increased (B). Images (40x) were taken by Leica SPEII confocal microscope.

In order to analyse if X-ALD hDPSCs reproduce pathological defects when are differentiated into neural lineage, we performed differentiation experiments and analysed specific X-ALD hallmarks. Firstly, both differentiated healthy and X-ALD cells expressed ALDP similarly as in their basal media with perinuclear and cytoplasmatic expression, although immunocytochemistry showed stronger expression in X-ALD neurons (Fig. 23, A). Interestingly, when we studied neutral lipid accumulation, we observed similar results to what we observed in basal hDPSCs. BODIPY 493/503 staining revealed differences between X-ALD and healthy differentiated cells. Even when X-ALD hDPSCs were differentiated into neural lineage, pathological hallmark features persisted with higher accumulation of neutral lipids (Fig. 23, B). This remarkable accumulation of neutral lipid was confirmed by quantification of fluorescence intensity by CTCF values (Fig. 23, C). Furthermore, slightly differences were found in Nav1.6 expression, a general marker for Na^+ channels. X-ALD neuron-like cells seemed to show less expression of this marker, suggesting an alteration in the excitability of these differentiated cells (Fig. 23, D). This hypothesis was consistent with obtained results of electrophysiological records. Whole-cell patch clamp records revealed significant differences between healthy and X-ALD differentiated cells in terms of amplitude and kinetics of Na^+ channels. In the case of X-ALD neuron-like cells, they showed evident lower peak amplitude and slower kinetics indicating an alteration in process of neuronal

differentiation that might be caused by pathological defects derived from the disease (Fig. 23, E). In addition to this fact, we found significant differences in terms of maximum intensity of Na^+ currents between cell populations confirming our hypothesis (Fig. 23, F). Altogether, X-ALD hDPSCs both in their basal or in their neural-differentiated status might be a feasible model to study X-ALD.

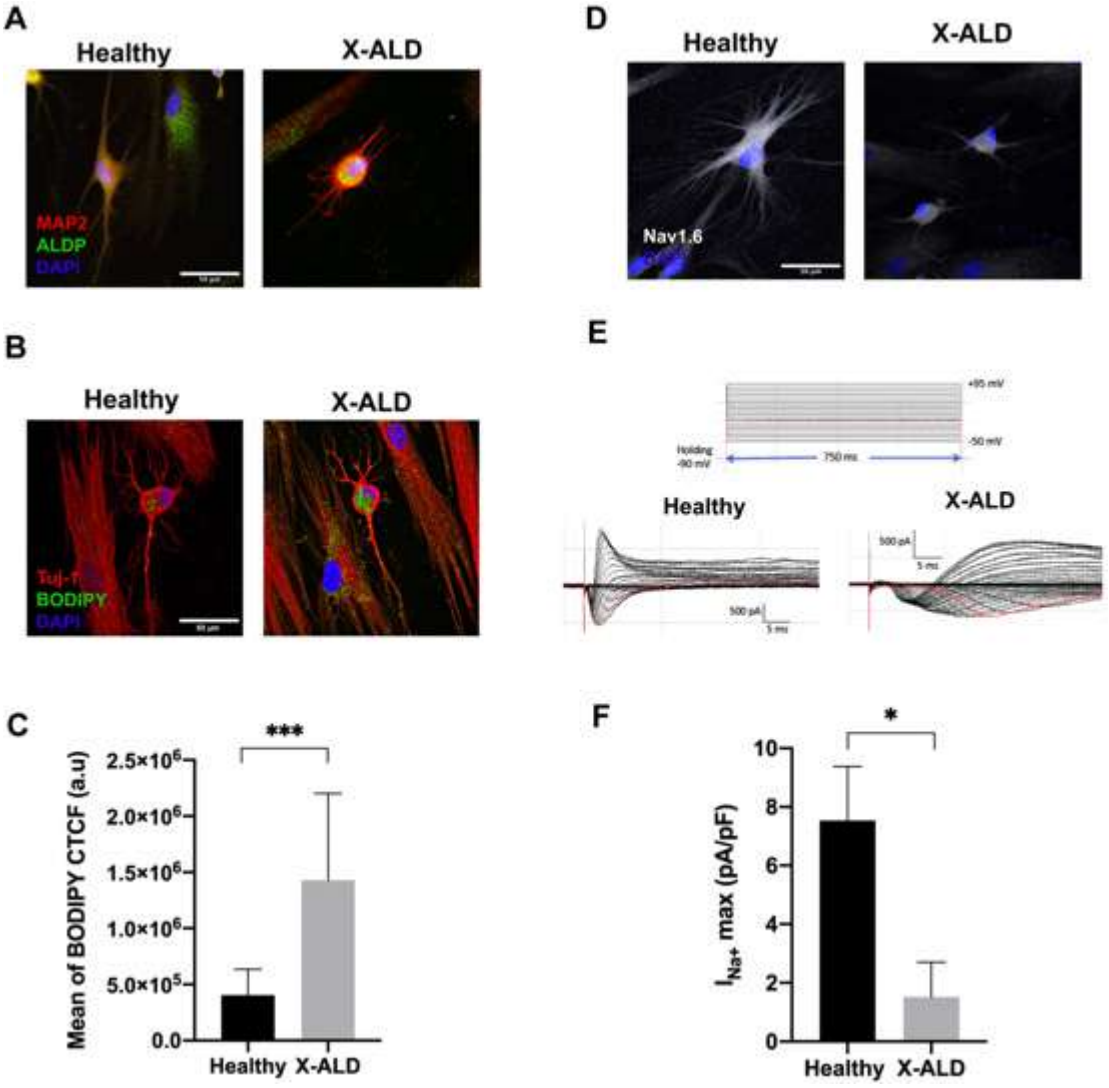

Figure 23. X-ALD hDPSCs differentiate into neural lineage and reproduce X-ALD hallmarks. Healthy and X-ALD differentiated cells showed immunoreactivity to ALDP (A). Alteration in neutral lipid accumulation was also evident in X-ALD differentiated cells, which exhibited higher accumulation than healthy differentiated cells (B). This difference was quantified in terms of CTCF showing significant differences between cell populations (C). Immunofluorescence of differentiated cells showed slight differences in Nav1.6 expression (D). Whole-cell patch clamp experiment revealed functional differences in amplitude and kinetics of Na^+ channels from X-ALD neuron-like cells (E). Measures of maximum intensity of Na^+ currents revealed significant differences between healthy and X-ALD neuron-like population (F). Graph show the meaning and SDs bar errors of CTCF of BODIPY 493/503 (C) and

maximum intensity currents of Na^+ (F). Comparisons between samples were made using tests for independent samples (Mann-Whitney tests). Images (40x) were taken by Leica SPEII confocal microscope. Asterisks indicate p value: p<.05 (*), p<.001 (***), a.u: arbitrary units, pA: picoamperes, pF: picofarads.

2. Therapeutic effect of hBMSCs

2.1 Cell characterization of hBMSCs.

Following the same protocol as hDPSCs and based on ISCT criteria, human bone marrow isolated cells were characterized in terms of mesenchymal stemness. Cell population showed adherence to plastic surface and exhibited fibroblast-like morphology under *in vitro* standard conditions (Fig. 24, A). Furthermore, analysis of expression of different surface receptors aligned with established criteria as they expressed CD90 (78.0 ± 2.3 %), CD44 (95.0 ± 2.9 %) and CD105 (79.2 ± 2.6 %) (Fig.23, B and C) while lacking expression of CD34 and CD45 (data not shown), more specific of HPCs.

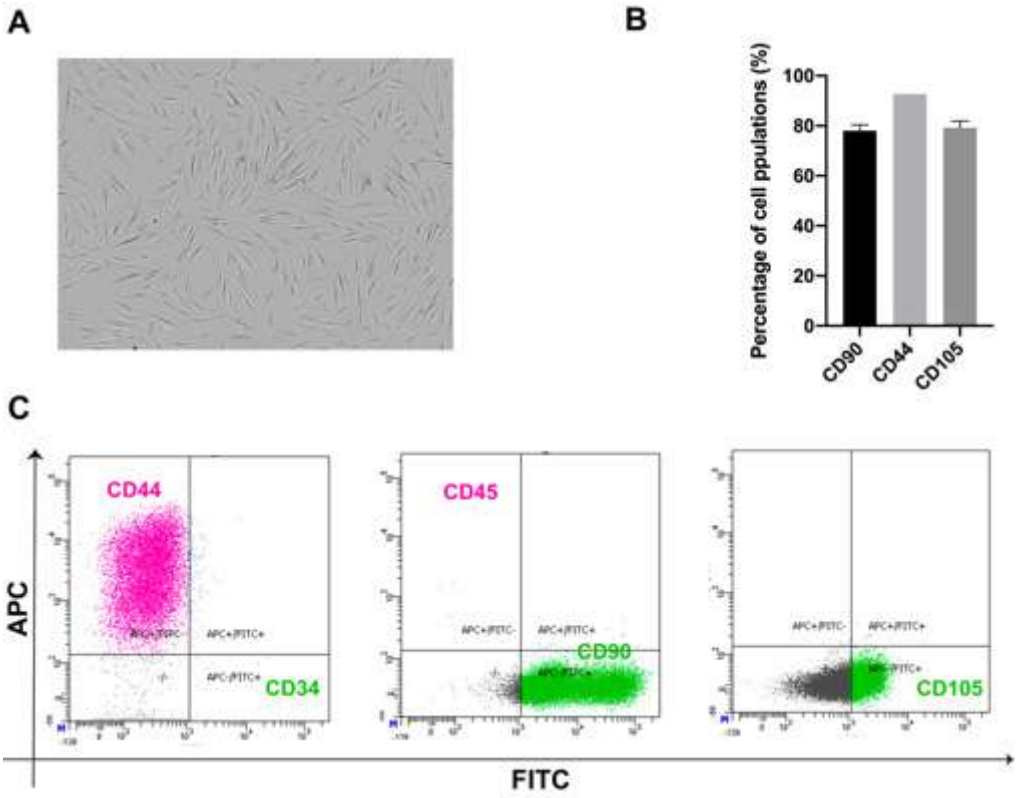

Figure 24. Mesenchymal characterisation of human bone marrow isolated cells.
Phase contrast image of hBMSCs under *in vitro* standard conditions (A). Graph showing mean of cell percentage (%) of different stem cell markers such as CD90, CD44 and CD105 (B). Flow cytometry scatter plots of mentioned markers (C). Each dot represents an individual cell and the density of dots indicates the relative abundance of cells in each quadrant. The phase contrast image (10x) was acquired with InCuCyte incubator.

2.2 EVs characterization of CM derived from hBMSCs.

As mentioned before, paracrine effect of hBMSCs is one of the most interesting therapeutic mechanisms of this cell population. Most of these beneficial effects are due to their paracrine activity and, as a consequence, partially due to the EVs release. In order to determine the presence of EVs in CM derived from hBMSCs, we isolated EVs through centrifugation and ultracentrifugation methods.

Using TEM imaging we could confirm the presence of EVs in CM derived from hBMSCs, confirming their morphology (Fig. 25, G). To better characterise these EVs, we also analysed ultracentrifugated CM by imaging flow cytometry. These results confirmed the presence of EVs of different sizes, corresponding to the different types of EVs that could be found in CM (MVs and Exos) (Fig. 25, A). Thus, we further classified CM population according to the expression of several markers of interest: CD63, Hsp70 and calnexin. Hence, we assured precise characterisation of EVs with their specific markers and excluded any type of cell debris related to calnexin expression (Fig. 25, B). EVs expressed CD63 (Fig. 25, C and F) and Hsp70 (Fig. 25, D and F) while lacking expression of calnexin (Fig. 25, E), confirming their intrinsic characteristic as EVs.

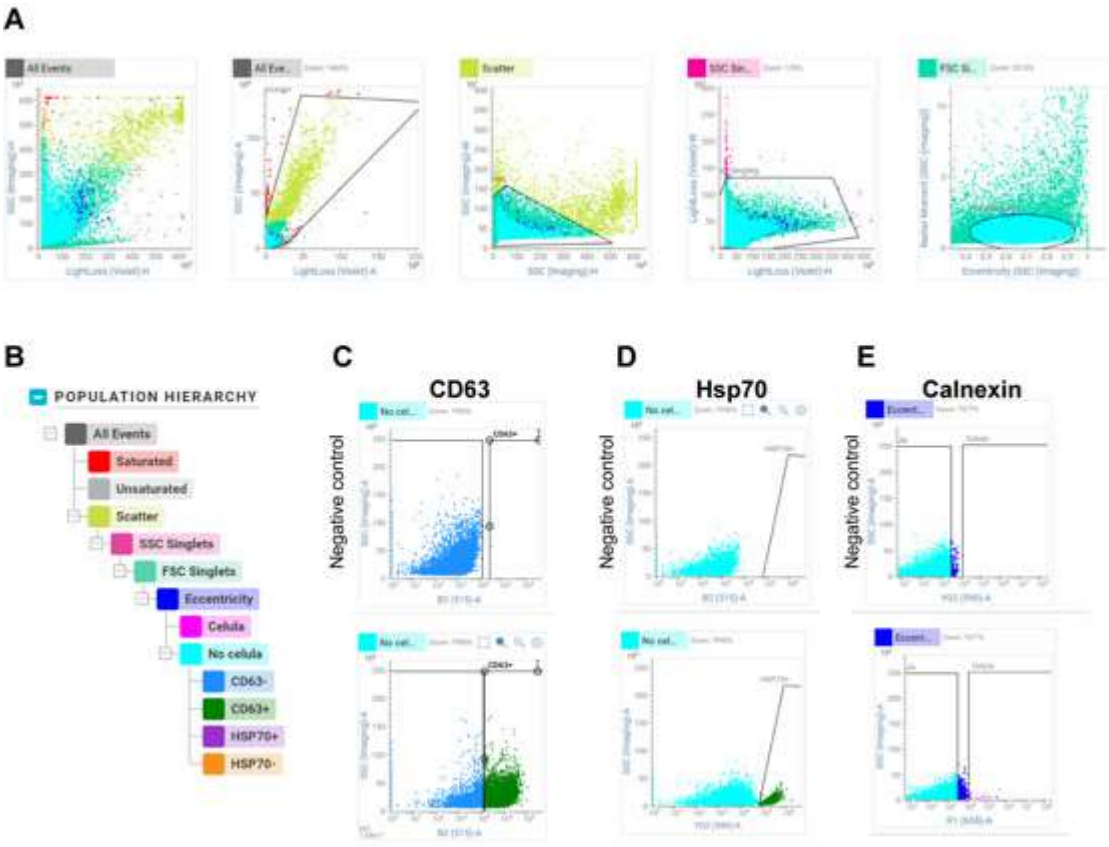

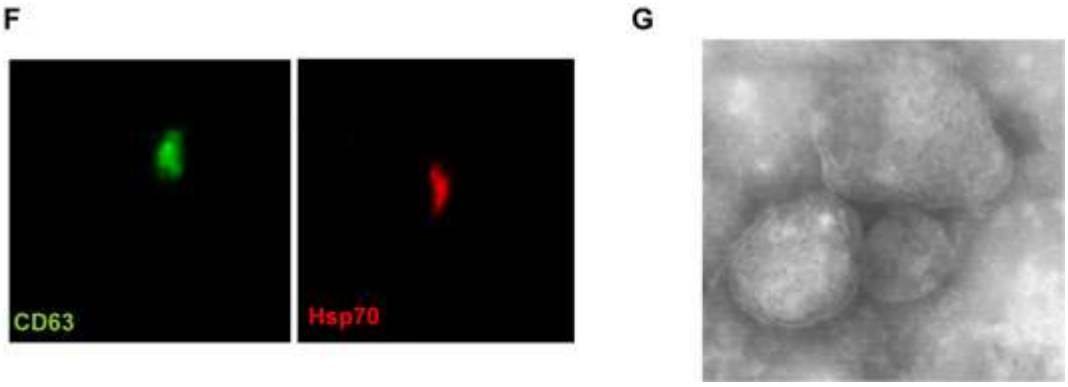

Figure 25. Flow cytometric and microscopic characterisation of EVs found hBMSCs-derived CM. Gating strategy employed to define EV population incorporating size, light scatter properties and eccentricity with precise identification of EVs based on their physical characteristics (A). Hierarchical classification of cell populations showing the segregation of various cellular and EVs subpopulations within the CM sample (B). Marker expression profiles for EVs highlighting presence of CD63 and Hsp70 on EVs while calnexin is found on cell population (C-E). Representative imaging of $CD63^{+}$/$Hsp70^{+}$ EVs processed by imaging flow cytometry (F). TEM image revealing morphology and distribution of EVs found in hBMSCs-derived CM.

2.3 Direct and indirect effect of hBMSCs on X-ALD hDPSCs.

After establishing the *in vitro* model of X-ALD using hDPSCs, the next step was to analyse the therapeutic effects of hBMSCs. To achieve this, we conducted both direct and indirect co-culture experiments. The direct co-cultures allowed us to study cell-to-cell interactions and the direct exchange of components between the different cell populations. In contrast, the indirect co-cultures enabled us to investigate the paracrine effects of hBMSCs through the release of soluble factors. These complementary approaches are essential for understanding the underlying mechanisms of potential cell-based and cell-free therapies for X-ALD.

2.4 Lentiviral transduction of hDPSCs and hBMSCs.

Prior to the establishment of direct co-cultures of hDPSCs and hBMSCs, cell cultures were transduced with different lentiviral constructs in order to distinguish cell populations *in vitro*. Due to their mesenchymal characteristics, both cell populations – hDPSCs and hBMSCs – exhibit same morphology with fibroblast-like shape and high adherence to plastic under standard *in vitro* conditions. Additionally, both cell populations express mesenchymal stem cell markers in line with ISCT criteria (Dominici et al., 2006). These shared characteristics reinforce the importance of using lentiviral constructs to discern between the cell populations during co-culture experiments.

Different lentiviral constructs were used depending on the specific co-culture experiment. To analyse cell-to-cell interactions and the potential exchange of cytoplasmatic and/or membrane material, we used lentiviral constructs with constitutive expression of GFP and RFP under the control of ubiquitin promoter allowing green or red fluorescence of cell cytoplasm. In these experiments, healthy and X-ALD hDPSCs were marked using RFP lentivirus (Fig. 26, A), while hBMSCs were marked with GFP lentivirus (Fig. 26, B).

In contrast, for experiments related to mitochondrial trafficking, X-ALD hDPSCs were labelled with GFP lentivirus (Fig. 26, C) and hBMSCs were transduced with a specific- RFP mitochondria lentiviral construct (Fig. 26, D). Cell viability of lentiviral transduced cells was analysed and no differences were observed compared to their non-transduced counterparts (data not shown). Thus, we established distinct direct co-culture in which each cell population could be easily distinguished.

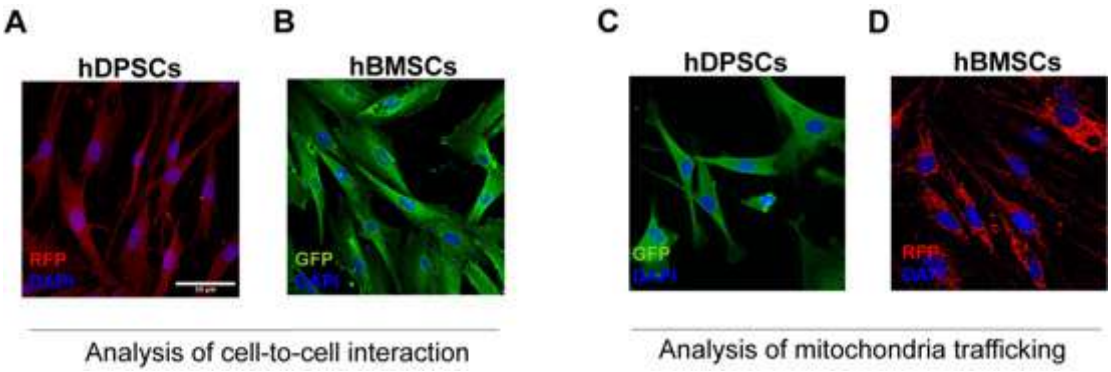

Figure 26. Lentiviral transduction of hDPSCs and hBMSCs.
Healthy and X-ALD hDPSCs transduced with Lentivirus RFP (A) and GFP (C) depending on the aim of study. hBMSCs transduced with Lentivirus GFP (B) when hDPSCs were transduced with RFP or mito-Red (D) when hDPSCs were transduced with GFP. Images (40x) were taken by Leica SPEII confocal microscope (A, C, D) and Thunder Leica microscope (B).

2.5 ALDP analysis of hDPSCs directly and indirectly co-cultured with hBMSCs.

In order to assess the effect of hBMSCs on ALDP expression, we performed direct and indirect co-cultures of X-ALD hDPSCs with hBMSCs or its CM-containing EVs. After three days of co-culture, we analysed ALDP expression by immunofluorescence. Neither the hBMSCs nor their CM induced apparent changes in ALDP expression in X-ALD hDPSCs. X-ALD hDPSCs maintained the same expression pattern observed in their standard culture media (basal), with positive immunoreactivity in the perinuclear zone and cytoplasm (Fig. 27, A and B). Interestingly, in the direct co-cultures, both in TNT formation (white arrows) and cell-to-

cell interaction zones (white arrowheads), we could observe regions of contact with immunoreactive for ALDP suggesting a possible exchange or traffic of healthy peroxisomes from hBMSCs to X-ALD cells (Fig. 27, C).

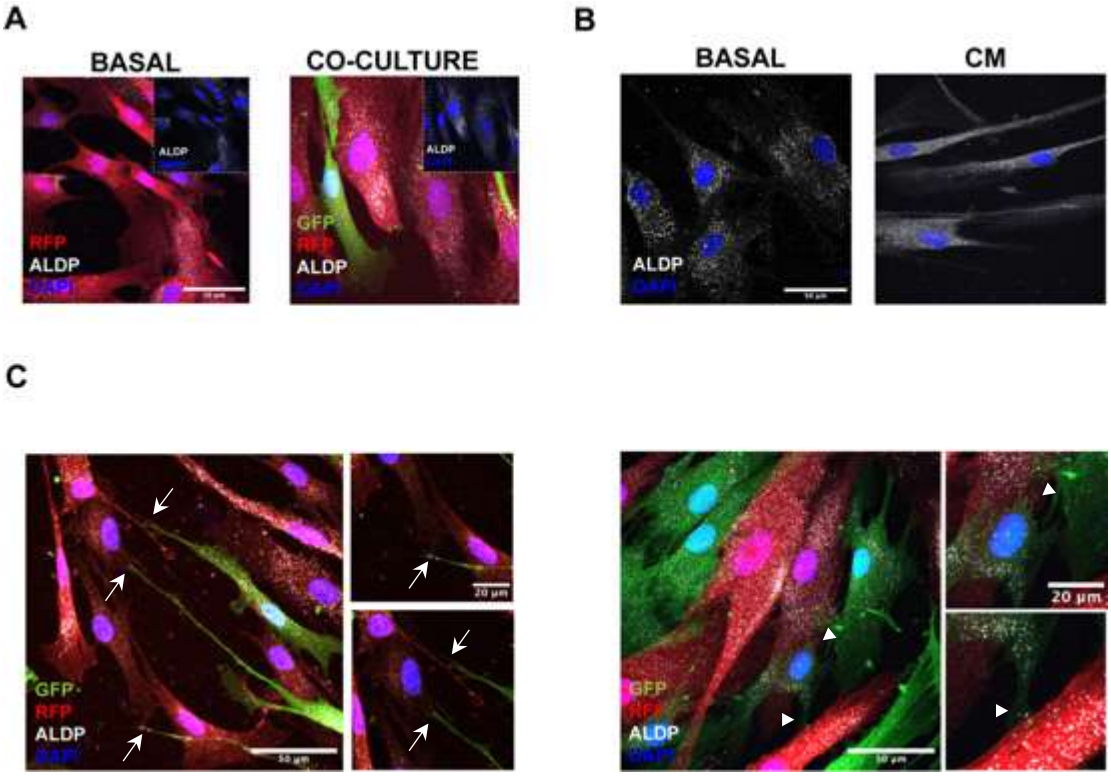

Figure 27. ALDP expression in X-ALD hDPSCs with different treatments of hBMSCs.
In standard *in vitro* conditions, in studied X-ALD hDPSCs, ALDP showed punctuate staining pattern across cytoplasm (A, B; basal). When X-ALD hDPSCs were co-cultured both with hBMSCs (A) and CM-containing EVs from hBMSCs (B), no changes in ALDP expression and distribution were noticed. However, in TNTs (left, arrows) and cell-to-cell contacts (right, arrowheads), immunopositive peroxisomes were observed suggesting a possible direct exchange of healthy peroxisomes to X-ALD hDPSCs (C). Images (40x) were acquired with Leica SPEII confocal microscope. Cropped and zoomed images were processed using Fiji software.

2.6 Neutral lipid accumulation study in presence of hBMSCs.

One of the hallmarks of X-ALD is the accumulation of VLCFA in bloodstream, cells and tissues (Moser et al., 1981). As mentioned before, X-ALD hDPSCs are a feasible model to *in vitro* reproduce X-ALD because, among other characteristics, they exhibited elevated neutral lipid accumulation within the cytoplasm and perinuclear regions compared to healthy cell populations. With the aim to study both the direct impact of hBMSCs and their paracrine effect on build-up of neutral lipids, we performed direct and indirect co-cultures of hBMSCs or their

CM-containing EVs and X-ALD hDPSCs. Once we established mentioned co-cultures, we analysed neutral lipid accumulation by BODIPY 493/503 and LipidTOX Deep Red staining following the same protocol than in the developing *in vitro* model. We tracked neutral lipid staining across time in both types of co-cultures. After three days, we observed a significant reduction of this aberrant accumulation when cells were incubated with presence of CM-containing EVs both in BODIPY 493/503 and LipidTOX Deep Red staining. To confirm that this fact is exclusively due to the paracrine function of hBMSCs, we parallely performed same experiments with basal media composed by DMEM 1X. In this control group (DMEM 1X), none evidence of neutral lipid reduction was noticed neither by BODIPY 493/503 nor LipidTOX Deep Red staining confirming our hypothesis (Fig. 28, A and C). This reduction was quantified in terms of CTCF and results were in line with what was observed in confocal images (Fig. 28, B and D).

The following step was to analyse the direct effect of hBMSCs on neutral lipid accumulation and its possible reduction. As mentioned before, in direct co-cultures, prior to their establishment, cell populations were transduced with different lentiviral constructs. In this case, X-ALD hDPSCs were transduced with Lentivirus-RFP while hBMSCs followed same protocol for Lentivirus-GFP. All cell populations showed same cell growing as their cell counterparts without lentiviral transduction. Likewise, X-ALD hDPSCs-RFP showed abnormal neutral lipid accumulation in comparison to healthy RFP cells assessed by LipidTOX Deep Red staining (Fig. 28, E). After three days of direct co-culture, we assessed neutral lipid accumulation by LipidTOX Deep Red staining and we identified that X-ALD hDPSCs-RFP showed a slight increase in neutral lipid accumulation (Fig. 28, E) assessed by CTCF quantification (Fig. 28, F). These results confirmed that EVs present in CM of hBMSCs have an important and significant effect on VLCFA metabolism not seen in their cellular counterpart.

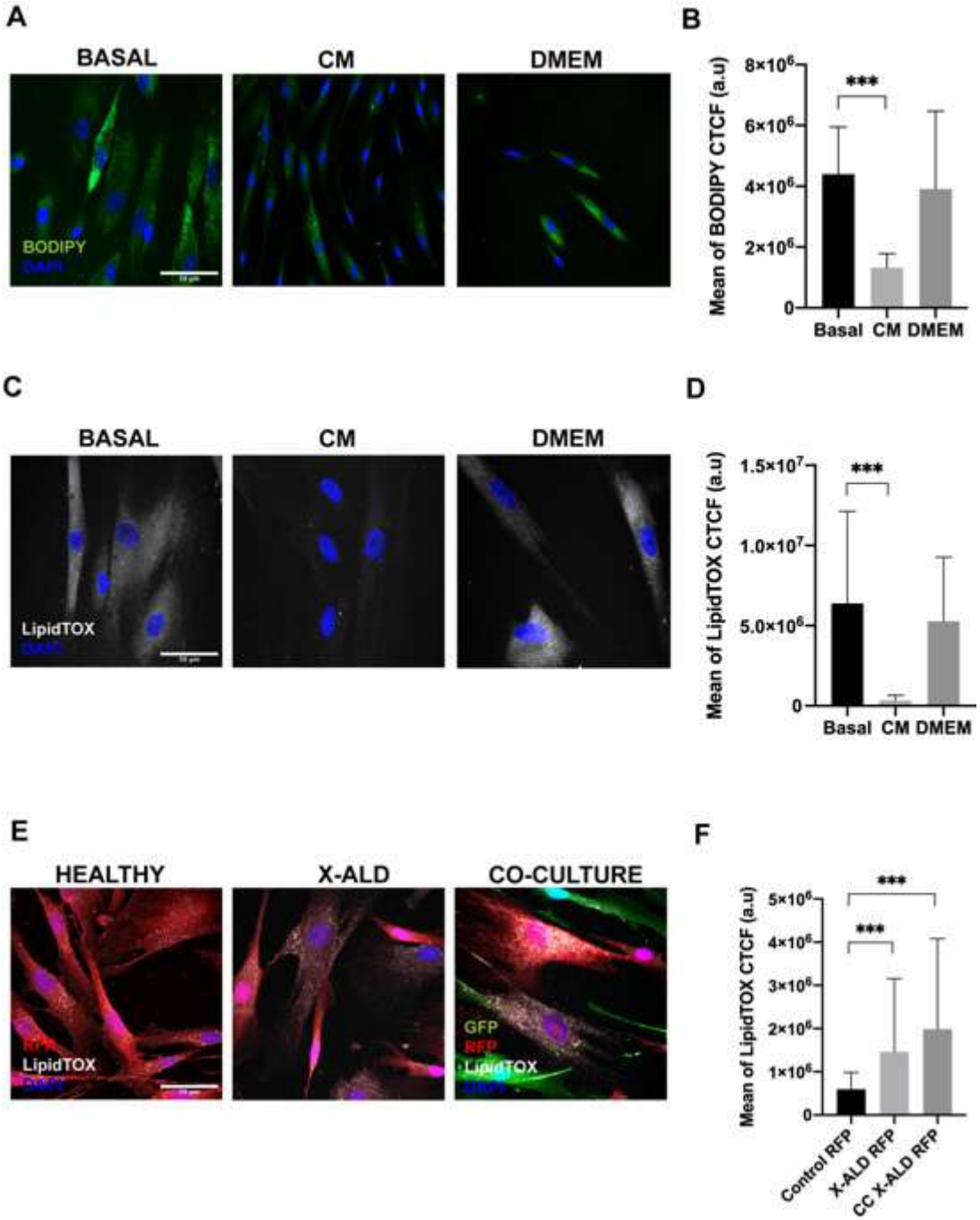

Figure 28. Direct and indirect effect of hBMSCs on neutral lipid metabolism and accumulation. CM-containing EVs from hBMSCs reduced altered neutral lipid accumulation, assessed by BODIPY 493/503 staining, in X-ALD hDPSCs within 72 hours compared to those incubated only with DMEM 1X (A). Reduction of fluorescence corresponding to neutral lipid was quantified in terms of CTCF (B). LipidTOX Deep Red staining revealed similar results with an evident decrease of neutral lipids accumulation when cells were cultured with CM-containing EVs from hBMSCs compared to those incubated only with DMEM 1X (C). This reduction was quantified in terms of CTCF (D). Healthy and X-ALD hDPSCs-RFP displayed significant differences in neutral lipid accumulation similarly to those observed in cells without lentiviral transduction. Direct co-culture of hBMSCs-GFP and X-ALD

hDPSCs-RFP resulted in a slight increase of neutral lipid accumulation after 72 hours (E) quantified by CTCF values (F). The histograms show mean of CTCF values of BODIPY 493/503 and LipidTOX Deep Red and SD bar errors. Multiple comparisons were made using tests for independent samples (Kruskal-Wallis test). Images (40x) were acquired using Leica SPEII confocal microscope. Asterisks indicate p value: p<.001 (***), a.u: arbitrary units, CC: co-culture.

2.7 Protective effect of CM under oxidative stress conditions and cytotoxicity.

One of mechanisms implicated into the pathophysiology of X-ALD is oxidative stress. Evidences of oxidative stress in X-ALD were reported both in *post-mortem* tissue (Powers et al., 2005), plasma (Vargas et al., 2004) and in *in vitro* experiments (Baarine et al., 2012; J. Zhou et al., 2021). In this work, we were interested in determining whether CM-containing EVs could protect X-ALD hDPSCs from oxidative stress conditions. Hence, oxidative stress was induced using H_2O_2 prior to the addition of CM-containing EVs to cell cultures. Induction of oxidative stress was confirmed after incubating 500 µM of H_2O_2 for two hours. The changes in cell cultures were observed as a transition from spindle-shaped fibroblast-like morphology to a more rounded and shrunken form when they were incubated with H_2O_2 (Fig. 29, A). Further, oxidative stress was confirmed by Caspase3/7 expression (Fig. 29, B) evidencing a considerable increase in the percentage of cells expressing this apoptotic marker (Fig. 29, C).

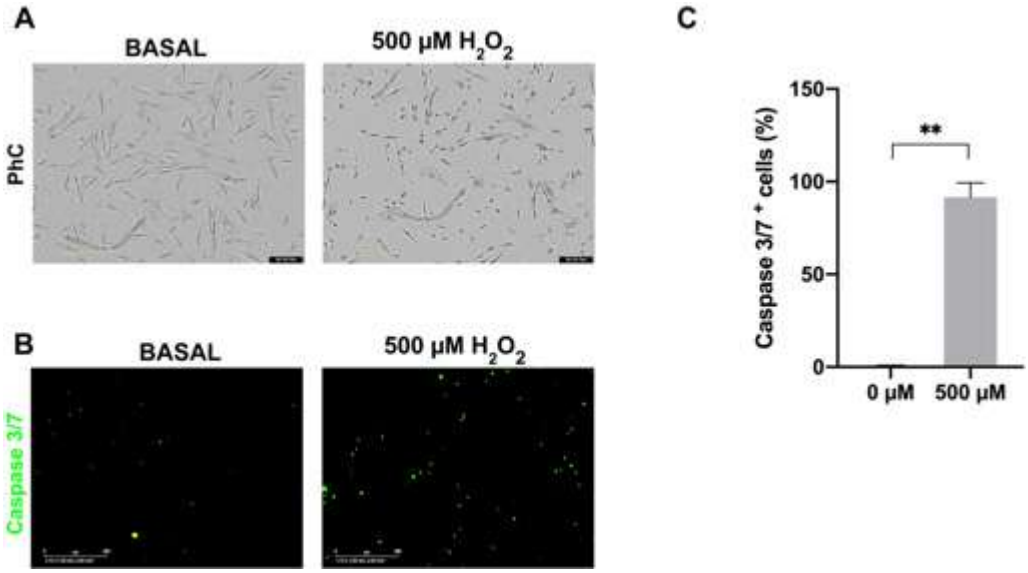

Figure 29. Induced oxidative stress in X-ALD hDPSCs by H_2O_2.

Phase contrast (PhC) images of X-ALD hDPSCs in their standard culture media, designated as basal, (left) and two hours after the addition of 500 µM of H_2O_2 (right) showing typical morphological changes due to apoptosis (A). Fluorescent images of X-ALD hDPSCs in basal media and after addition of 500 µM of H_2O_2 showing the expression of Caspase 3/7 (B), confirming cell apoptosis. Histogram shows

cell population percentage (%) positive to Caspase 3/7 and SDs bar errors. Comparison between samples were made using tests for paired samples (Mann Whitney tests). All images (10x) were taken using InCucyte incubator and processed by its software. Asterisks indicate p value: p<.01 (**).

Once cells were stressed, CM-containing EVs or DMEM 1X was added to cultures for 72 hours and evaluation of apoptosis was performed. First differences in apoptosis between cells incubated with CM-containing EVs or DMEM 1X were observed. Strikingly, most of cells incubated with DMEM 1X after oxidative stress induction were apparently dead or starting apoptotic process based on evident morphological changes under *in vitro* conditions. Most of cells incubated with DMEM 1X were damaged after 72 hours without any significant recovery of their *in vitro* morphology. By contrast, cells incubated with CM-containing EVs survived and returned to their original form with spindle-shape morphology (Fig. 30, A). Additionally, supernatants of these cultures were analysed by flow cytometry and significant differences were found between both groups. Stressed X-ALD cells incubated with DMEM 1X showed more particles in supernatants confirming more cell death in this group and also more cell debris compared to cells incubated with CM-containing EVs (Fig. 30, B).

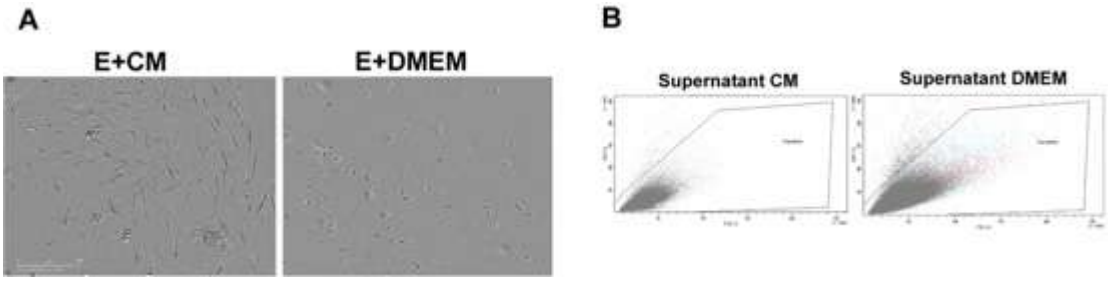

Figure 30. Effect of CM-containing EVs in cell viability of induced-oxidative stressed X-ALD hDPSCs.

Phase contrast images of stressed X-ALD hDPSCs after 72 hours incubated with DMEM 1X (right) and CM-containing EVs (left) with remarkable differences in cell viability. FSC vs SSC density plots from supernatants of CM (left) and DMEM group (right). DMEM group showed higher density of cell debris (B). Images (10x) were obtained from InCuCyte incubator and processed by its software.

Once we confirmed differences between cells incubated with CM-containing EVs or with DMEM 1X, the next step was to study specific markers of apoptosis. We choose the annexin V/7-AAD kit for flow cytometry as it enables the identification of different groups of the cell population based on their apoptotic damage: early apoptotic cells (Annexin V^+/ 7-AAD^-), late apoptotic cells (Annexin V^+/ 7-AAD^+) and dead cells (Annexin V^-/ 7-AAD^+).

Regarding results of Annexin V and 7-AAD expression, clearly differences were noticed in line with was previously observed. First of all, this kit also confirmed suitability of H_2O_2 as an inductor of oxidative stress as they notably increased cell percentage of cells expressing one or both markers (Fig. 31, A). Additionally, analysis of these apoptotic markers in stressed cells incubated with CM-containing EVs or DMEM 1X revealed evident differences (Fig. 31, B). As mentioned above, most of stressed cells incubated with DMEM were found in supernatants as cell debris. As a result, this group showed evident less cell population, restricted to only-surviving cells. In addition to this, stressed cells analysed by flow cytometry confirmed the presence of early (60.9 ± 5.1 %) and late apoptotic (17.4 ± 2.3 %) cells as well as death cells (16.9 ± 0.2 %). These categorized groups were also observed in stressed cells incubated with CM-containing EVs, but a reduced rate, being early apoptotic cells predominant (40.9 ± 4.7 %) followed by late (15.2 ± 0.7 %) and death cells (13.4 ± 0.9 %). These results confirmed the presumable protective effect of CM-containing EVs in oxidative stress environment, being able of rescuing a healthy phenotype of stressed X-ALD cells with a reduction of general apoptosis (Fig. 31, C) and cell death (Fig. 31, D).

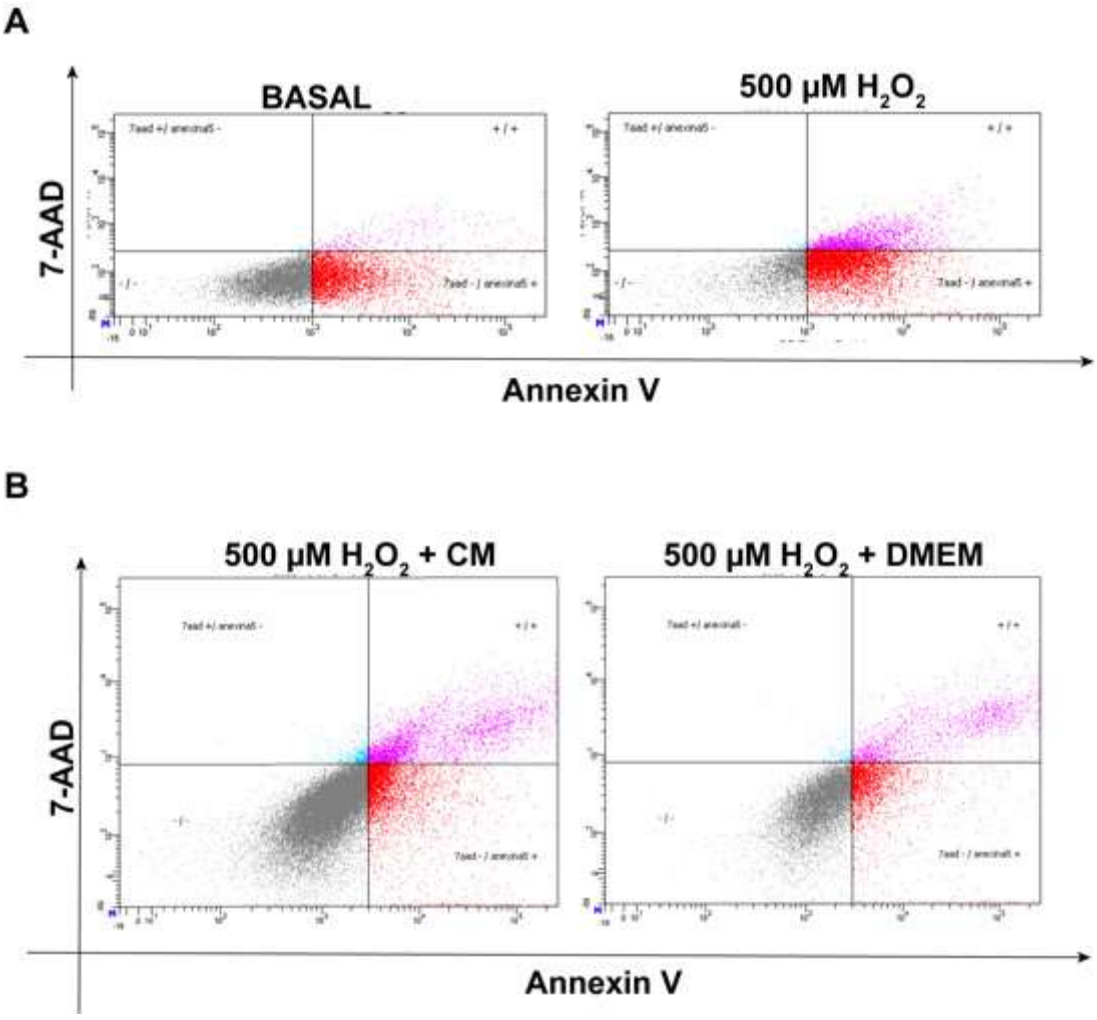

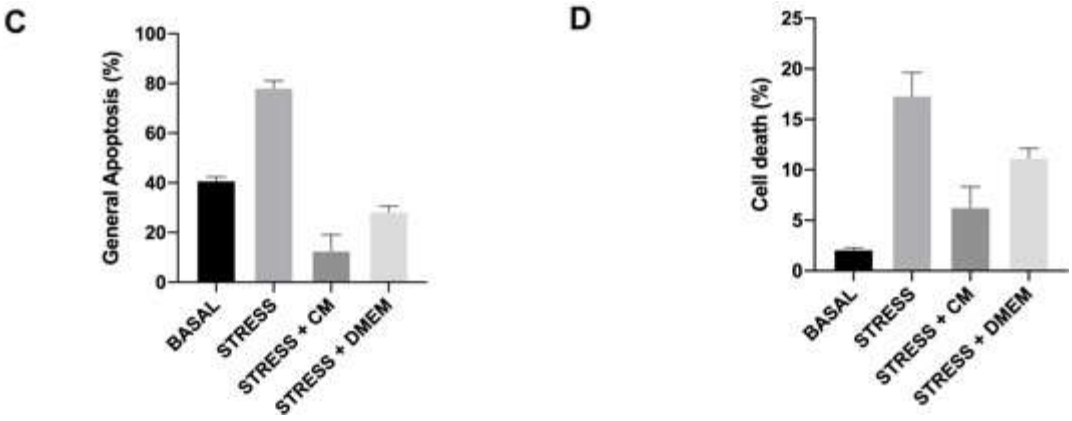

Figure 31. Analysis of protective effect of CM-containing EVs on stressed X-ALD hDPSCs through the expression of Annexin V and 7-AAD.

Flow cytometry scatter plots of Annexin V-PE and 7-AAD in X-ALD cells in basal and stress conditions (A) and incubated with CM-containing EVs or DMEM 1X after 72 hours (B). Each dot represents an individual cell and the density of dots indicates the relative abundance of cells in each quadrant. Graphs show mean of percentage of cells expressing early and late apoptotic markers (general apoptosis) (C) and cell death (D) and SDs bar errors of different examined conditions.

2.8 Effect of CM in X-ALD hDPSCs cultured with an excess of C26:0.

In the previous chapter we exposed the divergent effect of C26:0 in healthy and X-ALD hDPSCs. Whereas in healthy cell population, C26:0 did not induce any significant change in their cell growth or viability, in X-ALD hDPSCs, this type of VLCFA induced delayed in cell growth and even cell death when exposed to higher concentrations. This fact confirmed that X-ALD hDPSCs presented an alteration in C26:0 metabolism through peroxisomal β-oxidation, characteristic of the disease.

With the aim to analyse if the indirect use of hBMSCs could ameliorate the disruptive effect of C26:0 in X-ALD cell cultures, we performed indirect co-culture experiment using CM-containing EVs derived from hBMSCs. Based on previous experiments, we used the same concentrations of C26:0 and analysed same parameters: cell confluence and cell death percentages. Surprisingly, when X-ALD cells were incubated both with C26:0 and CM-containing EVs, notably changes were noticed. CM induced a rescue in cell growth of X-ALD hDPSCs exposed to 50 μM of C26:0. Without the presence of CM-containing EVs, C26:0 caused a delayed in cell growth, but CM normalized cell growth to basal conditions (Fig. 32, A). This cell growth was quantified in terms of cell confluence percentage (Fig. 32, B).

When used increased concentrations of C26:0, CM-containing EVs also caused significant changes. Concretely, CM rescued a healthy phenotype and induced a protective

effect against cytotoxicity of C26:0 to X-ALD cell cultures. When X-ALD cells were exposed to 100 μM of C26:0, most of them abruptly died. However, this high concentration of C26:0 did not induce such cell death if CM-containing EVs were present in the culture indicating an apparent correction in VLCFA metabolism (Fig. 32, C). Cell death and their rescue were quantified confirming our hypothesis (Fig. 32, D).

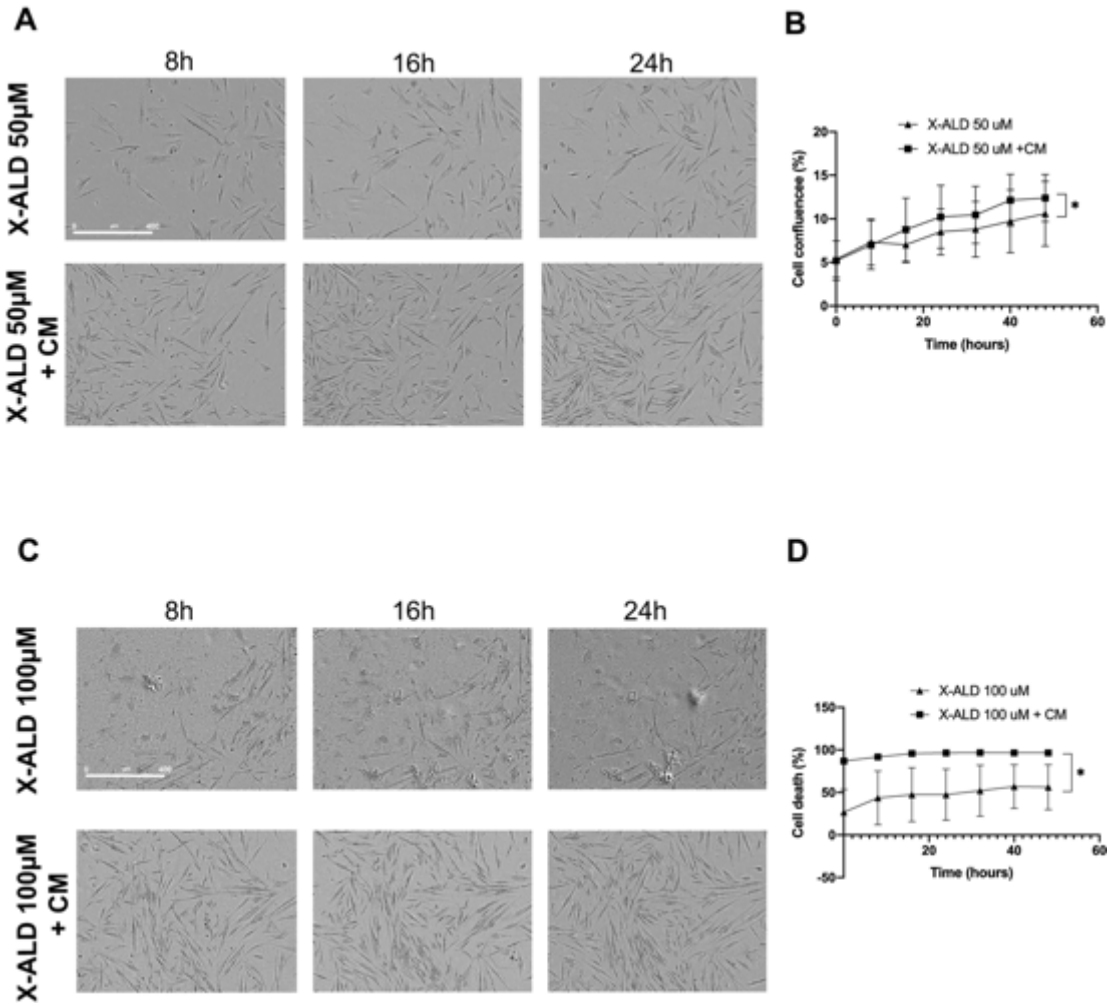

Figure 32. Protective effect of CM-containing EVs on X-ALD hDPSCs cultured with an excess of C26:0.

Phase contrast images of time-lapse cultures of X-ALD hDPSCs cultured with 50 μM (A) and 100 μM (B) of C26:0 with and without CM-containing EVs. Significant differences were found in X-ALD cells treated with CM-containing EVs in terms of cell growth (C) and viability (D). Comparisons were made using tests for paired samples (Wilcoxon matched pair signed rank test). All images (10x) were obtained from InCuCyte incubator and processed by its software. Asterisks indicate p value: p<.05 (*).

2.9 Direct effect of hBMSCs on neural-like cells.

The therapeutic role of hBMSCs on neuronal plasticity has been studied for several years (Azevedo-Pereira et al., 2024). In this case, we sought to analyse the direct effect of hBMSCs on neural differentiated X-ALD cells. In the previous chapter, we exposed significant functional differences of differentiated neural-like X-ALD cells in comparison to healthy differentiated cells. Knowing this, we attempted to determine the direct effect of hBMSCs on these differentiated cells in terms of functionality through electrophysiology experiments. X-ALD hDPSCs followed the neural differentiation protocol and, five days before analysis, hBMSCs-GFP were added to cell cultures. At day *in vitro* 40 (DIV), healthy and X-ALD neural-like cells were analysed by whole-cell patch clamp records. Interestingly, we found evident differences in X-ALD neural-like cells when were co-cultured with hBMSCs. In this case, the pattern of Na^+ currents restored their healthy status, changing their amplitude and kinetics being more similar to healthy differentiated cells (Fig. 33, A). In more detail, we examined this fact and quantified the maximum current of sodium normalised to cell size and found significant differences between healthy and X-ALD differentiated cells, evidencing an alteration in the neuronal differentiation process exclusively in the disease-case. This evident difference was not seen when hBMSCs were co-cultured with X-ALD cells (Fig. 33, B). In line with this, we also explored the time to peak value which corresponds to the interval between the onset of an electrical signal and its maximum amplitude, indicating the speed of cellular response or signal propagation. Consistent with the changes observed in Na^+ current kinetics, X-ALD neural-like cells showed slower time-to-peak than their healthy counterparts, suggesting delayed signal propagation and impaired neuronal activity. However, when these cells were directly co-cultured with hBMSCs-GFP, their time-to-peak was significantly reduced being more similar to healthy cells and indicating a striking rescue of phenotype (Fig. 33, C). This change further corroborated the idea that the presence of hBMSCs facilitated the restoration of normal neuronal activity and functionality in X-ALD cell population. Altogether, these results provide compelling evidence that hBMSCs can directly influence the electrophysiological properties of X-ALD neural-like cells, significantly improving their functionality. This highlights the potential of hBMSCs as a therapeutic approach for restoring neuronal plasticity and function in neurodegenerative diseases like X-ALD. Therapeutic effects of hBMSCs may be mediated through their ability to modulate ion channel activity, particularly in relation to Na^+ currents, and may involve mechanisms such as the release of soluble factors or direct cell-to-cell interactions that promote functional recovery.

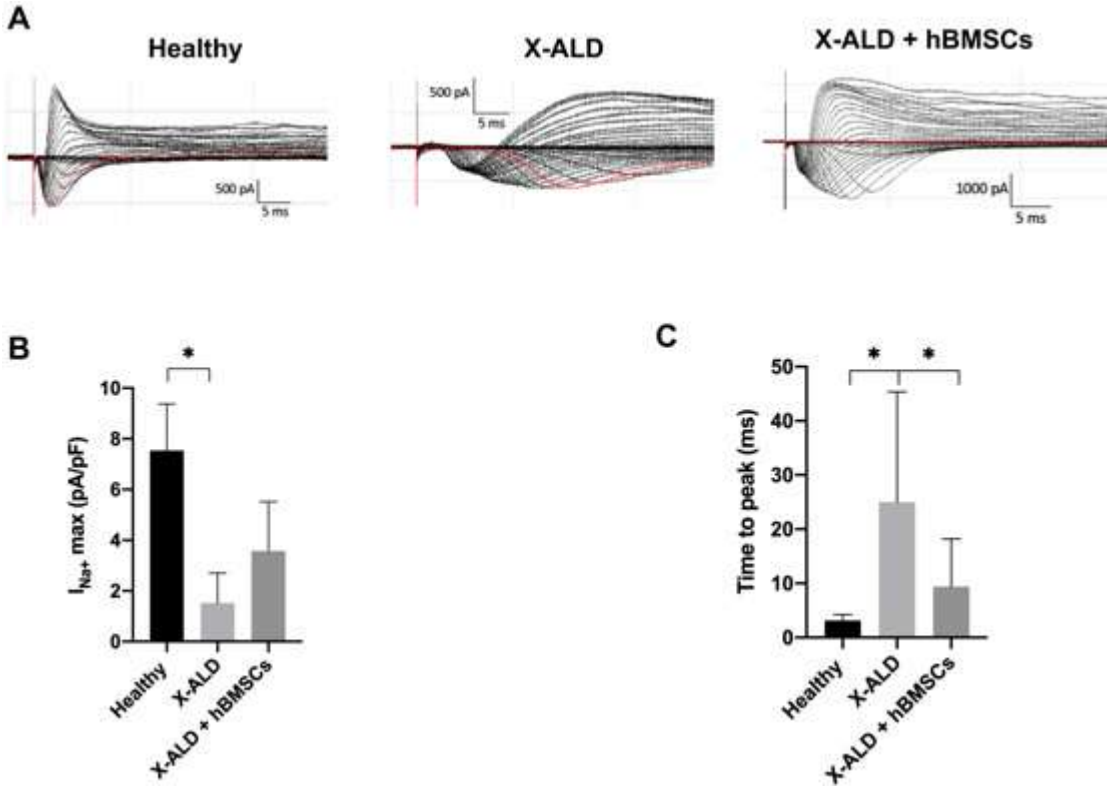

Figure 33. hBMSCs correct the deficient neuronal-like differentiation of X-ALD hDPSCs.
Electrophysiologic recordings (whole-cell patch clamp) of neural-like differentiated healthy and X-ALD hDPSCs (A). X-ALD neural-like cells showed Na^+ and K^+ currents with lower peak amplitude and slower kinetics than healthy neural-like cells. When X-ALD neural-like cells were co-cultured with hBMSCs, differentiated cells increased their maximum Na^+ current (B) and reduced their time-to-peak (C), rescuing a healthy phenotype. The histograms show mean values of maximum intensity current of Na^+ (B) and time to peak (C) and SDs. Comparisons between samples were made using tests for independent samples (Mann-Whitney tests). Asterisks indicate p value: p<.05 (*), pA: picoamperes, pF: picofarads, ms: milliseconds.

2.10 Intercellular communication and exchange of cytoplasmatic components.

Direct cell-to-cell communication is one of mechanisms of action of hBMSCs. Through the establishment of contacts, hBMSCs can exert their activity in different cell co-cultures. Within this context, we sought to analyse direct cellular communication between hBMSCs and X-ALD hDPSCs. As mentioned before, the different cell populations were transduced with different lentiviral constructs in order to discern between them. In this case, following the same strategy than in neutral lipid studies, we transduced X-ALD hDPSCs with Lentivirus-RFP and hBMSCs with Lentivirus-GFP. Thus, X-ALD hDPSCs-RFP and hBMSCs-GFP co-cultures were established in a ratio 1:1 for 72 hours. Three days after co-cultures were established, we analysed cell-to-cell contacts. First of all, we clearly noticed that both cell

populations interacted each other, with different types of contacts. We observed cell-to-cell communication between distant cells through the formation of TNTs, but also interaction between closer cells were reported (Fig. 34, A). To analyse these closer interactions in further detail, we studied the formation of gap junctions in cell-to-cell contacts. hBMSCs-GFP interacted with X-ALD hDPSCs-RFP through formation of gap junctions confirmed by the localization of Cx-43 (white arrows) at the intercellular contacting zones (Fig. 34, B).

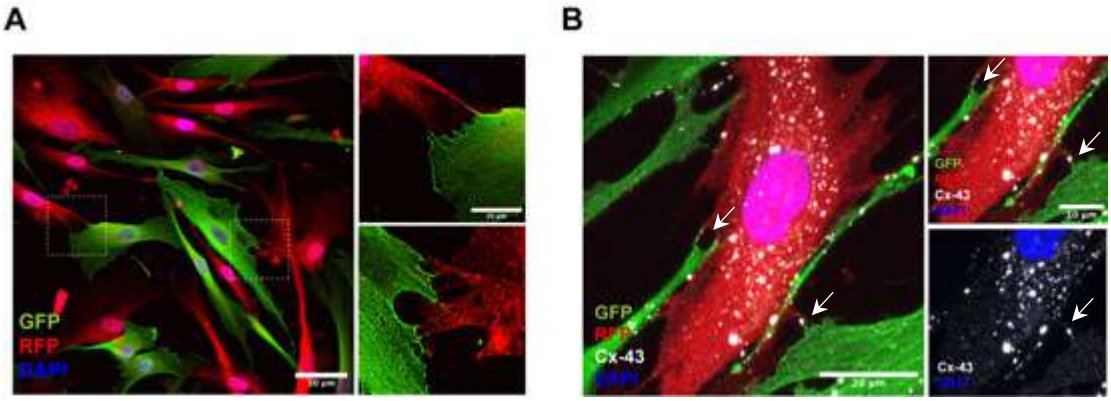

Figure 34. Cell-to-cell interactions of X-ALD hDPSCs and hBMSCs.

Direct co-cultures of hBMSCs-GFP and X-ALD hDPSCs-RFP revealed cell-to-cell interactions between different cell populations (A). These cell-to-cell interactions were established through GJ formation, confirmed by Cx-43 immunofluorescence (B. white arrows). All images (40x and 63x) were taken by Leica SPEII confocal microscope. Cropped and zoomed images were processed using Fiji software.

Through establishment of intime contacts between cell population, exchange of different factors could be done (Plotnikov et al., 2010; Velarde et al., 2022). In this case, we analysed a possible exchange of cytoplasmatic material from hBMSCs-GFP to X-ALD hDPSCs-RFP. Interestingly, we observed cytoplasmatic material derived from hBMSCs-GFP in X-ALD hDPSCs-RFP as a form of GFP material in X-ALD hDPSCs-RFP cytoplasm. To demonstrate the inclusion of this endogenous material, orthogonal projections of confocal images were studied and confirmed our hypothesis (Fig. 35, A). Next step was to study determinant components found in this exogenous GFP cytoplasmatic component as healthy ALDP. Thus, we performed ALDP expression analysis by immunofluorescence. Surprisingly, when orthogonal projections of this immunofluorescence images were analysed, we confirmed the presence of $ALDP^{+}$ peroxisomes, derived from hBMSCs, included in the cytoplasmatic material found in X-ALD cytoplasm (Fig. 35, B). Nevertheless, the cell percentage of X-ALD hDPSCs RFP presenting GFP material with healthy peroxisomes was low in comparison to the high percentage of X-ALD with GFP inclusions (Fig. 35, C). This fact confirmed donation of

healthy peroxisomes to X-ALD cell population and opens the possibility of a probable restoration of ALDP function.

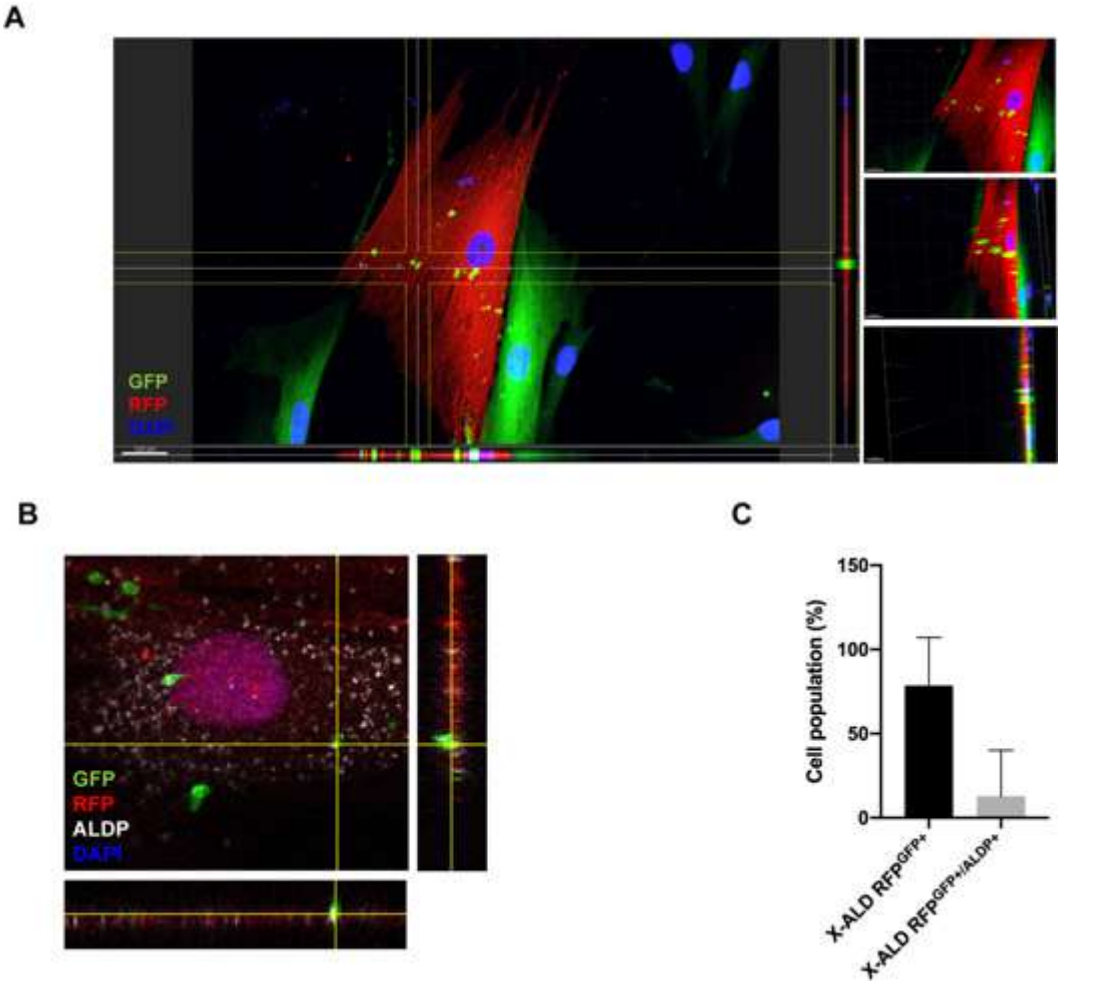

Figure 35. Direct co-culture of X-ALD hDPSCs and hBMSCs revealed cytoplasmatic material donation from hBMSCs.

Orthogonal projections of direct co-cultures demonstrated that X-ALD hDPSCs-RFP included GFP cytoplasmatic material in their cytoplasm, confirming exchange of cellular components (A). Immunofluorescence against ALDP confirmed presence of healthy peroxisomes in these GFP cytoplasmatic material included in X-ALD hDPSCs RFP, suggesting an exchange of healthy peroxisomes from hBMSCs (B). The histogram shows the meaning and SDs bar errors of cell percentage of X-ALD hDPSCs-RFP with GFP material and with GFP material and presence of ALDP immunoreactivity (C). Images (40x) were acquired using Leica SPEII confocal microscope. Cropped and zoomed images were processed by Fiji software. Orthogonal projections were obtained with Imaris (A) and Fiji software (B).

2.11 Direct cell-to-cell communication and exchange of healthy mitochondria

Once we confirmed the direct exchange of cytoplasmatic components through cell-to-cell contacts, we aimed to assess if there was an exchange of other cellular components such as mitochondria. The critical role of mitochondria in X-ALD was exhaustively studied before being determinant in oxidative stress (Fourcade et al., 2015). Thus, we performed direct co-cultures of hBMSCs-GFP and X-ALD hDPSCs-RFP in a ratio 1:1 for 72 hours. After that time, immunofluorescence against human mitochondria was performed and confirmed abundant presence of these organelle in cellular contacting zones. Interestingly, these mitochondria were evident in the different interacting contacts previously reported: close contacts (Fig. 36, A) and TNTs (Fig. 36, B). However, based on this conducted experiment, we could not confirm if the origin of these mitochondria was derived from hBMSCs and also, we could not discern between intrinsic and exogenous mitochondria.

Due to this problematic, we changed lentiviral strategy in direct co-cultures in order to confirm apparent mitochondria trafficking. As previously mentioned, we transduced hBMSCs cell population with a lentiviral construct that specifically label human mitochondria in red (Lenti-mitoDsRed). By contrast, X-ALD hDPSCs were transduced using Lentivirus-GFP. Direct co-cultures followed same protocol as previous experiments, seeded in a ratio 1:1 and maintained for 72 hours. Immunofluorescence confirmed colocalization of human mitochondria with RFP being able to discern between mitochondria derived from hBMSCs cell population (Fig. 36, C). Additionally, in order to confirm or discard presence of mitochondria derived from hBMSCs-mitoRed in cell-to-cell contacts, we assessed Cx-43 analysis and confirmed presence of these organelle in contacting zones where GJ were established through Cx-43 expression (Fig. 36, D).

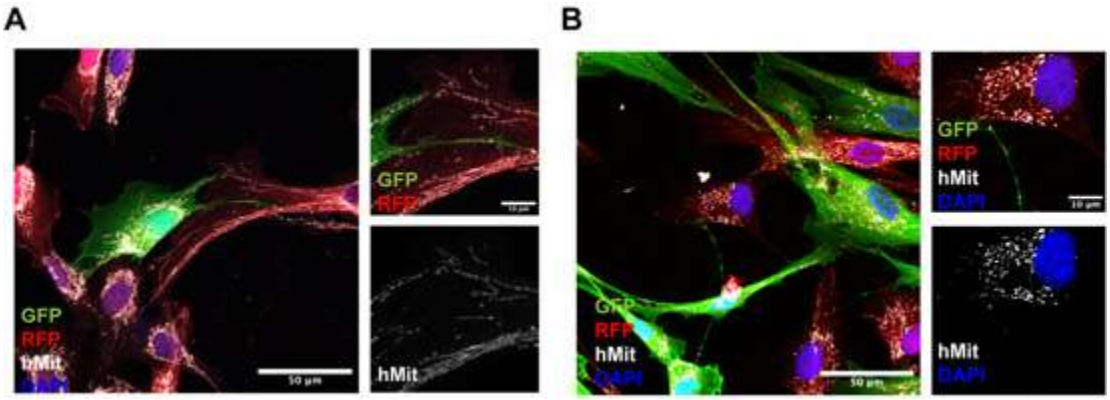

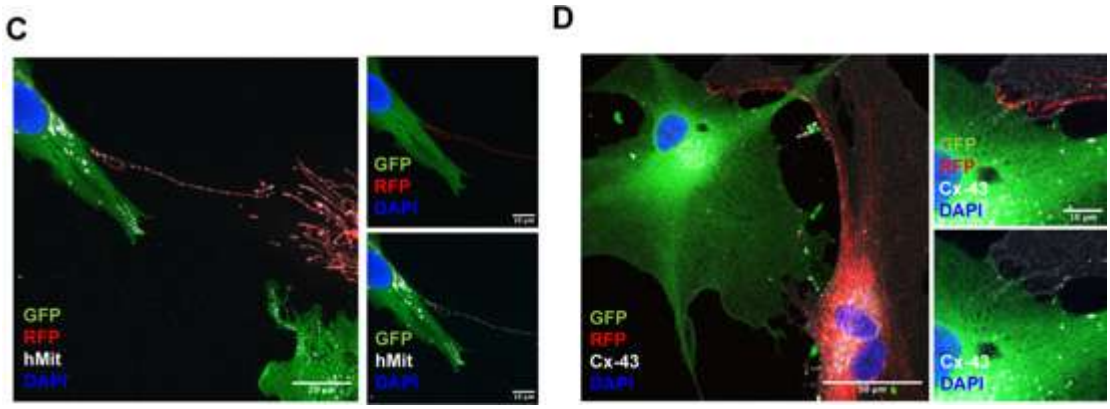

Figure 36. Mitochondria analysis in direct co-culture of hBMSCs and X-ALD hDPSCs.
Confocal images of direct co-cultures composed by hBMSCs-GFP and X-ALD hDPSCs RFP showing immunoreactivity for human mitochondria (hMit) and focused on intimal cell-to-cell contacts (A) and TNTs (B). Confocal images of direct co-culture of hBMSCs-mitoRed and X-ALD-GFP hDPSCs indicating expression of Cx-43, specific marker for GJ formation (C). All images (40x and 63x) were taken by Leica SPEII confocal microscope. Zoomed and cropped images were processed using Fiji software.

Apart from the presence of red mitochondria in contacting zones, we also analysed the likely existence of X-ALD cells with presence of red mitochondria included in their cytoplasm. After 72 hours of co-culture, we observed X-ALD cells with red mitochondria (Fig. 37, A). At this time, the number of mitochondria inclusions was extremely variable, reporting cells with high number of mitochondrial inclusions (43 red mitochondrial material in one cell), others with a few (1 red mitochondrial material in one cell) and others without any type of red mitochondria (data not shown). To firmly confirm that red mitochondria originating from hBMSCs was included in X-ALD cytoplasm, we performed orthogonal projections of analysed confocal images. In line with was observed, orthogonal projections confirmed donation of healthy mitochondria from hBMSCs to X-ALD (Fig. 37, B).

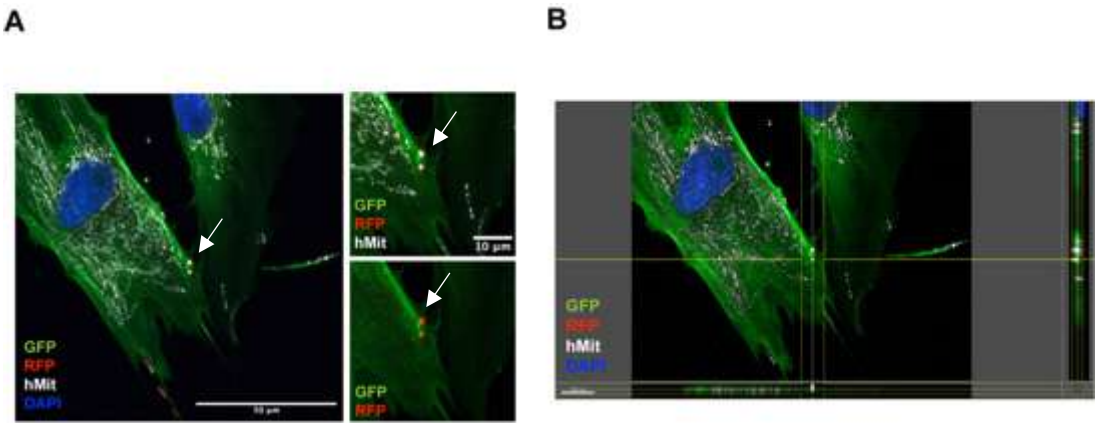

Figure 37. hBMSCs donate healthy mitochondria to X-ALD cells.
Confocal image of immunofluorescence against hMit. The image notices the existence of red mitochondria in X-ALD hDPSCs-GFP in their cytoplasm (white arrows) (A). Orthogonal projection of analysed confocal image confirming the inclusion of mitochondria (B). Images (40x and 63x) were taken by Leica SPEII confocal microscope. Orthogonal projection was performed using Imaris software.

Next step in these mitochondria trafficking analysis, was to elucidate if the number of cells with donated mitochondria in their cytoplasm increase over time. Thus, we analysed these co-cultures by flow cytometry at different times: 24, 48 and 72 hours. Results of flow cytometry analysis revealed an evident decrease in X-ALD cell population presenting red mitochondria (Fig. 38, A). To explain this fact, we performed time-lapse analysis of direct co-cultures and we noticed that there were cases in which X-ALD with few donated mitochondria divided and one of the two resulting cells did not show red mitochondria, being only present in one of them (Fig. 38, B). So, the constant division of growing X-ALD cells, increase the cell population but donated mitochondria did not distribute equally.

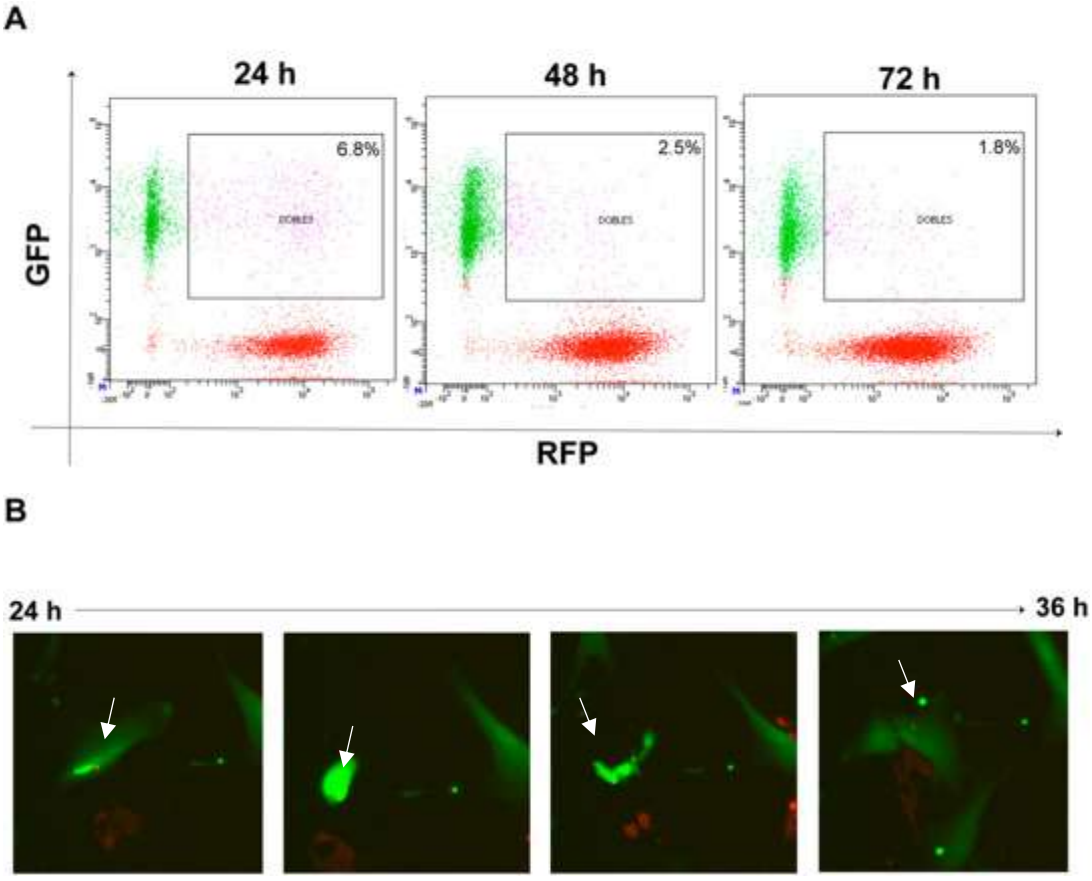

Figure 38. Analysis of donated mitochondria over the time in direct co-cultures of hBMSCs and X-ALD.

Flow cytometry scatter plots of direct co-cultures at 24, 48 and 72 hours showing the different cell populations: GFP corresponds to X-ALD cells, RFP corresponds to hBMSCs and double positive corresponds to X-ALD with donated mitochondria (A). Each dot represents an individual cell and the density of dots indicates the relative abundance of cells in each quadrant. Time-lapse images of X-ALD cell with one red mitochondrial inclusion dividing (B). Notice red mitochondria highlighted with white arrow. Images (10x) were obtained by InCuCyte incubator and software.

Organelle donation has been also reported by paracrine pathway (Thomas et al., 2022). In order to analyse an indirect plausible exchange of mitochondrial material, we used CM-containing EVs from hBMSCs-mitoRed cell cultures in X-ALD hDPSCs GFP during 72 hours. After this time, we observed healthy red mitochondrial material in X-ALD hDPSCs GFP (Fig.39, B). No colocalization was found with antibody against human mitochondria suggesting that this material suffered some type of fractioning process before being encapsulated in microvesicles. Orthogonal projections confirmed suspected inclusion (Fig. 39, C). We parallelly performed same experiments in X-ALD hDPSCs GFP without presence of CM-containing EVs from hBMSCs-mitoRed and we found no presence of RFP material in X-ALD cytoplasm (Fig. 39, A), suggesting mitochondrial specificity in direct co-cultures. We also analysed mitochondrial inclusions in X-ALD hDPSCs GFP over time and we found a slight decrease in number of mitochondrial materials per cell at 5 days of co-culture compared to 3 days (Fig. 39, D).

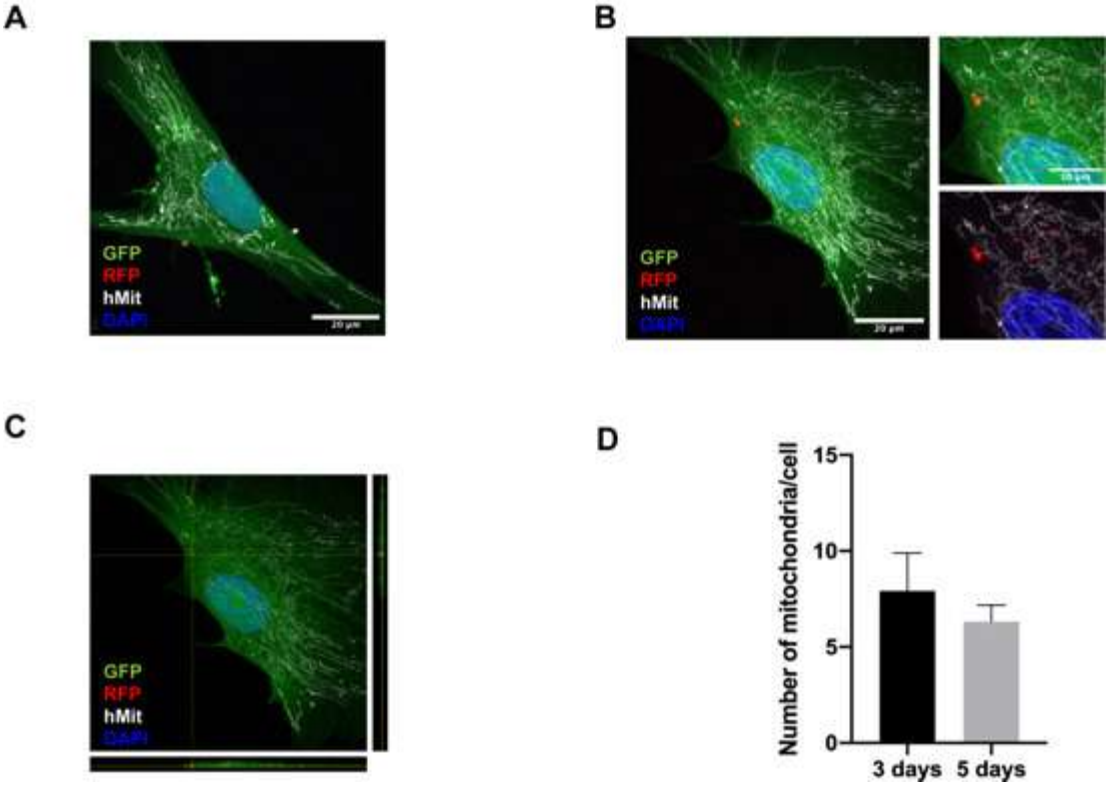

Figure 39. Indirect donation of mitochondrial components to X-ALD cell cultures.

Confocal image of immunofluorescence of X-ALD-GFP hDPSCs against hMit and RFP (A). Confocal images of immunofluorescence of indirect co-culture of X-ALD-GFP hDPSCs cells cultured with CM-mitoRed against hMit and RFP (B). Orthogonal projection of analysed confocal image confirming inclusion of red mitochondrial components in their cytoplasm (C). Graph shows mean of the number of mitochondria per cell and SDs bar errors of co-cultures maintained three or five days (D). All images (40x) were taken by Leica SPEII confocal microscope. Orthogonal projection was performed using Fiji software.

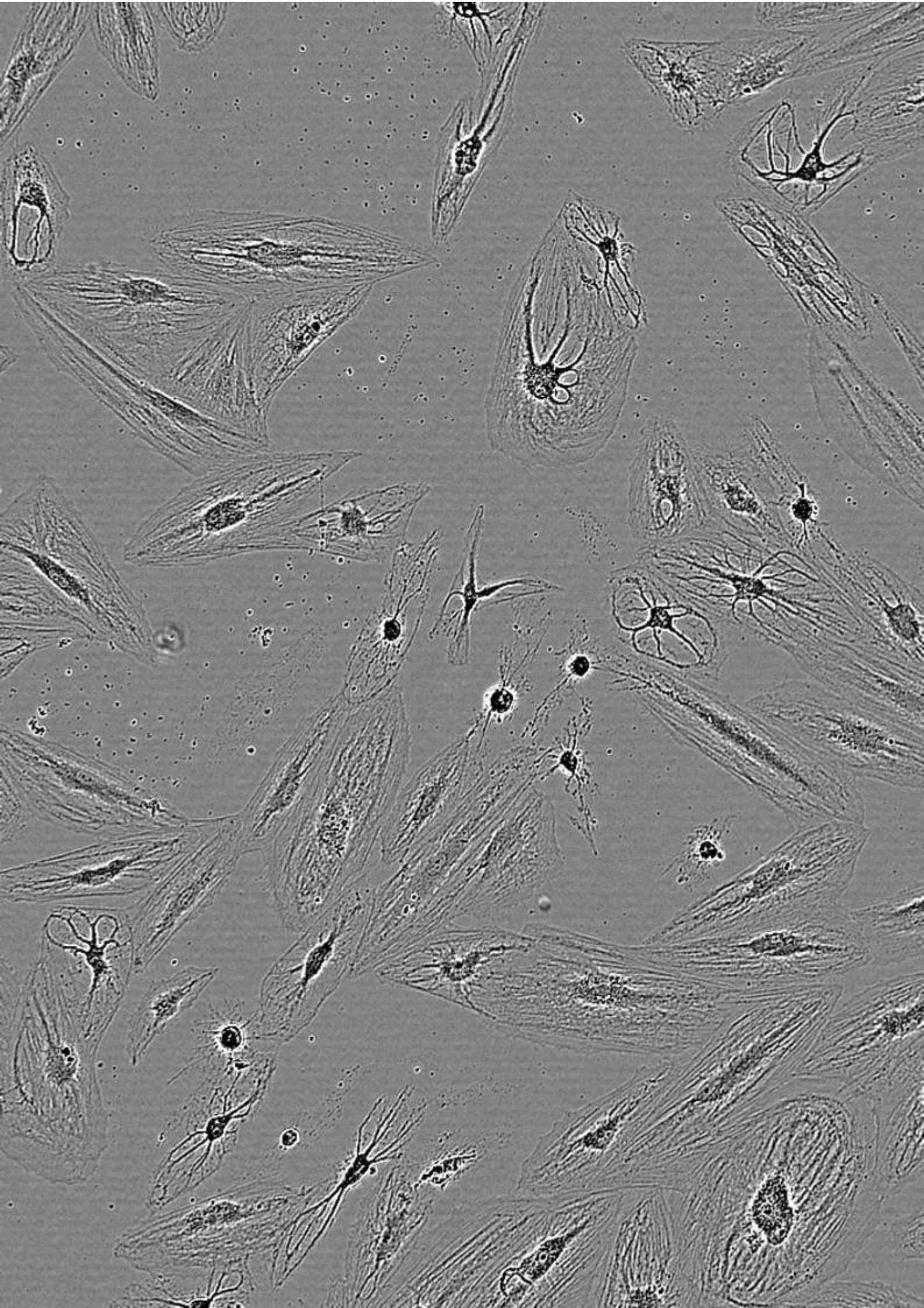

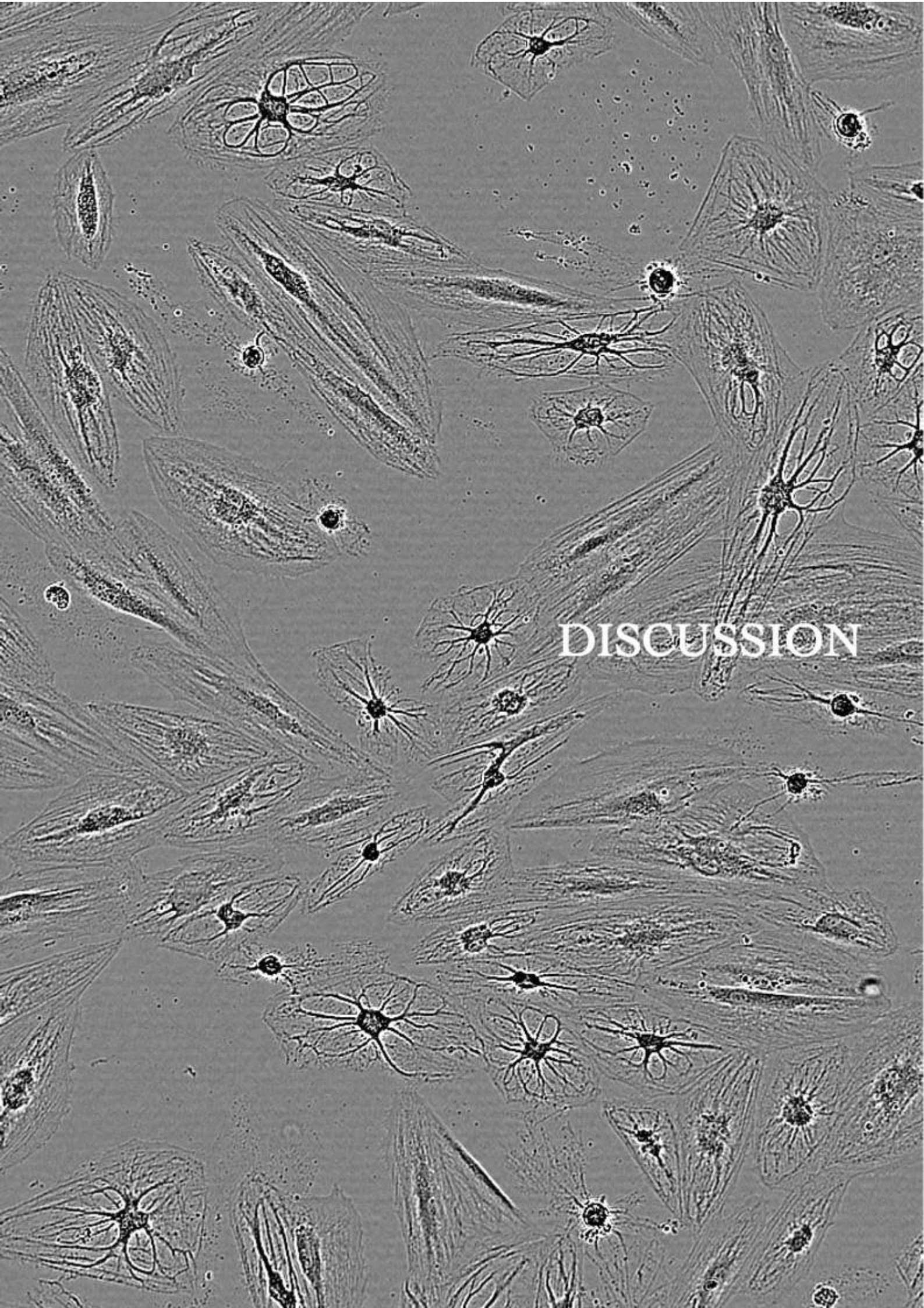

DISCUSSION

This image is property of Claudia Pérez García. Phase contrast image of neural differentiated human dental pulp stem cells. Image acquisition: Sartorious InCuCyte s3.

Discussion

The term of leukodystrophy (LD) is used to denote a heterogeneous group of disorders that affect the white matter of CNS with inheritable condition (Bonkowsky, 2021). Currently, more than 30 types of LDs have been described and classified based on several features such as RMI findings, cellular pathology or metabolic approach (Vanderver et al., 2015). LDs can be manifested at any stage of life and show highly variable clinical manifestations and pathologic mechanisms ranging from developmental delay to seizures and spasticity (Bonkowsky, 2021). One of the most common LDs is X-ALD with an estimated prevalence of 1 in 17,000 male births (Engelen et al., 2012c; Turk et al., 2020). As commented previously, therapeutic approach in X-ALD is limited due to their complex clinical manifestations, the absence of a genotype-phenotype correlation and pathophysiological mechanisms that remain unclear. Due to these considerations, in this Doctoral Thesis, we propose hDPSCs as a feasible source to study such a complex disease as X-ALD. In line with this, we also examinate the therapeutic potential of hBMSCs on this model.

- The use of hDPSCs for modelling X-ALD.

hDPSCs are a mesenchymal subpopulation, embryologically derived from multipotent neural crest cells, that reside inside the dental pulp, a highly vascularized connective tissue located at the core of the tooth (Gronthos et al., 2000). Among its characteristics, hDPSCs possess MSC characteristics such as self-renewal capability and multilineage differentiation potential (Gronthos et al., 2002), but they also have a great value due to their neural crest cell origin as they are able to differentiate into neurons and glia (Arthur et al., 2008) and to induce neurogenesis (Ishizaka et al., 2013).

As NCP, hDPSCs are a feasible source to study cell migration abilities in which ACE2 expression plays a critical role. In this dissertation, we observed that, under migrating conditions, healthy hDPSCs differently express ACE2 with high expression and accumulation in the cellular membrane of the leading pole compared to basal static cells. This fact suggests that increasing ACE2 expression and mobilization to the cell membrane may represent a general mechanism present in migratory cells to improve oxygen supply along migratory pathways. Since the discovery of hDPSCs in 2000 (Gronthos et al., 2000), the use of different types of dental pulp stem cells has been of special interest, not only because of their own potential characteristcs, but also because of their therapeutic potential.

In this Doctoral Thesis, the use of hDPSCs was specifically focused on the *in vitro* modelling of X-ALD. The first general hypothesis was to explore if donated X-ALD hDPSCs reproduced specific clinical hallmarks related to disease. As mentioned in the results chapter, these X-ALD cells mimic several X-ALD features making them a promising source to study such complex disease. Among those X-ALD features, we explored from their genetic status to their VLCFA tolerance. We first performed genetic analysis to better understand the possible pathologic characteristics of cells. However, despite our effort, we did not find any mutation or pathogenic variants in all sequenced regions of ABCD1 gene, the exclusive gene responsible of the disease. Thus, genetic mutation of ABCD1 might be found in non-explored regions such as 5' and 3'untranslated regions (UTRs) as well as in intronic intervening sequences (IVS). The next step was to evaluate ALDP expression in order to find any significant difference when compared to healthy hDPSCs. ALDP expression in X-ALD hDPSCs did not differ of analysed healthy hDPSCs, with an immunopunctuate pattern in perinuclear and cytoplasm. Although experiments assessing ALDP expression can provide valuable insights into the presence of X-ALD pathology in cells, such information would only be meaningful if the protein is found to be absent or significantly reduced. In our case, normal expression of ALDP cannot firmly confirm the existence of X-ALD pathologic defects in these cells, but it does not rule out either. This is because ALDP can be found at normal levels in X-ALD patients giving rise to same clinical manifestations than those who present absent or reduced protein as summarized Watkins et al (1995) (Watkins et al., 1995). Moreover, in the case of known missense pathogenic variants, there are cases in which ALDP is detectable (Fig. 40).

The heart of the issue resides into protein functionality and even if protein is structurally stable and expressing as basal, their main function might be compromised. For this reason, we aimed to analyse differences related to lipid accumulation in order to elucidate plausible alterations in ALDP function. In this case, we noticed remarkable differences in neutral lipid accumulation compared to healthy cells using different types of staining: ORO, BODIPY 493/503 and LipidTOX Deep Red. The most common technique to detect VLCFA in biological samples derived from X-ALD patients is gas chromatography/ mass spectrometry (GC/MS) measuring concentrations and ratios of hexacosanoic acid (C26:0), tetracosanoic acid (C24:0) and docosanoic acid (C22:0). However, in biological samples, fatty acyl chains are typically not found in their free state but are instead incorporated into complex lipids such as phospholipids (PLs) (O'Neill et al., 1981). Additionally, recent progress in comprehensive lipidomic analysis using liquid chromatography-tandem mass spectrometry (LC-MS/MS) has identified that, in X-ALD patients, VLCFAs are mainly present within PLs, glycolipids and neutral lipids (Abe et al., 2014; Lee et al., 2019). In line with this, all stains that were used for

analyse aberrant lipid accumulation revealed specific related-X-ALD differences between cell populations, being a starting point for developing the *in vitro* model.

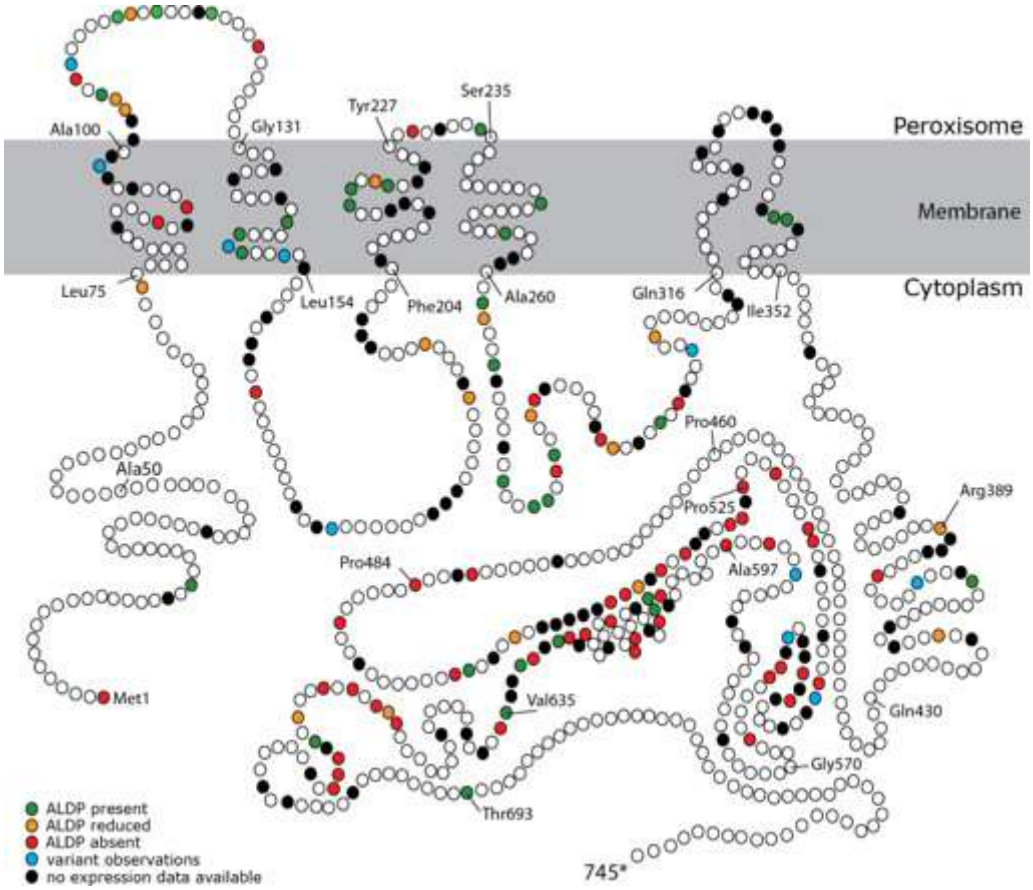

Figure 40. Pathogenic variants and ALDP stability.

Representative illustration of ALDP structure and the effect of missense (likely) pathogenic variants on its stability. Source: https://adrenoleukodystrophy.info/.

The alteration of neutral lipid accumulation, due to a non-functional but stable ALDP, demonstrates the existence of X-ALD in these analysed hDPSCs, but more specific assays were performed to better characterise the cells. As previously mentioned, C26:0 accumulation is one of hallmarks of X-ALD. We did not detect concentrations of these VLCFA in our cells, but we studied the effect of different concentrations in different cell cultures. The inability of X-ALD hDPSCs to correctly metabolize C26:0 compromised their normal growth and viability resulting in a delayed cell growth and even cell death at highest studied concentration. By contrast, in healthy cells none of these events occurred. These results were in accordance with previous reports that emphasize the cytotoxicity of C26:0 to X-ALD fibroblasts (Fourcade et

al., 2008), but being the first time to be identified in hDPSCs. Being demonstrated X-ALD features in the cells under their *in vitro* standard conditions, we further extended the study and exploited the advantages of hDPSCs in terms of neurogenic potential.

Since now, research focused on human neural cell types of X-ALD patients has been done with *post-mortem* tissue (Yska et al., 2024) or with reprogrammed fibroblasts (Baarine et al., 2015; Jang et al., 2011), but working with hDPSCs show advantages against other sources due to their intrinsic characteristics. Due to the extensive experience in the field, we choose a precise protocol for neural differentiation previously developed from our group (Bueno et al., 2021). Taking advantage of the benefits offered by several techniques, we were able to conduct a comprehensive analysis of X-ALD differentiated cells. Combining obtained results of immunofluorescence and electrophysiology, we determined that X-ALD showed clearly disease-related differences in comparison to healthy cells. X-ALD hDPSCs differentiated into neural-like cells as healthy cells do, but aberrant neutral lipid accumulation persisted. In addition to this fact, that was previously analysed in undifferentiated cells, X-ALD neural-like cells also presented differences in neuronal functionality as electrophysiologic records suggested. Whole-cell patch clamp demonstrated that, using this protocol, we could obtain functional neuronal-like cells with the ability to generate action potentials. These action potentials were analysed by characterizing the presence and activity of voltage-gated sodium channels. Thus, both healthy and X-ALD neural-like cells showed sodium and potassium currents, making possible to achieve a precise model of X-ALD. However, discrepancies in amplitude and kinetics of sodium channels were noticed between different cell population. X-ALD neural-like cells showed lower peak of amplitude and slower kinetics of sodium currents, suggesting an alteration in the process of neuronal differentiation. One possible explanation to this fact could be the distribution of fatty acids across sodium channels. The demonstrated alteration in fatty acid accumulation of X-ALD neural-like cells might be compromising the proper function of sodium channels. However, further studies are needed to explain this fact. Therefore, the process of neural differentiation of X-ALD hDPSCs is feasible and bring promising results not only related to same alterations studied in undifferentiated cells, but also to those related with the process of differentiation.

The use of hDPSCs as *in vitro* source for developing novel cell models of different genetic disorders is a promising tool which has numerous advantages versus the use of other studied sources. The lack of access to human neural cell types restricts the *in vitro* studies of several neurologic diseases and focuses the research exclusively to the use of animal models. In the case of X-ALD, animal models do not recapitulate human disease, since single knock-out does not present any type of demyelinating disease in CNS (Lu et al., 1997). Due to this problematic,

several authors used iPSCs from X-ALD fibroblasts to obtain different neural cell types and analyse X-ALD characteristics in these differentiated cells (Baarine et al., 2015; Jang et al., 2011). iPSCs are a promising source that allow the study of cells that are inaccessible due to invasiveness and bring valuable knowledge into the field (Takahashi et al., 2007). Nevertheless, in the specific case of modelling genetic diseases might not be the best or, at least, the exclusive option. Although iPSCs technology allows an unlimited source of human cells or tissues that carry specific-causing disease mutations, it has limitations which has to be emphasized. The main concerns of iPSCs for *in vitro* modelling diseases are related to their high variability in their biological properties, which can give rise to a high inconsistency of resulted disease phenotypes (Soldner & Jaenisch, 2012). The causes of these unpredictable results are diverse: from cellular changes resulted from the reprogramming process of somatic cells to differences in genetic background. Examples of these alterations are: disruption or dysregulation of genes if the vector integrates in the host genome (Soldner et al., 2009), transcriptional derepression of genes on the inactivated X chromosome (Mekhoubad et al., 2012) and genetic alterations such as point mutations and copy number variations (CNVs) (Gore et al., 2011; Hussein et al., 2011). Additionally, other challenges are disease-specific such as the difficulty of recapitulate human diseases that depend on complex interactions of multiple genetic or environmental factors. For this reason, not all human diseases can be modelled *in vitro* using iPSCs technology. By contrast, hDPSCs are a reasonable alternative to iPSCs technology specially in complex diseases such as X-ALD. In the case of X-ALD, the use of hDPSCs takes special relevance because their likely manifestation during childhood, when human dentition is taking place and deciduous teeth can be easily obtained without invasive surgery methods. Therefore, *in vitro* modelling of genetic diseases using hDPSCs is less costly than iPSCs cultures and differentiation protocols are generally more standardised and take less time. Obviously, genetic alterations that may be presented in iPSCs cultures, are not reported when hDPSCs are used for modelling genetic disease, assuring a genetically well-defined model system. Unfortunately, hDPSCs also show disadvantages related to their own properties as they have limitation rate of growth unlike iPSCs or immortalized cell lines (Masuda et al., 2021). Additionally, in specific disease-cases, the *in vitro* modelling of the disease using hDPSCs may be challenging due to the lack of precise differentiation protocols or the poorly studied methodology for certain types of mature cells such as excitatory and inhibitory neurons. Nevertheless, there are evidences of the use of hDPSCs in the study of neuropsychiatric genetic disorders with promising results (Urraca et al., 2018). Considering everything, hDPSCs are an excellent source of unique hMSCs that are easily and at low culturing cost extracted from tooth, biological tissue normally considered as a medical waste. Their intrinsic features such as their high plasticity, makes them a valuable option to be examinate in the field of *in vitro* modelling diseases with special attention to those with genetic alterations.

Regarding our specific use of hDPSCs for *in vitro* modelling X-ALD, we are aware of our limitations. The specific results obtained in this Doctoral Thesis are only representative of this specific donor. However, this study is the first to utilize hDPSCs as a model for X-ALD, successfully demonstrating that the disease pathology can be effectively replicated in this specific cell type. As mentioned before, one of the features of X-ALD is their wide spectrum of clinical manifestations that can be present independently of genotype. Increasing the number samples from different X-ALD donors could complete the study not only to define aberrant alterations but also to emphasize phenotypic differences between X-ALD individuals with different clinical manifestations. Nowadays, human teeth are not usually classified as a biological specimen suitable for donation, being more considered as a medical waste. This classification significantly limits the availability of hDPSCs in comparison to other sources such as umbilical cord blood and bone marrow. Promoting greater societal awareness of the potential of these valuable cells, which can be easily isolated from extracted teeth, is crucial. Such efforts would facilitate the development of future platforms as biobanks for the collection, preservation and utilization of hDPSCs both for *in vitro* modelling and for their therapeutic potential in regenerative medicine.

- Cellular therapeutics: the role of hBMSCs in the cell replacement therapy.

Currently, various types of hMSCs are being investigated for their significant therapeutic potential including adipose-derived hMSCs (Freitag et al., 2019), umbilical cord-derived hMSCs (Ding et al., 2015) and hDPSCs (Ding et al., 2015). Among these, hBMSCs stand out as the most prominent. Several factors contribute to the preference for hBMSCs over other hMSCs sources. Firstly, they are widely accessible, relatively easy to extract and manipulate *in vitro* and their use poses no ethical concerns (Steens & Klein, 2018). Additionally, the combination of their inherent properties and the extensive research supporting their therapeutic applications makes hBMSCs a more well-established option compared to hMSCs derived from other sources or other type of stem cells such as ESCs. In this Doctoral Thesis, the direct and indirect therapeutic role of hBMSCs was exhaustively studied in a specific pathological context of X-ALD.

In the specific case of X-ALD, it is known that the only available therapy for the cerebral form of the disease is HSCT. HSCT has shown significant success in halting the progression of cALD when administered to patients at an early stage (Cartier et al., 2014; Moser & Mahmood, 2007; Schönberger et al., 2007). Despite its success in X-ALD, HSCT fails in cross-correcting recipient hBMSCs although a successful engraftment is achieved, likely due to the

low cell density (Koç et al., 1999). Nevertheless, the use of hBMSCs in X-ALD has been explored with studies showing their beneficial long-term effects in cALD patients (Shapiro et al., 2000) and, more recently, in those with AMN (Siwek et al., 2024). These findings suggest that hBMSCs transplantation, like HSCT, represent a viable treatment for X-ALD. Moreover, the combination of hBMSCs along with HSCT brings favourable results enhancing the cell engraftment and avoiding the GVHD (Burnham et al., 2020). Pre-treatment with hBMSCs in X-ALD patients might help stabilize or slow down the progression of the Loes score, preserving neurological function and providing a therapeutic bridge to subsequent HSCT. Further research is needed to explore this combined approach, potentially enhancing the therapeutic landscape for X-ALD.

In this Doctoral Thesis, we have focused on the extensive therapeutic potential of hBMSCs in the context of the *in vitro* X-ALD. Attending to the direct effect which hBMSCs can exert on the novel *in vitro* model of X-ALD, we paid attention to functionality in neural differentiated cells and cell-to-cell interactions. The first evidence of direct therapeutic effect of hBMSCs was noticed in functional neural differentiation experiments. As mentioned before, X-ALD differentiated cells showed clearly impairments in sodium currents probably related to the process of differentiation. The direct addition of hBMSCs on the cell cultures during the last days of differentiation was fundamental to achieve a rescue of phenotype. hBMSCs directly induced changes in the sodium currents increasing their maximum and reducing their time to peak to similar values than healthy differentiated cells. These results are in line with previous studies that evidence the supportive role of hBMSCs on neuron primary cultures. As reported De Laorden et al (2023), mesenchymal stem cell populations have the ability to stimulate and restore neuronal activity (De Laorden et al, 2023) through establishment of physical contacts. These intimal contacts are essential to induce neuroprotection, but evidences of restoration of neuronal activity using EVs are also reported (Mauri et al, 2012). Currently, it is known that the crosstalk between mesenchymal stem cell populations and other cell types is achieving mainly through the establishment of GJ and TNTs (Tarasiuk et al., 2022). Knowing this, we also sought to analyse the direct communication between hBMSCs and hDPSCs. Since both cell populations have mesenchymal characteristics, their *in vitro* manipulation is easy and they share the same cell culture media, making feasible direct co-cultures. At the same time, regarding their same *in vitro* morphology, the identification of each cell population becomes compromised in this type of cultures. For this reason and as explained in previous chapters, we transduced cell populations using different reporters in order to identify each cell of co-culture. First results of these direct co-cultures revealed clearly interactions between cells, assessed by GJ and TNT formation, which prompted us to conduct an in-depth analysis. Thus, we sought to analyse a possible exchange of cytosolic material between hBMSCs and X-ALD cells.

Thanks to the different reporter genes employed in lentiviral constructs, we could notice presence of GFP material, coming from hBMSCs, in X-ALD hDPSCs cytoplasm confirmed by orthogonal projections. Despite being the first time that it is evidenced in hDPSCs, hBMSCs are able to donate cytoplasmatic and membrane components to recipient cells as Lehmann et al (2014) reported in an established co-culture of hBMSCs and human nucleus pulposus cells, where a bidirectional exchange mediated by TNT was assessed (Lehmann et al., 2014).

The evident exchange of healthy components motivated us to pursue a more rigorous and thorough analysis. As a consequence, we analysed ALDP expression in these direct co-cultures. First of all, we did not discern any change in number or distribution of peroxisomes in X-ALD hDPSCs, suggesting no changes in terms related to X-ALD disease. Nonetheless, through exchange of cytoplasmatic material, healthy peroxisomes might be coming from healthy hBMSCs. Taking as premise this hypothesis, we examined the presence of healthy peroxisomes in the characteristic GFP cytoplasmatic material found in X-ALD hDPSCs. Surprisingly, we could find ALDP immunoreactivity in those material suggesting trafficking of these organelle. We hypothesised that hBMSCs, across direct established contacts, donated healthy peroxisomes, among other organelle or molecules, to diseased cells. These healthy peroxisomes could replace lost of function of altered peroxisomes of X-ALD hDPSCs. We did not perform any assay to confirm such enhancement in functionality with a possible restoration in peroxisomal β-oxidation and we are aware that this fact might not be occurring, but it is a starting point to elucidate possible mechanisms of action of hBMSCs into X-ALD pathology. Moreover, through other studied direct co-cultures, we could confirm trafficking of other organelle: mitochondria. As well as in cytoplasmatic exchange, through GJ establishment and TNT formation, healthy mitochondria were able to be incorporated into X-ALD hDPSCs. The fact that hBMSCs donate healthy mitochondria to X-ALD hDPSCs is particularly relevant because of the critical role of oxidative stress in X-ALD pathophysiology. It is known that the combination of oxidative stress and mitochondrial and proteostasis malfunction contribute to X-ALD pathology, more concretely, to the axonal degeneration (Fourcade et al., 2015). Moreover, in the underlying mechanisms of onset and damage involved in oxidative stress and inflammation, mitochondrial ROS play an essential role. Due to an increase in VLCFA levels, production of mitochondrial ROS is increased giving rise to redox imbalance (Yu et al., 2022). In more detail, in a recent study of Launay et al (2024) highlighted the importance of mitochondria and their dynamics in the pathology of X-ALD (Launay et al., 2024). Knowing this, we could assume that integration of healthy mitochondria into X-ALD hDPSCs could be beneficious to X-ALD cells' phenotype. Nevertheless, according to conducted experiments, we did not perform any mitochondrial analysis based on their function and further research will shed light on the matter. Despite the limitations of our work, these results bring relevant

knowledge about the cell-to-cell communication between hBMSCs and X-ALD cells. We are conscious that results exposed in this dissertation are only specific to these donor cells and they must not be taken in account as general rule. Increasing number of cell samples will bring more precise data to analyse in depth the direct effects of hBMSCs on *in vitro* models of X-ALD.

The restoration of function lost as a result of damage by replacing dead cells with new healthy cells is one of most studied mechanisms of hBMSCs. This fact, known as cell replacement therapy, allows a therapeutic effect directly mediated by cell migration and differentiation. If we address the core of the issue, evidences of cell replacement are reported in terms of neurological involvement. An example of this fact was the study described by Chen et al (2008) in which used an experimental animal model of cerebral stroke treated with hBMSCs. Transplanted cells migrated to the lesion site and some of them expressed specific markers of astrocytes and oligodendrocytes (Chen et al., 2008). Nevertheless, the extent of direct cellular replacement, as the substitution of lost or damaged neurons, remains limited. This limitation highlights the need for further research to optimize protocols for enhancing the efficiency and functional integration of these cells into the damaged neural circuits. Most of the therapeutic benefits observed in hBMSCs-based studies appear to be linked to indirect mechanisms, such as the secretion of neurotrophic and anti-inflammatory factors. These secretions help to create a neuroprotective environment, reducing inflammation and promoting neuronal survival, rather than achieving full cellular replacement. Thus, while hBMSCs hold promise for neurodegenerative disease treatment, their role may be more supportive than directly regenerative, with future research necessary to unlock their fully potential in cell replacement therapies.

- Cell-free therapy: paracrine mediators as promising therapeutic agents.

As mentioned previously, hBMSCs exert their beneficial properties mainly through paracrine effects including secretion of trophic and anti-inflammatory factors. These secreted bioactive factors can be found in supernatants of *in vitro* cultures. More concretely, if hBMSCs are cultured in serum-depletion conditions *in vitro*, the resulting supernatant, known as CM, is full enriched of these beneficious components. A key component of paracrine signalling of hBMSCs is found in CM and are the EVs, which are rich in proteins, lipids and nucleic acids. EVs contribute to cellular communication and tissue regeneration. Notably, these EVs carry many of the beneficial effects traditionally attributed to the cells themselves, offering a promising avenue for cell-free therapy. By harnessing the regenerative properties of hBMSCs-

derived EVs, we can potentially achieve therapeutic outcomes without the complexities associated with direct cell transplantation.

In this dissertation, we have focused our attention to the significant and mostly studied paracrine effect of hBMSCs. In parallel to direct co-cultures, we performed indirect co-cultures to analyse their effect on the *in vitro* developed X-ALD model. To achieve this, we first confirmed the presence of EVs in the CM derived of hBMSCs. These EVs varied in sized and expressed general markers of Exos: CD63 and Hsp70. Their lack of expression of calnexin, specific of whole-cell lysates determined the specificity for EVs. Confirming the existence of these EVs in CM, we went on to specific experiments using these CM-containing EVs in order to achieve an indirect rescue of phenotype. In regard to ALDP expression, CM-containing EVs did not induce any change in X-ALD hDPSCs in terms of number and distribution of healthy $ALDP^{+}$ peroxisomes. Nonetheless, a plausible integration of healthy peroxisomes through EVs coming from hBMSCs might be occurring, but based on conducted experiments, we could not confirm this fact. Experiments using lentiviral constructs which label peroxisomes of hBMSCs may elucidate more knowledge at this issue and, consequently, confirm or reject this proposed hypothesis. Despite not evidenced apparently changes in the protein responsible of the disease, we sought to analyse the effect of CM in the neutral lipid accumulation. Surprisingly, three days after the addition of CM-containing EVs, X-ALD hDPSCs rescued an apparent healthy phenotype drastically reducing the aberrant neutral lipid accumulation in their cytoplasm. This fact was in line with previous investigations using CM-containing EVs in different animal models in the context of hepatic pathology (Yang et al., 2021) and spinal cord injury (SCI) (Guo et al., 2016). In our case, despite not having any confirmation of changes in peroxisome function, components of CM induce changes in lipid metabolism facilitating their elimination.

To study other impacts of CM-containing EVs on these studied cells, we conducted experiments related to X-ALD aspects. Since we previously reported cytotoxic effect of C26:0 only in X-ALD hDPSCs, we wanted to know if with the presence of CM-containing EVs could rescue related aspects of cytotoxicity to basal levels. Unexpectedly, when we added CM-containing EVs to cell media-containing C26:0, X-ALD hDPSCs normalized their cell growth and viability. However, the mechanisms by which these components rescue an apparent healthy phenotype remain obscure. Similar results were reported when stressed X-ALD hDPSCs were incubated with CM-containing EVs. Three days after the induction of oxidative stress, only the group of X-ALD hDPSCs that were incubated with CM-containing EVs survived, notably reducing the cell percentage of apoptotic population. Although involved mechanisms to achieve this were not deeply studied, several possible explanations might elucidate mechanisms involved in this protective effect. On one hand, among all components found in

CM-containing EVs, anti-oxidant proteins may have a critical role in inducing cell survivance as other authors demonstrated (Saleem et al., 2021). On the other hand, other research highlighted that components of CM activate PI3k/Akt pathway, which plays an important regulatory role in cell apoptosis, cell proliferation, angiogenesis, and other cellular processes and functions (Huang et al., 2021). Additionally, in relationship to aspects that were analysed by direct contact of cells, we also examined the presumable indirect transference of organelle or components from them. In this case, we obtained CM-containing EVs from hBMSCs-mitoRed to distinguish the exogenous material. When X-ALD hDPSCs were incubated with this specific labelled-mitochondria CM during three days, we noticed presence of RFP in their cytoplasm indicating some type of indirect transference of mitochondria. However, we could not confirm any functional improvement of the cells which showed mitochondrial components in comparison to those without them. Although we did not study mechanisms involved in this transference, the presence of mitochondrial components in EVs, and more concretely in exosomes, has been demonstrated in last years (Di Mambro et al., 2023; Liang et al., 2023). One aspect to be discussed about these specific experiments is the fact that RFP mitochondrial components did not show immunoreactivity to specific antibody used for human mitochondria. One possible explanation could be mitochondria portions found in EVs do not react with specific region of designed antibody due to a lack of recognized epitope.

The results obtained regarding the use of CM-containing EVs from hBMSCs are promising and align with the primary therapeutic mechanism of action of these cells: their paracrine effect. However, when working with CM-containing EVs, it is essential to recognize that it behaves like a “black box” and its components can vary significantly depending on the *in vitro* conditions or the nature of cells. For instance, factors such as cell culture conditions, passage number, oxygen levels and presence of serum or other supplements can all influence the composition of the CM. Moreover, donor variability and the inherent heterogeneity of hMSCs add further complexity. For these reasons, we have attempted to obtain CM in the most reproducible manner possible. Nevertheless, we are aware that despite demonstrating the presence of EVs in this CM, other components such as miRNA, proteins (growth factors, cytokines, enzymes…) and lipids have not been thoroughly analysed. Additionally, it is important to consider the possibility that the composition of CM may have changed due to factors beyond our control, such subtle shifts in culture media composition, contamination with exogenous proteins or unnoticed cell stress during handling.

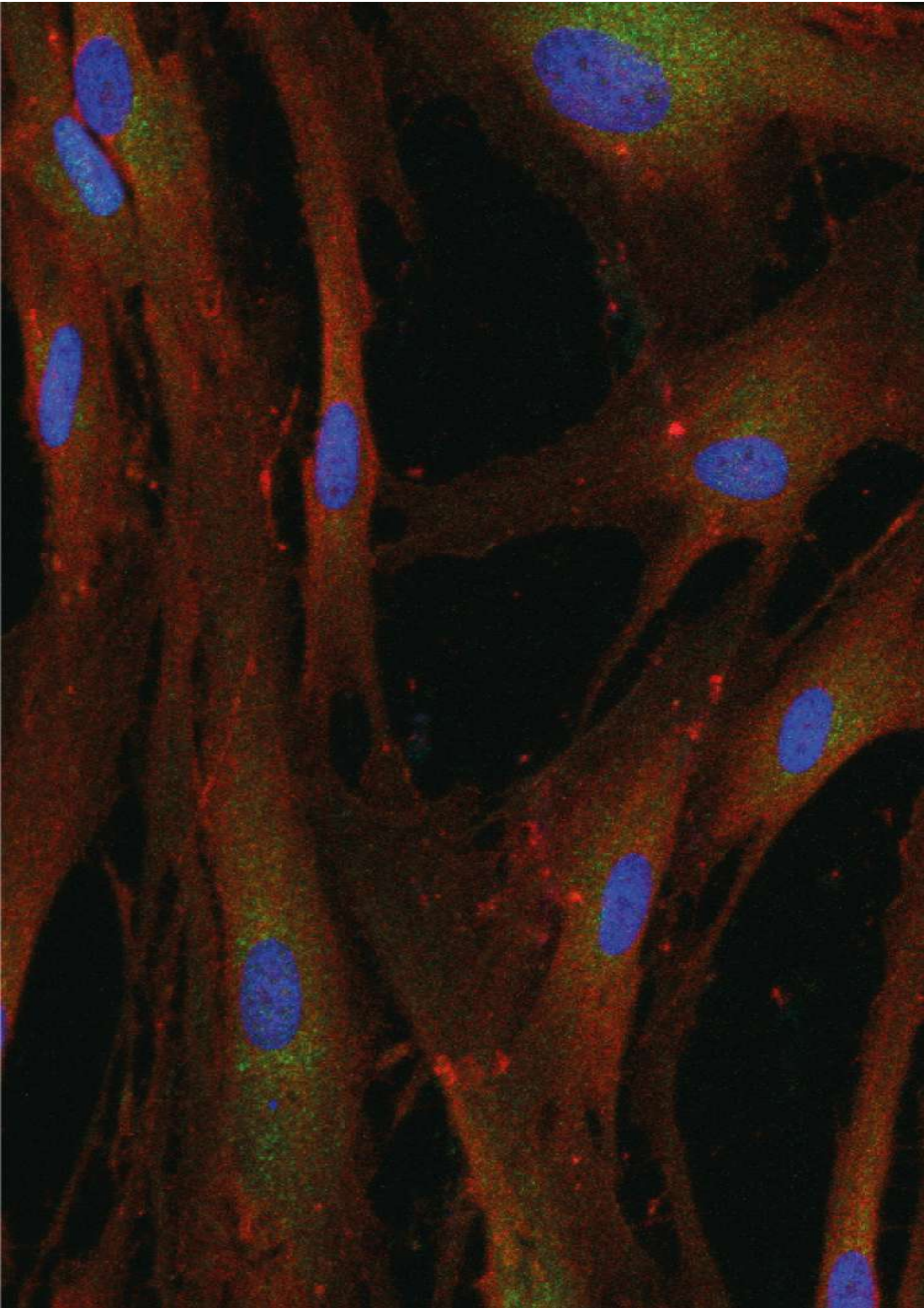

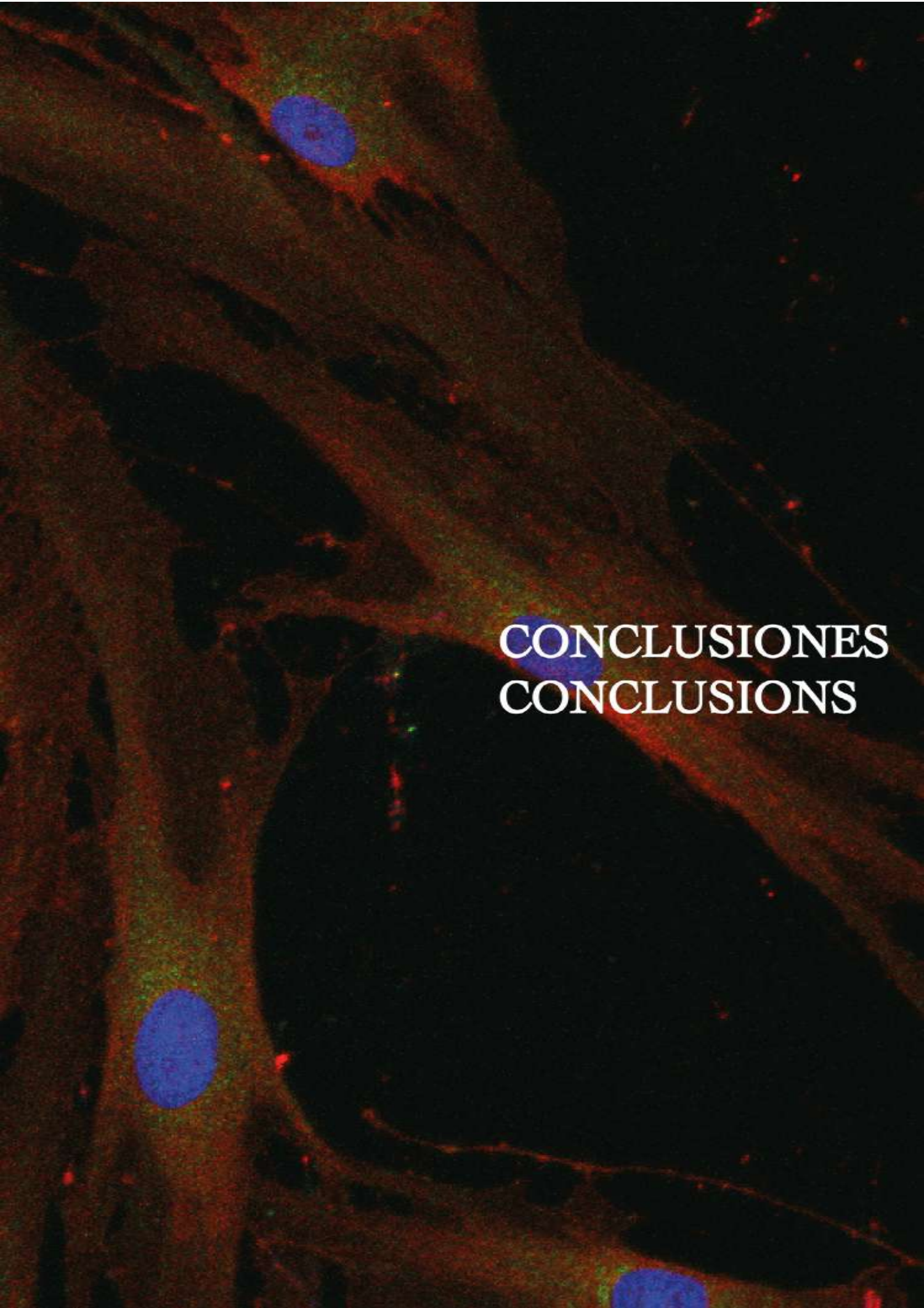

CONCLUSIONES
CONCLUSIONS

This image is property of Claudia Pérez García. Immunofluorescence of human dental pulp stem cells against Neuropilin-1 and ACE-2. Image acquisition: Leica SPEII confocal microscope.

Conclusiones

Tomando como base los objetivos formulados para esta Tesis Doctoral, las conclusiones de la presente disertación son las siguientes:

1. Las hDPSCs son una fuente viable para el estudio de la migración celular. Las hDPSCs, como células progenitoras neurales, presentan capacidad de migración celular asociada a procesos de reparación. En hDPSCs migratorias, la expresión de ACE2 se encuentra regulada diferencialmente en comparación con las basales estáticas. Las hDPSCs migratorias muestran una elevada expression de ACE2, con una polarización hacia la membrana celular, lo que evidencia el papel crucial de ACE2 en la migración celular y su posible contribución a la facilitación del suministro de oxígeno durante el movimiento.

2. Las hDPSCs del paciente con X-ALD muestran fenotipo específico de la enfermedad. Estas células presentan una acumulación aberrante de lípidos neutros en su citoplasma y una alta sensibilidad a la citotoxicidad del C26:0, lo que afecta a su crecimiento y viabilidad celular normal. Estas alteraciones no se observan en células sanas, lo que determina características específicas relacionadas con la patología en las hDPSCs de X-ALD.

3. Las células diferenciadas con fenotipo neural en X-ALD también presentan acumulación aberrante de lípidos neutros en sus somas. Esto indica que el fenotipo patológico persiste incluso tras la diferenciación. Además, se observan alteraciones en los canales de sodio, exclusivamente en las células diferenciadas con X-ALD, caracterizadas por una menor amplitud y una cinética más lenta en comparación con las células diferenciadas sanas.

4. Las hBMSCs ejercen funciones terapéuticas cuando se co-cultivan con las hDPSCs de X-ALD. A través del establecimiento de unions tipo gap y la formación de nanotúbulos, las hBMSCs transfieren peroxisomas y mitocondrias sanas endógenas a las hDPSCs de X-ALD, lo que podría facilitar una correción cruzada de las células afectadas. Además, las hBMSCs restaurant un fenotipo sano en las células diferenciadas con fenotipo neural de X-ALD, aumentando su amplitud y reduciendo su latencia hasta el pico en los canales de sodio.

5. El CM derivado de hBMSCs contiene EVs de distintos tamaños que expresan marcadores generales de exosomas como CD63 y Hsp70. Estas EVs presents en el CM muestran beneficios terapéuticos evidentes en las hDPSCs de X-ALD. A través de mecanismos mediados por señalización paracrina, las EVs del CM de hBMSCs restauran significativamente un fenotipo sano al mitigar defectos patológicos y proporcionar indirectamente componentes mitocondriales saludables. Este CM reduce la acumulación aberrante de lípidos neutros y protege a las hDPSCs de X-ALD del daño por estrés oxidativo y de la toxicidad inducida por altas concentraciones de C26:0, promoviendo su supervivencia y un crecimiento celular normal.

Conclusions

Based on the aims established for this Doctoral Thesis, the conclusions of the present dissertation can be formulated as follows:

1. hDPSCs are a feasible source to study cell migration. hDPSCs, as NCP, display healing cell migration abilities. ACE2 expression is differentially regulated in migrating hDPSCs compared to basal static hDPSCs. Migrating hDPSCs show high expression of ACE2 and polarized to cellular membrane of the leading pole, evidencing the critical role of ACE2 in cell migration potentially facilitating oxygen supply during movement.

2. X-ALD hDPSCs exhibit specific X-ALD hallmarks evidencing aberrant neutral lipid accumulation in their cytoplasm and being highy sensible to C26:0 cytotoxicity affecting their normal cell growth and viability. These alterations are not observed in healthy cells, determining specific disease-related characteristics in X-ALD hDPSCs.

3. Differentiated X-ALD neural-like cells also show aberrant neutral lipid accumulation in their cellular bodies indicating that the phenotype persists even in differentiated cells. Furthermore, alterations in sodium channels are also present exclusively in differentiated X-ALD cells with lower peak of amplitude and slower kinetics than healthy differentiated cells.

4. hBMSCs exert therapeutic functions when are directly co-culture with X-ALD hDPSCs. Through the establishment of GJ and TNT formation, hBMSCs donate endogenous healthy peroxisomes and mitochondria to X-ALD hDPSCs, promoting a possible cross-correction of diseased cells. Moreover, hBMSCs rescue a healthy phenotype in differentiated X-ALD neural-like cells by increasing their peak of amplitude and reducing their time-to-peak in sodium channels.

5. CM from hBMSCs contains EVs of different sizes that express general markers of Exos: CD63 and Hsp70. This CM-containing EVs shows evident therapeutic benefits in X-ALD hDPSCs. Through paracrine mediated mechanisms, CM-containing EVs from hBMSCs significantly rescues a healthy phenotype by mitigating pathologic defects and by indirect donation of healthy mitochondrial components. These CM

reduce altered neutral lipid accumulation and protect stressed X-ALD hDPSCs from oxidative stress damage and from high concentrations of C26:0, enhancing their survival and normal cell growth.

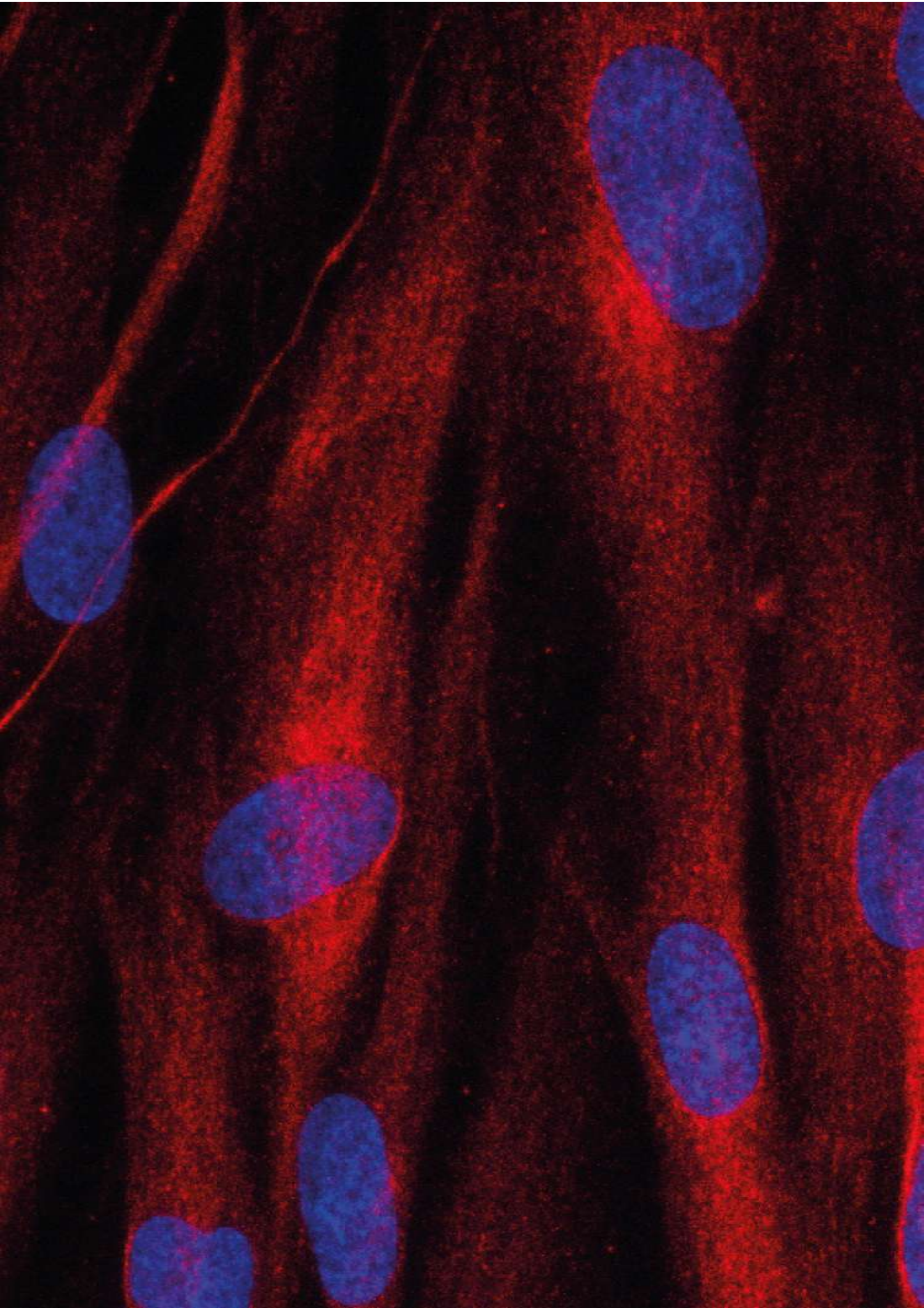

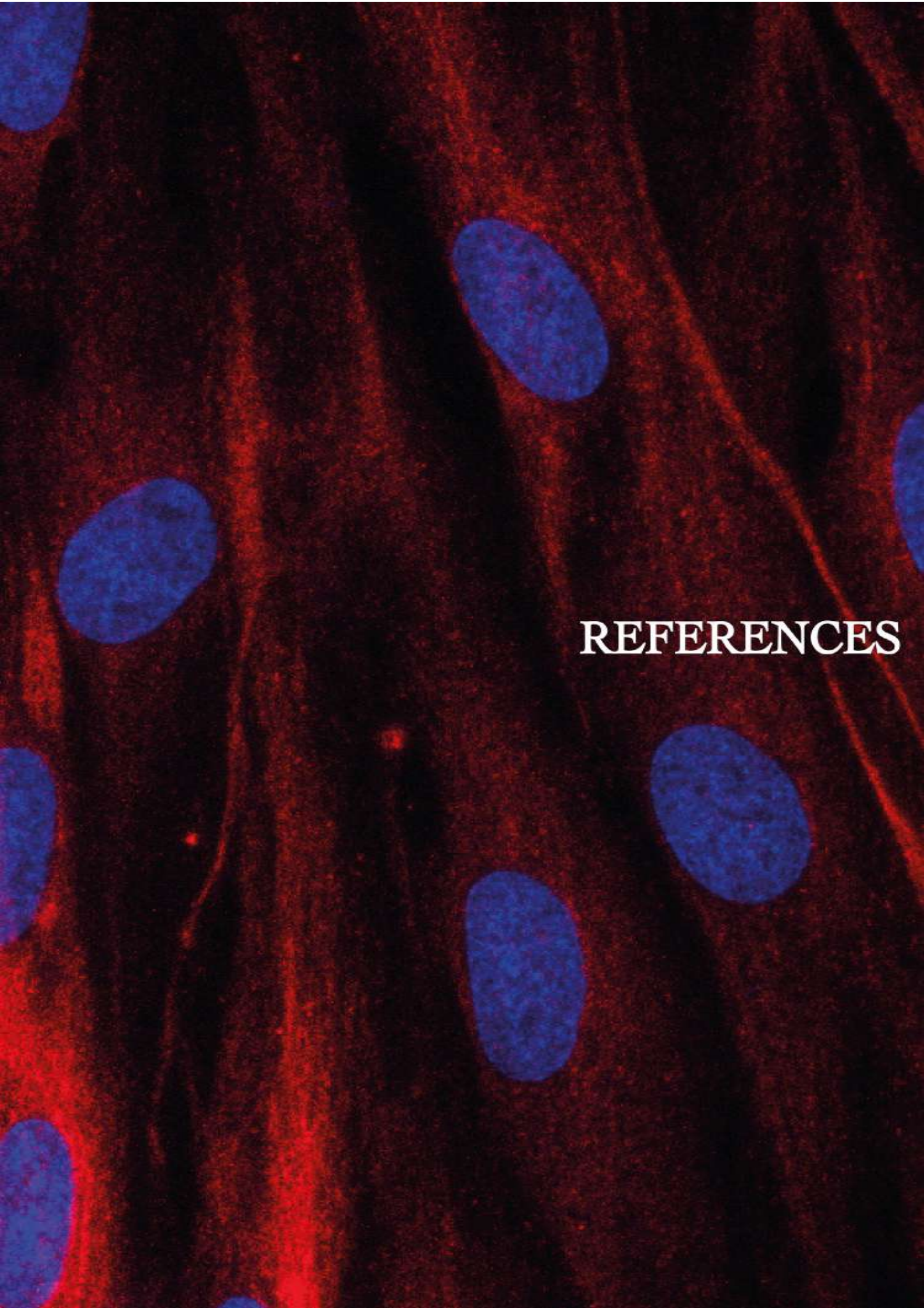

REFERENCES

This image is property of Claudia Pérez García. Immunofluorescence of human dental pulp stem cells against Nestin. Image acquisition: Leica SPEII confocal microscope.

References

Abe, Y., Honsho, M., Nakanishi, H., Taguchi, R., & Fujiki, Y. (2014). Very-long-chain polyunsaturated fatty acids accumulate in phosphatidylcholine of fibroblasts from patients with Zellweger syndrome and acyl-CoA oxidase1 deficiency. *Biochimica et Biophysica Acta (BBA) - Molecular and Cell Biology of Lipids*, *1841*(4), 610–619. https://doi.org/10.1016/j.bbalip.2014.01.001

Abrahams, J. J., Frisoli, J. K., & Dembner, J. (1995). Anatomy of the jaw, dentition, and related regions. *Seminars in Ultrasound, CT and MRI*, *16*(6), 453–467. https://doi.org/10.1016/S0887-2171(06)80020-x

Aguilar, P. S., Baylies, M. K., Fleissner, A., Helming, L., Inoue, N., Podbilewicz, B., Wang, H., & Wong, M. (2013). Genetic basis of cell-cell fusion mechanisms. *Trends in Genetics: TIG*, *29*(7), 427–437. https://doi.org/10.1016/J.TIG.2013.01.011

Albersen, M., Van Der Beek, S. L., Dijkstra, I. M. E., Alders, M., Barendsen, R.W., Bliek, J., Boelen, A., Ebberink, M.S., Ferdinandusse, S., Goorden, S. M. I., Heijboer, A.C., Jansen, M., Jaspers, Y. R. J., Metgod, I., Salomons, G. S., Vaz, F. M., Verschoof-Puite, R. K., Visser, W. F., Dekkers, E., Engelen, M., … Kemp, S. (2023). Sex-specific newborn screening for X-linked adrenoleukodystrophy. *Journal of inherited metabolic disease, 46*(1), 116-128. https://doi.org/10.1002/jimd.12571

Al Madhoun, A., Sindhu, S., Haddad, D., Atari, M., Ahmad, R., & Al-Mulla, F. (2021). Dental Pulp Stem Cells Derived From Adult Human Third Molar Tooth: A Brief Review. *Frontiers in cell and developmental biology, 9*, 717624. https://doi.org/10.3389/fcell.2021.717624

Alvarez-Dolado, M., Pardal, R., Garcia-Verdugo, J. M., Fike, J. R., Lee, H. O., Pfeffer, K., Lois, C., Morrison, S. J., & Alvarez-Bullia, A. (2003). Fusion of bone-marrow-derived cells with Purkinje neurons, cardiomyocytes and hepatocytes. *Nature*, *425*(6961), 968–973. https://doi.org/10.1038/nature02069

Anzalone, R., Lo Iacono, M., Corrao, S., Magno, F., Loria, T., Cappello, F., Zummo, G., Farina, F., & La Rocca, G. (2010). New emerging potentials for human Wharton's jelly mesenchymal stem cells: Immunological features and hepatocyte-like differentiative capacity. *Stem Cells and Development, 19*(4), 423-438. https://doi.org/10.1089/scd.2009.0299

Arabpour, M., Saghazadeh, A., & Rezaei, N. (2021). Anti-inflammatory and M2 macrophage polarization-promoting effect of mesenchymal stem cell-derived exosomes. *International Immunopharmacology*, *97*, 107823. https://doi.org/10.1016/j.intimp.2021.107823

Arthur, A., Rychkov, G., Shi, S., Koblar, S. A., & Gronthos, S. (2008). Adult human dental pulp stem cells differentiate toward functionally active neurons under appropriate environmental cues. *Stem Cells*, *26*(7), 1787–1795. https://doi.org/10.1634/stemcells.2007-0979

Aubourg, P., Adamsbaum, C., Lavallard-Rousseau, M. C., Rocchiccioli, F., Cartier, N., Jambaque, I., Jakobezak, C., Lemaitre, A., Boureau, F. & Wolf, C. (1993). A two-year trial of oleic and erucic acids ("Lorenzo's oil") as treatment for adrenomyeloneuropathy. *The New England Journal of Medicine*, *329*(11), 745–752. https://doi.org/10.1056/NEJM199309093291101

Avanzini, M. A., Mura, M., Percivalle, E., Bastaroli, F., Croce, S., Valsecchi, C., Lenta, E., Nykjaer, G., Cassaniti, I., Bagnarino, J., Baldanti, F., Zecca, M., Comoli, P., & Gnecchi, M. (2021). Human mesenchymal stromal cells do not express ACE2 and TMPRSS2 and are not permissive to SARS-CoV-2 infection. *Stem cells translational medicine*, 10(4), 636–642. https://doi.org/10.1002/sctm.20-0385

Azevedo-Pereira, R. L., Aizman, I., & Nejadnik, B. (2024). Mesenchymal Stem Cells Promote an Increase in Neuronal Oscillation via Glutamate Tonic Release. *Neuroscience, 552,* 76–88. https://doi.org/10.1016/j.neuroscience.2024.06.015

Baarine, M., Andréoletti, P., Athias, A., Nury, T., Zarrouk, A., Ragot, K., Vejux, A., Riedinger, J. M., Kattan, Z., Bessede, G., Trompier, D., Savary, S., Cherkaoui-Malki, M., & Lizard, G. (2012). Evidence

of oxidative stress in very long chain fatty acid - Treated oligodendrocytes and potentialization of ROS production using RNA interference-directed knockdown of ABCD1 and ACOX1 peroxisomal proteins. *Neuroscience*, *213*, 1–18. https://doi.org/10.1016/j.neuroscience.2012.03.058

Baarine, M., Khan, M., Singh, A., & Singh, I. (2015). Functional Characterization of IPSC-Derived Brain Cells as a Model for X-Linked Adrenoleukodystrophy. *PLOS ONE*, *10*(11), e0143238. https://doi.org/10.1371/journal.pone.0143238

Baghaei, K., Hashemi, S.M, Tokhanbigli, S., Asadi Rad, A., Assadzadeh-Aghdaei, H., Sharifian, A., & Zali, M.R. (2017). Isolation, differentiation, and characterization of mesenchymal stem cells from human bone marrow. *Gastroenterology and Hepatology From Bed to Bench, 10*(3), 208-213.

Bakopoulou, A., Leyhausen, G., Volk, J., Tsiftsoglou, A., Garefis, P., Koidis, P., & Geurtsen, W. (2011). Comparative analysis of in vitro osteo/odontogenic differentiation potential of human dental pulp stem cells (DPSCs) and stem cells from the apical papilla (SCAP). *Archives of Oral Biology*, *56*(7), 709–721. https://doi.org/10.1016/j.archoralbio.2010.12.008

Balistreri, C. R., De Falco, E., Bordin, A., Maslova, O., Koliada, A., & Vaiserman, A. (2020). Stem cell therapy: old challenges and new solutions. *Molecular biology reports, 47*(4), 3117–3131. https://doi.org/10.1007/s11033-020-05353-2

Bansal, R., & Jain, A. (2015). Current overview on dental stem cells applications in regenerative dentistry. *Journal of Natural Science, Biology and Medicine*, *6*(1), 29-34. https://doi.org/10.4103/0976-9668.149074

Bartsch, G., Yoo, J. J., De Coppi, P., Siddiqui, M. M., Schuch, G., Pohl, H. G., Fuhr, J., Perin, L., Soker, S., & Atala, A. (2005). Propagation, Expansion, and Multilineage Differentiation of Human Somatic Stem Cells from Dermal Progenitors. *Stem cells and development, 14* (3), 337-348. https://doi.org/10.1089/scd.2005.14.337

Barzilay, R., Melamed, E., & Offen, D. (2009). Introducing transcription factors to multipotent mesenchymal stem cells: making transdifferentiation possible. *Stem Cells (Dayton, Ohio)*, *27*(10), 2509–2515. https://doi.org/10.1002/stem.172

Berger, J., Molzer, B., Faé, I., & Bernheimer, H. (1994). X-linked adrenoleukodystrophy (X-ALD): a novel mutation of the ALD gene in 6 members of a family presenting with 5 different phenotypes. *Biochemical and Biophysical Research Communications*, *205*(3), 1638–1643. https://doi.org/10.1006/bbrc.1994.2855

Berger, J., Pujol, A., Aubourg, P., & Forss-Petter, S. (2010). Current and Future Pharmacological Treatment Strategies in X-Linked Adrenoleukodystrophy. *Brain Pathology*, *20*(4), 845-856. https://doi.org/10.1111/j.1750-3639.2010.00393.x

Bernardo, M. E., & Fibbe, W. E. (2013). Mesenchymal Stromal Cells: Sensors and Switchers of Inflammation. *Cell Stem Cell*, *13*(4), 392–402. https://doi.org/10.1016/j.stem.2013.09.006

Bilodeau, E. A., & Hunter, K. D. (2021). Odontogenic and Developmental Oral Lesions in Pediatric Patients. *Head and Neck Pathology*, *15*(1), 71–84. https://doi.org/10.1007/s12105-020-01284-3

Blaw, M. E. (1970). Melanodermic type leukodystrophy (adreno-leukodystrophy). In P. J. Vinken & C. W. Bruyn (Eds.), *Handbook of clinical neurology* (Vol. 10, pp. 128–133). American Elsevier.

Boles, D. J., Craft, D. A., Padgett, D. A., Loria, R. M., & Rizzo, W. B. (1991). Clinical Variation in X-Linked Adrenoleukodystrophy: Fatty Acid and Lipid Metabolism in Cultured Fibroblasts. In *Biochemical medicine and metabolic biology, 45*(1), 74-91. https://doi.org/10.1016/0885-4505(91)90010-i

Bonkowsky, J. L. (2021). New insights into genetic white matter disorders. *Developmental Medicine and Child Neurology*, *63*(9), 1010. https://doi.org/10.1111/dmcn.14891

Boyd, M. J., Collier, P. N., Clark, M. P., Deng, H., Kesavan, S., Ronkin, S. M., Waal, N., Wang, J., Cao, J., Li, P., Come, J., Davies, I., Duffy, J. P., Cochran, J. E., Court, J. J., Chandupatla, K., Jackson, K. L., Maltais, F., O'Dowd, H., Boucher, C., … Magavi, S. S. (2021). Discovery of Novel, Orally Bioavailable Pyrimidine Ether-Based Inhibitors of ELOVL1. *Journal of Medicinal Chemistry*, *64*(24), 17777–17794. https://doi.org/10.1021/acs.jmedchem.1c00948

Brown, F. R., van Duyn, M. A. S., Moser, A. B., Schulman, J. D., Rizzo, W. B., Snyder, R. D., Murphy, J. V., Kamoshita, S., & Migeon, C. J. (1982). Adrenoleukodystrophy: Effects of dietary restriction of very long chain fatty acids and of administration of carnitine and clofibrate on clinical status and plasma fatty acids. *Johns Hopkins Medical Journal*, *151*(4), 164–172.

Bueno, C., Ramirez, C., Rodríguez-Lozano, F. J., Tabarés-Seisdedos, R., Rodenas, M., Moraleda, J. M., Jones, J. R., Martinez, S. (2013). Human adult periodontal ligament-derived cells integrate and differentiate after implantation into the adult mammalian brain. *Cell Transplantation*, *22*(11), 2017–2028. https://doi.org/10.3727/096368912X657305

Bueno, C., Martínez-Morga, M., García-Bernal, D., Moraleda, J. M., & Martínez, S. (2021). Differentiation of human adult-derived stem cells towards a neural lineage involves a dedifferentiation event prior to differentiation to neural phenotypes. *Scientific Reports*, *11*(1), 12034. https://doi.org/10.1038/s41598-021-91566-9

Burnham, A. J., Daley-Bauer, L. P., & Horwitz, E. M. (2020). Mesenchymal stromal cells in hematopoietic cell transplantation. *Blood Advances*, *4*(22), 5877–5887. https://doi.org/10.1182/bloodadvances.2020002646

Campanella, V. (2018). Dental Stem Cells: Current research and future applications. *European Journal of Paediatric Dentistry*, *19*(4), 257. https://doi.org/10.23804/EJPD.2018.19.04.1

Caplan, A. I. (1991). Mesenchymal stem cells. *Journal of Orthopaedic Research*, *9*(5), 641–650. https://doi.org/10.1002/jor.1100090504

Caplan, A. I. (2017). Mesenchymal stem cells: Time to change the name! *Stem Cells Translational Medicine*, *6*(6), 1445–1451. https://doi.org/10.1002/sctm.17-0051

Cartier, N., Hacein-Bey-Abina, S., Bartholomae, C. C., Veres, G., Schmidt, M., Kutschera, I., Vidaud, M., Abel, U., Dal-Cortivo, L., Caccavelli, L., Mahlaoui, N., Kiermer, V., Mittelstaedt, D., Bellesme, C., Lahlou, N., Lefrère, F., Blanche, S., Audit, M., Payen, E., Leboulch, P., … Aubourg, P. (2009). Hematopoietic stem cell gene therapy with a lentiviral vector in X-linked adrenoleukodystrophy. *Science (New York, N.Y.)*, *326*(5954), 818–823. https://doi.org/10.1126/science.1171242

Cartier, N., & Aubourg, P. (2010). Hematopoietic Stem Cell Transplantation and Hematopoietic Stem Cell Gene Therapy in X-Linked Adrenoleukodystrophy. *Brain Pathology*, *20*(4), 857–862. https://doi.org/10.1111/j.1750-3639.2010.00394.x

Cartier, N., Lewis, C. A., Zhang, R., & Rossi, F. M. V. (2014). The role of microglia in human disease: therapeutic tool or target? *Acta Neuropathologica*, *128*(3), 363–380. https://doi.org/10.1007/s00401-014-1330-y

Casado-Díaz, A. (2022). Stem Cells in Regenerative Medicine. *Journal of Clinical Medicine, 11*(18), 5460. https://doi.org/10.3390/jcm11185460

Casasnovas, C., Ruiz, M., Schlüter, A., Naudí, A., Fourcade, S., Veciana, M., Castañer, S., Albertí, A., Bargalló, N., Johnson, M., Raymond, G. V., Fatemi, A., Moser, A. B., Villarroya, F., Portero-Otín, M., Artuch, R., Pamplona, R., & Pujol, A. (2019). Biomarker Identification, Safety, and Efficacy of High-Dose Antioxidants for Adrenomyeloneuropathy: a Phase II Pilot Study. *Neurotherapeutics: The Journal of the American Society for Experimental NeuroTherapeutics*, *16*(4), 1167–1182. https://doi.org/10.1007/s13311-019-00735-2

Chang, C.C., Chang, K.C., Tsai, S.J., Chang, H.H., & Lin, C.P. (2014). Neurogenic differentiation of dental pulp stem cells to neuron-like cells in dopaminergic and motor neuronal inductive media. *Journal of the Formosan Medical Association*, *113*(12), 956–965. https://doi.org/10.1016/j.jfma.2014.09.003

Chen, J.R., Cheng, G.Y., Sheu, C.C., Tseng, G.F., Wang, T.J., & Huang, Y.S. (2008). Transplanted bone marrow stromal cells migrate, differentiate and improve motor function in rats with experimentally induced cerebral stroke. *Journal of Anatomy*, *213*(3), 249–258. https://doi.org/10.1111/j.1469-7580.2008.00948.x

Chernomordik, L. V., Zimmerberg, J., & Kozlov, M. M. (2006). Membranes of the world unite! *The Journal of Cell Biology*, *175*(2), 201–207. https://doi.org/10.1083/jcb.200607083

Coelho, D., Kim, J. C., Miousse, I. R., Fung, S., Du Moulin, M., Buers, I., Suormala, T., Burda, P., Frapolli, M., Stucki, M., Nürnberg, P., Thiele, H., Robenek, H., Höhne, W.,Longo, N., Pasquali, M., Mengel, E., Watkins, D., Shoubridge, E. A., Majewski, J., … Baumgartner, M. R. (2012). Mutations in ABCD4 cause a new inborn error of vitamin B12 metabolism. *Nature Genetics*, *44*(10), 1152–1155. https://doi.org/10.1038/ng.2386

Come, J. H., Senter, T. J., Clark, M. P., Court, J. J., Gale-Day, Z., Gu, W., Krueger, E., Liang, J., Morris, M., Nanthakumar, S., O'Dowd, H., Maltais, F., Iyer, G., Andreassi, J., Boucher, C., Considine, T., Moody, C. S., Taylor, W., Mohanty, A. K., Huang, Y., … Magavi, S. S. (2021). Discovery and Optimization of Pyrazole Amides as Inhibitors of ELOVL1. *Journal of Medicinal Chemistry*, *64*(24), 17753-17776. https://doi.org/10.1021/acs.jmedchem.1c00944

Cook, H. W. (1996). Fatty acid desaturation and chain elongation in eukaryotes. In D. E. Vance & J. Vance (Eds.), *Biochemistry of lipids, lipoproteins, and membranes* (pp. 129–152). Elsevier. https://doi.org/10.1016/S0167-7306(08)60512-8

Corcione, A., Benvenuto, F., Ferretti, E., Giunti, D., Cappiello, V., Cazzanti, F., Risso, M., Gualandi, F., Mancardi, G. L., Pistoia, V., & Uccelli, A. (2006). Human mesenchymal stem cells modulate B-cell functions. *Blood*, *107*(1), 367–372. https://doi.org/10.1182/blood-2005-07-2657

Cui, L. L., Nitzsche, F., Pryazhnikov, E., Tibeykina, M., Tolppanen, L., Rytkönen, J., Huhtala, T., Mu, J. W., Khiroug, L., Boltze, J., & Jolkkonen, J. (2017). Integrin α4 overexpression on rat mesenchymal stem cells enhances transmigration and reduces cerebral embolism after intracarotid injection. *Stroke*, *48*(10), 2895–2900. https://doi.org/10.1161/STROKEAHA.117.017809

De Beer, M., Engelen, M., & Van Geel, B. M. (2014). Frequent occurrence of cerebral demyelination in adrenomyeloneuropathy. *Neurology*, *83*(24), 2227–2231. https://doi.org/10.1212/WNL.0000000000001074

Dean, M., & Annilo, T. (2005). Evolution of the ATP-binding cassette (ABC) transporter superfamily in vertebrates. *Annual Review of Genomics and Human Genetics*, *6*, 123–142. https://doi.org/10.1146/ANNUREV.GENOM.6.080604.162122

Dean, M., Moitra, K., & Allikmets, R. (2022). The human ATP-binding cassette (ABC) transporter superfamily. *Human Mutation, 43*(9), 1162-1182. https://doi.org/10.1002/humu.24418

De Laorden, E. H., Simón, D., Milla, S., Portela-Lomba, M., Mellén, M., Sierra, J., de la Villa, P., Moreno-Flores, M. T., & Iglesias, M. (2023). Human placenta-derived mesenchymal stem cells stimulate neuronal regeneration by promoting axon growth and restoring neuronal activity. *Frontiers in cell and developmental biology, 11*, 1328261. https://doi.org/10.3389/fcell.2023.1328261

Della Sala, F., di Gennaro, M., Lista, G., Messina, F., Ambrosio, L., & Borzacchiello, A. (2021). Effect of Hyaluronic Acid on the Differentiation of Mesenchymal Stem Cells into Mature Type II Pneumocytes. *Polymers, 13*(17), 2928. https://doi.org/10.3390/polym131729

De Miguel, M.P., Fuentes-Julián, S., & Alcaina, Y. (2010). Pluripotent stem cells: origin, maintenance and induction. *Stem cells reviews and reports, 6*(4), 633-649. https://doi.org/10.1007/s12015-010-9170-1

Deon, M., Sitta, A., Barschak, A. G., Coelho, D. M., Pigatto, M., Schmitt, G. O., Jardim, L. B., Giugliani, R., Wajner, M., & Vargas, C. R. (2007). Induction of lipid peroxidation and decrease of antioxidant defenses in symptomatic and asymptomatic patients with X-linked adrenoleukodystrophy. *International Journal of Developmental Neuroscience*, *25*(7), 441–444. https://doi.org/10.1016/J.IJDEVNEU.2007.08.008

Deon, M. y Sitta, A., Barschak, A. G., Coelho, D. M., Terroso, T., Schmitt, G. O., Wanderley, H. Y., Jardim, L. B., Giugliani, R., Wajner, M., & Vargas, C. R. (2008). Oxidative stress is induced in female carriers of X-linked adrenoleukodystrophy. *Journal of the Neurological Sciences*, *266*(1–2), 79–83. https://doi.org/10.1016/j.jns.2007.08.043

Di Biase, A., Salvati, S., Varí, R., Avellino, C., Sforza, F., Cappa, M., & Masella, R. (2000). Susceptibility to oxidation of plasma low-density lipoprotein in X-linked adrenoleukodystrophy: Effects of simvastatin treatment. *Molecular Genetics and Metabolism*, *71*(4), 651–655. https://doi.org/10.1006/mgme.2000.3100

Di Mambro, T., Pellielo, G., Agyapong, E. D., Carinci, M., Chianese, D., Giorgi, C., Morciano, G., Patergnani, S., Pinton, P., & Rimessi, A. (2023). The Tricky Connection between Extracellular Vesicles and Mitochondria in Inflammatory-Related Diseases. *International Journal of Molecular Sciences*, *24*(9), 8181. https://doi.org/10.3390/ijms24098181

Dilger, N., Neehus, A.L., Grieger, K., Hoffmann, A., Menssen, M., & Ngezahayo, A. (2020). Gap Junction Dependent Cell Communication Is Modulated During Transdifferentiation of Mesenchymal Stem/Stromal Cells Towards Neuron-Like Cells. *Frontiers in Cell and Developmental Biology*, *8,* 869. https://doi.org/10.3389/fcell.2020.00869

Ding, D.C., Chang, Y.H., Shyu, W.C., & Lin, S.Z. (2015). Human Umbilical Cord Mesenchymal Stem Cells: A New Era for Stem Cell Therapy. *Cell Transplantation*, *24*(3), 339–347. https://doi.org/10.3727/096368915X686841

Dominici, M., Le Blanc, K., Mueller, I., Slaper-Cortenbach, I., Marini, F., Krause, D., Deans, R., Keating, A., Prockop, D. J., & Horwitz, E. M. (2006). Minimal criteria for defining multipotent mesenchymal stromal cells. The International Society for Cellular Therapy position statement. *Cytotherapy*, *8*(4), 315–317. https://doi.org/10.1080/14653240600855905

Dörnen, J., & Dittmar, T. (2021). The Role of MSCs and Cell Fusion in Tissue Regeneration. *International Journal of Molecular Sciences*, *22*(20), 10980. https://doi.org/10.3390/ijms222010980

Dorshkind, K., Green, L., Godwin, A., & Fletcher, W. H. (1993). Connexin-43-Type Gap Junctions Mediate Communication Between Bone Marrow Stromal Cells. *Blood*, *82*(1), 38–45. https://doi.org/10.1182/BLOOD.V82.1.38.BLOODJOURNAL82138

Dubey, P., Raymond, G. V., Moser, A. B., Kharkar, S., Bezman, L., & Moser, H. W. (2005). Adrenal insufficiency in asymptomatic adrenoleukodystrophy patients identified by very long-chain fatty acid screening. *Journal of Pediatrics*, *146*(4), 528–532. https://doi.org/10.1016/j.jpeds.2004.10.067

Dulak, J., Szade, K., Szade, A., Nowak, W., & Józkowicz, A. (2015). Adult stem cells: hopes and hypes of regenerative medicine. *Acta Biochimica Polonica*, *62*(3), 329–337. https://doi.org/10.18388/abp.2015_1023

Dumitru, C. A., Hemeda, H., Jakob, M., Lang, S., & Brandau, S. (2014). Stimulation of mesenchymal stromal cells (MSCs) via TLR3 reveals a novel mechanism of autocrine priming. *FASEB Journal : Official Publication of the Federation of American Societies for Experimental Biology*, *28*(9), 3856–3866. https://doi.org/10.1096/FJ.14-250159

Dupin, E., & Sommer, L. (2012). Neural crest progenitors and stem cells: from early development to adulthood. *Developmental Biology*, *366*(1), 83–95. https://doi.org/10.1016/J.YDBIO.2012.02.035

Duque, G., Huang, D. C., Macoritto, M., Rivas, D., Yang, X. F., Ste-Marie, L. G., & Kremer, R. (2009). Autocrine Regulation of Interferon γ in Mesenchymal Stem Cells Plays a Role in Early Osteoblastogenesis. *Stem Cells*, *27*(3), 550–558. https://doi.org/10.1634/stemcells.2008-0886

Eichler, F., Duncan, C., Musolino, P. L., Orchard, P. J., De Oliveira, S., Thrasher, A. J., Armant, M., Dansereau, C., Lund, T. C., Miller, W. P., Raymond, G. V., Sankar, R., Shah, A. J., Sevin, C., Gaspar, H.B., Gissen, P., Amartino, H., Bratkovic, D., Smith, N. J. C., Paker, A.M., …Williams, D.A. (2017). Hematopoietic Stem-Cell Gene Therapy for Cerebral Adrenoleukodystrophy. *The New England Journal of Medicine, 377*(17), 1630-1638. https://doi.org/10.1056/NEJMoa1700554

Engelen, M., Ofman, R., Dijkgraaf, M. G., Hijzen, M., van der Wardt, L. A., van Geel, B. M., de Visser, M., Wanders, R. J., Poll-The, B. T., & Kemp, S. (2010). Lovastatin in X-linked adrenoleukodystrophy. *The New England Journal of Medicine*, *362*(3), 276–277. https://doi.org/10.1056/NEJMC0907735

Engelen, M., Tran, L., Ofman, R., Brennecke, J., Moser, A. B., Dijkstra, I. M., Wanders, R. J., Poll-The, B. T., & Kemp, S. (2012a). Bezafibrate for X-Linked Adrenoleukodystrophy. *PLoS ONE*, *7*(7), e41013. https://doi.org/10.1371/JOURNAL.PONE.0041013

Engelen, M., Schackmann, M. J., Ofman, R., Sanders, R. J., Dijkstra, I. M., Houten, S. M., Fourcade, S., Pujol, A., Poll-The, B. T., Wanders, R. J., & Kemp, S. (2012b). Bezafibrate lowers very long-chain fatty acids in X-linked adrenoleukodystrophy fibroblasts by inhibiting fatty acid elongation. *Journal of Inherited Metabolic Disease*, *35*(6), 1137-1145. https://doi.org/10.1007/S10545-012-9471-4

Engelen, M., Kemp, S., De Visser, M., Van Geel, B. M., Wanders, R. J., Aubourg, P., & Poll-The, B. T. (2012c). X-linked adrenoleukodystrophy (X-ALD): clinical presentation and guidelines for diagnosis, follow-up and management. *Orphanet Journal of Rare Diseases*, *7*(1), 51. https://doi.org/10.1186/1750-1172-7-51

Eom, Y. W., Oh, J. E., Lee, J. I., Baik, S. K., Rhee, K. J., Shin, H. C., Kim, Y. M., Ahn, C. M., Kong, J. H., Kim, H. S., & Shim, K. Y. (2014). The role of growth factors in maintenance of stemness in bone marrow-derived mesenchymal stem cells. *Biochemical and Biophysical Research Communications*, *445*(1), 16–22. https://doi.org/10.1016/J.BBRC.2014.01.084

Erdei, Z., Lőrincz, R., Szebényi, K., Péntek, A., Varga, N., Likó, I., Várady, G., Szakács, G., Orbán, T. I., Sarkadi, B., & Apáti, Á. (2014). Expression pattern of the human ABC transporters in pluripotent embryonic stem cells and in their derivatives. *Cytometry Part B: Clinical Cytometry*, *86*(5), 299–310. https://doi.org/10.1002/cyto.b.21168

Esterbauer, H., Schaur, R. J., & Zollner, H. (1991). Chemistry and biochemistry of 4-hydroxynonenal, malonaldehyde and related aldehydes. *Free Radical Biology and Medicine*, *11*(1), 81–128. https://doi.org/10.1016/0891-5849(91)90192-6

Evans, M. J., & Kaufman, M. H. (1981). Establishment in culture of pluripotential cells from mouse embryos. *Nature*, *292*(5819), 154–156. https://doi.org/10.1038/292154A0

Fanconi, A., Prader, A., Isler, W., Luethy, F., & Siebenmann, R. (1963). Addison's disease with cerebral sclerosis in childhood. A hereditary syndrome transmitted through chromosome X. *Helvetica Paediatrica Acta*, *18*, 480–501. https://pubmed.ncbi.nlm.nih.gov/14110277/

Foudah, D., Monfrini, M., Donzelli, E., Niada, S., Brini, A. T., Orciani, M., Tredici, G., & Miloso, M. (2014). Expression of Neural Markers by Undifferentiated Mesenchymal-Like Stem Cells from Different Sources. *Journal of Immunology Research*, *2014*, 1–16. https://doi.org/10.1155/2014/987678

Fourcade, S., Lopez-Erauskin, J., Galino, J., Duval, C., Naudi, A., Jove, M., Kemp, S., Villarroya, F., Ferrer, I., Pamplona, R., Portero-Otin, M., & Pujol, A. (2008). Early oxidative damage underlying neurodegeneration in X-adrenoleukodystrophy. *Human Molecular Genetics*, *17*(12), 1762–1773. https://doi.org/10.1093/hmg/ddn085

Fourcade, S., Ferrer, I., & Pujol, A. (2015). Oxidative stress, mitochondrial and proteostasis malfunction in adrenoleukodystrophy: A paradigm for axonal degeneration. *Free Radical Biology and Medicine*, *88*, 18–29. https://doi.org/10.1016/j.freeradbiomed.2015.05.041

Fransen, M., Lismont, C., & Walton, P. (2017). The Peroxisome-Mitochondria Connection: How and Why? *International journal of molecular sciences, 18*(6), 1126. https://doi.org/10.3390/ijms18061126

Freitag, J., Bates, D., Wickham, J., Shah, K., Huguenin, L., Tenen, A., Paterson, K., & Boyd, R. (2019). Adipose-Derived Mesenchymal Stem Cell Therapy in the Treatment of Knee Osteoarthritis: A Randomized Controlled Trial. *Regenerative Medicine*, *14*(3), 213–230. https://doi.org/10.2217/rme-2018-0161

Friedenstein, A. J., Chailakhjan, R. K., & Lalykina, K. S. (1970). The development of fibroblast colonies in monolayer cultures of guinea-pig bone marrow and spleen cells. *Cell Tissue Kinetics, 3*(4), 393-403. https://doi.org/10.1111/j.1365-2184.1970.tb00347.x

Friedman, J. R., & Nunnari, J. (2014). Mitochondrial form and function. *Nature, 505*(7483), 335-343. https://doi.org/10.1038/nature12985

Gabashvili, A. N., Baklaushev, V. P., Grinenko, N. F., Levinskii, A. B., Mel'nikov, P. A., Cherepanov, S. A., & Chekhonin, V. P. (2015). Functionally Active Gap Junctions between Connexin 43-Positive Mesenchymal Stem Cells and Glioma Cells. *Bulletin of Experimental Biology and Medicine*, *159*(1), 173–179. https://doi.org/10.1007/s10517-015-2916-7

Garside, S., Rosebush, P. I., Levinson, A.J., & Mazurek, M. F. (1999). Late-Onset Adrenoleukodystrophy Associated With Long-Standing Psychiatric Symptoms. *The Journal of Clinical Psychiatry*, *60*(7), 460-468. https://doi.org/10.4088/jcp.v60n0708

Geillon, F., Gondcaille, C., Charbonnier, S., Van Roermund, C. W., Lopez, T. E., Dias, A. M., De Barros, J. P., Arnould, C., Wanders, R. J., Trompier, D., & Savary, S. (2014). Structure-function analysis of peroxisomal ATP-binding cassette transporters using chimeric dimers. *Journal of Biological Chemistry*, *289*(35), 24511–24520. https://doi.org/10.1074/jbc.M114.575506

Geillon, F., Gondcaille, C., Raas, Q., Dias, A. M. M., Pecqueur, D., Truntzer, C., Lucchi, G., Ducoroy, P., Falson, P., Savary, S., & Trompier, D. (2017). Peroxisomal ATP-binding cassette transporters form mainly tetramers. *Journal of Biological Chemistry*, *292*(17), 6965–6977. https://doi.org/10.1074/jbc.M116.772806

Generali, M., Kehl, D., Wanner, D., Okoniewski, M. J., Hoerstrup, S. P., & Cinelli, P. (2022). Heterogeneous expression of ACE2 and TMPRRS2 in mesenchymal stromal cells. *Journal of cellular and molecular medicine*, 26(1), 228–234. https://doi.org/10.1111/jcmm.17048

Genin, E. C., Geillon, F., Gondcaille, C., Athias, A., Gambert, P., Trompier, D., & Savary, S. (2011). Substrate specificity overlap and interaction between adrenoleukodystrophy protein (ALDP/ABCD1) and adrenoleukodystrophy-related protein (ALDRP/ABCD2). *Journal of Biological Chemistry*, *286*(10), 8075–8084. https://doi.org/10.1074/jbc.M110.211912

Ghannam, S., Pène, J., Moquet-Torcy, G., Jorgensen, C., & Yssel, H. (2010). Mesenchymal Stem Cells Inhibit Human Th17 Cell Differentiation and Function and Induce a T Regulatory Cell Phenotype. *The Journal of Immunology*, *185*(1), 302–312. https://doi.org/10.4049/jimmunol.0902007

Gilg, A. G., Singh, A. K., & Singh, I. (2000). Inducible nitric oxide synthase in the central nervous system of patients with X-adrenoleukodystrophy. *Journal of Neuropathology and Experimental Neurology*, *59*(12), 1063–1069. https://doi.org/10.1093/JNEN/59.12.1063

Golan, K., Singh, A. K., Kollet, O., Bertagna, M., Althoff, M. J., Khatib-Massalha, E., Petrovich-Kopitman, E., Wellendorf, A. M., Massalha, H., Levin-Zaidman, S., Dadosh, T., Bohan, B., Gawali, M., Dasgupta, B., Lapidot, T., & Cancelas, J. A. (2020). Bone marrow regeneration requires mitochondrial transfer from donor Cx43-expressing hematopoietic progenitors to stroma. *Blood*, *136*(23), 2607–2619. https://doi.org/10.1182/BLOOD.2020005399

González-Nieto, D., Chang, K. H., Fasciani, I., Nayak, R., Fernandez-García, L., Barrio, L. C., & Cancelas, J. A. (2015). Connexins: Intercellular Signal Transmitters in Lymphohematopoietic Tissues. *International Review of Cell and Molecular Biology*, *318*, 27–62. https://doi.org/10.1016/BS.IRCMB.2015.06.001

Gore, A., Li, Z., Fung, H.L., Young, J. E., Agarwal, S., Antosiewicz-Bourget, J., Canto, I., Giorgetti, A., Israel, M. A., Kiskinis, E., Lee, J.H., Loh, Y.H., Manos, P. D., Montserrat, N., Panopoulos, A. D., Ruiz, S., Wilbert, M. L., Yu, J., Kirkness, E. F., Izpisua Belmonte, J.C., … Zhang, K. (2011). Somatic coding mutations in human induced pluripotent stem cells. *Nature*, *471*(7336), 63–67. https://doi.org/10.1038/nature09805

Gosalakkal, J., & Balky, A. P. (2010). Intra familial phenotypical variations in adrenoleukodystrophy. *Neurology India*, *58*(1), 109–111. https://doi.org/10.4103/0028-3886.60418

Gray, M. W. (2012). Mitochondrial Evolution. *Cold Spring Harbor Perspectives in Biology, 4*(9). https://doi.org/10.1101/cshperspect.a011403

Gronthos, S., Mankani, M., Brahim, J., Robey, P. G., & Shi, S. (2000). Postnatal human dental pulp stem cells (DPSCs) *in vitro* and *in vivo*. *Proceedings of the National Academy of Sciences*, *97*(25), 13625–13630. https://doi.org/10.1073/pnas.240309797

Gronthos, S., Brahim, J., Li, W., Fisher, L. W., Cherman, N., Boyde, A., DenBesten, P., Robey, P. G., & Shi, S. (2002). Stem Cell Properties of Human Dental Pulp Stem Cells. *Journal of Dental Research*, *81*(8), 531–535. https://doi.org/10.1177/154405910208100806

Guimarães, C. P., Domingues, P., Aubourg, P., Fouquet, F., Pujol, A., Jimenez-Sanchez, G., Sá-Miranda, C., Azevedo, J. E. (2004). Mouse liver PMP70 and ALDP: Homomeric interactions prevail in vivo. *Biochimica et Biophysica Acta*, *1689*(3), 235–243. https://doi.org/10.1016/j.bbadis.2004.04.001

Guo, L., Rolfe, A. J., Wang, X., Tai, W., Cheng, Z., Cao, K., Chen, X., Xu, Y., Sun, D., Li, J., He, X., Young, W., Fan, J., & Ren, Y. (2016). Rescuing macrophage normal function in spinal cord injury with embryonic stem cell conditioned media. *Molecular Brain*, *9*(1), 48. https://doi.org/10.1186/s13041-016-0233-3

Guo, Y., Guo, W., Chen, J., Chen, G., Tian, W., & Bai, D. (2018). Are Hertwig's epithelial root sheath cells necessary for periodontal formation by dental follicle cells? *Archives of Oral Biology*, *94*, 1–9. https://doi.org/10.1016/j.archoralbio.2018.06.014

Guo, S., Wang, H., & Yin, Y. (2022). Microglia Polarization From M1 to M2 in Neurodegenerative Diseases. *Frontiers in Aging Neuroscience*, *14,* 815347. https://doi.org/10.3389/FNAGI.2022.815347

Haberfeld, W., & Spieler, F. (1910). Zur diffusen Hirn-Rückenmarksklerose im Kindesalter. *Deutsche Zeitschrift Für Nervenheilkunde*, *40*(5–6), 436–463. https://doi.org/10.1007/BF01629013

Halliwell, B. (1999). Antioxidant defence mechanisms: From the beginning to the end (of the beginning). *Free Radical Research*, *31*(4), 261–272. https://doi.org/10.1080/10715769900300841

Halliwell, B. (2006). Reactive Species and Antioxidants. Redox Biology Is a Fundamental Theme of Aerobic Life. *Plant Physiology*, *141*(2), 312–322. https://doi.org/10.1104/PP.106.077073

Harrell, C. R., Jovicic, N., Djonov, V., Arsenijevic, N., & Volarevic, V. (2019). Mesenchymal Stem Cell-Derived Exosomes and Other Extracellular Vesicles as New Remedies in the Therapy of Inflammatory Diseases. *Cells*, *8*(12), 1605. https://doi.org/10.3390/cells8121605

Harris-Jones, J. N., & Nixon, P. G. (1955). Familial Addison's disease with spastic paraplegia. *The Journal of Clinical Endocrinology and Metabolism*, *15*(6), 739–744. https://doi.org/10.1210/JCEM-15-6-739

Hartley, M. D., Kirkemo, L. L., Banerji, T., & Scanlan, T. S. (2017). A Thyroid Hormone–Based Strategy for Correcting the Biochemical Abnormality in X-Linked Adrenoleukodystrophy. *Endocrinology*, *158*(5), 1328. https://doi.org/10.1210/EN.2016-1842

Hein, S., Schönfeld, P., Kahlert, S., & Reiser, G. (2008). Toxic effects of X-linked adrenoleukodystrophy-associated, very long chain fatty acids on glial cells and neurons from rat hippocampus in culture. *Human Molecular Genetics*, *17*(12), 1750–1761. https://doi.org/10.1093/HMG/DDN066

Hernandez-Lopez, J. M., Hernandez-Medina, C., Medina-Corvalan, C., Rodenas, M., Francisca, A., Perez-Garcia, C., Echevarria, D., Carratala, F., Geijo-Barrientos, E., & Martinez, S. (2023). Neuronal progenitors of the dentate gyrus express the SARS-CoV-2 cell receptor during migration in the developing human hippocampus. *Cellular and molecular life sciences: CMLS, 80*(6), 140. https://doi.org/10.1007/s00018-023-04787-8

Hindi, S. M., Tajrishi, M. M., & Kumar, A. (2013). Signaling Mechanisms in Mammalian Myoblast Fusion. *Science Signaling*, *6*(272). https://doi.org/10.1126/scisignal.2003832

Ho, J. K., Moser, H., Kishimoto, Y., & Hamilton, J. A. (1995). Interactions of a very long chain fatty acid with model membranes and serum albumin. Implications for the pathogenesis of adrenoleukodystrophy. *Journal of Clinical Investigation*, *96*(3), 1455-1463. https://doi.org/10.1172/JCI118182

Honczarenko, M., Le, Y., Swierkowski, M., Ghiran, I., Glodek, A. M., & Silberstein, L. E. (2006). Human Bone Marrow Stromal Cells Express a Distinct Set of Biologically Functional Chemokine Receptors. *Stem Cells*, *24*(4), 1030–1041. https://doi.org/10.1634/stemcells.2005-0319

Horn, M. A., Retterstøl, L., Abdelnoor, M., Skjeldal, O. H., & Tallaksen, C. M. (2013). Adrenoleukodystrophy in Norway: high rate of de novo mutations and age-dependent penetrance. *Pediatric Neurology*, *48*(3), 212–219. https://doi.org/10.1016/J.PEDIATRNEUROL.2012.12.007

Huang, G. T., Sonoyama, W., Liu, Y., Liu, H., Wang, S., & Shi, S. (2008). The Hidden Treasure in Apical Papilla: The Potential Role in Pulp/Dentin Regeneration and BioRoot Engineering. *Journal of Endodontics*, *34*(6), 645-651. https://doi.org/10.1016/J.JOEN.2008.03.001

Huang, G. T., Gronthos, S., & Shi, S. (2009). Critical reviews in oral biology & medicine: Mesenchymal stem cells derived from dental tissues vs. those from other sources: Their biology and role in Regenerative Medicine. *Journal of Dental Research, 88*(9), 792-806. https://doi.org/10.1177/0022034509340867

Huang, Y., Mei, X., Jiang, W., Zhao, H., Yan, Z., Zhang, H., Liu, Y., Hu, X., Zhang, J., Peng, W., Zhang, J., Qi, Q., & Chen, N. (2021). Mesenchymal Stem Cell-Conditioned Medium Protects Hippocampal Neurons From Radiation Damage by Suppressing Oxidative Stress and Apoptosis. *Dose-Response*, *19*(1), 155932582098494. https://doi.org/10.1177/1559325820984944

Hubbard, W. C., Moser, A. B., Liu, A. C., Jones, R. O., Steinberg, S. J., Lorey, F., Panny, S. R., Vogt, R. F., Macaya, D., Turgeon, C. T., Tortorelli, S., & Raymond, G. V. (2009). Newborn screening for X-linked adrenoleukodystrophy (X-ALD): Validation of a combined liquid chromatography–tandem mass spectrometric (LC–MS/MS) method. *Molecular Genetics and Metabolism*, *97*(3), 212–220. https://doi.org/10.1016/J.YMGME.2009.03.010

Huffnagel, I. C., Laheji, F. K., Aziz-Bose, R., Tritos, N. A., Marino, R., Linthorst, G. E., Kemp, S., Engelen, M., & Eichler, F. (2019). The Natural History of Adrenal Insufficiency in X-Linked Adrenoleukodystrophy: An International Collaboration. *The Journal of Clinical Endocrinology and Metabolism*, *104*(1), 118–126. https://doi.org/10.1210/JC.2018-01307

Hussein, S. M., Batada, N. N., Vuoristo, S., Ching, R. W., Autio, R., Närvä, E., Ng, S., Sourour, M., Hämäläinen, R., Olsson, C., Lundin, K., Mikkola, M., Trokovic, R., Peitz, M., Brüstle, O., Bazett-Jones, D. P., Alitalo, K., Lahesmaa, R., Nagy, A., & Otonkoski, T. (2011). Copy number variation and selection during reprogramming to pluripotency. *Nature*, *471*(7336), 58–62. https://doi.org/10.1038/nature09871

Hyvärinen, K., Holopainen, M., Skirdenko, V., Ruhanen, H., Lehenkari, P., Korhonen, M., Käkelä, R., Laitinen, S., & Kerkelä, E. (2018). Mesenchymal Stromal Cells and Their Extracellular Vesicles Enhance the Anti-Inflammatory Phenotype of Regulatory Macrophages by Downregulating the Production of Interleukin (IL)-23 and IL-22. *Frontiers in Immunology*, *9*, 771. https://doi.org/10.3389/fimmu.2018.00771

Igarashi, M., Schaumburg, H. H., Powers, J., Kishimoto, Y., Kolodny, E., & Suzuki, K. (1976). Fatty acid abnormality in adrenoleukodystrophy. *Journal of Neurochemistry,* 26(4), 851-860. https://doi.org/10.1111/j.1471-4159.1976.tb04462.x

Iohara, K., Zheng, L., Ito, M., Tomokiyo, A., Matsushita, K., & Nakashima, M. (2006). Side Population Cells Isolated from Porcine Dental Pulp Tissue with Self-Renewal and Multipotency for Dentinogenesis, Chondrogenesis, Adipogenesis, and Neurogenesis. *Stem cells*, *24*(11), 2493–2503. https://doi.org/10.1634/stemcells.2006-0161

Ishizaka, R., Hayashi, Y., Iohara, K., Sugiyama, M., Murakami, M., Yamamoto, T., Fukuta, O., & Nakashima, M. (2013). Stimulation of angiogenesis, neurogenesis and regeneration by side population cells from dental pulp. *Biomaterials*, *34*(8), 1888–1897. https://doi.org/10.1016/j.biomaterials.2012.10.045

Islam, M. N., Das, S. R., Emin, M. T., Wei, M., Sun, L., Westphalen, K., Rowlands, D. J., Quadri, S. K., Bhattacharya, S., & Bhattacharya, J. (2012). Mitochondrial transfer from bone-marrow-derived stromal cells to pulmonary alveoli protects against acute lung injury. *Nature Medicine*, *18*(5), 759–765. https://doi.org/10.1038/NM.2736

Issa, S. S., Shaimardanova, A. A., Valiullin, V. V., Rizvanov, A. A., & Solovyeva, V. V. (2022). Mesenchymal Stem Cell-Based Therapy for Lysosomal Storage Diseases and Other Neurodegenerative Disorders. *Frontiers in Pharmacology, 13,* 859516. https://doi.org/10.3389/fphar.2022.859516

Izgi, K., Sonmez, M. F., Canatan, H., & Iskender, B. (2017). Long Term Exposure to Myrtucommulone-A Changes CD105 Expression and Differentiation Potential of Mesenchymal Stem Cells. *Tissue Engineering and Regenerative Medicine*, *14*(2), 113–121. https://doi.org/10.1007/s13770-016-0020-3

Jakobsson, A., Westerberg, R., & Jacobsson, A. (2006). Fatty acid elongases in mammals: their regulation and roles in metabolism. *Progress in Lipid Research*, *45*(3), 237–249. https://doi.org/10.1016/J.PLIPRES.2006.01.004

Janebodin, K., Horst, O. V., Ieronimakis, N., Balasundaram, G., Reesukumal, K., Pratumvinit, B., & Reyes, M. (2011). Isolation and characterization of neural crest-derived stem cells from dental pulp of neonatal mice. *PloS One*, *6*(11), e27526. https://doi.org/10.1371/JOURNAL.PONE.0027526

Jang, J., Kang, H. C., Kim, H. S., Kim, J. Y., Huh, Y. J., Kim, D. S., Yoo, J. E., Lee, J. A., Lim, B., Lee, J., Yoon, T. M., Park, I. H., Hwang, D. Y., Daley, G. Q., & Kim, D. W. (2011). Induced pluripotent stem cell models from X-linked adrenoleukodystrophy patients. *Annals of Neurology*, *70*(3), 402–409. https://doi.org/10.1002/ANA.22486

Jaspers, Y. R. J., Ferdinandusse, S., Dijkstra, I. M. E., Barendsen, R. W., van Lenthe, H., Kulik, W., Engelen, M., Goorden, S. M. I., Vaz, F. M., & Kemp, S. (2020). Comparison of the Diagnostic Performance of C26:0-Lysophosphatidylcholine and Very Long-Chain Fatty Acids Analysis for Peroxisomal Disorders. *Frontiers in Cell and Developmental Biology*, *8*. 690. https://doi.org/10.3389/FCELL.2020.00690

Juuri, E., Isaksson, S., Jussila, M., Heikinheimo, K., & Thesleff, I. (2013). Expression of the stem cell marker, SOX2, in ameloblastoma and dental epithelium. *European Journal of Oral Sciences*, *121*(6), 509–516. https://doi.org/10.1111/eos.12095

Kanafi, M., Majumdar, D., Bhonde, R., Gupta, P., & Datta, I. (2014). Midbrain Cues Dictate Differentiation of Human Dental Pulp Stem Cells Towards Functional Dopaminergic Neurons. *Journal of Cellular Physiology*, *229*(10), 1369–1377. https://doi.org/10.1002/jcp.24570

Karakaş, N., Bay, S., Türkel, N., Öztunç, N., Öncül, M., Bilgen, H., Shah, K., Şahin, F., & Öztürk, G. (2020). Neurons from human mesenchymal stem cells display both spontaneous and stimuli responsive activity. *PLoS ONE*, *15*(5), e228510. https://doi.org/10.1371/journal.pone.0228510

Kashiwayama, Y., Seki, M., Yasui, A., Murasaki, Y., Morita, M., Yamashita, Y., Sakaguchi, M., Tanaka, Y., & Imanaka, T. (2009). 70-kDa peroxisomal membrane protein related protein (P70R/ABCD4) localizes to endoplasmic reticulum not peroxisomes, and NH2-terminal hydrophobic property determines the subcellular localization of ABC subfamily D proteins. *Experimental Cell Research*, *315*(2), 190–205. https://doi.org/10.1016/J.YEXCR.2008.10.031

Kaushik, S., & Cuervo, A. M. (2015). Proteostasis and aging. *Nature medicine, 21*(12), 1406–1415. https://doi.org/10.1038/nm.4001

Kemp, S., Mooyer, P. A., Bolhuis, P. A., Geel, B. M., Mandel, J. L., Barth, P. G., Aubourg, P., & Wanders, R. J. (1996). ALDP expression in fibroblasts of patients with X-linked adrenoleukodystrophy. *Journal of Inherited Metabolic Disease*, *19*(5), 667–674. https://doi.org/10.1007/BF01799844

Kemp, S., Wei, H.M., Lu, J.F., Braiterman, L. T., McGuinness, M. C., Moser, A. B., Watkins, P. A., & Smith, K. D. (1998). Gene redundancy and pharmacological gene therapy: Implications for X-linked adrenoleukodystrophy. *Nature Medicine*, *4*(11), 1261–1268. https://doi.org/10.1038/3242

Kemp, S., Pujol, A., Waterham, H. R., Van Geel, B. M., Boehm, C. D., Raymond, G. V., Cutting, G. R., Wanders, R. J., & Moser, H. W. (2001). ABCD1 Mutations and the X-linked Adrenoleukodystrophy Mutation Database: Role in Diagnosis and Clinical Correlations. *Human mutation, 18*(6), 499-515. https://doi.org/10.1002/humu.1227

Kemp, S., Valianpour, F., Denis, S., Ofman, R., Sanders, R. J., Mooyer, P., Barth, P. G., & Wanders, R. J. (2005). Elongation of very long-chain fatty acids is enhanced in X-linked adrenoleukodystrophy. *Molecular Genetics and Metabolism*, *84*(2), 144–151. https://doi.org/10.1016/J.YMGME.2004.09.015

Kemp, S., & Wanders, R. (2010). Biochemical aspects of X-linked adrenoleukodystrophy. *Brain Pathology*, *20*(4), 831–837. https://doi.org/10.1111/j.1750-3639.2010.00391.x

Kemp, S., Theodoulou, F. L., & Wanders, R. J. (2011). Mammalian peroxisomal ABC transporters: from endogenous substrates to pathology and clinical significance. *British journal of pharmacology, 164*(7), 1753-1766. https://doi.org/10.1111/bph.2011.164.issue-7

Kemp, S., Huffnagel, I. C., Linthorst, G. E., Wanders, R. J., & Engelen, M. (2016). Adrenoleukodystrophy - Neuroendocrine pathogenesis and redefinition of natural history. In *Nature Reviews Endocrinology, 12*(10), 606-615. https://doi.org/10.1038/nrendo.2016.90

Kemper, A. R., Brosco, J., Comeau, A. M., Green, N. S., Grosse, S. D., Jones, E., Kwon, J. M., Lam, W. K., Ojodu, J., Prosser, L. A., & Tanksley, S. (2017). Newborn screening for X-linked adrenoleukodystrophy: evidence summary and advisory committee recommendation. *Genetics in Medicine*, *19*(1), 121–126. https://doi.org/10.1038/gim.2016.68

Kerkis, I., Kerkis, A., Dozortsev, D., Stukart-Parsons, G. C., Gomes Massironi, S. M., Pereira, L. V., Caplan, A. I., & Cerruti, H. F. (2006). Isolation and characterization of a population of immature dental pulp stem cells expressing OCT-4 and other embryonic stem cell markers. *Cells, Tissues, Organs*, *184*(3–4), 105–116. https://doi.org/10.1159/000099617

Khan, M., Singh, J., Gilg, A. G., Uto, T., & Singh, I. (2010). Very long-chain fatty acid accumulation causes lipotoxic response via 5-lipoxygenase in cerebral adrenoleukodystrophy. *Journal of Lipid Research*, *51*(7), 1685–1695. https://doi.org/10.1194/JLR.M002329

Khattar, K. E., Safi, J., Rodriguez, A.M., & Vignais, M.-L. (2022). Intercellular Communication in the Brain through Tunneling Nanotubes. *Cancers*, *14*(5), 1207. https://doi.org/10.3390/cancers14051207

Kim, G. H., Kim, J. E., Rhie, S. J., & Yoon, S. (2015). The Role of Oxidative Stress in Neurodegenerative Diseases. *Experimental Neurobiology*, *24*(4), 325–340. https://doi.org/10.5607/EN.2015.24.4.325

Király, M., Kádár, K., Horváthy, D. B., Nardai, P., Rácz, G. Z., Lacza, Z., Varga, G., & Gerber, G. (2011). Integration of neuronally predifferentiated human dental pulp stem cells into rat brain in vivo. *Neurochemistry International*, *59*(3), 371–381. https://doi.org/10.1016/j.neuint.2011.01.006

Kishimoto, Y., Moser, H. W., Kawamura, N., Platt, M., Pallante, S. L., & Fenselau, C. (1980). Adrenoleukodystrophy: evidence that abnormal very long chain fatty acids of brain cholesterol esters are of exogenous origin. *Biochemical and Biophysical Research Communications*, *96*(1), 69–76. https://doi.org/10.1016/0006-291X(80)91182-1

Klemmensen, M. M., Borrowman, S. H., Pearce, C., Pyles, B., & Chandra, B. (2024). Mitochondrial dysfunction in neurodegenerative disorders. *Neurotherapeutics*, *21*(1), e00292. https://doi.org/10.1016/j.neurot.2023.10.002

Koç, O. N., Peters, C., Aubourg, P., Raghavan, S., Dyhouse, S., DeGasperi, R., Kolodny, E. H., BenYoseph, Y., Gerson, S. L., Lazarus, H. M., Caplan, A. I., Watkins, P. A., & Krivit, W. (1999). Bone marrow–derived mesenchymal stem cells remain host-derived despite successful hematopoietic engraftment after allogeneic transplantation in patients with lysosomal and peroxisomal storage diseases. *Experimental Hematology*, *27*(11), 1675–1681. https://doi.org/10.1016/S0301-472X(99)00101-0

Kou, M., Huang, L., Yang, J., Chiang, Z., Chen, S., Liu, J., Guo, L., Zhang, X., Zhou, X., Xu, X., Yan, X., Wang, Y., Zhang, J., Xu, A., Tse, H. F., & Lian, Q. (2022). Mesenchymal stem cell-derived extracellular vesicles for immunomodulation and regeneration: a next generation therapeutic tool? *Cell death & disease, 13*(7), 580. https://doi.org/10.1038/s41419-022-05034-x

Körbling, M., & Estrov, Z. (2003). Adult stem cells for tissue repair - a new therapeutic concept? *The New England Journal of Medicine*, *349*(6), 570–582. https://doi.org/10.1056/NEJMRA022361

Korenke, G. C., Christen, H. J., Kruse, B., Hunneman, D. H., & Hanefeld, F. (1997). Progression of X-linked adrenoleukodystrophy under interferon-β therapy. *Journal of Inherited Metabolic Disease*, *20*(1), 59–66. https://doi.org/10.1023/A:1005361607523

Kruska, N., Schönfeld, P., Pujol, A., & Reiser, G. (2015). Astrocytes and mitochondria from adrenoleukodystrophy protein (ABCD1)-deficient mice reveal that the adrenoleukodystrophy-associated very long-chain fatty acids target several cellular energy-dependent functions. *Biochimica et Biophysica Acta - Molecular Basis of Disease*, *1852*(5), 925–936. https://doi.org/10.1016/j.bbadis.2015.01.005

Kumar, S., Sait, H., Polipalli, S. K., Pradhan, G. S., Pruthi, S., & Kapoor, S. (2021). Loes Score: Clinical and Radiological Profile of 22 Patients of X-Linked Adrenoleukodystrophy: Case Series from a Single Center. *The Indian journal of radiology & imaging, 31*(2), 383–390. https://doi.org/10.1055/s-0041-1734366

Lan, T., Luo, M., & Wei, X. (2021). Mesenchymal stem/stromal cells in cancer therapy. *Journal of Hematology & Oncology*, *14*(1), 195. https://doi.org/10.1186/S13045-021-01208-W

Larsson, L.I., Bjerregaard, B., & Talts, J. F. (2008). Cell fusions in mammals. *Histochemistry and Cell Biology*, *129*(5), 551–561. https://doi.org/10.1007/s00418-008-0411-1

Launay, N., Lopez-Erauskin, J., Bianchi, P., Guha, S., Parameswaran, J., Coppa, A., Torreni, L., Schlüter, A., Fourcade, S., Paredes-Fuentes, A. J., Artuch, R., Casasnovas, C., Ruiz, M., & Pujol, A. (2024). Imbalanced mitochondrial dynamics contributes to the pathogenesis of X-linked adrenoleukodystrophy. *Brain*, *147*(6), 2069–2084. https://doi.org/10.1093/brain/awae038

Lee, B. C., Kim, H. S., Shin, T. H., Kang, I., Lee, J. Y., Kim, J. J., Kang, H. K., Seo, Y., Lee, S., Yu, K. R., Choi, S. W., & Kang, K. S. (2016). PGE2 maintains self-renewal of human adult stem cells via EP2-mediated autocrine signaling and its production is regulated by cell-to-cell contact. *Scientific Reports*, *6*, 26298. https://doi.org/10.1038/SREP26298

Lee, C. A. A., Seo, H. S., Armien, A. G., Bates, F. S., Tolar, J., & Azarin, S. M. (2018). Modeling and rescue of defective blood-brain barrier function of induced brain microvascular endothelial cells from childhood cerebral adrenoleukodystrophy patients. *Fluids and barriers of the CNS, 15*(1), 9. https://doi.org/10.1186/s12987-018-0094-5

Lee, D.K., Long, N. P., Jung, J., Kim, T. J., Na, E., Kang, Y. P., Kwon, S. W., & Jang, J. (2019). Integrative lipidomic and transcriptomic analysis of X-linked adrenoleukodystrophy reveals distinct lipidome signatures between adrenomyeloneuropathy and childhood cerebral adrenoleukodystrophy. *Biochemical and Biophysical Research Communications*, *508*(2), 563–569. https://doi.org/10.1016/j.bbrc.2018.11.123

Lehmann, T. P., Filipiak, K., Juzwa, W., Sujka-Kordowska, P., Jagodziński, P. P., Zabel, M., Głowacki, J., Misterska, E., Walczak, M., & Głowacki, M. (2014). Co-culture of human nucleus pulposus cells with multipotent mesenchymal stromal cells from human bone marrow reveals formation of tunnelling nanotubes. *Molecular Medicine Reports*, *9*(2), 574–582. https://doi.org/10.3892/mmr.2013.1821

Li, W., Moore, M. J., Vasilieva, N., Sui, J., Wong, S. K., Berne, M. A., Somasundaran, M., Sullivan, J. L., Luzuriaga, K., Greenough, T. C., Choe, H., & Farzan, M. (2003). Angiotensin-converting enzyme 2 is a functional receptor for the SARS coronavirus. *Nature*, 426(6965), 450–454. https://doi.org/10.1038/nature02145

Li, X., Corbett, A. L., Taatizadeh, E., Tasnim, N., Little, J. P., Garnis, C., Daugaard, M., Guns, E., Hoorfar, M., & Li, I. T. S. (2019). Challenges and opportunities in exosome research—Perspectives from biology, engineering, and cancer therapy. *APL Bioengineering*, *3*(1), 011503. https://doi.org/10.1063/1.5087122

Lian, X. L., Ji, L. M., & Zhang, L. N. (2021). Mannotriose induced differentiation of mesenchymal stem cells into neuron-like cells. *Journal of Integrative Neuroscience*, *20*(1), 125–130. https://doi.org/10.31083/J.JIN.2021.01.214

Liang, W., Sagar, S., Ravindran, R., Najor, R. H., Quiles, J. M., Chi, L., Diao, R. Y., Woodall, B. P., Leon, L. J., Zumaya, E., Duran, J., Cauvi, D. M., De Maio, A., Adler, E. D., & Gustafsson, Å. B. (2023). Mitochondria are secreted in extracellular vesicles when lysosomal function is impaired. *Nature Communications*, *14*(1), 5031. https://doi.org/10.1038/s41467-023-40680-5

Lindroos, B., Mäenpää, K., Ylikomi, T., Oja, H., Suuronen, R., & Miettinen, S. (2008). Characterisation of human dental stem cells and buccal mucosa fibroblasts. *Biochemical and Biophysical Research Communications*, *368*(2), 329–335. https://doi.org/10.1016/j.bbrc.2008.01.081

Liu, L. X., Janvier, K., Berteaux-Lecellier, V., Cartier, N., Benarous, R.., & Aubourg, P. (1999). Homo- and heterodimerization of peroxisomal ATP-binding cassette half-transporters. *The Journal of Biological Chemistry*, *274*(46), 32738–32743. https://doi.org/10.1074/JBC.274.46.32738

Liu, L., Ling, J., Wei, X., Wu, L., & Xiao, Y. (2009). Stem Cell Regulatory Gene Expression in Human Adult Dental Pulp and Periodontal Ligament Cells Undergoing Odontogenic/Osteogenic Differentiation. *Journal of Endodontics*, *35*(10), 1368–1376. https://doi.org/10.1016/j.joen.2009.07.005

Liu, K., Ji, K., Guo, L., Wu, W., Lu, H., Shan, P., & Yan, C. (2014). Mesenchymal stem cells rescue injured endothelial cells in an in vitro ischemia–reperfusion model via tunneling nanotube like structure-mediated mitochondrial transfer. *Microvascular Research*, *92*, 10–18. https://doi.org/10.1016/j.mvr.2014.01.008

Liu, X. (2019). ABC Family Transporters. *Advances in Experimental Medicine and Biology*, *1141*, 13–100. https://doi.org/10.1007/978-981-13-7647-4_2

Liu, D., Gao, Y., Liu, J., Huang, Y., Yin, J., Feng, Y., Shi, L., Meloni, B. P., Zhang, C., Zheng, M., & Gao, J. (2021). Intercellular mitochondrial transfer as a means of tissue revitalization. *Signal Transduction and Targeted Therapy*, *6*(1), 65. https://doi.org/10.1038/S41392-020-00440-Z

Lledó, B., Bernabeu, R., Ten, J., Galán, F. M., & Cioffi, L. (2007). Preimplantation genetic diagnosis of X-linked adrenoleukodystrophy with gender determination using multiple displacement amplification. *Fertility and Sterility*, *88*(5), 1327–1333. https://doi.org/10.1016/j.fertnstert.2007.01.034

Lo Sicco, C., Reverberi, D., Balbi, C., Ulivi, V., Principi, E., Pascucci, L., Becherini, P., Bosco, M. C., Varesio, L., Franzin, C., Pozzobon, M., Cancedda, R., & Tasso, R. (2017). Mesenchymal Stem Cell-Derived Extracellular Vesicles as Mediators of Anti-Inflammatory Effects: Endorsement of Macrophage Polarization. *Stem Cells Translational Medicine*, *6*(3), 1018–1028. https://doi.org/10.1002/sctm.16-0363

Loes, D. J., Hite, S., Moser, H., Stillman, A. E., Shapiro, E., Lockman, L., Latchaw, R. E., & Krivit, W. (1994). Adrenoleukodystrophy: a scoring method for brain MR observations. *AJNR. American journal of neuroradiology, 15*(9), 1761–1766.

Loes, D. J., Fatemi, A., Melhem, E. R., Gupte, N., Bezman, L., Moser, H. W., & Raymond, G. V. (2003). Analysis of MRI patterns aids prediction of progression in X-linked adrenoleukodystrophy. *Neurology*, *61*(3), 369–374. https://doi.org/10.1212/01.WNL.0000079050.91337.83

López-Erauskin, J., Fourcade, S., Galino, J., Ruiz, M., Schlüter, A., Naudi, A., Jove, M., Portero-Otin, M., Pamplona, R., Ferrer, I., & Pujol, A. (2011). Antioxidants Halt Axonal Degeneration in a Mouse Model of X-Adrenoleukodystrophy. *Annals of Neurology*, *70*(1), 84-92. https://doi.org/10.1002/ANA.22363

López-Erauskin, J., Galino, J., Ruiz, M., Cuezva, J. M., Fabregat, I., Cacabelos, D., Boada, J., Martínez, J., Ferrer, I., Pamplona, R., Villarroya, F., Portero-Otín, M., Fourcade, S., & Pujol, A. (2013). Impaired mitochondrial oxidative phosphorylation in the peroxisomal disease X-linked adrenoleukodystrophy. *Human Molecular Genetics*, *22*(16), 3296–3305. https://doi.org/10.1093/hmg/ddt186

Low, D., & Ginhoux, F. (2018). Recent advances in the understanding of microglial development and homeostasis. *Cellular Immunology*, *330*, 68–78. https://doi.org/10.1016/J.CELLIMM.2018.01.004

Lu, J.F., Lawler, A. M., Watkins, P. A., Powers, J. M., Moser, A. B., Moser, H. W., & Smith, K. D. (1997). A mouse model for X-linked adrenoleukodystrophy. *Proceedings of the National Academy of Sciences*, *94*(17), 9366–9371. https://doi.org/10.1073/pnas.94.17.9366

Maellaro, E., Del Bello, B., Sugherini, L., Santucci, A., Comporti, M., & Casini, A. F. (1994). Purification and characterization of glutathione-dependent dehydroascorbate reductase from rat liver. *The Biochemical Journal*, *301*(Pt 2), 471–476. https://doi.org/10.1042/BJ3010471

Mahmoudi, M., Taghavi-Farahabadi, M., Rezaei, N., & Hashemi, S. M. (2019). Comparison of the effects of adipose tissue mesenchymal stromal cell-derived exosomes with conditioned media on neutrophil function and apoptosis. *International Immunopharmacology*, *74*, 105689. https://doi.org/10.1016/j.intimp.2019.105689

Majore, I., Moretti, P., Stahl, F., Hass, R., & Kasper, C. (2011). Growth and Differentiation Properties of Mesenchymal Stromal Cell Populations Derived from Whole Human Umbilical Cord. *Stem Cell Reviews and Reports*, *7*(1), 17–31. https://doi.org/10.1007/s12015-010-9165-y

Mallack, E. J., Gao, K., Engelen, M., & Kemp, S. (2022). Structure and Function of the ABCD1 Variant Database: 20 Years, 940 Pathogenic Variants, and 3400 Cases of Adrenoleukodystrophy. *Cells*, *11*(2), 283. https://doi.org/10.3390/cells11020283

Mark, P., Kleinsorge, M., Gaebel, R., Lux, C. A. y Toelk, A., Pittermann, E., David, R., Steinhoff, G., & Ma, N. (2013). Human Mesenchymal Stem Cells Display Reduced Expression of CD105 after Culture in Serum-Free Medium. *Stem Cells International*, *2013*, 698076. https://doi.org/10.1155/2013/698076

Marone, M., De Ritis, D., Bonanno, G., Mozzetti, S., Rutella, S., Scambia, G., & Pierelli, L. (2002). Cell Cycle Regulation in Human Hematopoietic Stem Cells: From Isolation to Activation. *Leukemia & Lymphoma*, *43*(3), 493–501. https://doi.org/10.1080/10428190290011967

Martens, W., Wolfs, E., Struys, T., Politis, C., Bronckaers, A., & Lambrichts, I. (2012). Expression Pattern of Basal Markers in Human Dental Pulp Stem Cells and Tissue. *Cells Tissues Organs*, *196*(6), 490–500. https://doi.org/10.1159/000338654

Masuda, K., Han, X., Kato, H., Sato, H., Zhang, Y., Sun, X., Hirofuji, Y., Yamaza, H., Yamada, A., & Fukumoto, S. (2021). Dental Pulp-Derived Mesenchymal Stem Cells for Modeling Genetic Disorders. *International Journal of Molecular Sciences*, *22*(5), 2269. https://doi.org/10.3390/ijms22052269

Mauri, M., Lentini, D., Gravati, M., Foudah, D., Biella, G., Costa, B., Toselli, M., Parenti, M., & Coco, S. (2012). Mesenchymal stem cells enhance GABAergic transmission in co-cultured hippocampal neurons. *Molecular and cellular neurosciences, 49*(4), 395–405. https://doi.org/10.1016/j.mcn.2012.02.004

Mayo, V., Sawatari, Y., Huang, C.Y., & Garcia-Godoy, F. (2014). Neural crest-derived dental stem cells—Where we are and where we are going. *Journal of Dentistry*, *42*(9), 1043–1051. https://doi.org/10.1016/j.jdent.2014.04.007

McCormick, J. B., & Huso, H. A. (2010). Stem cells and ethics: current issues. *Journal of cardiovascular translational research, 3*(2), 122-127. https://doi.org/10.1007/s12265-009-9155-0

McQuillen, P. S., & Ferriero, D. M. (2004). Selective vulnerability in the developing central nervous system. *Pediatric Neurology*, *30*(4), 227–235. https://doi.org/10.1016/j.pediatrneurol.2003.10.001

Mekhoubad, S., Bock, C., de Boer, A. S., Kiskinis, E., Meissner, A., & Eggan, K. (2012). Erosion of Dosage Compensation Impacts Human iPSC Disease Modeling. *Cell Stem Cell*, *10*(5), 595–609. https://doi.org/10.1016/j.stem.2012.02.014

Melhem, E. R., Loes, D. J., Georgiades, C. S., Raymond, G. V., & Moser, H. W. (2000). X-linked Adrenoleukodystrophy: The Role of Contrast-enhanced MR Imaging in Predicting Disease Progression. *AJNR: American Journal of Neuroradiology*, *21*(5), 839-844. /pmc/articles/PMC7976769/

Melief, S. M., Zwaginga, J. J., Fibbe, W. E., & Roelofs, H. (2013). Adipose Tissue-Derived Multipotent Stromal Cells Have a Higher Immunomodulatory Capacity Than Their Bone Marrow-Derived Counterparts. *Stem Cells Translational Medicine*, *2*(6), 455–463. https://doi.org/10.5966/sctm.2012-0184

Melzer, C., von der Ohe, J., & Hass, R. (2019). In vivo cell fusion between mesenchymal stroma/stem-like cells and breast cancer cells. *Cancers*, *11*(2), 185. https://doi.org/10.3390/cancers11020185

Mezey, É., Key, S., Vogelsang, G., Szalayova, I., Lange, G. D., & Crain, B. (2003). Transplanted bone marrow generates new neurons in human brains. *Proceedings of the National Academy of Sciences*, *100*(3), 1364–1369. https://doi.org/10.1073/pnas.0336479100

Miike, T., Taku, K., Tamura, T., Ohta, J., Ozaki, M., Yamamoto, C., Sakai, T., Antoku, Y., & Yadomi, C. (1989). Clinical improvement of adrenoleukodystrophy following intravenous gammaglobulin therapy. *Brain and Development*, *11*(2), 134–137. https://doi.org/10.1016/S0387-7604(89)80083-X

Miura, M., Gronthos, S., Zhao, M., Lu, B., Fisher, L. W., Robey, P. G., & Shi, S. (2003). SHED: Stem cells from human exfoliated deciduous teeth. *Proceedings of the National Academy of Sciences*, *100*(10), 5807–5812. https://doi.org/10.1073/pnas.0937635100

Moloudizargari, M., Govahi, A., Fallah, M., Rezvanfar, M. A., Asghari, M. H., & Abdollahi, M. (2021). The mechanisms of cellular crosstalk between mesenchymal stem cells and natural killer cells: Therapeutic implications. *Journal of Cellular Physiology*, *236*(4), 2413–2429. https://doi.org/10.1002/jcp.30038

Morató, L., Galino, J., Ruiz, M., Calingasan, N. Y., Starkov, A. A., Dumont, M., Naudí, A., Martínez, J. J., Aubourg, P., Portero-Otín, M., Pamplona, R., Galea, E., Beal, M. F., Ferrer, I., Fourcade, S., & Pujol, A. (2013). Pioglitazone halts axonal degeneration in a mouse model of X-linked adrenoleukodystrophy. *Brain: a journal of neurology*, *136*(8), 2432-2443. https://doi.org/10.1093/BRAIN/AWT143

Morsczeck, C., Götz, W., Schierholz, J., Zeilhofer, F., Kühn, U., Möhl, C., Sippel, C., & Hoffmann, K. H. (2005). Isolation of precursor cells (PCs) from human dental follicle of wisdom teeth. *Matrix Biology*, *24*(2), 155–165. https://doi.org/10.1016/j.matbio.2004.12.004

Moser, H. W., Moser, A. B., Frayer, K. K., Chen, W., Schulman, J. D., O'Neill, B. P., & Kishimoto, Y. (1981). Adrenoleukodystrophy: increased plasma content of saturated very long chain fatty acids. *Neurology*, *31*(10), 1241–1249. https://doi.org/10.1212/WNL.31.10.1241

Moser, A. B., Borel, J., Naidu, S., Cornblath, D., Sanders, D. B., & Moser, H. W. (1987). A New Dietary Therapy for Adrenoleukodystrophy : Biochemical and Prehnary Clinical Results in 36 Patients. *Annals of Neurology*, *21*(3), 240–249. https://doi.org/10.1002/ana.410210305

Moser, H. W., Moser, A. B., Naidu, S., & Bergin, A. (1991). Clinical aspects of adrenoleukodystrophy and adrenomyeloneuropathy. *Developmental Neuroscience*, *13*(4–5), 254–261. https://doi.org/10.1159/000112170

Moser, A. B., Kreiter, N., Bezman, L., Lu, S., Raymond, G. V., Naidu, S., & Moser, H. W. (1999). Plasma very long chain fatty acids in 3,000 peroxisome disease patients and 29,000 controls. *Annals of Neurology*, *45*(1), 100–110. https://doi.org/10.1002/1531-8249(199901)45:1

Moser, A. B., & Moser, H. W. (1999). The Prenatal Diagnosis of X-linked Adrenoleukodystrophy. *Prenatal diagnosis, 19*(1), 46-48. https://doi.org/10.1002/(sici)1097-0223(199901)19:1

Moser, H. W., & Mahmood, A. (2007). New insights about hematopoietic stem cell transplantation in adrenoleukodystrophy. *Archives of Neurology*, *64*(5), 631–632. https://doi.org/10.1001/ARCHNEUR.64.5.631

Moser, H. W., Mahmood, A., & Raymond, G. V. (2007). X-linked adrenoleukodystrophy. *Nature Clinical Practice. Neurology*, *3*(3), 140–151. https://doi.org/10.1038/NCPNEURO0421

Mosser, J., Douar, A. M., Sarde, C. O., Kioschis, P., Feil, R., Moser, H., Poustka, A. M., Mandel, J. L., & Aubourg, P. (1993). Putative X-linked adrenoleukodystrophy gene shares unexpected homology with ABC transporters. *Nature, 361*(6414), 726–730. https://doi.org/10.1038/361726a0

Mosser, J., Lutz, Y., Stoeckel, M. E., Sarde, C. O., Kretz, C., Douar, A. M., Lopez, J., Aubourg, P., & Mandel, J. L. (1994). The gene responsible for adrenoleukodystrophy encodes a peroxisomal membrane protein. *Human Molecular Genetics*, *3*(2), 265–271. https://doi.org/10.1093/HMG/3.2.265

Naidu, S., Bresnan, M.J., Griffin, D., O'Toole, S., & Moser, H.W. (1988). Childhood Adrenoleukodystrophy: Failure of Intensive Immunosuppression to Arrest Neurologic Progression. *Archives of Neurology*, *45*(8), 846–848. https://doi.org/10.1001/ARCHNEUR.1988.00520320032011

Navas, P., Villalba, J. M., & Córdoba, F. (1994). Ascorbate function at the plasma membrane. *Biochimica et Biophysica Acta*, *1197*(1), 1–13. https://doi.org/10.1016/0304-4157(94)90016-7

Nielsen, M. S., Axelsen, L. N., Sorgen, P. L., Verma, V., Delmar, M., & Holstein-Rathlou, N. H. (2012). Gap Junctions. *Comprehensive Physiology*, *2*(3), 1981–2035. https://doi.org/10.1002/CPHY.C110051

Noden, D. M. (1983). The role of the neural crest in patterning of avian cranial skeletal, connective, and muscle tissues. *Developmental Biology*, *96*(1), 144–165. https://doi.org/10.1016/0012-1606(83)90318-4

Nourbakhsh, N., Soleimani, M., Taghipour, Z., Karbalaie, K., Mousavi, S.B., Talebi, A., Nadali, F., Tanhaei, S., Kiyani, G.A., Nematollahi, M., Rabiei, F., Mardani, M., Bahramiyan, H., Torabinejad, M., Nasr-Esfahani, M.H., & Baharvand, H. (2011). Induced in vitro differentiation of neural-like cells from human exfoliated deciduous teeth-derived stem cells. *The International Journal of Developmental Biology*, *55*(2), 189–195. https://doi.org/10.1387/ijdb.103090nn

Nuti, N., Corallo, C., Chan, B. M., Ferrari, M., & Gerami-Naini, B. (2016). Multipotent Differentiation of Human Dental Pulp Stem Cells: a Literature Review. *Stem Cell Reviews and Reports*, *12*(5), 511–523. https://doi.org/10.1007/s12015-016-9661-9

Ofman, R., Dijkstra, I. M., Van Roermund, C. W., Burger, N., Turkenburg, M., Van Cruchten, A., Van Engen, C. E., Wanders, R. J., & Kemp, S. (2010). The role of ELOVL1 in very long-chain fatty acid homeostasis and X-linked adrenoleukodystrophy. *EMBO Molecular Medicine*, *2*(3), 90–97. https://doi.org/10.1002/emmm.201000061

Ogawa, Y., Akamatsu, R., Fuchizaki, A., Yasui, K., Saino, O., Tanaka, M., Kikuchi-Taura, A., Kimura, T., & Taguchi, A. (2022). Gap Junction–Mediated Transport of Metabolites Between Stem Cells and Vascular Endothelial Cells. *Cell Transplantation*, *31,* 9636897221136151. https://doi.org/10.1177/09636897221136151

Oh, S. H., Muzzonigro, T. M., Bae, S. H., LaPlante, J. M., Hatch, H. M., & Petersen, B. E. (2004). Adult bone marrow-derived cells trans differentiating into insulin-producing cells for the treatment of type I diabetes. *Laboratory Investigation: a journal of technical methods and pathology*, *84*(5), 607–617. https://doi.org/10.1038/labinvest.3700074

O'Neill, B. P., Mannion, L. C., & Feringa, E. R. (1981). The adrenoleukomyeloneuropathy complex: expression in four generations. *Neurology*, *31*(2), 151–156. https://doi.org/10.1212/WNL.31.2.151

O'Neill, B. P., Moser, H. W., Saxena, K. M., & Marmion, L. C. (1984). Adrenoleukodystrophy: clinical and biochemical manifestations in carriers. *Neurology*, *34*(6), 798–801. https://doi.org/10.1212/WNL.34.6.798

Osathanon, T., Sawangmake, C., Nowwarote, N., & Pavasant, P. (2014). Neurogenic differentiation of human dental pulp stem cells using different induction protocols. *Oral Diseases*, *20*(4), 352–358. https://doi.org/10.1111/odi.12119

Özdemir, A. T., Özgül Özdemir, R. B., Kırmaz, C., Sarıboyacı, A. E., Ünal Halbutoğlları, Z. S., Özel, C., & Karaöz, E. (2016). The paracrine immunomodulatory interactions between the human dental pulp derived mesenchymal stem cells and CD4 T cell subsets. *Cellular Immunology*, *310*, 108–115. https://doi.org/10.1016/j.cellimm.2016.08.008

Petrillo, S., Piemonte, F., Pastore, A., Tozzi, G., Aiello, C., Pujol, A., Cappa, M., & Bertini, E. (2013). Glutathione imbalance in patients with X-linked adrenoleukodystrophy. *Molecular Genetics and Metabolism*, *109*(4), 366-370. https://doi.org/10.1016/J.YMGME.2013.05.009

Pierdomenico, L., Bonsi, L., Calvitti, M., Rondelli, D., Arpinati, M., Chirumbolo, G., Becchetti, E., Marchionni, C., Alviano, F.,Fossati, V., Staffolani, N., Franchina, M., Grossi, A., & Bagnara, G. P. (2005). Multipotent Mesenchymal Stem Cells with Immunosuppressive Activity Can Be Easily Isolated from Dental Pulp. *Transplantation*, *80*(6), 836–842. https://doi.org/10.1097/01.tp.0000173794.72151.88

Pittenger, M. F., Mackay, A. M., Beck, S. C., Jaiswal, R. K., Douglas, R., Mosca, J. D., Moorman, M. A., Simonetti, D. W., Craig, S., & Marshak, D. R. (1999). Multilineage potential of adult human mesenchymal stem cells. *Science, 284*(5411), 143-147. https://doi.org/10.1126/science.284.5411.143

Planat-Benard, V., Varin, A., & Casteilla, L. (2021). MSCs and Inflammatory Cells Crosstalk in Regenerative Medicine: Concerted Actions for Optimized Resolution Driven by Energy Metabolism. *Frontiers in Immunology*, *12,* 626755. https://doi.org/10.3389/fimmu.2021.626755

Plotnikov, E. Y., Khryapenkova, T. G., Galkina, S. I., Sukhikh, G. T., & Zorov, D. B. (2010). Cytoplasm and organelle transfer between mesenchymal multipotent stromal cells and renal tubular cells in co-culture. *Experimental Cell Research*, *316*(15), 2447–2455. https://doi.org/10.1016/j.yexcr.2010.06.009

Ponnaiyan, D., & Jegadeesan, V. (2014). Comparison of phenotype and differentiation marker gene expression profiles in human dental pulp and bone marrow mesenchymal stem cells. *European Journal of Dentistry*, *08*(3), 307–313. https://doi.org/10.4103/1305-7456.137631

Powers, J. M., & Schaumburg, H. H. (1974). Adreno-leukodystrophy. Similar ultrastructural changes in adrenal cortical and Schwann cells. *Archives of Neurology*, *30*(5), 406–408. https://doi.org/10.1001/ARCHNEUR.1974.00490350064011

Powers, J. M., Liu, Y., Moser, A. B., & Moser, H. W. (1992). The Inflammatory Myelinopathy of Adreno-Leukodystrophy: Cells, Effector Molecules, and Pathogenetic Implications. *Journal of Neuropathology and Experimental Neurology*, *51*(6), 630–643. https://doi.org/10.1097/00005072-199211000-00007

Powers, J. M., DeCiero, D. P., Ito, M., Moser, A. B., & Moser, H. W. (2000). Adrenomyeloneuropathy: a neuropathologic review featuring its noninflammatory myelopathy. *Journal of Neuropathology and Experimental Neurology*, *59*(2), 89–102. https://doi.org/10.1093/JNEN/59.2.89

Powers, J. M., Pei, Z., Heinzer, A. K., Deering, R., Moser, A. B., Moser, H. W., Watkins, P. A., & Smith, K. D. (2005). Adreno-leukodystrophy: oxidative stress of mice and men. *Journal of Neuropathology and Experimental Neurology*, *64*(12), 1067–1079. https://doi.org/10.1097/01.JNEN.0000190064.28559.A4

Raas, Q., Gondcaille, C., Hamon, Y., Leoni, V., Caccia, C., Ménétrier, F., Lizard, G., Trompier, D., & Savary, S. (2019). CRISPR/Cas9-mediated knockout of Abcd1 and Abcd2 genes in BV-2 cells: novel microglial models for X-linked Adrenoleukodystrophy. *Biochimica et Biophysica Acta - Molecular and Cell Biology of Lipids*, *1864*(5), 704–714. https://doi.org/10.1016/j.bbalip.2019.02.006

Raffaghello, L., Bianchi, G., Bertolotto, M., Montecucco, F., Busca, A., Dallegri, F., Ottonello, L., & Pistoia, V. (2008). Human Mesenchymal Stem Cells Inhibit Neutrophil Apoptosis: A Model for Neutrophil Preservation in the Bone Marrow Niche. *Stem Cells*, *26*(1), 151–162. https://doi.org/10.1634/stemcells.2007-0416

Ran, L. J., Zeng, Y., Wang, S. C., Zhang, D. S., Hong, M., Li, S. Y., Dong, J., & Shi, M. X. (2018). Effect of co-culture with amniotic epithelial cells on the biological characteristics of amniotic mesenchymal stem cells. *Molecular Medicine Reports*, *18*(1), 723–732. https://doi.org/10.3892/mmr.2018.9053

Ransohoff, R. M. (2016). How neuroinflammation contributes to neurodegeneration. *Science*, *353*(6301), 777–783. https://doi.org/10.1126/SCIENCE.AAG2590

Rasmussen, M., Moser, A. B., Borel, J., Khangoora, S., & Moser, H. W. (1994). Brain, Liver, and Adipose Tissue Erucic and Very Long Chain Fatty Acid Levels in Adrenoleukodystrophy Patients Treated with Glyceryl Trierucate and Trioleate Oils (Lorenzo's Oil). *Neurochemical Research, 19*(8), 1073-1082. https://doi.org/10.1007/BF00968719

Ratajczak, M. Z., Zuba-Surma, E., Kucia, M., Poniewierska, A., Suszynska, M., & Ratajczak, J. (2012). Pluripotent and multipotent stem cells in adult tissues. *Advances in Medical Sciences*, *57*(1), 1–17. https://doi.org/10.2478/V10039-012-0020-Z

Ren, G., Zhang, L., Zhao, X., Xu, G., Zhang, Y., Roberts, A. I., Zhao, R. C., & Shi, Y. (2008). Mesenchymal Stem Cell-Mediated Immunosuppression Occurs via Concerted Action of Chemokines and Nitric Oxide. *Cell Stem Cell*, *2*(2), 141–150. https://doi.org/10.1016/j.stem.2007.11.014

Renner, P., Eggenhofer, E., Rosenauer, A., Popp, F. C., Steinmann, J. F., Slowik, P., Geissler, E. K., Piso, P., Schlitt, H. J., & Dahlke, M. H. (2009). Mesenchymal Stem Cells Require a Sufficient, Ongoing Immune Response to Exert Their Immunosuppressive Function. *Transplantation Proceedings*, *41*(6), 2607–2611. https://doi.org/10.1016/j.transproceed.2009.06.119

Rizk, A., Paul, G., Incardona, P., Bugarski, M., Mansouri, M., Niemann, A., Ziegler, U., Berger, P., & Sbalzarini, I. F. (2014). Segmentation and quantification of subcellular structures in fluorescence microscopy images using Squassh. *Nature protocols, 9*(3), 586–596. https://doi.org/10.1038/nprot.2014.037

Rizzo, W. B. (1993). Lorenzo's oil--hope and disappointment. *The New England Journal of Medicine*, *329*(11), 801–802. https://doi.org/10.1056/NEJM199309093291110

Rodríguez-Lozano, F. J., Insausti, C. L., Iniesta, F., Blanquer, M., Ramírez, M. D., Meseguer, L., Meseguer-Henarejos, A. B., Marín, N., Martínez, S., & Moraleda, J. M. (2012). Mesenchymal dental stem cells in regenerative dentistry. *Medicina oral, patologia oral y cirugia bucal, 17*(6), e1062–e1067. https://doi.org/10.4317/medoral.17925

Roermund, C. W., Visser, W. F., IJlst, L., Cruchten, A., Boek, M., Kulik, W., Waterham, H. R., Wanders, R. J. (2008). The human peroxisomal ABC half transporter ALDP functions as a homodimer and accepts acyl–CoA esters. *The FASEB Journal*, *22*(12), 4201–4208. https://doi.org/10.1096/fj.08-110866

Rombouts, W. J., & Ploemacher, R. E. (2003). Primary murine MSC show highly efficient homing to the bone marrow but lose homing ability following culture. *Leukemia*, *17*(1), 160–170. https://doi.org/10.1038/sj.leu.2402763

Romer, A. S. (1972). The Vertebrate as a Dual Animal — Somatic and Visceral. *Evolutionary Biology* (Vol. 6, pp. 121–156). Springer US. https://doi.org/10.1007/978-1-4684-9063-3_5

Rose, R. C., & Bode, A. M. (1993). Biology of free radical scavengers: an evaluation of ascorbate. *FASEB Journal: Official Publication of the Federation of American Societies for Experimental Biology*, *7*(12), 1135–1142.

Rossant, J. (2001). Stem Cells from the Mammalian Blastocyst. *Stem Cells*, *19*(6), 477–482. https://doi.org/10.1634/STEMCELLS.19-6-477

Rossant, J. (2008). Stem Cells and Early Lineage Development. *Cell*, *132*(4), 527–531. https://doi.org/10.1016/j.cell.2008.01.039

Rothová, M., Feng, J., Sharpe, P. T., Peterková, R., & Tucker, A. S. (2011). Contribution of mesoderm to the developing dental papilla. *The International Journal of Developmental Biology*, *55*(1), 59–64. https://doi.org/10.1387/ijdb.103083mr

Rustom, A., Saffrich, R., Markovic, I., Walther, P., & Gerdes, H.H. (2004). Nanotubular highways for intercellular organelle transport. *Science, 303*(5660), 1007-1010. https://doi.org/10.1126/science.1093133

Sackstein, R. (2005). The lymphocyte homing receptors: gatekeepers of the multistep paradigm. *Current opinion in hematology, 12*(6), 444-450. https://doi.org/10.1097/01.moh.0000177827.78280.79

Saleem, R., Mohamed-Ahmed, S., Elnour, R., Berggreen, E., Mustafa, K., & Al-Sharabi, N. (2021). Conditioned Medium from Bone Marrow Mesenchymal Stem Cells Restored Oxidative Stress-Related Impaired Osteogenic Differentiation. *International Journal of Molecular Sciences*, *22*(24), 13458. https://doi.org/10.3390/ijms222413458

Salgado, A.J., Reis, R.L., Sousa, N.J., & Gimble, J.M. (2010). Adipose Tissue Derived Stem Cells Secretome: Soluble Factors and Their Roles in Regenerative Medicine. *Current Stem Cell Research & Therapy*, *5*(2), 103–110. https://doi.org/10.2174/157488810791268564

Sarde, C. O., Mosser, J., Kioschis, P., Kretz, C., Vicaire, S., Aubourg, P., Poustka, A., & Mandel, J. L. (1994). Genomic organization of the adrenoleukodystrophy gene. *Genomics*, *22*(1), 13–20. https://doi.org/10.1006/GENO.1994.1339

Scarfe, L., Taylor, A., Sharkey, J., Harwood, R., Barrow, M., Comenge, J., Beeken, L., Astley, C., Santeramo, I., Hutchinson, C., Ressel, L., Smythe, J., Austin, E., Levy, R., Rosseinsky, M. J., Adams, D. J., Poptani, H., Park, B. K., Murray, P., & Wilm, B. (2018). Non-invasive imaging reveals conditions that impact distribution and persistence of cells after in vivo administration. *Stem Cell Research and Therapy*, *9*(1), 332. https://doi.org/10.1186/s13287-018-1076-x

Schindelin, J., Arganda-Carreras, I., Frise, E., Kaynig, V., Longair, M., Pietzsch, T., Preibisch, S., Rueden, C., Saalfeld, S., Schmid, B., Tinevez, J. Y., White, D. J., Hartenstein, V., Eliceiri, K., Tomancak, P., & Cardona, A. (2012). Fiji: an open-source platform for biological-image analysis. *Nature methods, 9*(7), 676–682. https://doi.org/10.1038/nmeth.2019

Schlüter, A., Espinosa, L., Fourcade, S., Galino, J., López, E., Ilieva, E., Morató, L., Asheuer, M., Cook, T., McLaren, A., Reid, J., Kelly, F., Bates, S., Aubourg, P., Galea, E., & Pujol, A. (2012). Functional genomic analysis unravels a metabolic-inflammatory interplay in adrenoleukodystrophy. *Human Molecular Genetics*, *21*(5), 1062–1077. https://doi.org/10.1093/HMG/DDR536

Schlüter, A., Sandoval, J., Fourcade, S., Díaz-Lagares, A., Ruiz, M., Casaccia, P., Esteller, M., & Pujol, A. (2018). Epigenomic signature of adrenoleukodystrophy predicts compromised oligodendrocyte differentiation. *Brain pathology, 28*(6), 902–919. https://doi.org/10.1111/bpa.12595

Schneider, S., Unger, M., Van Griensven, M., & Balmayor, E. R. (2017). Adipose-derived mesenchymal stem cells from liposuction and resected fat are feasible sources for regenerative medicine. *European Journal of Medical Research*, *22*(1), 17. https://doi.org/10.1186/s40001-017-0258-9

Schönberger, S., Roerig, P., Schneider, D. T., Reifenberger, G., Göbel, U., & Gärtner, J. (2007). Genotype and protein expression after bone marrow transplantation for adrenoleukodystrophy. *Archives of Neurology*, *64*(5), 651–657. https://doi.org/10.1001/ARCHNEUR.64.5.NOC60105

Seo, B. M., Miura, M., Gronthos, S., Bartold, P. M., Batouli, S., Brahim, J., Young, M., Robey, P. G., Wang, C. Y., & Shi, S. (2004). Investigation of multipotent postnatal stem cells from human periodontal ligament. *Lancet*, *364*(9429), 149–155. https://doi.org/10.1016/S0140-6736(04)16627-0

Shadrin, I. Y., Yoon, W., Li, L., Shepherd, N., & Bursac, N. (2015). Rapid fusion between mesenchymal stem cells and cardiomyocytes yields electrically active, non-contractile hybrid cells. *Scientific Reports*, *5,* 12043. https://doi.org/10.1038/srep12043

Shao, Y., Zhou, F., He, D., Zhang, L., & Shen, J. (2019). Overexpression of CXCR7 promotes mesenchymal stem cells to repair phosgene-induced acute lung injury in rats. *Biomedicine and Pharmacotherapy*, *109*, 1233–1239. https://doi.org/10.1016/j.biopha.2018.10.108

Shapiro, E., Krivit, W., Lockman, L., Jambaqué, I., Peters, C., Cowan, M., Harris, R., Blanche, S., Bordigoni, P., Loes, D., Ziegler, R., Crittenden, M., Ris, D., Berg, B., Cox, C., Moser, H., Fischer, A., & Aubourg, P. (2000). Long-term effect of bone-marrow transplantation for childhood-onset cerebral X-linked adrenoleukodystrophy. *The Lancet*, *356*(9231), 713–718. https://doi.org/10.1016/S0140-6736(00)02629-5

Sharpe, P. T. (2016). Dental mesenchymal stem cells. *Development*, *143*(13), 2273–2280. https://doi.org/10.1242/dev.134189

Shevde N. (2012). Stem Cells: Flexible friends. *Nature, 483*(7387), S22–S26. https://doi.org/10.1038/483S22a

Shi, S., & Gronthos, S. (2003). Perivascular Niche of Postnatal Mesenchymal Stem Cells in Human Bone Marrow and Dental Pulp. *Journal of Bone and Mineral Research*, *18*(4), 696–704. https://doi.org/10.1359/jbmr.2003.18.4.696

Shi, Y., Wang, Y., Li, Q., Liu, K., Hou, J., Shao, C., & Wang, Y. (2018). Immunoregulatory mechanisms of mesenchymal stem and stromal cells in inflammatory diseases. *Nature Reviews Nephrology, 14*(8), 493–507. https://doi.org/10.1038/s41581-018-0023-5

Siemerling, E., & Creutzfeldt, H. G. (1923). Bronzekrankheit und sklerosierende Encephalomyelitis - Diffuse Sklerose. *Archiv Für Psychiatrie Und Nervenkrankheiten*, *68*(1), 217–244. https://doi.org/10.1007/BF01835678/METRICS

Singh, I., Moser, H. W., Moser, A. B., & Kishimoto, Y. (1981). Adrenoleukodystrophy: impaired oxidation of long chain fatty acids in cultured skin fibroblasts an adrenal cortex. *Biochemical and Biophysical Research Communications*, *102*(4), 1223–1229. https://doi.org/10.1016/S0006-291X(81)80142-8

Singh, I., Khan, M., Key, L., & Pai, S. (1998). Lovastatin for X-linked adrenoleukodystrophy. *The New England Journal of Medicine*, *339*(10), 702–703. https://doi.org/10.1056/NEJM199809033391012

Singh, J., Khan, M., & Singh, I. (2009). Silencing of Abcd1 and Abcd2 genes sensitizes astrocytes for inflammation: implication for X-adrenoleukodystrophy. *Journal of Lipid Research*, *50*(1), 135-147. https://doi.org/10.1194/JLR.M800321-JLR200

Singh, I., & Pujol, A. (2010). Pathomechanisms underlying X-adrenoleukodystrophy: A three-hit hypothesis. *Brain Pathology*, *20*(4), 838–844. https://doi.org/10.1111/j.1750-3639.2010.00392.x

Singh, J., Khan, M., Pujol, A., Baarine, M., & Singh, I. (2013). Histone Deacetylase Inhibitor Upregulates Peroxisomal Fatty Acid Oxidation and Inhibits Apoptotic Cell Death in Abcd1-Deficient Glial Cells. *PLoS ONE*, *8*(7), e70712. https://doi.org/10.1371/journal.pone.0070712

Siwek, T., Zwiernik, B., Jezierska-Woźniak, K., Jezierska, K., Mycko, M. P., & Selmaj, K. W. (2024). Intrathecal administration of mesenchymal stem cells in patients with adrenomyeloneuropathy. *Frontiers in Neurology*, *15,* 1345503. https://doi.org/10.3389/fneur.2024.1345503

Söhl, G., & Willecke, K. (2004). Gap junctions and the connexin protein family. *Cardiovascular Research*, *62*(2), 228–232. https://doi.org/10.1016/J.CARDIORES.2003.11.013

Soldner, F., Hockemeyer, D., Beard, C., Gao, Q., Bell, G. W., Cook, E. G., Hargus, G., Blak, A., Cooper, O., Mitalipova, M., Isacson, O., & Jaenisch, R. (2009). Parkinson's Disease Patient-Derived Induced Pluripotent Stem Cells Free of Viral Reprogramming Factors. *Cell*, *136*(5), 964–977. https://doi.org/10.1016/j.cell.2009.02.013

Soldner, F., & Jaenisch, R. (2012). iPSC Disease Modeling. *Science*, *338*(6111), 1155–1156. https://doi.org/10.1126/science.1227682

Solleiro-Villavicencio, H., & Rivas-Arancibia, S. (2018). Effect of Chronic Oxidative Stress on Neuroinflammatory Response Mediated by CD4 + T Cells in Neurodegenerative Diseases. *Frontiers in Cellular Neuroscience, 12,* 114. https://doi.org/10.3389/fncel.2018.00114

Sonoyama, W., Liu, Y., Fang, D., Yamaza, T., Seo, B.M., Zhang, C., Liu, H., Gronthos, S., Wang, C.Y., Shi, S., & Wang, S. (2006). Mesenchymal Stem Cell-Mediated Functional Tooth Regeneration in Swine. *PLoS ONE*, *1*(1), e79. https://doi.org/10.1371/journal.pone.0000079

Spaeth, E., Klopp, A., Dembinski, J., Andreeff, M., & Marini, F. (2008). Inflammation and tumor microenvironments: Defining the migratory itinerary of mesenchymal stem cells. *Gene Therapy,15*(10), 730-738. https://doi.org/10.1038/gt.2008.39

Spaggiari, G. M., Capobianco, A., Becchetti, S., Mingari, M. C., & Moretta, L. (2006). Mesenchymal stem cell-natural killer cell interactions: Evidence that activated NK cells are capable of killing MSCs, whereas MSCs can inhibit IL-2-induced NK-cell proliferation. *Blood*, *107*(4), 1484–1490. https://doi.org/10.1182/blood-2005-07-2775

Spaggiari, G. M., Abdelrazik, H., Becchetti, F., & Moretta, L. (2009). MSCs inhibit monocyte-derived DC maturation and function by selectively interfering with the generation of immature DCs: central role of MSC-derived prostaglandin E2. *Blood*, *113*(26), 6576–6583. https://doi.org/10.1182/blood-2009-02-203943

Steens, J., & Klein, D. (2018). Current strategies to generate human mesenchymal stem cells in vitro. *Stem Cells International*, *2018,* 6726185. https://doi.org/10.1155/2018/6726185

Stock, P., Brückner, S., Winkler, S., Dollinger, M. M., & Christ, B. (2014). Human bone marrow mesenchymal stem cell-derived hepatocytes improve the mouse liver after acute acetaminophen intoxication by preventing progress of injury. *International Journal of Molecular Sciences*, *15*(4), 7004–7028. https://doi.org/10.3390/ijms15047004

Stumpf, D. A., Hayward, A., Haas, R., Frost, M., & Schaumburg, H. H. (1981). Adrenoleukodystrophy: Failure of Immunosuppression to Prevent Neurological Progression. *Archives of Neurology*, *38*(1), 48–49. https://doi.org/10.1001/ARCHNEUR.1981.00510010074014

Sugimura-Wakayama, Y., Katagiri, W., Osugi, M., Kawai, T., Ogata, K., Sakaguchi, K., & Hibi, H. (2015). Peripheral Nerve Regeneration by Secretomes of Stem Cells from Human Exfoliated Deciduous Teeth. *Stem Cells and Development*, *24*(22), 2687–2699. https://doi.org/10.1089/scd.2015.0104

Szabó, A., & Mayor, R. (2018). Mechanisms of neural crest migration. *Annual Review of Genetics*, *52*, 43–63. https://doi.org/10.1146/ANNUREV-GENET-120417-031559

Takahashi, K., & Yamanaka, S. (2006). Induction of Pluripotent Stem Cells from Mouse Embryonic and Adult Fibroblast Cultures by Defined Factors. *Cell*, *126*(4), 663–676. https://doi.org/10.1016/j.cell.2006.07.024

Takahashi, K., Tanabe, K., Ohnuki, M., Narita, M., Ichisaka, T., Tomoda, K., & Yamanaka, S. (2007). Induction of Pluripotent Stem Cells from Adult Human Fibroblasts by Defined Factors. *Cell*, *131*(5), 861–872. https://doi.org/10.1016/j.cell.2007.11.019

Takeyasu, M., Nozaki, T., & Daito, M. (2006). Differentiation of dental pulp stem cells into a neural lineage. *Pediatric Dental Journal*, *16*(2), 154–162. https://doi.org/10.1016/S0917-2394(06)70081-7

Tang, D.Q., Cao, L.Z., Burkhardt, B. R., Xia, C.Q., Litherland, S. A., Atkinson, M. A., & Yang, L.J. (2004). In Vivo and In Vitro Characterization of Insulin-Producing Cells Obtained From Murine Bone Marrow. *Diabetes, 53*(7), 1721-1732. https://doi.org/10.2337/diabetes.53.7.1721

Tarasiuk, O., Ballarini, E., Rodriguez-Menendez, V., Bossi, M., Cavaletti, G., & Scuteri, A. (2022). Making Connections: Mesenchymal Stem Cells Manifold Ways to Interact with Neurons. *International Journal of Molecular Sciences*, *23*(10), 5791. https://doi.org/10.3390/ijms23105791

Teleanu, D. M., Niculescu, A.G., Lungu, I. I., Radu, C. I., Vladâcenco, O., Roza, E., Costăchescu, B., Grumezescu, A. M., & Teleanu, R. I. (2022). An Overview of Oxidative Stress, Neuroinflammation, and Neurodegenerative Diseases. *International journal of molecular sciences, 23*(11), 5938. https://doi.org/10.3390/ijms23115938

Terada, N., Hamazaki, T., Oka, M., Hoki, M., Mastalerz, D. M., Nakano, Y., Meyer, E. M., Morel, L., Petersen, B. E., & Scott, E. W. (2002). Bone marrow cells adopt the phenotype of other cells by spontaneous cell fusion. *Nature*, *416*(6880), 542–545. https://doi.org/10.1038/nature730

Thesleff, I. (1995). Homeobox genes and growth factors in regulation of craniofacial and tooth morphogenesis. *Acta Odontologica Scandinavica*, *53*(3), 129–134. https://doi.org/10.3109/00016359509005962

Thomas, M. A., Fahey, M. J., Pugliese, B. R., Irwin, R. M., Antonyak, M. A., & Delco, M. L. (2022). Human mesenchymal stromal cells release functional mitochondria in extracellular vesicles. *Frontiers in Bioengineering and Biotechnology*, *10,* 870193. https://doi.org/10.3389/fbioe.2022.870193

Tikellis, C., & Thomas, M. C. (2012). Angiotensin-Converting Enzyme 2 (ACE2) Is a Key Modulator of the Renin Angiotensin System in Health and Disease. *International journal of peptides*, 2012, 256294. https://doi.org/10.1155/2012/256294

Tremblay, M. È., Stevens, B., Sierra, A., Wake, H., Bessis, A., & Nimmerjahn, A. (2011). The role of microglia in the healthy brain. *The Journal of Neuroscience : The Official Journal of the Society for Neuroscience*, *31*(45), 16064–16069. https://doi.org/10.1523/JNEUROSCI.4158-11.2011

Trubiani, O., Zalzal, S. F., Paganelli, R., Marchisio, M., Giancola, R., Pizzicannella, J., Bühring, H. J., Piattelli, M., Caputi, S., & Nanci, A. (2010). Expression profile of the embryonic markers nanog, OCT-4, SSEA-1, SSEA-4, and frizzled-9 receptor in human periodontal ligament mesenchymal stem cells. *Journal of Cellular Physiology*, *225*(1), 123–131. https://doi.org/10.1002/JCP.22203

Tsuji, S., Sano, T., Ariga, T., & Miyatake, T. (1981). Increased synthesis of hexacosanoic acid (C23:0) by cultured skin fibroblasts from patients with adrenoleukodystrophy (ALD) and adrenomyeloneuropathy (AMN). *Journal of Biochemistry*, *90*(4), 1233–1236. https://doi.org/10.1093/OXFORDJOURNALS.JBCHEM.A133578

Turk, B. R., Theda, C., Fatemi, A., & Moser, A. B. (2020). X-linked adrenoleukodystrophy: Pathology, pathophysiology, diagnostic testing, newborn screening and therapies. *International Journal of Developmental Neuroscience*, *80*(1), 52–72. https://doi.org/10.1002/jdn.10003

Uccelli, A., Moretta, L., & Pistoia, V. (2008). Mesenchymal stem cells in health and disease. *Nature reviews. Immunology, 8*(9), 726–736. https://doi.org/10.1038/nri2395

Urraca, N., Memon, R., El-Iyachi, I., Goorha, S., Valdez, C., Tran, Q. T., Scroggs, R., Miranda-Carboni, G. A., Donaldson, M., Bridges, D., & Reiter, L. T. (2015). Characterization of neurons from immortalized dental pulp stem cells for the study of neurogenetic disorders. *Stem Cell Research*, *15*(3), 722–730. https://doi.org/10.1016/j.scr.2015.11.004

Urraca, N., Hope, K., Victor, A. K., Belgard, T. G., Memon, R., Goorha, S., Valdez, C., Tran, Q. T., Sanchez, S., Ramirez, J., Donaldson, M., Bridges, D., & Reiter, L. T. (2018). Significant transcriptional changes in 15q duplication but not Angelman syndrome deletion stem cell-derived neurons. *Molecular Autism*, *9*(1), 6. https://doi.org/10.1186/s13229-018-0191-y

Uto, T., Contreras, M. A., Gilg, A. G., & Singh, I. (2008). Oxidative imbalance in non-stimulated X-Adrenoleukodystrophy derived lymphoblasts. *Developmental Neuroscience*, *30*(6), 410-418. https://doi.org/10.1159/000191212

Valianpour, F., Selhorst, J. J., Van Lint, L. E., Van Gennip, A. H., Wanders, R. J., & Kemp, S. (2003). Analysis of very long-chain fatty acids using electrospray ionization mass spectrometry. *Molecular Genetics and Metabolism*, *79*(3), 189–196. https://doi.org/10.1016/S1096-7192(03)00098-2

Valiunas, V., Doronin, S., Valiuniene, L., Potapova, I., Zuckerman, J., Walcott, B., Robinson, R. B., Rosen, M. R., Brink, P. R., & Cohen, I. S. (2004). Human mesenchymal stem cells make cardiac connexins and form functional gap junctions. *The Journal of Physiology*, *555*(Pt 3), 617–626. https://doi.org/10.1113/JPHYSIOL.2003.058719

Van der Knaap, M. S., & Bugiani, M. (2018). Leukodystrophies — much more than just diseases of myelin. *Nature Reviews Neurology,14*(12), 747–748. https://doi.org/10.1038/s41582-018-0093-9

Van Geel, B. M., Assies, J., Haverkort, E. B., Koelman, J. H., Verbeeten, B., Wanders, R. J., & Barth, P. G. (1999). Progression of abnormalities in adrenomyeloneuropathy and neurologically asymptomatic X-linked adrenoleukodystrophy despite treatment with "Lorenzo's oil." *Journal of Neurology, Neurosurgery, and Psychiatry*, *67*(3), 290-299. https://doi.org/10.1136/JNNP.67.3.290

Van Geel, B. M., Bezman, L., Loes, D. J., Moser, H. W., & Raymond, G. V. (2001). Evolution of Phenotypes in Adult Male Patients with X-Linked Adrenoleukodystrophy. *Annals of Neurology, 49*(2), 186-194. https://doi.org/10.1002/1531-8249(20010201)49:2

Van Roermund, C. W., Visser, W. F., Ijlst, L., Waterham, H. R., & Wanders, R. J. (2011). Differential substrate specificities of human ABCD1 and ABCD2 in peroxisomal fatty acid β-oxidation. *Biochimica et Biophysica Acta - Molecular and Cell Biology of Lipids*, *1811*(3), 148–152. https://doi.org/10.1016/j.bbalip.2010.11.010

Van Roermund, C. W., Ijlst, L., Wagemans, T., Wanders, R. J., & Waterham, H. R. (2014). A role for the human peroxisomal half-transporter ABCD3 in the oxidation of dicarboxylic acids. *Biochimica et Biophysica Acta*, *1841*(4), 563–568. https://doi.org/10.1016/J.BBALIP.2013.12.001

Van Veldhoven, P. P. (2010). Biochemistry and genetics of inherited disorders of peroxisomal fatty acid metabolism. *Journal of Lipid Research*, *51*(10), 2863-2895. https://doi.org/10.1194/JLR.R005959

Vanderver, A., Prust, M., Tonduti, D., Mochel, F., Hussey, H. M., Helman, G., Garbern, J., Eichler, F., Labauge, P., Aubourg, P., Rodriguez, D., Patterson, M. C., Van Hove, J. L., Schmidt, J., Wolf, N. I., Boespflug-Tanguy, O., Schiffmann, R., van der Knaap, M. S & GLIA Consortium. (2015). Case definition and classification of leukodystrophies and leukoencephalopathies. *Molecular Genetics and Metabolism*, *114*(4), 494–500. https://doi.org/10.1016/j.ymgme.2015.01.006

Vargas, C. R., Wajner, M., Sirtori, L. R., Goulart, L., Chiochetta, M., Coelho, D., Latini, A., Llesuy, S., Bello-Klein, A., Giugliani, R., Deon, M., & Mello, C. F. (2004). Evidence that oxidative stress is increased in patients with X-linked adrenoleukodystrophy. *Biochimica et Biophysica Acta - Molecular Basis of Disease*, *1688*(1), 26–32. https://doi.org/10.1016/j.bbadis.2003.10.004

Vasandan, A. B., Jahnavi, S., Shashank, C., Prasad, P., Kumar, A., & Prasanna, S. J. (2016). Human Mesenchymal stem cells program macrophage plasticity by altering their metabolic status via a PGE2-dependent mechanism. *Scientific Reports*, *6*(1), 38308. https://doi.org/10.1038/srep38308

Vassilopoulos, G., Wang, P. R., & Russell, D. W. (2003). Transplanted bone marrow regenerates liver by cell fusion. *Nature*, *422*(6934), 901–904. https://doi.org/10.1038/NATURE01539

Velarde, F., Ezquerra, S., Delbruyere, X., Caicedo, A., Hidalgo, Y., & Khoury, M. (2022). Mesenchymal stem cell-mediated transfer of mitochondria: mechanisms and functional impact. *Cellular and Molecular Life Sciences : CMLS*, *79*(3), 177. https://doi.org/10.1007/S00018-022-04207-3

Vizoso, F. J., Eiro, N., Cid, S., Schneider, J., & Perez-Fernandez, R. (2017). Mesenchymal stem cell secretome: Toward cell-free therapeutic strategies in regenerative medicine. *International Journal of Molecular Sciences, 18*(9), 1852 (Vol. 18, Issue 9). https://doi.org/10.3390/ijms18091852

Von Bahr, L., Batsis, I., Moll, G., Hägg, M., Szakos, A., Sundberg, B., Uzunel, M., Ringden, O., & Le Blanc, K. (2012). Analysis of Tissues Following Mesenchymal Stromal Cell Therapy in Humans Indicates Limited Long-Term Engraftment and No Ectopic Tissue Formation. *Stem Cells*, *30*(7), 1575–1578. https://doi.org/10.1002/stem.1118

Wagner, W., Wein, F., Seckinger, A., Frankhauser, M., Wirkner, U., Krause, U., Blake, J., Schwager, C., Eckstein, V., Ansorge, W., & Ho, A. D. (2005). Comparative characteristics of mesenchymal stem cells from human bone marrow, adipose tissue, and umbilical cord blood. *Experimental Hematology*, *33*(11), 1402–1416. https://doi.org/10.1016/j.exphem.2005.07.003

Wanders, R. J., & Brites, P. (2010). Biosynthesis of ether-phospholipids including plasmalogens, peroxisomes and human disease: New insights into an old problem. *Clinical Lipidology, 15*(3), 379-386. https://doi.org/10.2217/clp.10.16

Wang, J., Wang, X., Sun, Z., Wang, X., Yang, H., Shi, S., & Wang, S. (2010). Stem Cells from Human-Exfoliated Deciduous Teeth Can Differentiate into Dopaminergic Neuron-Like Cells. *Stem Cells and Development*, *19*(9), 1375–1383. https://doi.org/10.1089/scd.2009.0258

Wang, X., Willenbring, H., Akkari, Y., Torimaru, Y., Foster, M., Al-Dhalimy, M., Lagasse, E., Finegold, M., Olson, S., & Grompe, M. (2003). Cell fusion is the principal source of bone-marrow-derived hepatocytes. *Nature*, *422*(6934), 897–901. https://doi.org/10.1038/NATURE01531

Wang, Y., Busin, R., Reeves, C., Bezman, L., Raymond, G., Toomer, C. J., Watkins, P. A., Snowden, A., Moser, A., Naidu, S., Bibat, G., Hewson, S., Tam, K., Clarke, J. T., Charnas, L., Stetten, G., Karczeski, B., Cutting, G., & Steinberg, S. (2011). X-linked adrenoleukodystrophy: ABCD1 de novo mutations and mosaicism. *Molecular Genetics and Metabolism*, *104*(1–2), 160–166. https://doi.org/10.1016/J.YMGME.2011.05.016

Wang, Y., Wang, F., Zhao, H., Zhang, X., Chen, H., & Zhang, K. (2014). Human adipose-derived mesenchymal stem cells are resistant to HBV infection during differentiation into hepatocytes in vitro. *International Journal of Molecular Sciences*, *15*(4), 6096–6110. https://doi.org/10.3390/ijms15046096

Wang, J., & Feng, J. Q. (2017). Signaling Pathways Critical for Tooth Root Formation. *Journal of Dental Research*, *96*(11), 1221–1228. https://doi.org/10.1177/0022034517717478

Waterham, H. R., Ferdinandusse, S., & Wanders, R. J. (2016). Human disorders of peroxisome metabolism and biogenesis. *Biochimica et Biophysica Acta - Molecular Cell Research*, *1863*(5), 922–933. https://doi.org/10.1016/j.bbamcr.2015.11.015

Waterman, R. S., Tomchuck, S. L., Henkle, S. L., & Betancourt, A. M. (2010). A New Mesenchymal Stem Cell (MSC) Paradigm: Polarization into a Pro-Inflammatory MSC1 or an Immunosuppressive MSC2 Phenotype. *PLoS ONE*, *5*(4), e10088. https://doi.org/10.1371/journal.pone.0010088

Watkins, P. A., Gould, S. J., Smith, M. A., Braiterman, L. T., Wei, H. M., Kok, F., Moser, A. B., Moser, H. W., & Smith, K. D. (1995). Altered expression of ALDP in X-linked adrenoleukodystrophy. *American Journal of Human Genetics*, *57*(2), 292. /pmc/articles/PMC1801558/?report=abstract

Weber, F. D., Wiesinger, C., Forss-Petter, S., Regelsberger, G., Einwich, A., Weber, W. H., Köhler, W., Stockinger, H., & Berger, J. (2014). X-linked adrenoleukodystrophy: very long-chain fatty acid metabolism is severely impaired in monocytes but not in lymphocytes. *Human Molecular Genetics*, *23*(10), 2542–2550. https://doi.org/10.1093/hmg/ddt645

Weinhofer, I., Zierfuss, B., Hametner, S., Wagner, M., Popitsch, N., MacHacek, C., Bartolini, B., Zlabinger, G., Ohradanova-Repic, A., Stockinger, H., Köhler, W., Höftberger, R., Regelsberger, G., Forss-Petter, S., Lassmann, H., & Berger, J. (2018). Impaired plasticity of macrophages in X-linked adrenoleukodystrophy. *Brain : A Journal of Neurology*, *141*(8), 2329–2342. https://doi.org/10.1093/BRAIN/AWY127

Weiss, A. R. R., & Dahlke, M. H. (2019). Immunomodulation by Mesenchymal Stem Cells (MSCs): Mechanisms of Action of Living, Apoptotic, and Dead MSCs. *Frontiers in Immunology*, *10*, 1191. https://doi.org/10.3389/fimmu.2019.01191

Wells, W. W., & Xu, D. P. (1994). Dehydroascorbate Reduction. *Journal of Bioenergetics and Biomembranes, 26*(4), 369-377. https://doi.org/10.1007/BF00762777

Wiesinger, C., Kunze, M., Regelsberger, G., Forss-Petter, S., & Berger, J. (2013). Impaired Very Long-chain Acyl-CoA-Oxidation in Human X-linked Adrenoleukodystrophy Fibroblasts Is a Direct Consequence of ABCD1 Transporter Dysfunction. *The journal of biological chemistry, 288*(26), 19269-19279. https://doi.org/10.1074/jbc.M112.445445

Wiesinger, C., Eichler, F. S., & Berger, J. (2015). The genetic landscape of X-linked adrenoleukodystrophy: inheritance, mutations, modifier genes, and diagnosis. *The Application of Clinical Genetics*, *8*, 109-121. https://doi.org/10.2147/TACG.S49590

Willkomm, L., & Bloch, W. (2015). State of the Art in Cell–Cell Fusion. *Methods in molecular biology, 1313,* 1-19. https://doi.org/10.1007/978-1-4939-2703-6_1

Witwer, K. W., Goberdhan, D. C., O'Driscoll, L., Théry, C., Welsh, J. A., Blenkiron, C., Buzás, E. I., Di Vizio, D., Erdbrügger, U., Falcón-Pérez, J. M., Fu, Q. L., Hill, A. F., Lenassi, M., Lötvall, J., Nieuwland, R., Ochiya, T., Rome, S., Sahoo, S., & Zheng, L. (2021). Updating MISEV: Evolving the minimal requirements for studies of extracellular vesicles. *Journal of Extracellular Vesicles, 10*(14), e12182. https://doi.org/10.1002/jev2.12182

Wyss-Coray, T., & Mucke, L. (2002). Inflammation in Neurodegenerative Disease—A Double-Edged Sword. *Neuron*, *35*(3), 419–432. https://doi.org/10.1016/S0896-6273(02)00794-8

Xiao, L., & Tsutsui, T. (2013). Characterization of human dental pulp cells-derived spheroids in serum-free medium: Stem cells in the core. *Journal of Cellular Biochemistry*, *114*(11), 2624–2636. https://doi.org/10.1002/jcb.24610

Xu, J., Wang, W., Kapila, Y., Lotz, J., & Kapila, S. (2009). Multiple differentiation capacity of STRO-1+/CD146+ PDL mesenchymal progenitor cells. *Stem Cells and Development*, *18*(3), 487–496. https://doi.org/10.1089/SCD.2008.0113

Yamamoto, T., Osako, Y., Ito, M., Murakami, M., Hayashi, Y., Horibe, H., Iohara, K., Takeuchi, N., Okui, N., Hirata, H., Nakayama, H., Kurita, K., & Nakashima, M. (2016). Trophic Effects of Dental Pulp Stem Cells on Schwann Cells in Peripheral Nerve Regeneration. *Cell Transplantation*, *25*(1), 183–193. https://doi.org/10.3727/096368915X688074

Yang, M., Cui, Y., Song, J., Cui, C., Wang, L., Liang, K., Wang, C., Sha, S., He, Q., Hu, H., Guo, X., Zang, N., Sun, L., & Chen, L. (2021). Mesenchymal stem cell-conditioned medium improved mitochondrial function and alleviated inflammation and apoptosis in non-alcoholic fatty liver disease by regulating SIRT1. *Biochemical and Biophysical Research Communications*, *546*, 74–82. https://doi.org/10.1016/j.bbrc.2021.01.098

Yan, F., Wang, W., Ying, H., Li, H., Chen, J., & Xu, C. (2017). S149R, a novel mutation in the ABCD1 gene causing X-linked adrenoleukodystrophy. *Oncotarget,* *8*(50), 87529–87538. https://doi.org/10.18632/oncotarget.20974

Yao, S., Chen, S., Clark, J., Hao, E., Beattie, G. M., Hayek, A., & Ding, S. (2006). Long-term self-renewal and directed differentiation of human embryonic stem cells in chemically defined conditions. *Proceedings of the National Academy of Sciences of the United States of America*, *103*(18), 6907. https://doi.org/10.1073/PNAS.0602280103

Yao, S., Pan, F., Prpic, V., & Wise, G. E. (2008). Differentiation of Stem Cells in the Dental Follicle. *Journal of Dental Research*, *87*(8), 767–771. https://doi.org/10.1177/154405910808700801

Yao, Y., Fan, X. L., Jiang, D., Zhang, Y., Li, X., Xu, Z., Bin Fang, S., Bin Chiu, S., Tse, H. F., Lian, Q., & Fu, Q. L. (2018). Connexin 43-Mediated Mitochondrial Transfer of iPSC-MSCs Alleviates Asthma Inflammation. *Stem Cell Reports*, *11*(5), 1120–1135. https://doi.org/10.1016/J.STEMCR.2018.09.012

Yeo, R. W., Lai, R. C., Zhang, B., Tan, S. S., Yin, Y., Teh, B. J., & Lim, S. K. (2013). Mesenchymal stem cell: An efficient mass producer of exosomes for drug delivery. *Advanced Drug Delivery Reviews*, *65*(3), 336–341. https://doi.org/10.1016/j.addr.2012.07.001

Ying, Q. L., Nichols, J., Evans, E. P., & Smith, A. G. (2002). Changing potency by spontaneous fusion. *Nature 2002 416:6880*, *416*(6880), 545–548. https://doi.org/10.1038/nature729

Yska, H. A., Engelen, M., & Bugiani, M. (2024). The pathology of X-linked adrenoleukodystrophy: tissue specific changes as a clue to pathophysiology. *Orphanet Journal of Rare Diseases*, *19*(1), 138. https://doi.org/10.1186/s13023-024-03105-0

Yu, B., Zhang, X., & Li, X. (2014). Exosomes Derived from Mesenchymal Stem Cells. *International Journal of Molecular Sciences*, *15*(3), 4142–4157. https://doi.org/10.3390/ijms15034142

Yu, T., & Klein, O. D. (2020). Molecular and cellular mechanisms of tooth development, homeostasis and repair. *Development*, *147*(2). https://doi.org/10.1242/dev.184754

Yu, J., Chen, T., Guo, X., Zafar, M. I., Li, H., Wang, Z., & Zheng, J. (2022). The Role of Oxidative Stress and Inflammation in X-Link Adrenoleukodystrophy. *Frontiers in Nutrition*, *9*. https://doi.org/10.3389/fnut.2022.864358

Zakrzewski, W., Dobrzyński, M., Szymonowicz, M., & Rybak, Z. (2019). Stem cells: Past, present, and future. In *Stem Cell Research and Therapy, 10*(1). https://doi.org/10.1186/s13287-019-1165-5

Zarrouk, A., Vejux, A., Nury, T., El Hajj, H. I., Haddad, M., Cherkaoui-Malki, M., Riedinger, J. M., Hammami, M., & Lizard, G. (2012). Induction of mitochondrial changes associated with oxidative stress on very long chain fatty acids (C22:0, C24:0, or C26:0)-treated human neuronal cells (SK-NB-E). *Oxidative Medicine and Cellular Longevity*. https://doi.org/10.1155/2012/623257

Zhang, F., Hong, Y., Liang, W., Ren, T., Jing, S., & Lin, J. (2012). Co-culture with Sertoli cells promotes proliferation and migration of umbilical cord mesenchymal stem cells. *Biochemical and Biophysical Research Communications*, *427*(1), 86–90. https://doi.org/10.1016/j.bbrc.2012.09.007

Zhang, B., Yin, Y., Lai, R. C., Tan, S. S., Choo, A. B., & Lim, S. K. (2014). Mesenchymal Stem Cells Secrete Immunologically Active Exosomes. *Stem Cells and Development*, *23*(11), 1233–1244. https://doi.org/10.1089/scd.2013.0479

Zhang, W., & Yelick, P. C. (2021). Tooth Repair and Regeneration: Potential of Dental Stem Cells. *Trends in Molecular Medicine*, *27*(5), 501–511. https://doi.org/10.1016/j.molmed.2021.02.005

Zhidkova, O. V., Andreeva, E. R., & Buravkova, L. B. (2018). Endothelial Cells Modulate Differentiation Potential and Mobility of Mesenchymal Stromal Cells. *Bulletin of Experimental Biology and Medicine*, *165*(1), 127–131. https://doi.org/10.1007/s10517-018-4113-y

Zhou, J., Terluk, M. R., Orchard, P. J., Cloyd, J. C., & Kartha, R. V. (2021). N-Acetylcysteine Reverses the Mitochondrial Dysfunction Induced by Very Long-Chain Fatty Acids in Murine Oligodendrocyte Model of Adrenoleukodystrophy. *Biomedicines*, *9*(12). https://doi.org/10.3390/BIOMEDICINES9121826

Zhou, C., Zhang, B., Yang, Y., Jiang, Q., Li, T., Gong, J., Tang, H., & Zhang, Q. (2023). Stem cell-derived exosomes: emerging therapeutic opportunities for wound healing. *Stem Cell Research and Therapy, 14*(1). https://doi.org/10.1186/s13287-023-03345-0

Zohrabian, V. M., Poon, C. S., & Abrahams, J. J. (2015). Embryology and Anatomy of the Jaw and Dentition. *Seminars in Ultrasound, CT and MRI*, *36*(5), 397–406. https://doi.org/10.1053/j.sult.2015.08.002

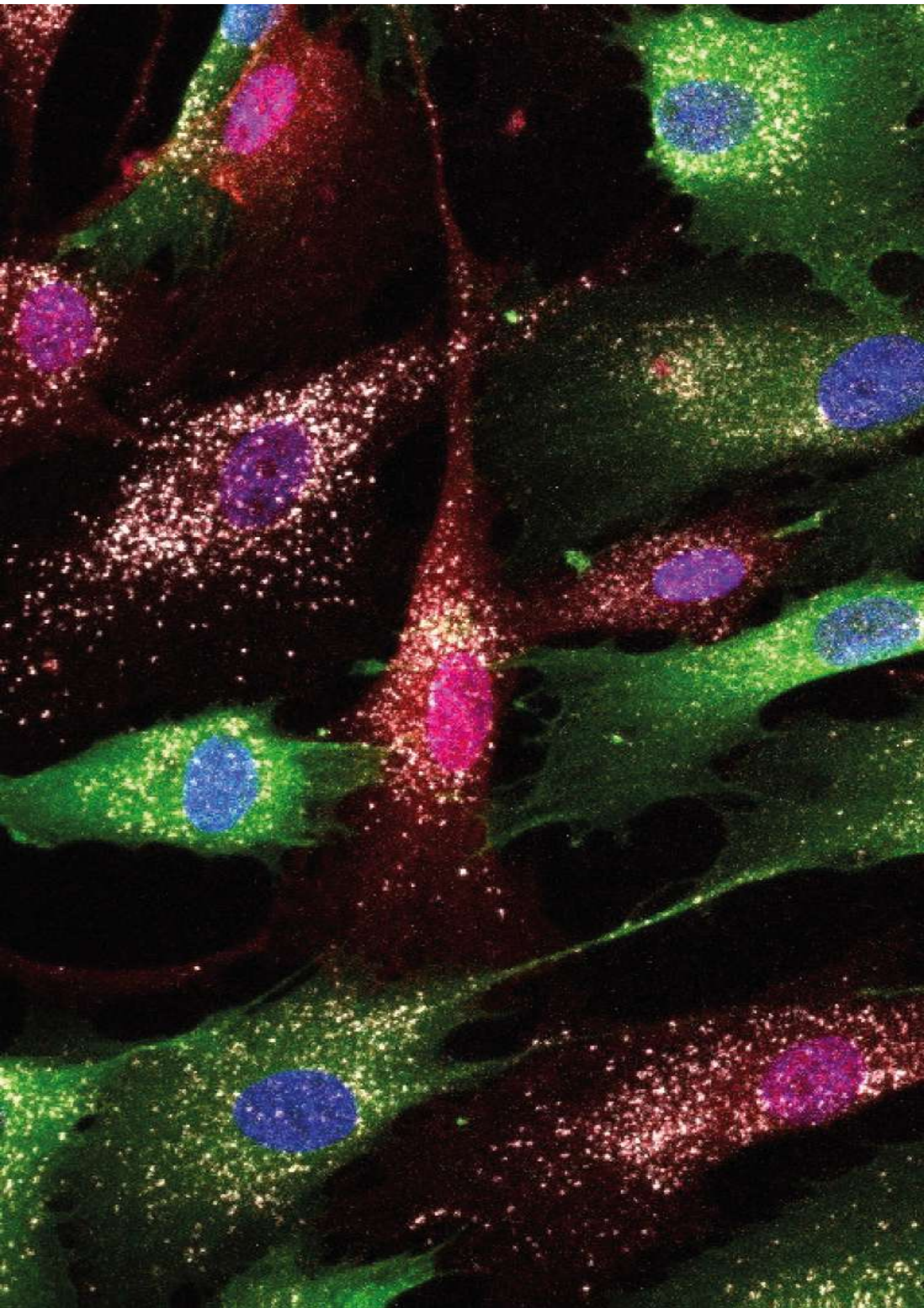

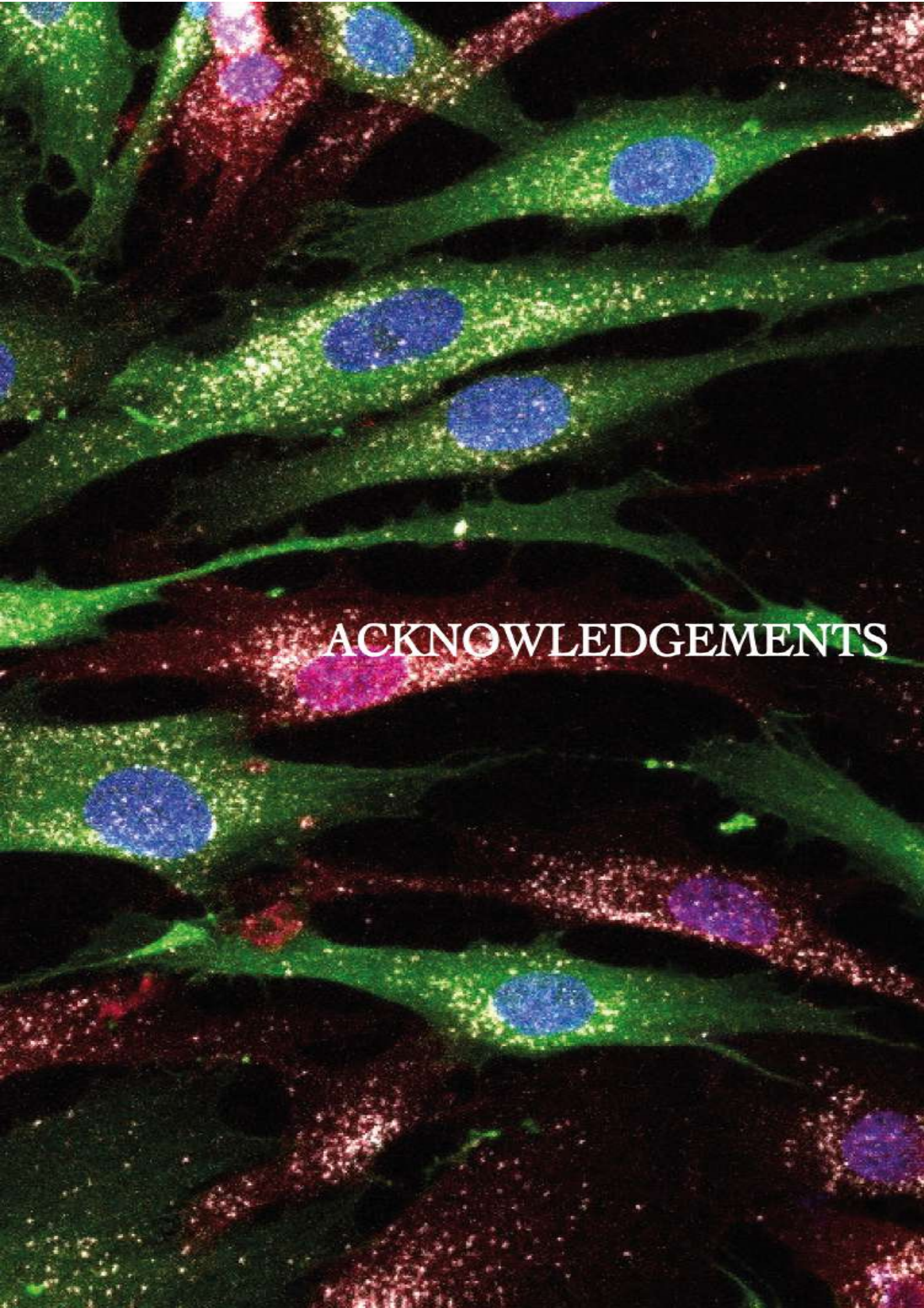

ACKNOWLEDGEMENTS

This image is property of Claudia Pérez García. Immunofluorescence of direct co-cultures of human dental pulp and bone marrow stem cells against GFP, RFP and ALDP. Image acquisition: Leica SPEII confocal microscope.

Acknowledgements

"¿Os habéis preguntado alguna vez cuántas veces en la vida habéis dado realmente las gracias? Unas gracias sinceras. La expresión de vuestra gratitud, de vuestro agradecimiento, de vuestra deuda."

— Delphine de Vigan, Las gratitudes

Si a la Claudia de 2018, que entró por primera vez al Instituto de Neurociencias con su tarjeta de visitante temporal, le dijesen que lo de "temporal" se acabaría extendiendo bastante en el tiempo y terminaría haciendo una tesis doctoral, probablemente no se lo creería. Sin embargo, a consecuencia de una serie de acontecimientos, hoy estoy aquí escribiendo estas palabras.

Desde luego que todo esto no estaría sucediendo sin la ayuda de mi director de tesis, Salvador. Gracias infinitas, en primer lugar, por confiar plenamente en la joven inexperta que apareció por el laboratorio y que no sabía muy bien qué hacer con su vida. Segundo, por haberme formado como científica, por haberme dado la libertad para indagar, cuestionar y buscar respuestas a cuestiones complejas. Por todas las lecciones científicas y vitales que me has dado.

Bien es sabido que la ciencia se hace en equipo y esta tesis doctoral no iba a ser menos. Me gustaría agradecer a todo el equipo del laboratorio, por haberme acompañado en esta travesía. A las primeras personas que conocí en cuanto entré en el laboratorio: Ana, Raquel y Alicia. Recuerdo que lo primero que hicisteis fue invitarme a desayunar con vosotras y a partir de entonces, entre café y café, fui ubicándome. Ana y Raquel, muchísimas gracias por todos vuestros consejos y ayuda en todo momento, nunca olvidaré el turismo exprés por París. Alicia, qué decir de ti. Has sido uno de los pilares fundamentales de esta tesis. Siempre te voy a estar eternamente agradecida, por haber estado presente en todos los momentos en los que he querido tirar la toalla. Que esté hoy escribiendo esto significa que has conseguido que no lo hiciera.

A la pieza clave de este laboratorio, el engranaje que hace que todo funcione: su personal técnico. Paqui, me falta tesis para agradecerte toda la ayuda prestada en todo momento. Muchas gracias porque de un problema siempre me has ofrecido múltiples soluciones. Mónica, por toda la alegría que desprendes y por hacerlo todo tan fácil. Ana, llegaste en la última etapa de mi tesis, pero siempre has estado dispuesta a ayudar. No puedo olvidarme de Marusa, por tu manera de facilitar las cosas y apagar fuegos a golpe de click.

A Tono, por toda la ayuda con los cultivos celulares, algo que era totalmente nuevo para mí. A Carlos Bueno, todavía recuerdo cuando me dijiste que si todo saliese a la primera, todas las enfermedades se habrían curado. Gracias por haber calmado mi impaciencia en aquellos inicios tan difíciles para mí. A Maria Luisa, por haber formado parte del proyecto con la parte de la electrofisiología y haberme explicado todo lo que no entendía. A Diego Pastor, porque me dejaste invadir tu escritorio y hacerlo mío, aunque nunca conseguí que me cedieras tu cajonera. Mil gracias por haber tenido la infinita paciencia de enseñarme todo lo relativo a la experimentación animal y no haber perdido los nervios cuando la he liado mezclando hembras y machos en una misma jaula.

A Abra, por toda la ayuda desinteresada. Porque gracias a ti estos años se han hecho mucho más llevaderos. A Vero, por todos los consejos realistas mientras se "construía" esta tesis. Créeme, me han servido de mucho. A Pili, por todo el perfeccionismo y eficacia que desprendes (y contagias). A Carla, por todas las risas y buen rollo, aunque ahora tenga que subir una planta más para verte. A Marta y a Dani, porque entre pintxo y pintxo nos fuimos conociendo más, pero no me olvido de que queda pendiente un "pizza-roll". A Nica, por toda tu dedicación y entusiasmo, bien sea para enseñarme a diseccionar un pie o para compartirme nuevos sitios donde probar tartas de queso. A Edu, por confiar en mí para adentrarme en la docencia y hacerme descubrir un nuevo mundo. A Diego, por todas las anécdotas y por ser el mejor guía turístico del País Vasco. A Emilio, por su templanza, paciencia y dedicación. A Mari Carmen Lillo, porque aunque nos veamos poco siempre has estado dispuesta a echar un cable. A Iris, por todo el apoyo en mis primeros años de tesis. A María, porque, aunque basemos nuestra personalidad en el último trend de moda de Tiktok, ya podemos decir que somos expertas en western blot. A Claudia, aunque tu paso por el laboratorio fue fugaz, fue suficiente para estrechar lazos, compartir crisis existenciales, técnicas de manejo de ansiedad y rollos de canela. Cosas de Claudias, supongo. A todos los/as estudiantes que han pasado por el laboratorio durante este periodo (Ana Moreno, Ana Glasgow, Coti, Paula…) y, en especial, a JM y Cristina. Porque siempre voy a recordar vuestra estancia con risas y, desde entonces, Mazarrón (puerto) tiene un huequito en mi corazón.

A todas las fundaciones privadas que han financiado la investigación realizada en esta tesis: Fundación San Antonio UCAM y WOP. A la Fundación ELA España por hacer de puente entre investigadores y pacientes y proporcionar dientes de leche. A todas las personas con adrenoleucodistrofia y a sus familiares, por no hacerme olvidar que detrás de cada flask de cultivo hay una historia.

A todos los servicios del Instituto de Neurociencias, porque hacen que algo tan complejo como la investigación sea un poco más fácil. A la unidad de lavado, a Trini, por lo gran profesional y persona que eres. Porque no conozco a una persona que contagie tanta alegría como tú. Al servicio de microscopía, por todas las horas dedicadas a cuadrar settings, darme formación y consejos con los experimentos. Todas las imágenes de esta tesis también son fruto de vuestro trabajo. Al servicio de ómicas, por todas las veces que he bajado con mil dudas y problemas y he salido de allí con todo mucho más claro y con muchas soluciones. Al servicio de limpieza y conserjería, porque sois la base de todo y sin vosotros nada funcionaría. A la CAPD, por toda la ayuda con la tramitación y papeleo. A todos los laboratorios que han prestado su ayuda desinteresada cuando la he necesitado. A Sergio y Carlos, por involucrarse tanto en enseñarme todos los entresijos del western blot. A Rocío Pérez, por responder todas mis dudas con las microvesículas. A Salu y Mariangeles, por la ayuda prestada en las ultracentrífugas. A todas las personas que me han cuestionado, corregido y aconsejado en los seminarios. A Carmen, porque has sido un soplo de aire fresco y has conseguido que este último año fuese mucho más divertido.

Sin embargo, sin las personas con las que haces la vida, no hay vida. Una mención especial en estos agradecimientos son aquellas personas que han presenciado la montaña rusa emocional que ha causado en mí la tesis doctoral. Porque nunca me iba a imaginar que unos compañeros de piso se iban a convertir en familia. Sergio, no te imaginas cuánto me has ayudado a lo largo de estos años. No sólo porque ahora conozco una lista interminable de curiosidades random de la medicina, sino además porque has estado siempre disponible ante

cualquier problema. Marcos, porque eres lo más parecido a mí y no sabes cuánto agradezco el sentirme comprendida y respaldada contigo. Yai, por todas tus locuras impulsivas y por todas las conversaciones de horas y horas que teníamos en el pasillo cuando salíamos un "segundo" a coger algo a la cocina. No puedo no mencionar a la mejor perrita de apoyo emocional, la Jinger, que, sin duda, también forma parte de esto. De Lilo tampoco me olvido, mi bicho de plumas favorito, que me ha acompañado en la mayor parte de escritura de esta tesis. Gracias simplemente por haber sido hogar y por haberme dado mi espacio siempre que lo he necesitado. Tampoco puedo olvidarme de Natalia, o más bien conocida en el piso como "la Nati", porque una vez me dijiste que si mi objetivo era acabar la tesis, el tuyo era que yo tuviera las herramientas para ello. Mil gracias porque no sólo has conseguido eso.

Esta tesis también le debe mucho a aquellas personas con las que comencé a adentrarme en el mundo de la ciencia: mi Sede de la Biotecnología. Porque con vosotras el slogan de la UMH de "los mejores años de tu vida" se ve elevado a la potencia infinita. Azucena, por todo lo aprendido juntas y, sobre todo, por todo lo (des)aprendido. Gracias infinitas por toda la ayuda, por las casualidades (campanita) y por todos los "sabías qué" que aprendo de ti. Ya sabes que nadaría océanos por ti (y de paso, te subo la bici a casa). Eli, desde el chiste de los macarrones hasta tu fatídico viaje a Punta Cana (o mejor dicho, Punta Caca). Si la inmortalidad existiese, desde luego que la tendrías toda tú. Gracias a ti esta tesis ha sido patrocinada por los post-its de la Roche Posay, pero no me pidas que vayamos caminando al Mc Donald's nunca más. Jorge, el que soporta el peso de tener siempre la razón, gran poseedor de mis fotos robadas, mi paparazzi personal y el Willy fog que aspiro ser. Si algo tengo claro después de todos estos años es que secretos contigo nunca podré tener, menos mal que grandes anécdotas sí. Tam, no podías faltar en esta primera (y única) edición de la tesis. Tus consejos como Sra Dra me han servido de mucho en este último empujón (y tus recomendaciones de libros, más aún). Gemma (o Chema), responsable de que sepa ubicar Enguera en el mapa, nos vemos menos de lo que me gustaría, pero siempre es guay el reencuentro (y más si hay helado de Nutella para desayunar). Marcos, porque me sigues hablando (y soportando) a pesar de olvidar tu cumpleaños varios años y casi matarte por sobredosis de lactosa y eso me deja en mal lugar a mí, pero dice mucho de lo gran persona que eres.

A mi piña del máster. Carol, por amenizar todas las quedadas con todas tus historietas únicas. Paula, por todos los kilómetros mal cuadrados juntas, porque siempre habrá una coca-colita al final de cada etapa. Inés, por haberme acogido con los brazos abiertos ya sea en Madrid, en Asturias o donde haga falta. Dani, el internacional del grupo, aunque ya nos conocíamos de la carrera, te ganaste un puesto especial cuando me cocinaste arroz al horno y eso nunca se olvida.

A la colchoneta salvavidas que me sostuvo en los primeros años de esta tesis: los atrapaos del CrossFit (team calidad). Aunque a día de hoy ya no sepa hacer un clean and jerk decente y sea una desertora, no podíais no tener un huequito en estos agradecimientos. Carlos, Shere, Pablo y Nieves, fuisteis un rayito de luz en momentos en los que sentía el mundo patas arriba. Mención especial a Juanda, porque muchos de los "nombrajos" de esta tesis le serán familiares e incluso sería capaz de explicar algunos de los experimentos, lo que le hace partícipe directo de esto. Gracias por estar, por escuchar, por querer entender y, sobre todo, por los bailes flamenco fusión.

Gracias interminables a las amistades de toda la vida, por saber perdonar mis ausencias y por haber estado siempre pendientes de esta tesis a pesar de no entender muy bien toda esta historia. A Iván, María y Laura, porque después de 27 años juntos, tengo recuerdos con vosotros en todas las etapas de mi vida y quiero que siga siendo así en las siguientes. Porque por fin os puedo decir que la tesis, bien. Estoy deseando que nos peguemos un homenaje de los nuestros. Marta y Jose, aparecisteis más tarde, pero también sois partícipe de esto. A María Navarro, porque una clase de biología en el instituto nos unió y desde entonces me has demostrado que puedo contar contigo en todo momento. A Irene, porque siempre que nos reencontramos es como si el tiempo no hubiese pasado. A todos mis amigos de La Marina, porque siempre tengo motivos para volver a casa.

A las personas que me sostienen desde que estoy en este mundo: mi familia. Si hay alguien que se merece un mayor agradecimiento en esta tesis, sois vosotros. Mamá y papá, mil gracias por los valores y educación que me habéis transmitido, por haberme permitido ser y elegir, por haber celebrado todos mis logros por pequeños que fueran y por haber estado al pie de cañón cuando he sentido que las cosas no iban tan bien. Gracias por la paciencia infinita en esta etapa de mi vida, por hacerme entender que las cosas van poquito a poquito. Es un orgullo ser vuestra hija. A mi hermana Laura, porque, aunque siempre se piensen que soy yo la mayor, ejerces como hermana mayor a la perfección. Por ser más que una hermana, por haberme apoyado en todo momento y porque siempre te voy a avisar cuando llegue a casa. A Carlos, por todos los consejos útiles de vida adulta que me das.

Y, por último, a mí. A mi "yo" de ayer, por todas las veces que te viste incapaz y aún así persististe. Has logrado que hoy esté escribiendo esto. A mi "yo" del mañana, para que sea consciente de todo lo conseguido y no le falten motivos para confiar en sí misma.